Topics in Resource Optimization in Wireless Networks with Limited Feedback

YuanYuan He

Submitted in total fulfilment of the requirements of the degree of

Doctor of Philosophy

Department of Electrical and Electronic Engineering
THE UNIVERSITY OF MELBOURNE

April 2011

Produced on archival quality paper.

Abstract

THIS thesis focuses on the design of various optimal resource allocation algorithms for wireless communication networks with imperfect channel state information (CSI) available at the transmitter obtained via a finite-rate feedback channel from the receiver (the so-called limited feedback technique).

We first look at an M parallel block-Nakagami-fading channels where we seek to design an optimal power allocation scheme that minimize the outage probability under a long term average transmit power (ATP) constraint with quantized CSI. A simultaneous perturbation stochastic approximation algorithm (SPSA) based simulation-optimization method is applied to obtain a locally optimal power codebook. As this method is computationally intensive and time-consuming, we then derive a number of reduced-complexity suboptimal finite-rate power codebook design algorithms. For the large number of parallel channels case, a Gaussian approximation based low-complexity power allocation strategy is provided.

We then consider a secondary user (SU) transmit power control problem in a spectrum sharing cognitive radio networks scenario with quantized channel feedback for optimizing relevant performance measures such as secondary ergodic capacity or outage probability under interference power constraints (which can be restricted either by an average (AIP) or a peak (PIP) constraint) at primary user (PU) receivers to protect the PU, and an average transmit power (ATP) constraint on SU. Firstly, we study the problem of ergodic capacity maximization over M parallel channels (each of which is licensed to a distinct PU) of SU subject to an ATP constraint at SU and M individual AIP constraints on each PU with quantized feedback of the joint channel space of SU transmitter to SU receiver and SU transmitter to PU receivers. We develop a "modified

generalized Lloyds-type algorithm (GLA)" for finding a locally optimal quantized power codebook. An approximate but computationally efficient quantized power allocation algorithm is then derived for the case of large number of feedback bits. It is seen that only 3-4 bits of feedback per channel band achieves SU ergodic capacity close to the full CSI based performance. We also extend these results to the noisy limited feedback case. We then consider the problem of throughput maximization of SU with a finite rate power codebook under an ATP constraint at SU and N individual PIP constraints on each PU receiver. With quantized channel (from the SU-TX to each PU-RX) knowledge, three different quantized power allocation schemes are proposed corresponding to three distinct forms of CSI obtained regarding the channel from SU-TX to SU-RX link at SU-TX : full CSI, noisy estimated CSI and quantized CSI. Finally, we consider the joint optimization of the quantization regions and the transmission power codebook such that the outage probability of the SU is minimized while an ATP constraint at the SU and an AIP constraint on the PU are met. Explicit expressions for asymptotic behavior of the SU outage probability at high rate quantization are also developed.

Declaration

This is to certify that

1. the thesis comprises only my original work towards the PhD,
2. due acknowledgement has been made in the text to all other material used,
3. the thesis is less than 100,000 words in length, exclusive of tables, maps, bibliographies and appendices.

YuanYuan He, April 2011

Acknowledgements

First of all, I would like to express my most sincere gratitude to my supervisor Professor Subhrakanti Dey. It is his encouraging, patient, kindness and enthusiasm that constantly fuel me with strength, hope and support to take on challenges and overcome frustrations. It is his wide knowledge, stimulating suggestions, endless source of brilliant ideas, logical way of thinking that guide me through these three and half years PhD study, and contribute greatly to the contents of this thesis. Without him, none of these research work would exist. I am also genuinely thankful to my co-supervisor Dr. Brian Krongold who provided the detail suggestions to guide me to start the PhD study and also help me improve the presentation skill.

I would like to give my special thanks to the committee member, Professor Jamie Evans, whose insightful comments and valuable advices greatly helped me to improve my research. And I also would like to thank him for organizing the weekly Wireless on the Whiteboard (WoW) seminars, where I have learned a lot of valuable information and knowledge about the latest research results, and also provide me good opportunities to share and discuss my research work with other people.

I also wish to thank the ARC Special Research Center for Ultra-Broadband Information Networks (CUBIN) (now the name has been changed to CEET) for providing a great working environment and facilities for me to do the research, where I made a lot of good friends. I am also grateful for the funding support provided by my supervisors and the ARC Communication Research Networks (ACoRN) for me to attend the conferences and visit University of Illinois at Urbana-Champaign. And I also would like to thank John Papandriopoulos for providing the template for this thesis.

Finally, I owe a debt of gratitude to my family and friends for their unconditional

love, encouragement, support, patience and understanding.

Contents

List of Figures

Chapter 1

Introduction

Optimizing the utilization of limited wireless resources, such as, transmission power control, rate allocation, multiple access scheme, spectrum access strategy, and so on, so as to improve the system performance, to ensure the basic quality of services, or to diminish the cost for the network infrastructures, plays a crucial role in wireless communication networks design. The randomly time-varying nature of wireless communication channels, also known as "fading channels", makes this task of optimal resource allocation extremely challenging. Research over the last two decades has well demonstrated that dramatically improvement on almost any information theoretic performance measure of wireless networks can be achieved by designing system resources adaptation based on full channel information available at the transmitter and receiver. However, while availability of full channel state information at the receiver (CSIR) is certainly feasible (at least in the form of channel estimates), the assumption of channel state information at the transmitter (CSIT) is impractical due to the reasons such as bandwidth constrained nature of the feedback channel and the substantial amount of communication overhead involved for a time-varying wireless channel. Recent research on various types of wireless communication networks has addressed this concern by investigating performance analysis with only partial channel knowledge available at the transmitter. This thesis will concentrate on designing optimal resource allocation algorithms for important wireless communication systems such as a single user point-to-point communication system involving parallel fading channels (technologically relevant for multi-carrier systems such as OFDM) and emerging technologies such as cognitive radio networks with quantized channel information at the transmitter using "limited feedback" over the finite-rate feed-

back channel.

In this chapter, we will first briefly introduce some useful information theoretic notions related to the topics in this thesis. Then, we will give an overview of the thesis and its main contributions. We will finally conclude the chapter with a list of publications resulting from this thesis.

1.1 Resource Optimization in Wireless Communication Networks

The increasing demand for high data rate wireless services requires high performance (such as capacity or reliability) wireless communication networks. To meet this goal, efficiently and adaptively utilizing limited wireless resources, such as transmit power, rate, etc, is essential. The channel quality of wireless communication systems is usually characterized by high variability due to the factors such as mobility, interference, multipath propagation environment, and so on [37]. Traditional fixed resource based management schemes, where resources have to be chosen to ensure an acceptable quality performance even with the worst-case channel conditions [16], results in a very inefficient and inflexible utilization of the available resource. In contrast, resources allocated adaptively based on the instantaneous channel conditions can dramatically improve the system performance. Due to the promise of such benefits, designing optimal resource allocation schemes in order to maximize the performance of various kinds of wireless communication networks have earned a significant interest from researchers and have been widely studied in the literature in recent years, such as [79],[64],[42],[19],[104].

Various notions of capacity for a wireless fading channel include *ergodic capacity* [10], *capacity versus outage probability* [40] and *delay-limited capacity* [99], which constitute some of the very important performance criteria for analyzing the information theoretic performance limits of wireless communication networks. For delay-insensitive applications such as wireless data networks, ergodic capacity, which is defined as the maximum achievable rate averaged over all channel realizations [117], is a good performance metric. But for delay-sensitive services such as real-time speech and video, the latter two notions are more appropriate. These two performance measures are closely related. The

notion of outage probability denotes the probability that the instantaneous mutual information of a wireless channel falls below a required rate threshold and the delay-limited capacity is defined as the maximum achievable constant transmission rate at which the outage probability is zero [40].

Deriving a resource optimization strategy which can adapt to the instantaneous channel conditions requires the transmitter to have access to some form of knowledge of the channel conditions, often referred to as channel state information (CSI) [34] in the literature. Due to the fact that in many wireless communication environments, changes in the propagation environment occur on a very slow time scale with respect to the signaling rate [40], the block-fading channel model [89],[36],[68] can be effective. In this model, channel information changes independently from block to block, but the channels within each transmission block experience the same CSI. Blocks can be viewed of as separated in time (e.g., in a TDMA system) or as separated in frequency (e.g., in a multicarrier system (OFDM))[40].

One issue which can significantly affect the resource optimization performance is to what degree of accuracy or resolution the transmitter can obtain the CSI. Many of the existing research work on resource optimization assume that the transmitter can obtain perfect CSI through the techniques such as training, in order to maximize the information theoretic performance measures of wireless communication systems. With the full CSI assumption, it is well known that the optimal power allocation strategy for maximizing the capacity of a OFDM system with a total power constraint is 'waterfilling' [35], which is obtained by solving this concave optimization problem with the Karush-Kuhn-Tucker (KKT) conditions (KKT conditions are the necessary conditions for optimality of an optimization problem, and if the problem is convex, the solution obtained by KKT is a global optimum). Here the notion of 'waterfilling' means that the transmitter allocates more power to the stronger sub-carriers (which have better channel conditions), and less or even no power to the weaker ones [35]. The optimal power control schemes for minimizing the outage probablilty of a block-fading channel under a short or long term average power constraint have been studied in [40]. In [53], the authors investigated the service outage based power allocation problem which combines the concepts

of both ergodic capacity and outage capacity for fading channels.

Unfortunately, the perfect CSI assumption is unrealizable in a practical system, due to bandwidth constraints on the reverse feedback link as well as the considerable communication overhead cost involved. This assumption is also not suitable for wireless communication systems using frequency-division duplexing (FDD), where the transmitter cannot obtain the forward link CSI from pilot based training techniques for the reverse link (or vice versa) since the forward link and the reverse link in FDD generally operate on different frequencies [34].

1.2 Limited Feedback Strategy

The use of limited channel information feedback has addressed the problem of obtaining partial information about instantaneous CSIT practically at the transmitter [34]. The general idea of the limited feedback approach is that, the receiver utilizes the reverse link as a feedback channel and conveys a low rate data stream about the information of forward channel conditions (such as the CSI, power, rate, etc.) to the transmitter, and then the transmitter exploits this information to adapt its transmission on the forward link. Such practical systems are commonly referred to as "limited feedback" or "finite-rate feedback" systems. Over the last few years, it has been demonstrated that the system performance obtained through the use of a small number of information bits about the forward link conditions sent from the receiver to the transmitter, is nearly identical to the impractical case of full CSI at the transmitter. Such encouraging results lead to the popularity of the application of limited feedback strategy in recent years, especially in wireless communication field, and the interest has continued to grow. In the following, we will briefly summarize the application of limited feedback in wireless communication systems over the past few years.

Single-user single-antenna wireless communication systems: In [107], the authors assumed perfect CSIR and utilized quantized version of the magnitude of channel CSI as feedback for channel adaptation in flat-fading systems, subject to either a short-term power constraint or a long-term power constraint. The idea of limited feedback strategy here is

that a fixed codebook about quantized CSI information with size 2^B is pre-computed and known to both transmitter and receiver. The receiver employs its channel estimate to pick the optimal transmitter-side CSI from the codebook. And then the B-bit binary label representing the index of the chosen CSI in the codebook is sent over the feedback channel to the transmitter. After that the transmitter will use the codebook element associated with the feedback index to adapt its transmission strategy. Obviously, the key technique here is the quantized codebook design. In [73], the authors considered periodic feedback, where channel CSI is fed back to the transmitter at regular fixed time-intervals. The performance degradation of an adaptive modulation due to feedback imperfections was evaluated in [3]. In [111], the authors showed that utilizing the channel side information can help reduce the complexity of code design. In [94],[57], another approach of feedback i.e, automatic repeat request (ARQ) scheme, where power adaptation is derived based on ACK/NAK feedback, was proposed. To make the system performance robust, in [11], the authors investigated rate adaptation based on both partial CSIT feedback as well as ACK/NAK signaling. In broadband systems, OFDM technique is used in multipath fading channels. In [121], the authors derived an optimal on-off subcarrier power allocation and quantized rate control (adaptive modulation) with limited feedback through a slow frequency-selective fading channel. Jointly optimizing the power allocations on the OFDM frequency tones has been studied in [32]. Power loading over sub-channel groups with limited feedback was discussed in [74].

Single-user multiple-antenna wireless communication systems: In [23], the authors designed a fixed covariance codebook using the Lloyd-like algorithm to maximize the ergodic capacity of an isolated MIMO link with flat Rayleigh fading, where the receiver only sends the label of the best covariance matrix in this predetermined covariance codebook to the transmitter. The covariance codebook also can be randomly generated. Random covariance codebooks design for MIMO channel, generated from the uniform distribution on the complex unit sphere, was proposed by [2]. Except for covariance quantization, other channel quantization approaches like channel CSI vector quantization (as addressed in [15] for a MISO system), beamforming vector quantization and linear precoding quantization. In [119], the authors provided quantized transmit beamformer designs

for the MISO case and the MIMO case under the uniform elemental power constraint. A quantized maximum signal-to-noise ratio beamforming technique was proposed in [33] for the MIMO case, where the beamforming vector codebooks is designed related to the Grassmannian line packing problem. Grassmannian line packing is the problem of finding the set or packing of lines that has maximum minimum distance between any pair of lines. In [50], the authors proposed a new quantizer design criterion to construct the beamforming quantization codebooks using a Lloyd-type vector quantization (VQ) algorithm (i.e, Generalized Lloyd Algorithm (GLA)) for the MISO case. The basic idea of VQ is to represent a large set of vectors by a smaller set of vectors in the best possible way. To implement vector quantization, GLA, a clustering technique, is often used to design the vector quantizer. It formulates a distortion function, and then iteratively runs the two optimality conditions until convergence, so as to obtain a locally solution. The two conditions are: (1) the nearest neighborhood condition, i.e, finding an optimum partition which divide a large set of points (vectors) into groups for given codebook vectors; (2) the centroid condition, i.e, finding optimum codebook vectors that minimize the distortion function for a fixed partition. The conditions for the convergence and consistency of the GLA with empirical distributions were established in [76]. The consistency property of GLA is defined by a performance which is nearly as good as in the case of known source statistics, and can be achieved with a large enough observed training set [102]. Another approach to designing a limited feedback beamforming codebook is using random vector quantization (RVQ), as shown in [29] for the MISO case. In this approach, the codebook is generated independently from a uniform distribution on the complex unit sphere. All these beamforming codebook design methods (Grassmannian, VQ, RVQ) can be applied to linear precoding codebook design, see [113],[26],[114]. Furthermore, the beamforming and the linear precoding techniques proposed for narrowband channels can be easily extended to broadband case by employing OFDM. In [52], the authors designed the optimal beamforming vector quantization scheme and computed the beamforming vectors for all subcarriers through interpolation for a MIMO-OFDM system. In [103], a geodesic sampling approach was used as a linear interpolation on the Grassmann manifold to obtain the precoder matrices for nonpilot subcarriers based on optimal quantized precoder

codebooks of pilot subcarriers in a MIMO-OFDM system.

Multi-user single-antenna wireless communication systems: In a multi-user cellular network, one bit feedback per user about the quality (SNR) of their channel (threshold-based technique) was studied in [98], and it also showed that such a 1-bit scheduling can capture most of the possible throughput gain. In [85], the authors investigated the capacity performance of the broadcast channel with limited feedback using superposition coding. As shown in [87], an opportunistic feedback protocol for an uplink MAC system was proposed . In a broadband MAC system, multiple access can be achieved through be orthogonal frequency-division based multiple access (OFDMA), time-division multiple access (TDMA), or code-division multiple access (CDMA). In [51], the authors considered using one bit feedback per subchannel to allocate the subchannels to users in a downlink OFDMA system. Allocation of scarce feedback resources optimally in downlink OFDMA systems was studied in [86]. OFDMA frequency scheduling algorithms design with limited feedback was discussed in [54],[63]. Optimal and suboptimal bit, power and subcarrier allocation schemes for OFDMA with limited-rate feedback were derived in [4]. In [5], the authors designed optimal power loading, quantization regions and time slots allocation to users so as to minimize the total average transmit power for TDMA system. To avoid interference, [115] analyzed the performance of signature optimization using limited feedback for a DS-CDMA system, where RVQ scheme is utilized to design a quantized signature codebook. And low rate feedback was also applied to peer-to-peer multi-carrier CDMA networks [1].

Multi-user multi-antenna wireless communication systems: In downlink multiuser MIMO systems with one receive antenna per user, the base station needs to precode the signals so as to eliminate the inter-user interference. There exist principally two different feedback approaches for designing the precoding matrix with limited feedback. One is to design the precoding matrix at the base station based on channel vector quantization together with user channel quality (SNR) as proposed in [58]. Multiuser opportunistic beamforming, where the base station picks the best subset of users and schedules them for transmission based on a quantized precoder codebook together with user channel quality (SNR), is an alternative limited feedback strategy for MIMO downlink channels

[41]. The comparison between these two schemes was also discussed in [41]. For multiuser MIMO with multiple receive antenna users, block diagonalization transmission technique with limited feedback was investigated in [80]. Coordinated beamforming with limited feedback for downlink multiuser MIMO with multiple receive antenna per user was studied in [27], where the transmit beamformers and receive combining vectors are jointly optimized based on quantizing the symmetric Hermitian matrices derived from the channel CSI. In (synchronous) multiuser MIMO uplinks, as shown in [48], the limited feedback approach is similar to the point-to-point single user MIMO case.

A new exciting area where feedback can generate significant impact is cognitive radio networks. In this thesis (Chapters 3, 4 and 5), we will analyze the performance of cognitive radio networks with finite rate feedback. There are also many other interesting applications of limited feedback in wireless communication field, such as the effect of errant feedback analysis, relay system with limited feedback, and so on. An excellent overview of limited feedback in wireless communication systems is available in [34]. The future research in limited feedback involve the consideration of imperfect CSI at the receiver, jointly encoding message information with channel feedback, considering the effect of feedback delay, an so on.

1.3 Cognitive Radio Networks

Radio spectrum is a limited and precious natural resource, which, traditionally, is licensed to users by regulatory authorities in a very rigid manner where in order to avoid interference, the licensed owner has an exclusive right to access the allocated frequency band [7]. Consequently, as the number of wireless communication systems and services grows, the availability of vacant spectrum becomes severely scarce. However, recent measurements by the Federal Communications Commission reveal that many portions of spectrum are mostly under utilized or even unoccupied. This led to the idea of cognitive radios (CR) technology, originally introduced by J. Mitola [49], which holds a tremendous promise for dramatically improving the efficiency of spectral utilization.

The key idea behind CR is that a CR is allowed to communicate over a frequency band

originally licensed to some non-cognitive users, as long as its operation does not generate unfavorable impact on these existing users' communication. The CR users exploit the information about activity, channel conditions, coding and massages of the non-cognitive users in the sharing spectrum [9], to carefully design their transmission strategy so as to minimal the interference they cause on non-cognitive users and improve performance and spectral efficiency as well. Based on the type of available information that CR can obtain, three main categories of CR network paradigms have been proposed: underlay, overlay and interweave [9].

In underlay paradigm, CR users (often called secondary users (SUs) in this setting) are permitted to operate over a spectrum, regardless the activity status of the non-cognitive users (referred to as primary users (PUs)) in this spectrum, by guaranteeing that the interference inflicted by SUs is below a certain regulatory limit. Obviously, the channel information knowledge of the interference channels (the link from SU transmitter to PU receiver) is crucial for SUs's transmission adaptation. This type of CR is also known as the "spectrum sharing" [7] model. In overlay systems, the CR users require the knowledge of non-cognitive users' channel, codebooks and messages, and can transmit concurrently with non-cognitive users by sacrificing part of their power, which is utilized to offset the resulting interference to non-cognitive users. In interweave systems, the CR users periodically detect/sense the activity information of non-cognitive users in the spectrum, and then opportunistically communicate over spectral holes that are not occupied by non-cognitive users, to ideally avoid any interference to non-cognitive users. These three different CR network strategies can also be combined to create new hybrid CR schemes to overcome some drawbacks of the individual paradigms. An overview of these three CR approaches is available in [9].

The cognitive radio networks studied in this thesis will focus on the underlay paradigm. In [30], the interference temperature concept was proposed by FCC as a suitable criterion to measure the tolerable interference level caused by SUs at PUs receivers. Based on this concept, instead of placing constraints only on the transmit power as always, imposing a constraint on the received power at the PU receiver seems much more appropriate in order to protect the PUs. Thus, the underlay CR can be modelled as cognitive communica-

tion with certain constraints imposed on the received interference signals at PUs receivers induced by SUs' transmission [9]. These constraints are closely related to the transmission strategy of SUs. Therefore, transmit power of SUs should be controlled properly in a spectrum sharing CR network to achieve the best tradeoff between efficiently sharing of the licensed spectrum (i.e, maximizing CR system performance) and at the same time, minimizing the interference caused to the PUs (i.e, total interference power at the PUs receivers remains below a certain level.)[69].

Transmit power adaptation for SUs in a CR network under various received power constraints have attracted significant interest in resent years. The behavior of capacities of various types of additive white Gaussian noise (AWGN) channels under received-power constraints at the PU-RX was first studied in [43], which showed that for point-to-point non-fading AWGN channels, the capacity performances with transmit and received power constraints are essentially similar. While in [7], the authors illustrated that with the identical limit on the received-power constraint, better capacity performance can be achieve in severe fading channels compared to the AWGN case due to more spectrum access opportunity for the SU. On performance analysis of spectrum sharing model in fading environments, two common received interference constraints, average interference power constraint (AIP) and peak interference power constraint (PIP), are considered. In [7], the authors investigated the ergodic capacity of a dynamic narrowband spectrum sharing model with one SU and one PU under either AIP or PIP constraint at PU-RX in various fading environments. It showed that with the AIP constraint, the optimal power allocation policy for maximizing the capacity is similar to the waterfilling with a nonconstant water level which depends on the CSI of the interference channel (the link from SU transmitter (SU-TX) to PU receiver (PU-RX)). In [45], the authors extended the work in [7] to asymmetric fading environments. It was shown in [123] that an AIP constraint is more favorable than a peak constraint especially in fading channels, since the AIP constraint is more flexible and can achieve a larger SU capacity with less PU capacity loss than that achieved by PIP. In [66], the authors studied optimum power allocation for three different capacity notions under both AIP and PIP constraints. In [117], the authors also considered the transmit power constraints at the SU-TX, and investigated the opti-

mal power allocation strategies for maximizing secondary ergodic capacity or minimizing outage probability under various combinations of secondary transmit peak/average power constraints and interference peak/average power constraints. For CR networks with multiple SUs and PUs (i.e, cognitive multiple-access channels networks and cognitive broadcast channels networks), the sum rate maximization problem for SUs under various combinations of transmit power constraints and interference power constraints was addressed in [90]. In non-cognitive MAC networks, TDMA is optimal for achieving the ergodic sum rate, while [90] showed TDMA was not always the optimum for CR MAC case and investigated the conditions for the optimality of TDMA. In [28], the authors addressed a joint subcarrier and power allocation algorithm for multiuser OFDM cognitive radio systems, where the peak power constraint is used to protect the primary user.

It can be easily observed that the knowledge of the channel information of CR network is essential to the power control optimization design. Most of above results assume the availability of full CSI knowledge at SU-TX. However, since the primary and secondary networks are usually independent and not cooperative with each other. It is difficult for PUs to feed back the required interference channel CSI to the SUs. As a result, imperfect CSI should be taken into account for the design of practical CR systems. This motivates a new and challenging research direction on cognitive networks with limited feedback, which is the focus of this thesis.

1.4 Outline and Contributions of Thesis

The focus of this thesis is on the design and the performance analysis of optimal resource allocation algorithms for wireless communication networks with imperfect CSI knowledge available at the transmitter obtained via the limited feedback technique. The main contributions of this thesis are contained in Chapters 2 to 5. Chapter 2 deals with the resource allocation problem with limited feedback for a single user wireless communication system using parallel fading channels, while Chapter 3, Chapter 4 and Chapter 5 study the various resource optimization schemes related to cognitive radio networks

(within the spectrum sharing paradigm) with limited feedback. A brief description of the major contributions of each of these chapters is given below.

In Chapter 2, we address an optimal power allocation problem for minimizing the notion of information theoretic outage for an M parallel block-Nakagami-fading channels under a sum (across all channels) long-term average transmit power constraint with finite rate feedback. First, a simulation-based optimization technique called simultaneous perturbation stochastic approximation algorithm (SPSA) is employed to numerically derive a locally optimal power codebook. SPSA is an algorithmic method generally used in nonlinear optimizing system with many variables where the objective function gradient is difficult or impossible to obtain. It is a type of stochastic approximation algorithm. Due to the high computational complexity and long convergence time of SPSA, we make an ordering assumption on the power codebook entries and derive effective hyperplane based approximations to the channel quantization regions in order to design a number of low-complexity suboptimal quantized power codebook design algorithms. Unlike previous work on outage minimization for MIMO channels, we do not assume that the same transmit power is used per channel or use the Gaussian approximation in general. Based on our power ordering assumption and hyperplane based approximations, we show that it is not generally optimal to allocate identical power to all channels, and that this is only asymptotically optimal at high average power (or SNR) for the Rayleigh fading case, whereas for the general Nakagami case, the transmit power allocation for an individual channel within each quantized region is asymptotically proportional to the corresponding Nakagami fading parameter (severity of fading); and the Gaussian approximation is seen to perform inefficiently for small number of parallel channels compared to our low-complexity algorithms. We also present a novel diversity order result for the outage probability for the Nakagami fading case. Finally, we derive a suitable Gaussian approximation based low-complexity power allocation scheme for large number of parallel channels, which has important practical applications in multi-carrier systems such as OFDM. Extensive numerical results illustrate that only a few bits of feedback (for $M = 4$ or $M = 6$) closes the gap substantially in outage performance with the full instantaneous channel information at the transmitter. For large number of channels, less than 1 bit of

(broadcast) feedback per channel can achieve the same outage probability (10^{-2}) with approximately only a 2.8 dB average power or SNR gap where all channels undergo severe Nakagami fading with the same fading parameter $m = 0.5$.

In Chapter 3, we consider a wideband spectrum sharing cognitive radio network where a secondary user can share a number of orthogonal frequency bands each licensed to a distinct primary user. We study the problem of optimum secondary transmit power allocation for its ergodic capacity maximization subject to a long term average sum (across the bands) transmit power constraint on the secondary user and individual average interference power constraint on each primary user, with quantized CSI(for the vector channel space consisting of all secondary-to-secondary and secondary-to-primary channels) at the secondary transmitter. A modified Generalized Lloyds-type algorithm (GLA) is designed for deriving the optimal power codebook, which is proved to be globally convergent and empirically consistent. We also provide a number of useful and interesting properties of the quantized powers. Based on these properties, an approximate quantized power allocation (AQPA) algorithm is designed, which performs very close to its modified GLA based counterpart for large number of feedback bits and is significantly faster, making it an attractive choice for practical implementation. And it is also seen to have a far superior performance compared to other suboptimal algorithms. After that, we also present an extension of the modified GLA based quantized power codebook design algorithm for the noisy limited feedback case. We believe our work in this chapter is the first to provide a systematic quantized power allocation algorithm with limited feedback for the spectrum sharing scenario in cognitive radio.

In Chapter 4, a spectrum sharing scenario in a cognitive radio network where a secondary user (SU) shares a narrowband with N primary users (PUs) is considered. We investigate the SU ergodic capacity maximization problem under an average transmit power constraint on the SU and N individual peak interference power constraints at each PU receiver with various forms of imperfect CSI knowledge available at the SU transmitter. For easy exposition, we first look at the case when the SU transmitter can obtain perfect knowledge of the CSI from the SU-TX to SU receiver (SU-RX) link, denoted as g_1, but only can access partial CSI knowledge from the SU-TX to each PU-RX link,

denoted as $g_{0i}, i = 1, \ldots, N$. Then a quantized power allocation scheme (codebook) is obtained with quantized $g_{0i}, i = 1, \ldots, N$ information, by using the Karush-Kuhn-Tucker (KKT) necessary optimality conditions to numerically solve the SU maximization problem. We also analyze the asymptotic SU ergodic capacity performance for the case when there is a large number of PUs ($N \to \infty$) operating. For the interference-limited regime, where the average transmit power constraint is inactive, an alternative scheme, termed as the quantized rate allocation strategy based on quantized ratio $\frac{g_1}{\max_i g_{0i}}$ information is proposed. Subsequently, we relax the strong assumption of full CSI knowledge of g_1 at the SU-TX to imperfect g_1 knowledge available at the SU-TX as well. Depending on the way the SU-TX obtains the g_1 information, two different quantized power codebooks: one with estimated g_1 and quantized $g_{0i}, i = 1, \ldots, N$ knowledge and another with both quantized g_1 and $g_{0i}, i = 1, \ldots, N$ information, are derived for the SU ergodic capacity maximization problem. Efficacy of these proposed algorithms are illustrated via numerical simulation results.

In Chapter 5, we study an optimal transmit power allocation problem that minimizes the outage probability of a SU who is allowed to coexist with a PU in a narrowband spectrum sharing cognitive radio network, under a long term average transmit power constraint at the SU-TX and an average interference power constraint on the PU-RX, with quantized CSI (including both the channel from SU-TX to SU-RX, denoted as g_1 and the channel from SU-TX to PU-RX, denoted as g_0) at the SU-TX. The optimal quantization regions in the vector channels space is proven to have a 'stepwise' structure. With this structure, the above outage minimization problem can be explicitly formulated and solved by employing the KKT necessary conditions to obtain a locally optimal quantized power codebook. A low-complexity near-optimal quantized power allocation algorithm is derived for the case of large number of feedback bits. More interestingly, we show that as the number of partition regions tends to infinity, when the average interference power constraint is active, the length of interval between any two adjacent quantization thresholds on g_0 axis is asymptotically equal; while when the average interference power constraint is inactive, the ratio between any two adjacent quantization thresholds on g_1 axis is asymptotically identical. Lastly, an explicit expression for the asymptotic SU out-

age probability at high rate quantization (as the number of feedback bits goes to infinity) is also provided, and is shown to approximate the optimal outage behavior extremely well for large number bits of feedback via numerical simulations.

1.5 List of Publications

Journal Papers

1. Y. Y. He and S. Dey. "Power Allocation in Spectrum Sharing Cognitive Radio Networks with Quantized Channel Information". *IEEE Trans. Commun.*, vol. 59, no. 6, pages 1644 - 1656, Jun. 2011.
2. Y. Y. He and S. Dey. "Throughput maximization in cognitive radio with limited feedback under peak interference constraints". *IEEE Transactions on Vehicular Technology*, submitted for publication.
3. Y. Y. He and S. Dey. "Outage Minimization for Parallel Fading Channels with Limited Feedback". *EURAPSIP Journal of Wireless Communications & Networking*, submitted for publication.
4. Y. Y. He and S. Dey. "Power Allocation in Outage Minimization of cognitive radio networks with limited feedback". *IEEE Transactions on Communications*, submitted for publication.

Conference Papers

1. Y. Y. He and S. Dey. "Throughput maximization in cognitive radio with limited feedback in the interference-limited regime" In *Proc. 11th European wireless conference (EW 2011)* , pages 1-8, Vienna, Austria, April 2011.
2. Y. Y. He, S. Dey and V. Raghavan. "Spectrum sharing in cognitive radio with quantized channel information." In *Proc. MILCOM 2010* , pages 1672-1677, San Jose, CA, USA, Oct. 2010.
3. Y. Y. He and S. Dey. "Efficient algorithms for outage minimization in parallel fading channels with limited feedback." In *Proc. 47th Annual Allerton Conference on Communication, Control, and Computing (Allerton 2009)*, pages 762-770, Monticello,

IL, USA, Sep. 2009.

4. B. S. Krongold and Y. Y. He. "Multiuser Efficient Ergodic Loading for OFDMA Systems." In *Proc. IEEE 70th Vehicular Technology Conference (VTC2009-Fall)*, pages 1-5, Anchorage, Alaska, USA, Sep. 2009.
5. B. S. Krongold and Y. Y. He. "Efficient Ergodic Discrete Loading for OFDM Systems." In *Proc. IEEE Global Telecommunications Conference (GLOBECOM'08)*, pages 1-5, New Orleans, LA, USA, Nov. 2008.

Chapter 2

Outage Minimization for Parallel Fading Channels with Limited Feedback

2.1 Introduction

Determining the information theoretic capacity of block-fading wireless channels has been an important area of research over the past decade. Various notions of capacity for single-user fading channels include *ergodic capacity* [10], *delay-limited capacity* [99] and *capacity versus outage probability* [40]. For delay-sensitive traffic such as voice and video, the latter two notions are rather important. In particular, the notion of outage probability signifies the probability that the capacity of a wireless channel falls below a required rate threshold. In [40], optimal power allocation for outage minimization in the case of parallel fading channels (single user) was obtained with the assumption of full channel state information (CSI) at the transmitter. However, full CSI at the transmitter is hard to obtain in practice due to limited bandwidth in the feedback channel from the receiver to the transmitter, and it is more common to have full CSI at the receiver. This has motivated researchers over the last decade to analyze performances of wireless systems with various forms of partial CSI at the transmitter (CSIT), such as noisy CSIT, statistical CSIT and quantized CSIT. In particular, the idea of Grassmannian line packing was used to design optimal beamforming codebooks for MIMO systems in [31], whereas in a related work [61], the authors derived a lower bound on the outage performance of multiple-antenna systems using beamforming based on quantized CSIT. More recently, in [107],

maximization of expected rate over a single-input single-output slowly fading channel is investigated using optimized discrete rate and power control with quantized CSIT. The same authors have also investigated the diversity-multiplexing tradeoff in MIMO channels with quantized CSIT in [106] (see also [105]). A number of recent papers have investigated outage minimization for fading channels with limited feedback for MIMO or multi-antenna systems. Such works include [12, 14, 71, 78, 105]. In particular, the authors of [71] looks at outage minimization with a finite-rate power codebook for MIMO systems. The key finding of [71] (see also [106]) is that the optimal power codebook has a circular structure in that the same transmit power is allocated to the outage region and the best channel region. In order to design the optimal power codebook, it assumes however that the same transmit power (as a function of the entire channel matrix) is used in all transmit antennas. This allows the authors of [71] to reduce the finite-rate power codebook design problem to an equivalent scalar quantization problem. Even then, finding the cumulative density function for the equivalent scalar random variable requires computing multi-dimensional probability integrals which is computationally complex. Furthermore, the optimal power codebook entries are found via generic gradient search techniques which can take unreasonably long time to converge. Using a similar setting, the same authors have investigated the outage diversity behaviour for multiple-antenna systems with quantized CSIT in [14] (see also [12]). In [78], the problem of outage minimization using quantized CSIT is investigated for the fading relay channel. In [105], a Gaussian approximation is used to capture the probability distribution of the mutual information for a MIMO system in order to study the outage behaviour. Finally, many of the above results only apply to Rayleigh fading channels (where the MIMO channel matrix is assumed to have complex circularly symmetric Gaussian distributed entries). Note however that the circular nature of the optimal power codebook and some of the useful approximations developed in [12] for asymptotically large number of channel feedback bits are also relevant for our work and we duly acknowledge this fact. Our focus is however on designing practical low-complexity but sub-optimal algorithms for designing the quantized power codebook and derive theoretical properties of these power allocation schemes in order to justify the various approximations used in designing the sub-optimal

schemes.

In this chapter, we look at an M-parallel fading channels system (thus consider a simpler setting than the MIMO setup) where we aim to minimize the outage probability under a sum (across all channels) long term average power constraint with quantized CSIT. We formulate the above problem and provide an iterative algorithm : simultaneous perturbation stochastic approximation algorithm to numerically solve for the optimal power allocation. Based on a power ordering assumption and a hyperplane based approximation to the basic rate achieving mutual information curve in the vector channel space, we derive a number of low-complexity suboptimal finite-rate power codebook design algorithms for outage minimization without having to assume the same transmit power per channel or use the Gaussian approximation in general. We derive these results for a more general Nakagami-m fading model, albeit with the assumption of independence between any two parallel channels. Since the optimal power allocation results for parallel fading channels with full CSIT are known [40], we are able to provide a fair comparison of our power allocation algorithms with the full CSIT based performance. Technologically, M-parallel fading channels are useful models for various multi-carrier transmission systems such as OFDM, MC-CDMA etc. We present a number of important and novel findings in this chapter. We show that in the high average power (or SNR) it is asymptotically optimal to allocate transmit power proportional to the Nakagami m fading parameter for the individual channels within each quantized region. In the Rayleigh fading case, this corresponds to allocating the same power across all channels within each quantized region (but only in the high average power regime). We also derive a novel diversity order result for the outage probability in the Nakagami fading case. Finally, motivated by technological applications such as in OFDM systems, we investigate the suitability of a Gaussian approximation scheme for the case of a large number of parallel channels. The Gaussian approximation is seen to perform poorly for small number of parallel channels compared to our low-complexity algorithms based on a simple approximation to the quantized regions under power ordering assumption. However, the derived Gaussian approximation based optimal power allocation schemes perform efficiently for large number of channels (e.g. $M \geq 16$), thus having important practical applications to multi-

carrier systems such as OFDM. Extensive numerical results are presented which illustrate that only 4 bits of feedback close the gap with the outage performance of the full CSI algorithm substantially for $M = 4$ or $M = 6$. For a large number of channels ($M = 16$), our Gaussian approximation based algorithm performs approximately within 2.8 dB (SNR gap) of the full CSI based algorithm at an outage probability of 10^{-2} with less than 1 bit of (broadcast) feedback per channel when all channels undergo severe Nakagami fading with identical fading parameter $m = 0.5$.

The organization of the chapter is as follows. Section 2.2 presents the fading channel model and the typical outage problem based on full CSIT. Section 2.3 presents the outage minimization problem with quantized CSIT followed by the modified problem formulation using the power ordering and hyperplane based approximation. Various suboptimal algorithms are then presented for finding the power codebook in high average power regime along with their associated theoretical properties. A new result on the diversity order for the outage probability is presented for the Nakagami fading case using our power allocation algorithm based on the power ordering and hyperplane based approximation. Section 2.4 presents a Gaussian approximation based sub-optimal algorithm applicable to the case of a large number of parallel channels. Section 2.5 presents an extensive set of numerical results illustrating the efficiency of our algorithms measured by closeness of their outage performance as compared to the full CSIT based solution. Finally, Section 2.6 presents some concluding remarks and ideas for future extensions of this work. All proofs are relegated to the appendix section 2.7 in this chapter.

2.2 Channel Model and Outage Minimization

We consider an M-parallel flat-fading channel model similar to that in [53], where a transmitted codeword spans M subchannels in one fading block. For each subchannel $i, i \in \{1, 2, ..., M\}$, the received signal can be written as:

$$y_i = \sqrt{h_i} x_i + w_i \tag{2.1}$$

where h_i denotes the channel power gain and x_i is the channel input symbol. The noise sequences $w_1, \ldots, w_M$ are independent and identically distributed (i.i.d) Gaussian random variables with zero mean and unit variance. It is assumed that the components of channel state vector $\mathbf{h} = (h_1, \ldots, h_M)$ are mutually independent, individually i.i.d. across fading blocks and ergodic and fading is sufficiently slow so that the input symbols transmitted over the same fading block experience the same channel state. It is also assumed that the fading block length $N \to \infty$ so that information theoretic results can be applied. The individual fading distributions may not be identical. However, they (and hence the joint channel fading distribution) are assumed to be continuous.

Given a channel realization $\mathbf{h}$, and assuming the availability of full channel state information (CSI) at the transmitter and receiver, denote the corresponding power allocation to the M subchannels by the vector $\mathbf{p}(\mathbf{h}) = (p_1(\mathbf{h}), \ldots, p_M(\mathbf{h}))$. Then the maximum mutual information of an M-parallel Gaussian channel is given by [53]

$$r(\mathbf{h}, \mathbf{p}(\mathbf{h})) = \frac{1}{M} \sum_{i=1}^{M} \frac{1}{2} \log(1 + h_i p_i(\mathbf{h})) \tag{2.2}$$

where, the rate unit is nats per channel use.

Thus, the outage probability, defined as the probability that the instantaneous mutual information of the channel is less than a pre-specified transmission rate r_0 (nats/channel use), can be expressed as

$$P_{out}(\mathbf{h}, \mathbf{p}(\mathbf{h}), r_0) = Prob\left[r(\mathbf{h}, \mathbf{p}(\mathbf{h})) < r_0\right] \tag{2.3}$$

Under a long term average power constraint defined by $E[\langle \mathbf{p}(\mathbf{h}) \rangle] \leq P_{av}$, (where $\langle x \rangle$ denotes the arithmetic mean of the vector x with length M, namely, $\langle x \rangle = \frac{1}{M} \sum_{i=1}^{M} x$), the outage minimization problem can be described as

$$\begin{aligned} &\min_{\mathbf{p}(\mathbf{h}) \geq 0} \; Prob\left[\frac{1}{M} \sum_{i=1}^{M} \frac{1}{2} \log(1 + h_i p_i(\mathbf{h})) < r_0\right] \\ &s.t. \;\; E[\langle \mathbf{p}(\mathbf{h}) \rangle] \leq P_{av} \end{aligned} \tag{2.4}$$

The optimal power allocation with full CSI at the transmitter for this problem can be found explicitly by using convex optimization techniques and was presented in Proposition 4 of [40]. The readers are referred to [40] for further details. Note that here P_{av} can be thought of effectively as the transmitter side signal-to-noise ratio (since noise variance has been normalized to unity). In the following we will address the optimal power allocation problem for outage minimization where only partial or limited CSI is available at the transmitter. For the purpose of analysis, we will assume that each channel h_i is gamma distributed (Nakagami fading) with mean $\frac{1}{\lambda_i}$, which probability density function (pdf) is given by

$$f(h_i) = (m_i\lambda_i)^{m_i}\frac{h_i^{m_i-1}}{\Gamma(m_i)}e^{-m_i\lambda_i h_i}, \quad h_i > 0 \tag{2.5}$$

where $\Gamma(.)$ is gamma function ($\Gamma(s) = \int_0^\infty t^{s-1}e^{-t}dt$) and constant $m_i \geq 0.5$. m_i is called the fading parameter. Larger values of the fading parameter m_i imply less severe fading environments. When $m_i = 1$, the above distribution boils down to an exponential distribution (corresponding to Rayleigh fading) and the nonfading case corresponds to $m_i = \infty$.

2.3 Optimum Quantized Power Control with Finite-rate Feedback

It is well known that having perfect CSI at both transmitter and receiver is hard to satisfy in a practical system due to bandwidth constraints on the receiver to transmitter feedback link as well as considerable communication cost overhead. In this section, we consider designing a power allocation procedure for M-parallel flat-fading channels based on quantized vector CSI $\mathbf{h} = (h_1, \ldots, h_M)$ (in M dimensions) acquired via a no-delay and error-free feedback link with limited rate from the receiver to the transmitter.

2.3.1 Optimal power allocation with limited feedback strategy

We assume that the receiver can perfectly estimate the full CSI information. Given B bits of feedback, a power codebook $\mathcal{P} = \{\mathbf{P}_1, \ldots, \mathbf{P}_L\}$, where $\mathbf{P}_j = \{p_{1j}, \ldots, p_{Mj}\}, j = 1, \ldots, L$

(note that power levels for different channels here are distinct as opposed to [71, 105] where the same transmit power was allocated to all transmit antennas in the MIMO setting), of cardinality $L = 2^B$, is designed off-line purely on the basis of the statistics of $\mathbf{h}$. This codebook is known *a priori* by both the transmitter and the receiver. Given a channel realization $\mathbf{h}$,

• First, the receiver applies a deterministic mapping denoted as I from current instantaneous $\mathbf{h}$ information into one of L integer indices [105], where the mapping I partitions the entire M-dimensional space of $\mathbf{h}$ into L regions $\mathcal{R}_1, \mathcal{R}_2, \ldots, \mathcal{R}_L$, given as $I(\mathbf{h}) = j$, if $\mathbf{h} \in \mathcal{R}_j$, $j = 1, \ldots, L$.

• Second, the receiver sends the corresponding index $j = I(\mathbf{h})$ to the transmitter via the feedback link.

• Then, the j^{th} entry of the power codebook $\mathcal{P}$, i.e. $\mathbf{P}_j$, will be employed by the transmitter for transmission.

Therefore the key steps involved in the limited feedback design problem constitute obtaining (off-line) the jointly optimal CSI partitions and power codebook design. Our objective is to design efficient algorithms for solving this joint optimization problem of the channel partition regions and the power codebook, so as to minimize the outage probability while satisfying a long term average power constraint.

Let $Pr(\mathcal{R}_j)$, $E[\bullet|\mathcal{R}_j]$ denote $Pr(\mathbf{h} \in \mathcal{R}_j)$ (the probability that $\mathbf{h}$ falls in the region $\mathcal{R}_j$) and $E[\bullet|\mathbf{h} \in \mathcal{R}_j]$, respectively. Define the indicator function x_j, $j = 1, \ldots, L$ as

$$x_j = \begin{cases} 1, & if \ \ \frac{1}{M}\sum_{i=1}^{M} \frac{1}{2}\log(1 + h_i p_{ij}) < r_0, \\ 0, & \text{otherwise.} \end{cases} \tag{2.6}$$

Then outage minimization problem (2.4) with limited feedback can be formulated as

$$\begin{aligned} &\min_{\mathbf{P}_j \geq 0,\ \mathcal{R}_j,\ \forall j} \ \sum_{j=1}^{L} E[x_j|\mathcal{R}_j]Pr(\mathcal{R}_j) \\ &s.t. \ \sum_{j=1}^{L} E[\mathbf{P}_j{}^{\Sigma}|\mathcal{R}_j]Pr(\mathcal{R}_j) \leq P_{av} \end{aligned} \tag{2.7}$$

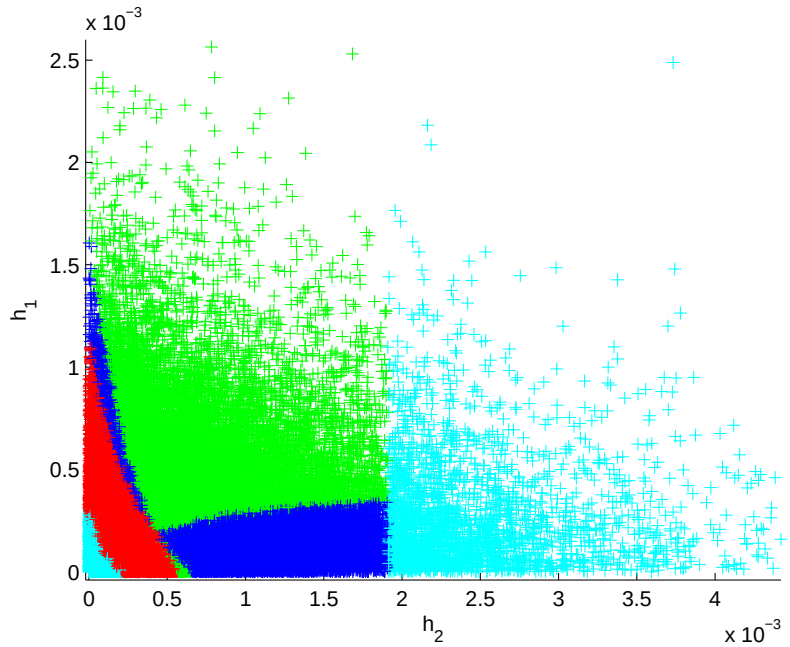

Figure 2.1: Structure of the optimal vector quantization regions for 2 channels with $B = \log_2 4$ bits of feedback.

where $\mathbf{P}_j{}^{\Sigma} = \frac{1}{M}\sum_{i=1}^{M} p_{ij}$, i.e, the average sum of all the elements in vector $\mathbf{P}_j$. It can be easily verified that the above optimization problem satisfies the long term average power constraint with equality.

The dual problem of (2.7) is expressed as

$$\min_{\lambda>0} \; g(\lambda) - \lambda P_{av}, \tag{2.8}$$

where λ is nonnegative Lagrange multiplier associated with the long term average power constraint in Problem (2.7), and the Lagrange dual function $g(\lambda)$ is defined as

$$g(\lambda) = \min_{\mathbf{P}_j \geq 0,\, \mathcal{R}_j,\, \forall j} \; \sum_{j=1}^{L} E[x_j + \lambda \mathbf{P}_j{}^{\Sigma} | \mathcal{R}_j] Pr(\mathcal{R}_j) \tag{2.9}$$

With a fixed λ, we can employ an iterative simulation-based optimization algorithm called the simultaneous perturbation stochastic approximation algorithm (SPSA) to find the optimal power codebook of problem (2.9). A step-by-step guide to implementation of SPSA can be found in [100], which, when applied to our problem, can be summarized

by the following steps.

Step 1 *Initialization and Coefficient Selection:* Set counter index $k = 0$. Pick initial guess of the power codebook $\hat{\mathcal{P}}_0$ and non-negative coefficients a, c, A, α and γ in the SPSA gain sequences $a_k = \frac{a}{(A+k+1)^\alpha}$ and $c_k = \frac{c}{(k+1)^\gamma}$. For guideline on choosing these coefficients see [100].

Step 2 *Generation of Simultaneous Perturbation Vector:* Generate a p-dimensional ($p = ML$) random perturbation vector Δ_k, where each component of Δ_k are i.i.d Bernoulli ± 1 distributed with probability of $\frac{1}{2}$ for each outcome.

Step 3 *Loss Function Evaluations:* Obtain two measurements of the loss function $\mathcal{L}(\cdot)$ based on the simultaneous perturbation around the current power codebook $\hat{\mathcal{P}}_k$: $\mathcal{L}(\hat{\mathcal{P}}_k + c_k\Delta_k)$ and $\mathcal{L}(\hat{\mathcal{P}}_k - c_k\Delta_k)$ with c_k and Δ_k from Steps 1 and 2.

Step 4 *Gradient Approximation:* Generate the simultaneous perturbation approximation to the unknown gradient $\hat{g}_k(\hat{\mathcal{P}}_k)$ given as,

$$\hat{g}_k(\hat{\mathcal{P}}_k) = \frac{\mathcal{L}(\hat{\mathcal{P}}_k + c_k\Delta_k) - \mathcal{L}(\hat{\mathcal{P}}_k - c_k\Delta_k)}{2c_k} \begin{bmatrix} \Delta_{k1}^{-1} \\ \Delta_{k2}^{-1} \\ \vdots \\ \Delta_{kp}^{-1} \end{bmatrix}$$

where Δ_{ki} is the ith component of the Δ_k vector.

Step 5 *Updating power codebook:* Use the algorithm

$$\hat{\mathcal{P}}_{k+1} = \hat{\mathcal{P}}_k - a_k\hat{g}_k(\hat{\mathcal{P}}_k)$$

to update $\hat{\mathcal{P}}_k$ to a new value $\hat{\mathcal{P}}_{k+1}$.

Step 6 *Iteration or Termination:* Return to Step 2 with $k + 1$ replacing k. Terminate the algorithm if there is little change in several successive iterations or the maximum allowable number of iterations has been reached.

Note that in the Step 3 of the SPSA which involves calculating a loss function with a given power codebook, we use the objective function of problem (2.9) as the loss function. And then given a power codebook, we use the nearest neighbor condition of a generalized

Lloyd algorithm with a Lagrangian distortion $d(\mathbf{h}, \mathbf{P}_j) = x_j + \lambda \mathbf{P}_j{}^{\Sigma}$ to generate the optimal partition regions [83], given as, $j = 1, \ldots, L$,

$$\mathcal{R}_j = \{\mathbf{h} | x_j + \lambda \mathbf{P}_j{}^{\Sigma} \leq x_i + \lambda \mathbf{P}_i{}^{\Sigma}, \forall i \neq j\}. \tag{2.10}$$

Therefore, with a given power codebook and resulting quantization regions, we can numerically calculate the loss function. We repeatedly apply Step 2 to Step 5 of SPSA until the resulting outage probability converges within a pre-specified accuracy (Step 6 of SPSA). After that, we solve the dual problem for finding the optimal λ by using a subgradient based search method, i.e, updating λ until convergence using $\lambda^{l+1} = [\lambda^l - \alpha^l (P_{av} - \sum_{j=1}^{L} E[\mathbf{P}_j{}^{\Sigma} | \mathcal{R}_j] Pr(\mathcal{R}_j))]^+$, where l is the iteration number, and α^l is a positive scalar step sizes for the l-th iteration satisfying $\sum_l \alpha^l = \infty$ and $\sum_l {\alpha^l}^2 < \infty$. Due to the fact that problem (2.7) is not convex, in general, the optimal solution we obtain here is only locally optimal.

Fig. 2.1 gives an example about what optimal quantization structure looks like by using SPSA for the $M = 2$ channels case. From Fig. 2.1, we can see that, in general, it is difficult to compute the surface area (or in general volumes in higher dimensional space) of these regions which have irregular shapes. Although we can use SPSA to numerically obtain a locally optimal power codebook and partition regions, it takes a very long time to converge and is computationally highly complex especially when the number of feedback bits or the number of channels is large. In the next few sections, we therefore focus on designing sub-optimal algorithms by introducing appropriate assumptions and approximations to the quantized regions and power codebook.

2.3.2 Power ordering assumption and hyper plane approximation (POHPA)

Let $\mathbf{P}(\mathbf{h})$ represent the optimal power allocation strategy which maps the channel realization $\mathbf{h}$ to a power level in $\mathcal{P}$. Without loss of generality, we assume that power levels are such that $\mathbf{P}_1{}^{\Sigma} > \cdots > \mathbf{P}_L{}^{\Sigma}$ corresponding to the partition $\mathcal{R}_1, \mathcal{R}_2, \ldots, \mathcal{R}_L$, then we have

Lemma 2.1. *Let $\boldsymbol{P}^*(\boldsymbol{h})$ denote as the minimum power level required to have no outage, i.e,*

$\frac{1}{M}\sum_{i=1}^{M}\frac{1}{2}\log(1+h_i p_i^*(\boldsymbol{h}))=r_0$. *The optimal solution satisfies :*

$$\begin{aligned}&\boldsymbol{P}(\boldsymbol{h})=\boldsymbol{P}_j,\ \ \textit{if}\ \ \boldsymbol{P}_{j+1}^{\Sigma}<(\boldsymbol{P}^*(\boldsymbol{h}))^{\Sigma}\le\boldsymbol{P}_j^{\Sigma},\quad j=1,\ldots,L-1;\\&\boldsymbol{P}(\boldsymbol{h})=\boldsymbol{P}_L,\ \ \textit{if}\ \ (\boldsymbol{P}^*(\boldsymbol{h}))^{\Sigma}\le\boldsymbol{P}_L^{\Sigma}\ \ \textit{or}\ \ (\boldsymbol{P}^*(\boldsymbol{h}))^{\Sigma}>\boldsymbol{P}_1^{\Sigma}.\end{aligned}\tag{2.11}$$

Proof: The proof is similar to [105],[71], and can be found in the appendix of this chapter.

If the same transmit power is allocated to all transmit channels, i.e, $p_{1j}=\cdots=p_{Mj}=\mathbf{P}_j^{\Sigma}$, the above Lemma result reduces to the case of [105],[71]. From Lemma 2.1, we also have that there is no outage in the first $L-1$ regions and outage only occurs in the last region $\mathcal{R}_L$; the optimal partition satisfies that a channel realization $\mathbf{h}=\{h_1,\ldots,h_M\}$ either belongs to the region $\mathcal{R}_j$ where $j\in\{1,\ldots,L\}$ is the maximum index that can guarantee zero outage for it or belongs to $\mathcal{R}_L$; $\mathcal{R}_L$ includes two parts : $\{\mathbf{h}|(\mathbf{P}^*(\mathbf{h}))^{\Sigma}>\mathbf{P}_1^{\Sigma}\}$ (outage) and $\{\mathbf{h}|(\mathbf{P}^*(\mathbf{h}))^{\Sigma}\le\mathbf{P}_L^{\Sigma}\}$, denoted as $\mathcal{R}_{L,1}$ and $\mathcal{R}_{L,2}$ respectively.

From Lemma 2.1, we have the boundary between $\mathcal{R}_{j-1}$ and $\mathcal{R}_j$, $j=2,\ldots,L-1$ is a hypersurface denoted as $g(h_1,\ldots,h_{M-1},\mathbf{P}_j)$, which is obtained by solving for h_M from equation $r(\mathbf{h},\mathbf{P}_j)=\frac{1}{M}\sum_{i=1}^{M}\frac{1}{2}\log(1+h_i p_{ij})=r_0$, namely,

$$g(h_1,\ldots,h_{M-1},\mathbf{P}_j)=\frac{k-\prod_{i=1}^{M-1}(1+h_i p_{ij})+1}{p_{Mj}\prod_{i=1}^{M-1}(1+h_i p_{ij})}\tag{2.12}$$

where $k=e^{2Mr_0}-1$. The boundaries between $\mathcal{R}_L$ and $\mathcal{R}_1$, $\mathcal{R}_{L-1}$ is given by $g(h_1,\ldots,h_{M-1},\mathbf{P}_1)$, $g(h_1,\ldots,h_{M-1},\mathbf{P}_L)$ respectively. Let $\{r_{i1},\ldots,r_{iL}\}$ represent the quantization thresholds on h_i axes ($i=1,\ldots,M$), from (2.12), it can be easily verified that $r_{ij}=\frac{k}{p_{ij}}$, $i\in\{1,2,\ldots,M\}$, $j\in\{1,2,\ldots,L\}$. Therefore if we assume that the power levels in power codebook are in descending order, i.e, $\mathbf{P}_1>\cdots>\mathbf{P}_L$ which means $p_{i1}>\cdots>p_{iL}$, $i=1,\ldots,M$ and also implies $\mathbf{P}_1^{\Sigma}>\cdots>\mathbf{P}_L^{\Sigma}$, we can obtain $r_{i1}<\cdots<r_{iL}$, $i=1,\ldots,M$, which gives a simple partition structure allowing easy numerical computation of the surface area (or volumes in higher dimensions) of the quantized regions. We call it the power ordering (PO) assumption. Fig. 2.2 gives an example of the optimal quantization struc-

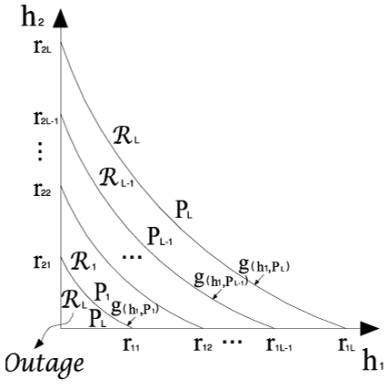

Figure 2.2: Structure of the quantization regions for 2 channels with $B = \log_2 L$ feedback bits under PO assumption.

ture with the PO assumption for the $M = 2$ channels case. With this PO assumption, the area below the hypersurface $g(h_1, \ldots, h_{M-1}, \mathbf{P}_1)$ defines the outage region $\mathcal{R}_{L,1}$.

Denoting $F(\mathbf{P}_j)$ as the probability that the channel state information $(h_1, \ldots, h_M)$ lies below $g(h_1, \ldots, h_{M-1}, \mathbf{P}_j)$, $j = 1, \ldots, L$, we have

$$F(\mathbf{P}_j) = \int \ldots \int_{\mathcal{R}_{L,1} \cup \mathcal{R}_1 \cup \ldots \cup \mathcal{R}_{j-1}} f(h_1, \ldots, h_M) dh_1 \ldots dh_M \tag{2.13}$$

where $f(h_1, \ldots, h_M)$ is the pdf for the channels vector $\{h_1, \ldots, h_M\}$, given by $f(h_1, \ldots, h_M) = \prod_{i=1}^{M} (m_i \lambda_i)^{m_i} \frac{h_i^{m_i - 1}}{\Gamma(m_i)} e^{-m_i \lambda_i h_i}$ for Nakagami fading (due to independence amongst the parallel channels). Thus, the probability that the channel realization $\mathbf{h} \in \mathcal{R}_j$ is $F(\mathbf{P}_{j+1}) - F(\mathbf{P}_j)$ for $j = 1, \ldots, L-1$, and $1 - F(\mathbf{P}_L) + F(\mathbf{P}_1)$ for $j = L$. The outage minimization problem with limited feedback (2.7) can thus be simplified as

$$\begin{aligned} \min_{\{\mathbf{P}_1 > \ldots > \mathbf{P}_{L-1} > \mathbf{P}_L \geq 0\}} \quad & P_{out} = F(\mathbf{P}_1) \\ s.t. \quad & \sum_{j=1}^{L-1} (p_{1j} + \ldots + p_{Mj})(F(\mathbf{P}_{j+1}) - F(\mathbf{P}_j)) \\ & + (p_{1L} + \ldots + p_{ML})(1 - F(\mathbf{P}_L) + F(\mathbf{P}_1)) = MP_{av} \end{aligned} \tag{2.14}$$

The Problem (2.14) is in general a nonlinear non-convex optimization problem. Since $g(h_1, \ldots, h_{M-1}, \mathbf{P}_j)$, $j = 1, \ldots, L$ is highly nonlinear, it's hard to obtain a closed-form ex-

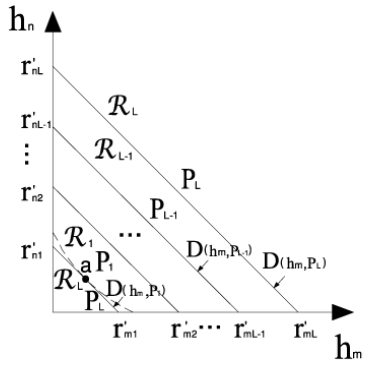

Figure 2.3: The projection of structure of quantization regions on h_n versus h_m coordinate plane with HPA (approximating $g(h_m, \mathbf{P}_j)$ by $D(h_m, \mathbf{P}_j)$).

pression for $F(\mathbf{P}_j)$. Although one can use numerical integrals to calculate $F(\mathbf{P}_j)$, and use randomized search techniques to find the optimum solution of problem (2.14), the associated computational complexity increases exponentially with the number of feedback bits and channels. Next, we will employ another approach by deriving an approximation for $g(h_1, \ldots, h_{M-1}, \mathbf{P}_j)$, such that an analytical (approximate) closed-form expression for $F(\mathbf{P}_j)$ can be easily obtained (unlike [105] where a Gaussian distribution was used to approximate the distribution of the mutual information to evaluate an analytical expression for $F(\mathbf{P}_j)$), thus significantly reducing the computational complexity of solving problem (2.14). Then based on the obtained optimal power allocation using this approximation, one can use Monte Carlo simulations to evaluate the "real outage" (corresponding outage probability performance given by $F(\mathbf{P}_1)$). More details on this can be found in the *Numerical Results* Section.

From (2.12), the intersection of hypersurface $h_M = g(h_1, \ldots, h_{M-1}, \mathbf{P}_j),\ j = 1, \ldots, L$ with any arbitrary two-channel coordinate plane, i.e, h_n versus h_m, $n, m \in \{1, 2, \ldots, M\}, n \neq m$, is a curve expressed as

$$h_n = g(h_m, \mathbf{P}_j) = \frac{k - h_m p_{mj}}{p_{nj}(1 + h_m p_{mj})}, \tag{2.15}$$

where $k = e^{2Mr_0} - 1$. It's easy to test that the above curve is convex. And the curve

intersects h_n axis and h_m axis at quantization thresholds r_{nj} and r_{mj} respectively. We can approximate the curve (2.15) by a straight line $r'_{nj}r'_{mj}$, as displayed in Fig.2.3, which is parallel to $r_{nj}r_{mj}$ and a tangent to the curve (2.15) at the intersection point 'a'. The straight line intersects h_n axis and h_m axis at point r'_{nj} and r'_{mj} respectively. The line $r'_{nj}r'_{mj}$ is expressed as

$$h_n = D(h_m, \mathbf{P}_j) = \frac{K - h_m p_{mj}}{p_{nj}} \quad h_m \in [0, \frac{K}{p_{mj}}] \tag{2.16}$$

where $K = 2(\sqrt{k+1} - 1)$, $r'_{nj} = \frac{K}{p_{nj}}$, $r'_{mj} = \frac{K}{p_{mj}}$ (new quantization thresholds), and point 'a' is $(\frac{K}{2p_{mj}}, \frac{K}{2p_{nj}})$. We name this approximation as hyperplane approximation (HPA)(we could also use the straight line $r_{nj}r_{mj}$ to do the approximation, but simulations demonstrate that the $r'_{nj}r'_{mj}$ approximation is always better than $r_{nj}r_{mj}$). To see clearly, Fig.2.4 gives an example of the HPA in three-dimensional (3D) space.

Thus, with PO and HPA (POHPA), the boundaries between $\mathcal{R}_{L,1}$ and $\mathcal{R}_1$, $\mathcal{R}_1$ and $\mathcal{R}_2$,

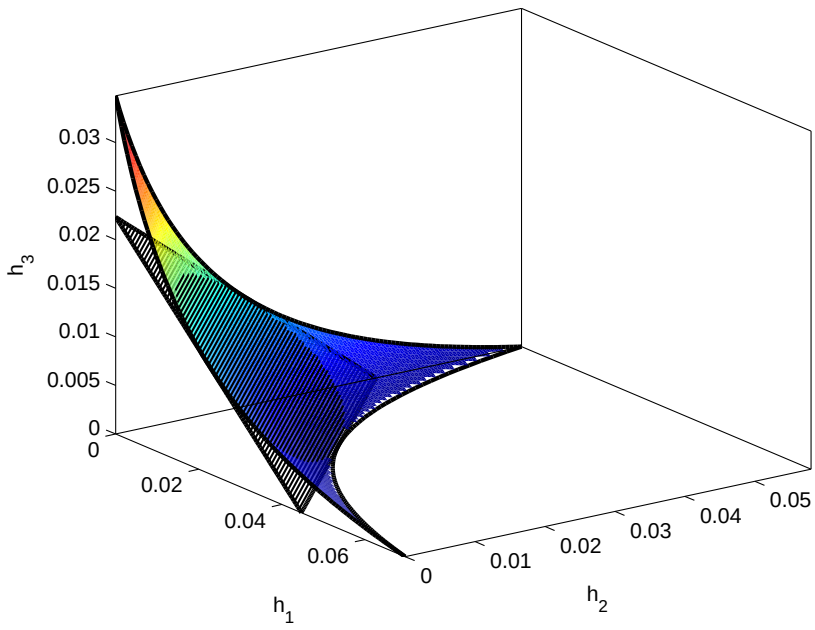

Figure 2.4: 3D of HPA.

..., $\mathcal{R}_{L-1}$ and $\mathcal{R}_{L,2}$ can be approximated as

$$D(h_1,\ldots,h_{M-1},\mathbf{P}_j)=\frac{K-\sum_{i=1}^{M-1}h_i p_{ij}}{p_{Mj}}, j=1,\ldots,L. \tag{2.17}$$

Any channel vector below $D(h_1,\ldots,h_{M-1},\mathbf{P}_1)$ is said to be in outage. Since $D(h_1,\ldots,h_{M-1},\mathbf{P}_j)$ is linear, an analytical closed-form approximation for $F(\mathbf{P}_j)$ can be obtained, which is denoted as $F'(\mathbf{P}_j)$. In this case, by definition we have

$$F'(\mathbf{P}_j)=Pr(D(h_1,\ldots,h_{M-1},\mathbf{P}_j)<\frac{K-\sum_{i=1}^{M-1}h_i p_{ij}}{p_{Mj}})=Pr(\sum_{i=1}^{M}h_i p_{ij}<K) \tag{2.18}$$

$\sum_{i=1}^{M}h_i p_{ij}$ is a weighted sum of independent gamma random variables, and $F'(\mathbf{P}_j)$ can be treated as the cumulative distribution function (cdf) of $\sum_{i=1}^{M}h_i p_{ij}$. Thus a closed-form expression for (2.18) can be obtained by using any of the following three equivalent results, which however differ in their analytical derivations.

1) *Multiple Infinite Series Representation:* This analytical expression was derived in [109],

$$\begin{aligned}F'(\mathbf{P}_j)=&\frac{1}{\Gamma(1+\sum_{i=1}^{M}m_i)}[\prod_{i=1}^{M}(\frac{m_i\lambda_i K}{p_{ij}})^{m_i}]\\&\times\Phi_2^{(M)}(m_1,m_2,\ldots,m_M;1+\sum_{i=1}^{M}m_i;-\frac{m_1\lambda_1 K}{p_{1j}},-\frac{m_2\lambda_2 K}{p_{2j}},\ldots,-\frac{m_M\lambda_M K}{p_{Mj}})\end{aligned} \tag{2.19}$$

where $\Phi_2^{(M)}(\ldots)$ is the confluent Lauricella multivariate hypergeometric function, involving multiple infinite sums [109]:

$$\begin{aligned}&\Phi_2^{(M)}(m_1,\ldots,m_M;1+\sum_{i=1}^{M}m_i;-\frac{m_1\lambda_1 K}{p_{1j}},\ldots,-\frac{m_M\lambda_M K}{p_{Mj}})\\&=\sum_{n_1=0}^{\infty}\cdots\sum_{n_M=0}^{\infty}\frac{[\prod_{i=1}^{M}(m_i)_{n_i}(-\frac{m_i\lambda_i K}{p_{ij}})^{n_i}\frac{1}{n_i!}]}{(1+\sum_{i=1}^{M}m_i)_{n_\tau}}\end{aligned} \tag{2.20}$$

where $n_\tau=\sum_{i=1}^{M}n_i$ and the Pochhammer symbol is defined as $(\alpha)_k=\frac{\Gamma(\alpha+k)}{\Gamma(k)}$ [109]. (2.19) can be numerically calculated. However, as M becomes large, computation of the multiple infinite sum may become too prohibitive to implement.

2) *Single Infinite Series Representation:* The second result provides a simpler expression for (2.18) involving only a single infinite sum [81], which was proposed by Moschopoulos (1985) [77].

$$F'(\mathbf{P}_j) = \prod_{i=1}^{M}(\frac{\beta_1}{\beta_{ij}})^{m_i}\sum_{n=0}^{\infty}\frac{\delta_n\gamma(\rho+n,\frac{K}{\beta_1})}{\Gamma(\rho+n)} \tag{2.21}$$

where $\rho=\sum_{i=1}^{M}m_i, \beta_{ij}=\frac{p_{ij}}{m_i\lambda_i}, \beta_1=\min(\beta_{ij}), \gamma(.)$ is incomplete gamma function ($\gamma(s,x)=\int_0^x t^{s-1}e^{-t}dt$) and the coefficients δ_n are obtained recursively by

$$\delta_{n+1}=\frac{1}{n+1}\sum_{l=1}^{n+1}[\delta_{n+1-l}\sum_{i=1}^{M}m_i(1-\frac{\beta_1}{\beta_{ij}})^l], n=0,1,\ldots,\ \delta_0=1 \tag{2.22}$$

Special Cases

• If $\rho=\sum_{i=1}^{M}m_i$ is an integer, (2.21) can be further simplified as [81]

$$F'(\mathbf{P}_j) = \prod_{i=1}^{M}(\frac{\beta_1}{\beta_{ij}})^{m_i}\sum_{n=0}^{\infty}\delta_n\{1-e^{-\frac{K}{\beta_1}}\sum_{l=0}^{\rho+n-1}\frac{(\frac{K}{\beta_1})^l}{l!}\} \tag{2.23}$$

• If $M=2$, let $\beta_2=\max(\beta_{ij})$, and m_θ is the corresponding fading parameter for β_2, we have

$$F'(\mathbf{P}_j) = (\frac{\beta_1}{\beta_2})^{m_\theta}\sum_{n=0}^{\infty}\frac{(m_\theta)_n(1-\frac{\beta_1}{\beta_2})^n}{n!}\frac{\gamma(\rho+n,\frac{K}{\beta_1})}{\Gamma(\rho+n)} \tag{2.24}$$

where $(m_\theta)_{n+1}$ represents the Pochhammer symbol.

3) *Integral Representation:* The third expression for the cdf of $\sum_{i=1}^{M}h_ip_{ij}$ is given as [75]

$$F'(\mathbf{P}_j) = \frac{1}{2}-\frac{1}{\pi}\int_0^\infty W(t)sin[\theta(t)-tK]\frac{dt}{t} \tag{2.25}$$

where

$$W(t)=\prod_{i=1}^{M}[1+(\frac{p_{ij}}{m_i\lambda_i}t)^2]^{-\frac{m_i}{2}},\quad \theta(t)=\sum_{i=1}^{M}m_i\tan^{-1}(\frac{p_{ij}}{m_i\lambda_i}t) \tag{2.26}$$

With POHPA, Problem (2.14) can be approximated as

$$\begin{aligned} &\min_{\{\mathbf{P}_1>\ldots>\mathbf{P}_{L-1}>\mathbf{P}_L\geq 0\}} F'(\mathbf{P}_1) \\ s.t. \quad &\sum_{j=1}^{L-1}(p_{1j}+\ldots+p_{Mj})(F'(\mathbf{P}_{j+1})-F'(\mathbf{P}_j)) \\ &+(p_{1L}+\ldots+p_{ML})(1-F'(\mathbf{P}_L)+F'(\mathbf{P}_1))=MP_{av} \end{aligned} \tag{2.27}$$

It's not hard to verify that Problem (2.27) is still nonconvex. However, we can employ the Karush-Kuhn-Tucker (KKT) necessary conditions to achieve locally optimal solutions.

Remark 2.1. *Note that KKT necessary conditions usually require* regularity *of a local optimum, which amounts to (in the context of Problem (2.27)) linear independence of the gradients of the active inequality constraints evaluated at the local optimum (see Proposition 3.3.1, pg. 310 in [21]). In Problem (2.27), if a local optimum of the power vector satisfies* $\boldsymbol{P}_1 > \ldots > \boldsymbol{P}_{L-1} > \boldsymbol{P}_L > 0$*, then the only active inequality constraint is the average power constraint, in which case the linear independence property is trivially satisfied. In the case where the local optimum for* $\boldsymbol{P}_L = 0$*, it can be easily shown by simple linear algebra that the gradients corresponding to these two (*$\boldsymbol{P}_L = 0$ *and the average power constraint) active inequality constraints satisfy the linear independence condition.*

Since regularity of a local optimum is thus established, one can now use KKT necessary conditions to obtain the following result:

Theorem 2.1. *Suppose* $\{p_{1j}{}^*,\ldots,p_{Mj}{}^*\}_{j=1}^{L}$ *be an optimum to Problem (2.27). Then we have*

$$\frac{\partial F'(\boldsymbol{P}_j)}{\partial p_{1j}{}^*}=\ldots=\frac{\partial F'(\boldsymbol{P}_j)}{\partial p_{Mj}{}^*},\ \ j=1,\ldots,L \tag{2.28}$$

where

$$\begin{aligned} \frac{\partial F'(\boldsymbol{P}_j)}{\partial p_{M1}{}^*} &= -\frac{\mu(F'(\boldsymbol{P}_2)-F'(\boldsymbol{P}_1))}{1-\mu\sum_{i=1}^{M}(p_{i1}-p_{iL})}, \\ \frac{\partial F'(\boldsymbol{P}_j)}{\partial p_{Mj}{}^*} &= -\frac{F'(\boldsymbol{P}_{j+1})-F'(\boldsymbol{P}_j)}{\sum_{i=1}^{M}(p_{i,j-1}-p_{ij})},\ \ j=2,\ldots,L-1, \end{aligned}$$

$$\frac{\partial F'(\boldsymbol{P}_L)}{\partial {p_{ML}}^*} = -\frac{1 - F'(\boldsymbol{P}_L) + F'(\boldsymbol{P}_1)}{\sum_{i=1}^{M}(p_{i,L-1} - p_{iL})}. \tag{2.29}$$

Proof: The proof can be found in the appendix of this chapter.

Combining the above result with the average power constraint in (2.27), we have following system of $(ML+1)$ nonlinear equations.

$$\begin{cases} \sum_{j=1}^{L-1}(p_{1j} + \ldots + p_{Mj})(F'(\mathbf{P}_{j+1}) - F'(\mathbf{P}_j)) + (p_{1L} + \ldots + p_{ML})(1 - F'(\mathbf{P}_L) + F'(\mathbf{P}_1)) \\ = MP_{av} \\ \frac{\partial F'(\mathbf{P}_j)}{\partial {p_{1j}}^*} = \ldots = \frac{\partial F'(\mathbf{P}_j)}{\partial {p_{Mj}}^*}, \;\; j = 1, \ldots, L \\ \frac{\partial F'(\mathbf{P}_j)}{\partial {p_{M1}}^*} = -\frac{\mu(F'(\mathbf{P}_2) - F'(\mathbf{P}_1))}{1 - \mu\sum_{i=1}^{M}(p_{i1} - p_{iL})} \\ \frac{\partial F'(\mathbf{P}_j)}{\partial {p_{Mj}}^*} = -\frac{F'(\mathbf{P}_{j+1}) - F'(\mathbf{P}_j)}{\sum_{i=1}^{M}(p_{i,j-1} - p_{ij})}, \;\; j = 2, \ldots, L-1 \\ \frac{\partial F'(\mathbf{P}_L)}{\partial {p_{ML}}^*} = -\frac{1 - F'(\mathbf{P}_L) + F'(\mathbf{P}_1)}{\sum_{i=1}^{M}(p_{i,L-1} - p_{iL})}, \\ \mathbf{P}_1 > \cdots > \mathbf{P}_L \end{cases} \tag{2.30}$$

A solution to (2.30) provides a locally optimum power allocation policy $\{{\mathbf{P}_j}^*\}_{j=1}^{L}$. For small values of L and M, the above system of nonlinear equations can be solved by various optimization softwares. However, the complexity of solving the above set of nonlinear equations is still too high for moderately large numbers of feedback bits and channels. Therefore, we consider several low-complexity suboptimal schemes suited to special cases of high or low P_{av} as described below.

2.3.3 High Average Power Approximation (HP_{av}A)

Theorem 2.2. *For arbitrary M, in high average power (as $P_{av} \to \infty$), the Multiple Infinite Series Representation (2.19), $F'(\boldsymbol{P}_j), j = 1, \ldots, L$ can be further approximated as*

$$F'(\boldsymbol{P}_j) \approx \frac{1}{\Gamma(1 + \sum_{i=1}^{M} m_i)} \prod_{i=1}^{M} (\frac{m_i \lambda_i K}{p_{ij}})^{m_i} \tag{2.31}$$

and a locally optimum power allocation scheme for (2.27) satisfies the following approximate relationship:

$$\frac{m_i}{{p_{ij}}^*} \approx \frac{m_l}{{p_{lj}}^*}, \quad i,l \in \{1,2,\ldots,M\},\ i \neq l,\ j = 1,\ldots,L \tag{2.32}$$

Proof: The proof can be found in the appendix of this chapter.

(2.32) implies that in high P_{av}, for each quantization region, the power allocated to each channel asymptotically depends only on the severity of fading (represented by the parameter m).

Special Cases:

• *Identical Fading Parameters*: If $m_1 = \ldots = m_M$, from (2.32), we have

$${p_{1j}}^* \approx \ldots \approx {p_{Mj}}^* \ \ j = 1,\ldots,L \tag{2.33}$$

which means, in high P_{av}, with identical fading parameters for all channels, for each quantization region, the power assigned to each channel is asymptotically equal, and we call this solution as 'Equal Power Per Channel (EPPC)'.

• *Rayleigh fading*: ($m_1 = \ldots = m_M = 1$), from Theorem 2.2, (2.31) reduces to

$$F'(\mathbf{P}_j) \approx \frac{1}{M!}\prod_{i=1}^{M}(\frac{\lambda_i K}{p_{ij}}) \tag{2.34}$$

and (2.32) reduces to EPPC.

For the general case (2.32), without loss of generality, by letting $p_{ij} = \frac{m_i}{m_M} p_{Mj},\ \forall i \in \{1,2,\ldots,M-1\}$ and denoting p_{Mj} as p_j for simplicity, the above $ML+1$ equations system (2.30) can be simplified into an $L+1$ equations system only:

$$\begin{cases} \sum_{j=1}^{L-1} p_j(F'(p_{j+1}) - F'(p_j)) + p_L(1 - F'(p_L) + F'(p_1)) = P'_{av} \\ \frac{\partial F'(p_j)}{\partial p_j} = -\frac{F'(p_{j+1}) - F'(p_j)}{(p_{j-1} - p_j)},\ \ j = 2,\ldots,L-1 \\ \frac{\partial F'(p_L)}{\partial p_L} = -\frac{1 - F'(p_L) + F'(p_1)}{(p_{L-1} - p_L)} \end{cases} \tag{2.35}$$

where $P'_{av} = P_{av}\frac{M m_M}{\sum_{i=1}^{M} m_i}$.

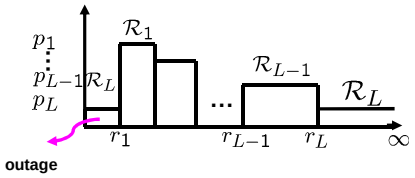

Figure 2.5: PFPPC

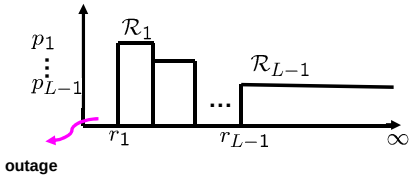

Figure 2.6: PFPPC+ZPiOR

Thus HP_{av}A reduces the M-dimensional vector quantization problem into a one-dimensional scalar quantization problem, as illustrated in Fig. 2.5, with corresponding quantization thresholds $r_1, \ldots, r_L$, where $r_j = r'_{Mj} = K/p_j$, and remarkably reduces the complexity. We call this suboptimal scheme as the 'Proportional to Fading Parameter Per Channel (PFPPC)' scheme. For small values of L, the above L nonlinear equations (where one can evaluate $F'(p_j)$ using the Single Infinite Series Representation (2.21)) can be solved by various optimization softwares.

For large values of L (e.g. $L \geq 16$ or $B \geq 4$), one can use the so-called equal average power per region (EPPR) approximation for such a scalar quantization problem by using the mean value theorem [12]. This essentially implies that when L goes to infinity, the total average power assigned to each quantization region is asymptotically equal and the performance using this approximation is close to optimum for large number of bits of feedback. In this case, we need to solve the following set of L equations instead of (2.35)

$$\begin{aligned} p_j(F'(p_{j+1}) - F'(p_j)) &= \frac{P'_{av}}{L}, \quad j = 1, \ldots, L-1; \\ p_L(1 - F'(p_L) + F'(p_1)) &= \frac{P'_{av}}{L}. \end{aligned} \tag{2.36}$$

which can be carried out by an iterative algorithm employing the standard bisection search method. We call this algorithm as 'PFPPC+EPPR'.

Let P_{tot}^{j} represent the total average power allocated to region $\mathcal{R}_j$ at PFPPC case. Then the average power constraint in (2.35) can be rewritten as,

$$\sum_{j=1}^{L} \frac{P_{tot}^{j}}{p_j} = 1 \tag{2.37}$$

Since $p_1 > p_2 > \ldots > p_L$, $\sum_{j=1}^{L} P_{tot}^{j} = P'_{av}$, it follows that

$$p_1 > P'_{av} \tag{2.38}$$

Thus, in the high P_{av} regime ($P_{av} \to \infty$), $r_1 = \frac{K}{p_1} \to 0$, and we have the following result which indicates that the total power allocated to the outage region is asymptotically (as $P_{av} \to \infty$) negligible:

Lemma 2.2. *In the high P_{av} regime, $\lim_{r_1 \to 0} P_{tot}^{L,1} = 0$, if $\sum_{j=1}^{L} \rho^j > 1$, where $\rho = \sum_{i=1}^{M} m_i$.*

Proof: The proof can be found in the appendix of this chapter.

Therefore another effective scheme for large L is to additionally (to PFPPC) employ what we call the 'Zero Power in Outage Region'(ZPiOR) approximation (PFPPC+ZPiOR), by letting the power level $p_L = 0$ resulting in $r_L = \frac{K}{p_L} \to \infty$, as showed in Fig. 2.6. Thus we have the total average power allocated to outage region $\mathcal{R}_{L,1}$, $P_{tot}^{L,1} = p_L * F'(p_1) = 0$.

Remark 2.2. *Note that if $\rho \geq 1$, the condition $\sum_{j=1}^{L} \rho^j > 1$ is clearly satisfied for any $L \geq 2$. For $0.5 < \rho < 1$ (which is the case of no diversity with $M = 1$ or the single channel case), one can show that there exists a finite L for which the condition $\sum_{j=1}^{L} \rho^j > 1$ is satisfied. This is easily seen by noting that the condition $\sum_{j=1}^{L} \rho^j > 1$ is equivalent to $\rho^{L+1} < 2\rho - 1$ for $\rho < 1$. It is interesting to note however that when $\rho = 0.5$ (which is the case when one has as single Nakagami channel with $m = 0.5$, the worst possible fading parameter), there is no finite value of L that can achieve $\sum_{j=1}^{L} \rho^j > 1$. Thus in high P_{av}, it is near optimal to allocate zero power to the outage region as long as $\rho \geq 1$ with any $L \geq 2$, or a single channel with $0.5 < m < 1$ and a sufficiently large L. For a single channel with $m = 0.5$, it seems that even in high P_{av}, one needs to allocate nonzero power to the outage region.*

Therefore the performance of the ZPiOR approximation (except for the single channel case with $m = 0.5$, in which case one can use the EPPR approximation to reduce complexity) (PFPPC+ ZPiOR) becomes asymptotically (as $L \to \infty$) close to that of the PFPPC scheme.

In this case, (2.35) can be simplified as

$$\begin{cases} \sum_{j=1}^{L-1} p_j(F'(p_{j+1}) - F'(p_j)) = P'_{av} \\ p_{j-1} = p_j + \frac{F'(p_{j+1}) - F'(p_j)}{-\frac{\partial F'(p_j)}{\partial p_j}} \quad j = 2, \ldots, L-1, F'(p_L) = 1 \end{cases} \tag{2.39}$$

which can be easily solved by using a standard bisection method. In fact, numerical studies illustrate (as we will see later) that the ZPiOR approximation has a near-optimum (for Problem (2.27)) performance for large number of quantization regions. Thus, the ZPiOR approximation achieves a better complexity-performance tradeoff than PFPPC+EPPR.

Remark 2.3. *For the low P_{av} scenario, we can apply the ZPiOR approximation as well. This is because it is easy to verify that*

$$\frac{1}{M}(p_{1L} + \ldots + p_{ML}) \quad < \quad P_{av} \tag{2.40}$$

then when the average power is small ($P_{av} \to 0$), $p_{iL} \to 0, i = 1, \ldots, M$ as well, and the corresponding quantization threshold $r_{iL} \to \infty$. In this case, the region $\mathcal{R}_L$ only includes $\mathcal{R}_{L,1}$ (the outage region) and the corresponding power level $\boldsymbol{P}_L = 0$, thus making the ZPiOR approximation applicable. A similar observation was also made in [105].

2.3.4 Asymptotic Behavior of Outage Probability

Here we briefly comment on the diversity behaviour of the outage minimization algorithm using POHPA. Define the diversity gain d as

$$d \quad = \quad -\lim_{P_{av} \to \infty} \frac{\log P_{out}}{\log P_{av}} \tag{2.41}$$

Then we have the following result:

Theorem 2.3. *For an arbitrary M, with $\log_2 L$ bits of quantized feedback, using the optimal power allocation employing the POHPA approximation, we have*

$$P_{out} \approx \frac{(\frac{\rho L}{M m_M})^{\rho^L+\ldots+\rho} c^{\rho^{L-1}+\ldots+\rho+1}}{P_{av}^{\rho^L+\ldots+\rho}} \tag{2.42}$$

The diversity order can be approximated as

$$d \approx \sum_{j=1}^{L} (\sum_{i=1}^{M} m_i)^j \tag{2.43}$$

Proof: The proof can be found in the appendix of this chapter.

Special Case: Note that for Rayleigh fading case where $m_i = 1, \forall i = 1, 2, \ldots, M$, (2.43) becomes $d \approx \sum_{j=1}^{L} M^j$, which is consistent with similar results in [105] and [12].

Remark 2.4. *It is possible that the result in Theorem 2.3 may hold with equality, rather than being an approximation for the diversity order. However, due to the various levels of approximations involved in deriving this, we are unable to prove an exact equality at this stage. This will involve computing orders of approximation errors and showing that the error goes to zero as P_{av} goes to infinity. We leave this for future work.*

2.4 Large Number of Channels Analysis

The previous algorithms can be effectively applied to find locally optimal solutions or suitable approximations for them for moderate number of parallel channels, such as $M < 10$. Once $M \geq 10$, these algorithms become computationally demanding. Given that practical multi-carrier systems such as OFDM can have large number of sub-carriers such as $M = 64$ or $M = 128$ sub-carriers, one needs to find outage minimizing power allocation algorithms with limited feedback for large M. Below we provide such an algorithm using a Gaussian approximation for large M in high P_{av}.

Note that in high average power, we have

$$\sum_{i=1}^{M}\log(1+p_{ij}h_i)\approx\sum_{i=1}^{M}\log(p_{ij}h_i)=\sum_{i=1}^{M}\log(p_{ij}\frac{f_i}{\lambda_i})=\sum_{i=1}^{M}\log(\frac{p_{ij}}{\lambda_i})+\sum_{i=1}^{M}\log(f_i) \quad (2.44)$$

where $f_i = h_i\lambda_i$, $\frac{1}{\lambda_i}$ is the mean of channel gain h_i, and under the Nakagami fading model, the pdf of f_i is $\frac{(m_i)^{m_i}}{\Gamma(m_i)}f_i^{m_i-1}e^{-m_i f_i}, \forall i$.

Thus $F(\mathbf{P}_j), j = 1,\ldots,L$ for M channels can be approximated as

$$F(\mathbf{P}_j)=Prob(\frac{1}{M}\sum_{i=1}^{M}\frac{1}{2}\log(1+p_{ij}h_i)<r_0)\approx Prob(\frac{1}{M}\sum_{i=1}^{M}\log(f_i)<s_j)=V(s_j) \quad (2.45)$$

where $s_j = 2r_0 - \frac{1}{M}\sum_{i=1}^{M}\log(\frac{p_{ij}}{\lambda_i}) = c' - \frac{1}{M}\sum_{i=1}^{M}\log(p_{ij})$, $c' = 2r_0 + \frac{1}{M}\sum_{i=1}^{M}\log(\lambda_i)$ and the function $V(.)$ denotes the cdf of $\frac{1}{M}\sum_{i=1}^{M}\log(f_i)$. It is easy to show that the pdf of $z_i = \log(f_i)$ is $f_{z_i} = \frac{(m_i)^{m_i}}{\Gamma(m_i)}e^{-m_i e^{z_i}}e^{m_i z_i}$. Denote its mean and variance by $E[z_i]$ and $Var[z_i]$ respectively. For the Rayleigh fading case, the pdf of $z_i = \log(f_i)$ is $e^{-e^{z_i}}e^{z_i}$, which is the well known *Gumbel Distribution* with mean $E[z_i] = -r$, where r is Euler-Mascheroni constant ($r = 0.5772156649...$) and variance $Var[z_i] = \frac{\pi^2}{6}$.

Note that for large M, if $m_1 = \cdots = m_M$ or in the special case of Rayleigh fading ($m_i = 1,\ \forall i$), z_i is i.i.d with finite mean and variance and then the *Central Limit Theorem* directly applies whereby one can use a Gaussian approximation for the pdf of $\frac{1}{M}\sum_{i=1}^{M}z_i$. However, in the general case where the fading parameters m_i are different for different channels, $z_i,\ i = \{1,2,\ldots,M\}$ are independent but not necessarily identically distributed. In this case, we can analytically proved that

Theorem 2.4. *The sequence* $\{z_i - E[z_i]\}$ *satisfies the* Lindeberg condition *(for a statement of this condition, see page 262, [39]).*

Proof: The proof can be found in the appendix of this chapter.

Therefore when the number of channels $M \to \infty$, the cdf of $\frac{1}{M}\sum_{i=1}^{M}z_i$ can still be approximated (by applying Theorem 3, Chapter VIII.4 in [39]) by a Gaussian cdf with mean and variance given by

$$\mu = \frac{1}{M}\sum_{i=1}^{M}E[z_i],\ \sigma^2 = \frac{1}{M^2}\sum_{i=1}^{M}Var[z_i] \quad (2.46)$$

Thus, we have

$$V(s_j) \approx \int_{-\infty}^{s_j} \frac{1}{\sigma\sqrt{2\pi}} e^{-\frac{(x-\mu)^2}{2\sigma^2}} dx = \frac{1}{2}[1 + erf(\frac{s_j - \mu}{\sigma\sqrt{2}})] \tag{2.47}$$

The original problem (2.14) for a large number of channels case can be approximated as

$$\begin{aligned} &\min_{\{\mathbf{P}_1 > \mathbf{P}_2 > \ldots > \mathbf{P}_L \geq 0\}} V(s_1) \\ &s.t. \quad \sum_{j=1}^{L-1} (p_{1j} + \ldots + p_{Mj})(V(s_{j+1}) - V(s_j)) \\ &\qquad + (p_{1L} + \ldots + p_{ML})(1 - V(s_L) + V(s_1)) = MP_{av} \end{aligned} \tag{2.48}$$

Using the KKT necessary conditions, we again get

$$\frac{\partial V(s_j)}{\partial p_{1j}} = \ldots = \frac{\partial V(s_j)}{\partial p_{Mj}}, j = 1, \ldots, L \tag{2.49}$$

Note that

$$\frac{\partial V(s_j)}{\partial p_{ij}} = f(s_j)\frac{\partial s_j}{\partial p_{ij}} = \frac{1}{\sigma\sqrt{2\pi}} e^{-\frac{(c - \frac{1}{M}\sum_{i=1}^{M} \log(p_{ij}) - \mu)^2}{2\sigma^2}} - \frac{1}{M}\frac{1}{p_{ij}} \tag{2.50}$$

where $f(s) = \frac{1}{\sigma\sqrt{2\pi}} e^{-\frac{(s-\mu)^2}{2\sigma^2}}$. It is easily seen that the above expression for $\frac{\partial V(s_j)}{\partial p_{ij}}$ is a monotonically increasing function of p_{ij} for all $i = 1, 2, \ldots, M$ and $j = 1, 2, \ldots, L$. Therefore, from (2.49), we have

$$p_{1j} = \ldots = p_{Mj}, \; j = 1, \ldots, L \tag{2.51}$$

The above result implies that at a local optimum, using the Gaussian approximation, the power levels (for each quantization region) for all channels are identical, which is identical to the EPPC scheme. With a slight abuse of notation, denote $p_j = p_{ij}, j = 1, \ldots, L$. Then we have $s_j = c' - \log(p_j)$ and the vector quantization problem (2.48) can be converted into the scalar quantization problem below with quantization thresholds $s_1, \ldots, s_L$:

$$\min_{\{p_1 > \ldots > p_L \geq 0\}} V(s_1)$$

$$s.t. \quad \sum_{j=1}^{L-1} p_j(V(s_{j+1}) - V(s_j)) + p_L(1 - V(s_L) + V(s_1)) = P_{av} \tag{2.52}$$

After employing the corresponding KKT necessary optimality conditions and simplifying, we have the system of L nonlinear equations below:

$$\begin{cases} \sum_{j=1}^{L-1} p_j(V(s_{j+1}) - V(s_j)) + p_L(1 - V(s_L) + V(s_1)) = P_{av} \\ p_{j-1} = p_j(\frac{V(s_{j+1}) - V(s_j)}{f(s_j)} + 1), \ \ j = 2, \ldots, L-1 \\ p_{L-1} = p_L(\frac{1 - V(s_L) + V(s_1)}{f(s_L)} + 1) \end{cases} \tag{2.53}$$

When L is not large, one can solve the above equations using optimization tools 1stOpt. When L is large (roughly $L \geq 16$), we can also use the EPPR approximation or the ZPiOR approximation to solve them, as discussed in the section on high P_{av} approximations. Table 2.1 below shows the applicability of various algorithms discussed so far according to different ranges of M, L and high P_{av}, where "GA" denotes the Gaussian approximation based algorithms.

Table 2.1: Proposed power allocation strategies

Number of Channels	$M < 10$	$M \geq 10$
Optimal approach	SPSA	-
Approximation	POHPA	-
High P_{av}	PFPPC ($L \geq 16$, PFPPC+ZPiOR or PFPPC+EPPR)	GA ($L \geq 16$, GA+ZPiOR or GA+EPPR)

2.5 Numerical Results

To numerically illustrate the performance of the designed power allocation strategies, we consider an M-parallel (independent) Nakagami block-fading channels where the mean value of the gamma distributed fading gain for each channel is assumed to be inversely proportional to the square of the wireless propagation distance d, and the required transmission rate is taken to be $r_0 = 0.25$ nats per channel use. Outage performance with full CSI at the transmitter is obtained with the optimal power allocation results presented in

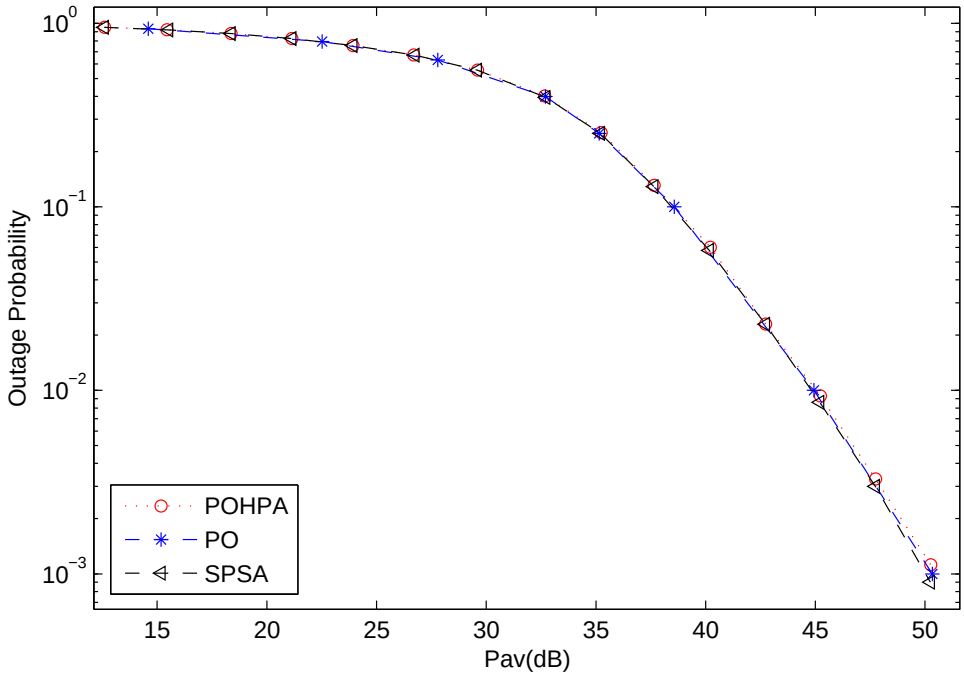

Figure 2.7: Outage performance comparison between SPSA, PO and POHPA for 2 channels 1 bit feedback ($m_1 = m_2 = 0.5$).

[40]. It should be noted that the results illustrate the "real outage" performance of the proposed algorithms (the power codebook designed via the algorithms is used to obtain the average outage probability over a large number of Monte-Carlo simulated channel realizations). As a result, the average power required for a given *real* outage may not strictly be the same as the original average power based on which the power codebook is designed. However, for a given algorithm, the graphs can and should be used to determine the minimum outage probability obtainable for a given average power and vice versa.

Experiment 1 : The first experiment examines the performance of POHPA. Fig. 2.7 compares the outage performance of SPSA, an exhaustive search over the space of all possible power allocation policies implementing the power ordering (PO) approximation only, and POHPA with 1 bit feedback for 2 channels case ($d_1 = 40m, d_2 = 60m$, $m_1 = m_2 = 0.5$). It can be observed that when P_{av} is small, the performance of these three methods have negligible difference, while when P_{av} is large, SPSA is slightly better

than PO and POHPA. Fig. 2.8 shows the outage performance of SPSA and POHPA for a higher dimensional case (4 channels case, $d_1 = 30m, d_2 = 40m, d_1 = 60m, d_2 = 70m$, $m_1 = m_2 = m_3 = m_4 = 1$). Again, it can be seen clearly that with identical number of feedback bits, the outage probability gap between SPSA and POHPA gradually increases as P_{av} increases. From Fig. 2.7 and Fig. 2.8, it seems that in a higher dimensional space (larger number of channels), with the same number of feedback bits, the outage probability gap between the two methods is bigger than the one in a low dimensional space, especially in high P_{av}. And with the same value of M, as the number of feedback bits increases, this gap seems to decrease, as shown in Fig. 2.8. This can be explained due to the fact that to achieve a fixed outage probability, a larger number of feedback bits requires less P_{av}.

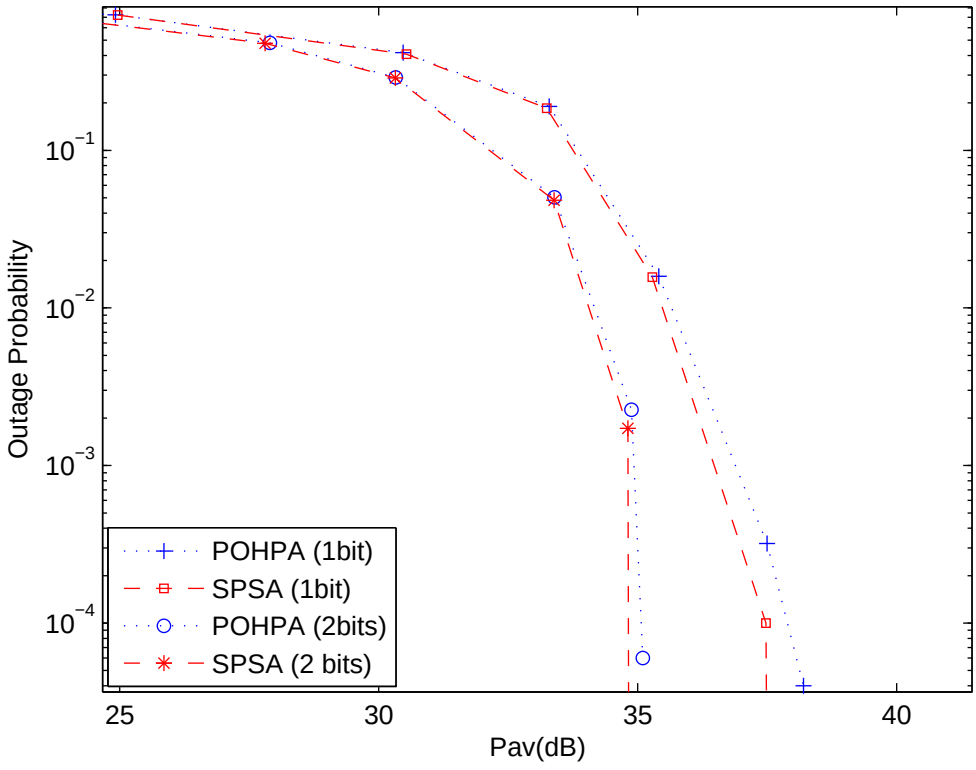

Figure 2.8: Outage performance comparison between SPSA and POHPA for 4 channels ($m_1 = m_2 = m_3 = m_4 = 1$).

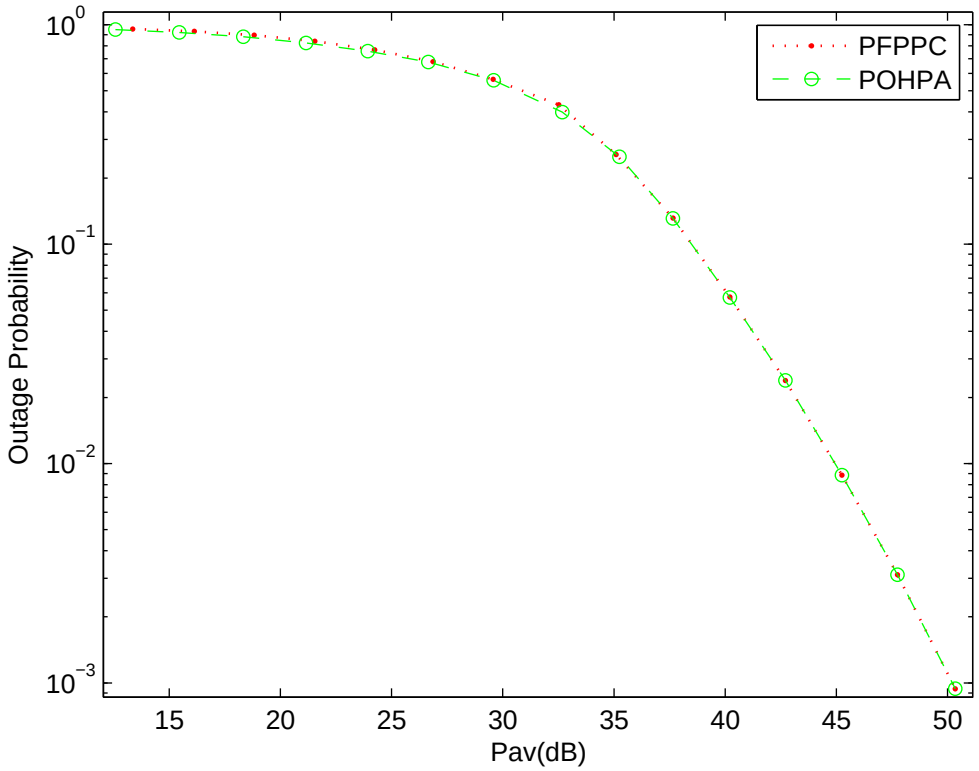

Figure 2.9: Outage performance of HPavA (PFPPC) scheme ($M = 2, B = 1, m_1 = m_2 = 0.5$).

Experiment 2 : This experiment tests the performance of suboptimal scheme HP_{av}A (namely, PFPPC). Fig. 2.9 compares the outage performance of PFPPC approximation with its optimal case (POHPA) for 2 channels ($d_1 = 40m, d_2 = 60m$) with 1 bit feedback ($m_1 = m_2 = 0.5$). The striking observation in Fig. 2.9 is that when $P_{av} \leq 32dB$, POHPA only slightly outperforms PFPPC, while when $P_{av} > 32dB$, the performance of PFPPC and POHPA almost overlaps each other (i.e, the performance of PFPPC is very close to its optimum), indicating that PFPPC is an efficient near-optimal scheme for POHPA especially at high P_{av}. In addition, Fig.2.10 illustrate the efficiency of using PFPPC+EPPR and PFPPC+ZPiOR schemes for HP_{av}A (PFPPC) at large number of feedback bits. As shown in Fig.2.10, with 4 bits of feedback (16 regions), PFPPC with ZPiOR approximation (PFPPC+ZPiOR) achieves almost equivalent performance to PFPPC with EPPR approximation (PFPPC+EPPR), and both schemes are very close to their optimal case (PFPPC). This

result illustrates the fact that ZPiOR can be combined with PFPPC as a computationally simpler alternative to PFPPC+EPPR for large number of feedback bits.

Experiment 3 : The third simulation, as illustrated in Fig. 2.11 for 4 channels case

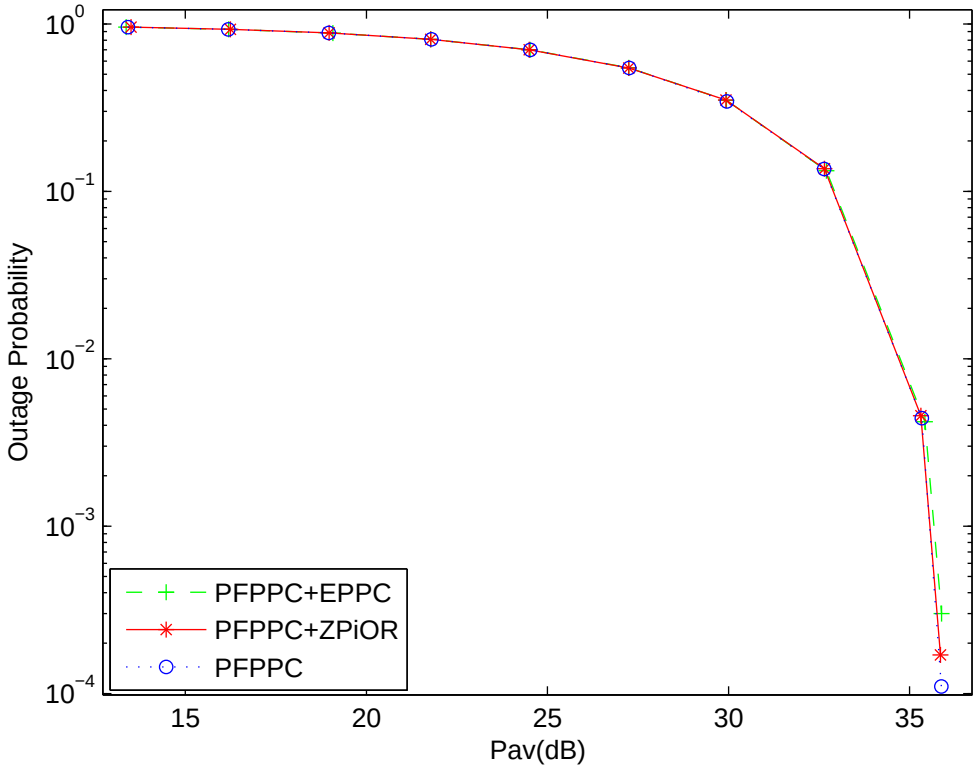

Figure 2.10: Outage performance of PFPPC+EPPR and PFPPC+ZPiOR schemes with 4bits feedback for 2channels and $m_1 = m_2 = 1$ ($\rho > 1$).

(**d**=[30m,40m,60m,70m] and $m_1 = m_2 = m_3 = m_4 = 0.5$), studies the effect of increasing the number of feedback bits on the outage performance using the proposed schemes. For comparison, the performance of the optimal power control policy with full CSI [40] is also shown. Instead of comparing the performance with the POHPA scheme, we plot the outage probabilities of its computationally efficient near-optimal schemes (PFPPC and its variants). With a small number of bits (1 bit and 2 bits) of feedback, PFPPC can be implemented by using the optimization software 1stopt, and with 4 bits of feedback ($L = 16$), we plot the performances of PFPPC+ZPiOR instead. The important observation from this figure is that the introducing one extra bit of feedback substantially reduces the gap with

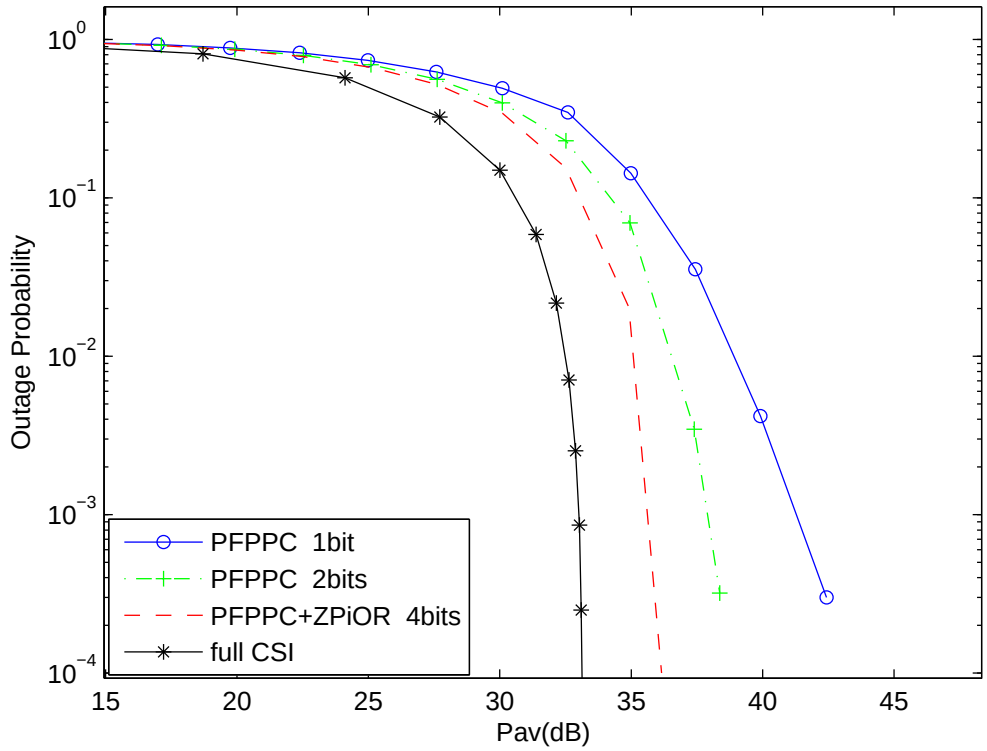

Figure 2.11: Effect of increasing feedback bits on outage performance for 4 channels ($m_1 = m_2 = m_3 = m_4 = 0.5$).

the full CSI performance and only a few bits of feedback can eliminate most of the gap with the full CSI performance. For example, at an outage probability of 10^{-2}, with 4 bits of feedback, there is only around 2.5 dB power loss compared to the full CSI case. This confirms that power allocation with limited feedback (only with a few feedback bits) can provide a dramatic performance advantage over no CSI (channel non-adaptive power allocation across all channels).

Fig. 2.12 depicts the diversity behaviour of the proposed outage minimization scheme POHPA using the derived bound given in (2.42) for 4 channels with $m_1 = m_2 = m_3 = m_4 = 0.5$. In high P_{av}, the outage performance of the PFPPC scheme is very close to optimum (POHPA), thus here we plot the performance of the computationally efficient PFPPC scheme instead of POHPA. We also use (2.31) to approximate the outage expression when the outage probability $\leq 10^{-10}$. As we can see from Fig. 2.12, the derived

bound captures the slope of outage behaviour in high P_{av} extremely well.

Experiment 4 : Fig. 2.13 shows the effect of the fading parameter m on the outage performance. It depicts the outage performance with 4 bits of feedback over 6 Nakagami fading channels with different values of the fading parameter: $m = 0.5$, $m = 1$ and $m = 2$ (here we use identical fading parameter for each channel, i.e. $m_1 = \ldots = m_6 = m$, and $d = [20, 30, 40, 60, 70, 80]$). It can be noticed that as m increases, i.e., the fading severity decreases, significant performance gains can be easily observed. To achieve a target out-

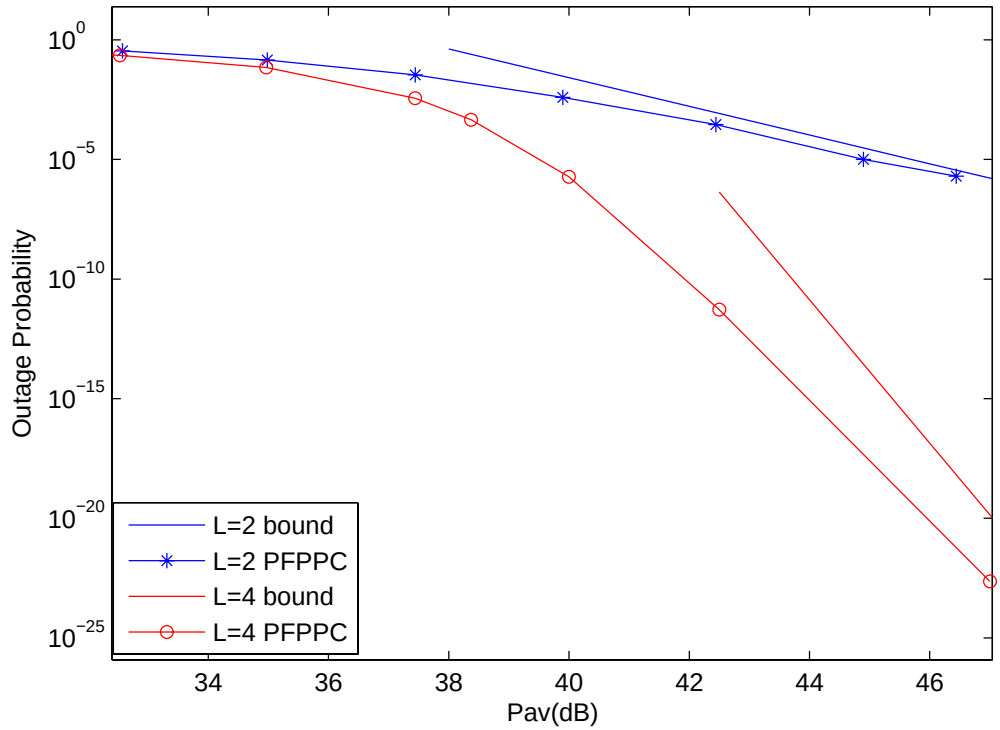

Figure 2.12: Bound on diversity order for L=2 and 4 with PFPPC scheme (M=4, $m_1 = m_2 = m_3 = m_4 = 0.5$).

age probability 10^{-2}, 4 bits of feedback with $m = 2$ provides around 2.65 dB and 1.18 dB improvements over 4 bits of feedback with $m = 0.5$ and $m = 1$ respectively, as measured by the SNR gap with respect to their respective full CSI performances.

Experiment 5: Fig. 2.14 compares the outage performance between the PFPPC scheme and the Gaussian approximation (GA) for 4 channels case ($m_1 = m_2 = m_3 = m_4 = 0.5$). It can be seen very clearly that the PFPPC scheme outperforms GA, the benefit of the PFPPC

scheme becoming more pronounced as P_{av} increases. For instance, with the same feedback bits, at an outage probability of 10^{-3}, PFPPC with 1 bit requires roughly 7.8 dB less power than GA does; and PFPPC with 2 and 4 bits feedback provide around 5.6 dB and

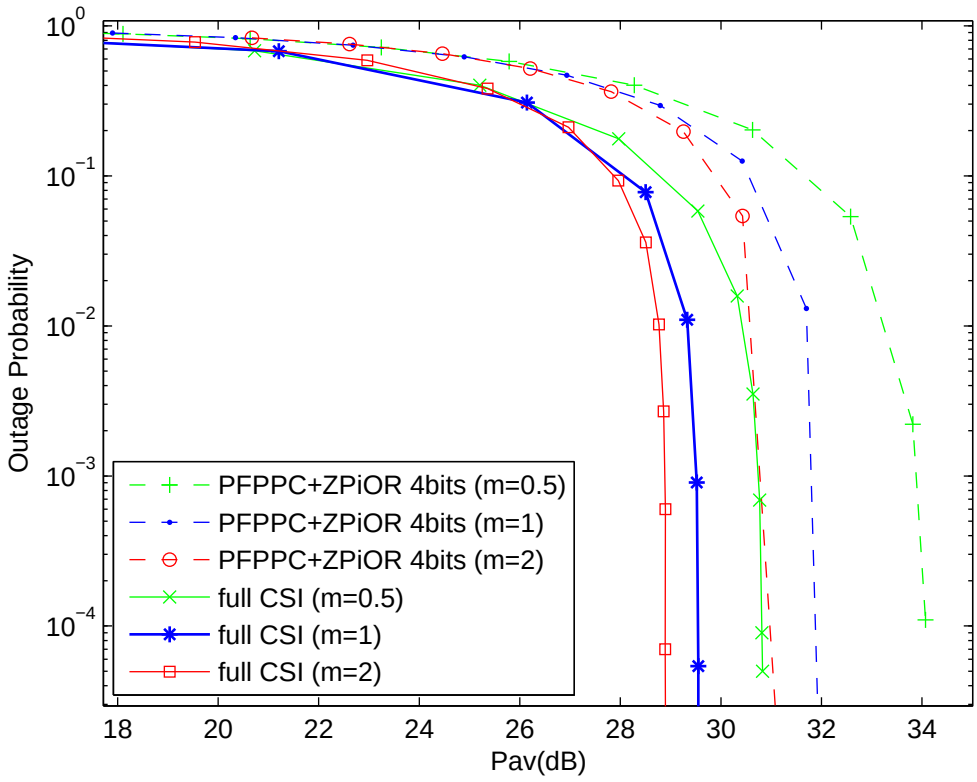

Figure 2.13: Effect of the fading parameter m on outage performance for 6 channels.

2.3 dB power savings over GA respectively. Even with only with 1 bit of feedback, PFPPC can achieve a better performance than GA with 2 bits of feedback in high P_{av}. These results indicate that the POHPA (with the PFPPC approximation) can achieve remarkable performance advantage over GA, especially in high P_{av}. However, when the number of channels is large, POHPA becomes computationally prohibitive. And in this case, GA is an efficient alternative, which is consistent with similar observations (for MIMO settings) in [25].

Fig. 2.15 illustrates the outage probability over large number of channels (16 channels) using GA, with the values of distances $d_1, \ldots, d_{16}$ randomly obtained (with a uni-

form distribution) from the range [20m,100m] and different identical fading parameters ($m_1 = \ldots = m_{16} = m$) m= 0.5 and $m = 2$ respectively. We again see that only a few bits of feedback are required to close the gap with the performance with full CSI. For instance, to achieve a target outage probability 10^{-2}, with $m = 2$, the power consumption gap between 10 bits of feedback (less than one bit per channel) and its full CSI based counterpart is only about 2.4 dB, while with $m = 0.5$, the gap is 2.8 dB. On the other hand, as m decreases, i.e., the fading severity increases, the outage performance of the limited feedback schemes deteriorates as expected.

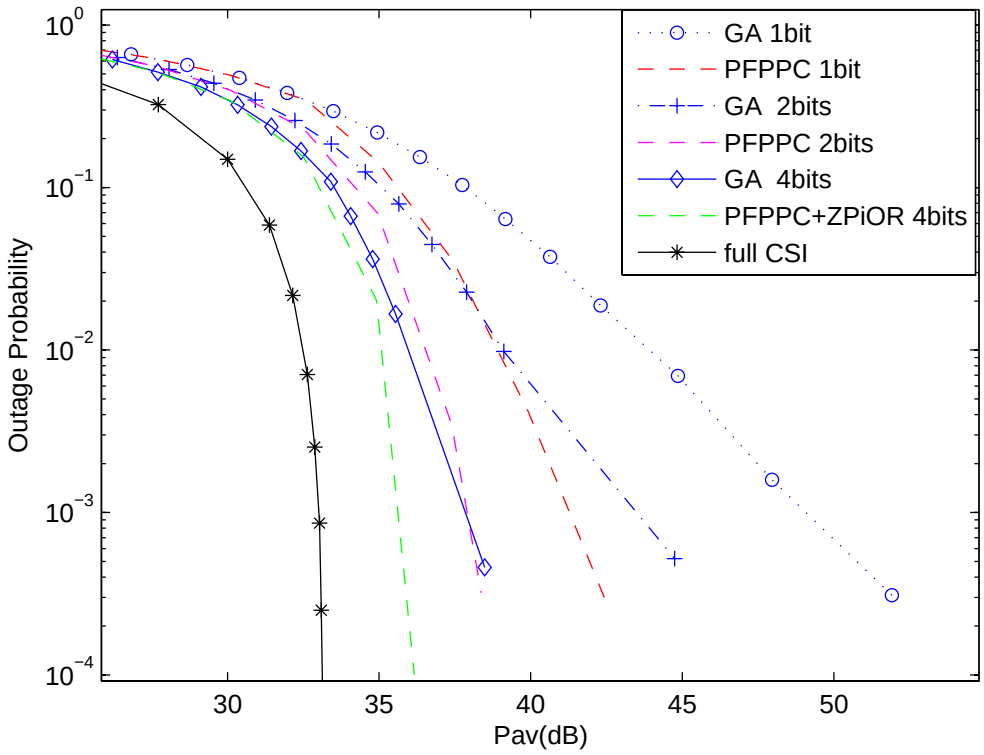

Figure 2.14: Outage performance comparison between POHPA and GA (M=4, B=1,2,4 bits, $m_1 = m_2 = m_3 = m_4 = 0.5$).

2.6 Conclusion

In this chapter, we have derived a simulation based optimization algorithm using SPSA and presented various low-complexity sub-optimal outage minimization algorithms via optimal power allocation with finite-rate or quantized channel feedback for an M-parallel block-fading channels under a long term average power constraint. Numerical results illustrate the effectiveness of these algorithms via their outage performance in comparison with the performance of the optimal power allocation with full CSI. Future work includes extension of these results to correlated fading channels, consideration of noisy or erroneous feedback as investigated in [92] and quantized CSIT based power allocation to more general optimization problems such as the service-outage based power and rate allocation in [53].

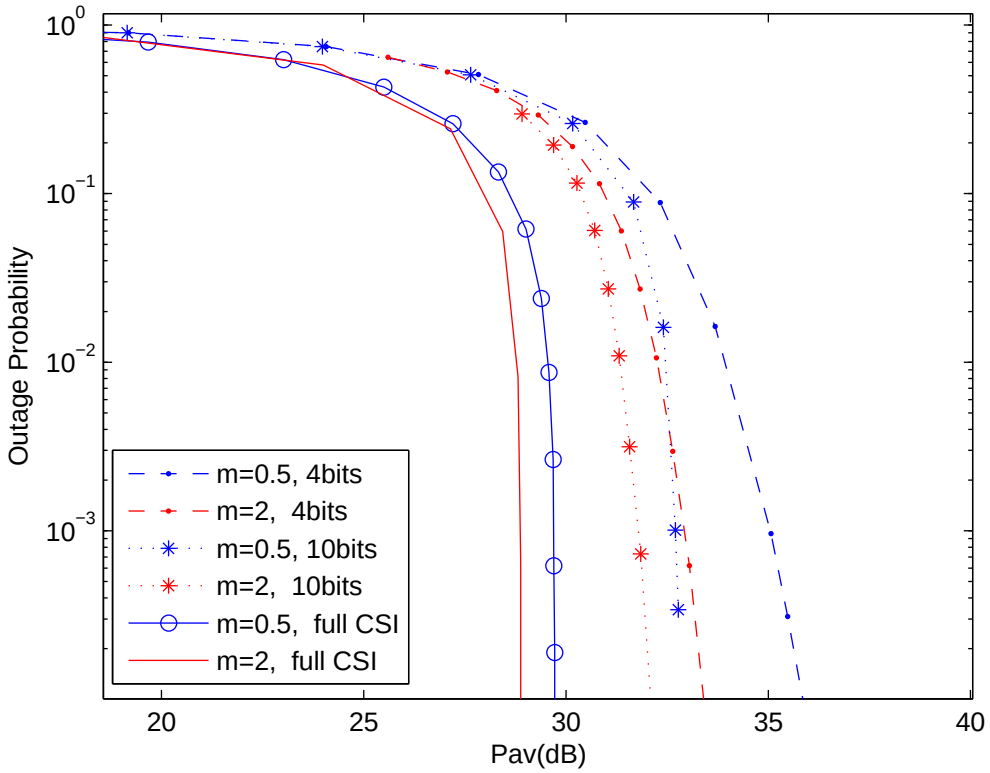

Figure 2.15: The outage performance of $M = 16$ channels with GA (m=0.5 and m=2).

2.7 Appendix

2.7.1 Proof of Lemma 2.1

The proof is similar to [105][71]. For all $j, 1 \leq j \leq L-1$, $\mathbf{P}(\mathbf{h}) = \mathbf{P}_j$, if $\mathbf{h} \in \mathcal{R}_j$, let $\mathcal{R}_j^*$ be the set of all $\mathbf{h}$ such that $\mathbf{P}_{j+1}^{\Sigma} < (\mathbf{P}^*(\mathbf{h}))^{\Sigma} \leq \mathbf{P}_j^{\Sigma}$, we need to prove that $\mathcal{R}_j^* = \mathcal{R}_j$. Assume the contrary, that $\mathcal{R}_j^* \backslash \mathcal{R}_j$ is a non empty set ($\backslash$ denotes the set subtraction operation), i.e, if $\mathbf{h} \in \mathcal{R}_j^* \backslash \mathcal{R}_j$, then $\mathbf{h} \in \mathcal{R}_j^*$ and $\mathbf{h} \notin \mathcal{R}_j$. And we can partition the set $\mathcal{R}_j^* \backslash \mathcal{R}_j$ into two subsets $\mathcal{R}_j^- = (\mathcal{R}_j^* \backslash \mathcal{R}_j) \bigcap (\bigcup_{k=1}^{j-1} \mathcal{R}_k)$ and $\mathcal{R}_j^+ = (\mathcal{R}_j^* \backslash \mathcal{R}_j) \bigcap (\bigcup_{k=j+1}^{L} \mathcal{R}_k)$. If the set $\mathcal{R}_j^-$ has nonzero probability, then we can construct a new scheme by assigning all elements of this set to $\mathcal{R}_j$ instead. Since $\forall \mathbf{h} \in \mathcal{R}_j^-, \mathbf{P}^*(\mathbf{h})^{\Sigma} \leq \mathbf{P}_j^{\Sigma}$, such rearrangement achieves the same outage probability but with less average power due to $\mathbf{P}_j^{\Sigma} < \mathbf{P}_k^{\Sigma}, 1 \leq k \leq j-1$, which is in contradiction with the optimality of the optimal solution $\mathcal{P}$ and $\mathcal{R}$. On the other hand, the set $\mathcal{R}_j^+$ is also an empty set, otherwise, we can easily see that this set is in outage (since $\forall \mathbf{h} \in \mathcal{R}_j^+, (\mathbf{P}^*(\mathbf{h}))^{\Sigma} > \mathbf{P}_{j+1}^{\Sigma}$), thus we have larger overall outage probability , which is also a contradiction. Therefore, we have $\mathcal{R}_j^* \subseteq \mathcal{R}_j$. We also can similarly prove $\mathcal{R}_L^* \subseteq \mathcal{R}_L$ as [105] did. Since $\bigcup_{j=1}^{L} \mathcal{R}_j^* = \bigcup_{j=1}^{L} \mathcal{R}_j$, we can conclude that $\mathcal{R}_j^* = \mathcal{R}_j, \forall j$.

2.7.2 Proof of Theorem 2.1

We introduce μ as the Lagrange multiplier associated with the average power constraint. The Lagrangian can be written as

$$\begin{aligned} J(\mathbf{P}, \mu) &= F'(\mathbf{P}_1) + \mu[\sum_{j=1}^{L-1}(\sum_{i=1}^{M} p_{ij})(F'(\mathbf{P}_{j+1}) - F'(\mathbf{P}_j)) \\ &\quad + (\sum_{i=1}^{M} p_{iL})(1 - F'(\mathbf{P}_L) + F'(\mathbf{P}_1)) - MP_{av}] \end{aligned} \tag{2.54}$$

Setting the first-order partial derivatives to zero (i.e, $\frac{\partial J}{\partial p_{ij}{}^*} = 0, i = 1, \ldots, M$, for $j = 1, \ldots, L$), produces

$$\frac{\partial J}{\partial p_{i1}{}^*} = (1 - \mu \sum_{i=1}^{M} p_{i1} + \mu \sum_{i=1}^{M} p_{iL}) \frac{\partial F'(\mathbf{P}_1)}{\partial p_{i1}{}^*} + \mu(F'(\mathbf{P}_2) - F'(\mathbf{P}_1)) = 0,$$

$$\begin{aligned}\frac{\partial J}{\partial {p_{ij}}^*} &= \mu[(\sum_{i=1}^{M} p_{i,j-1} - \sum_{i=1}^{M} p_{ij})\frac{\partial F'(\mathbf{P}_j)}{\partial {p_{ij}}^*} + (F'(\mathbf{P}_{j+1}) - F'(\mathbf{P}_j))] = 0, \quad 2 \le j \le L-1 \\ \frac{\partial J}{\partial {p_{iL}}^*} &= \mu[(\sum_{i=1}^{M} p_{i,L-1} - \sum_{i=1}^{M} p_{iL})\frac{\partial F'(\mathbf{P}_L)}{\partial {p_{ij}}^*} + (1 - F'(\mathbf{P}_L) + F'(\mathbf{P}_1))] = 0 \end{aligned} \tag{2.55}$$

Since $\mu \neq 0$ (note that otherwise $\frac{\partial F'(\mathbf{P}_1)}{\partial {p_{i1}}^*} = 0, i = 1, \ldots, M$ and since $F'(\mathbf{P}_1)$ is monotonically decreasing with p_{i1}, $\frac{\partial F'(\mathbf{P}_1)}{\partial {p_{i1}}^*} = 0$ implies ${p_{i1}}^* = \infty$, corresponding to infinite average power which is impossible), $F'(\mathbf{P}_2) \neq F'(\mathbf{P}_1)$, thus $(1 - \mu \sum_{i=1}^{M} p_{i1} + \mu \sum_{i=1}^{M} p_{iL})) \neq 0$. Simplifying (2.55), we have,

$$\begin{aligned}\frac{\partial F'(\mathbf{P}_1)}{\partial {p_{11}}^*} = \ldots = \frac{\partial F'(\mathbf{P}_1)}{\partial {p_{M1}}^*} &= -\frac{\mu(F'(\mathbf{P}_2) - F'(\mathbf{P}_1))}{1 - \mu \sum_{i=1}^{M}(p_{i1} - p_{iL})} \\ \frac{\partial F'(\mathbf{P}_j)}{\partial {p_{1j}}^*} = \ldots = \frac{\partial F'(\mathbf{P}_j)}{\partial {p_{Mj}}^*} &= -\frac{F'(\mathbf{P}_{j+1}) - F'(\mathbf{P}_j)}{\sum_{i=1}^{M}(p_{i,j-1} - p_{ij})}, \quad 2 \le j \le L-1 \\ \frac{\partial F'(\mathbf{P}_L)}{\partial {p_{1L}}^*} = \ldots = \frac{\partial F'(\mathbf{P}_L)}{\partial {p_{ML}}^*} &= -\frac{1 - F'(\mathbf{P}_L) + F'(\mathbf{P}_1)}{\sum_{i=1}^{M}(p_{i,L-1} - p_{iL})} \end{aligned} \tag{2.56}$$

Therefore, finally, we have

$$\frac{\partial F'(\mathbf{P}_j)}{\partial {p_{1j}}^*} = \ldots = \frac{\partial F'(\mathbf{P}_j)}{\partial {p_{Mj}}^*}, j = 1, \ldots, L \tag{2.57}$$

This completes the proof.

2.7.3 Proof of Theorem 2.2

In the multiple infinite series representation (2.19), for a sufficiently high P_{av}, we have $|-\frac{m_i \lambda_i K}{p_{ij}}| < 1, \ \forall i, j$. Thus from [38], the conditions of the convergence of the power series (2.20) are satisfied.

From (2.19), we have

$$\begin{aligned} F'(\mathbf{P}_j) &= \frac{1}{\Gamma(1 + \sum_{i=1}^{M} m_i)}[\prod_{i=1}^{M}(\frac{m_i \lambda_i K}{p_{ij}})^{m_i}] \sum_{n_1=0}^{\infty} \cdots \sum_{n_M=0}^{\infty} \frac{[\prod_{i=1}^{M}(m_i)_{n_i}(-\frac{m_i \lambda_i K}{p_{ij}})^{n_i} \frac{1}{n_i!}]}{(1 + \sum_{i=1}^{M} m_i)_{n_\tau}} \\ &= \frac{1}{\Gamma(1 + \sum_{i=1}^{M} m_i)}[\prod_{i=1}^{M}(\frac{m_i \lambda_i K}{p_{ij}})^{m_i}](1 + \sum_{\{n_1, \ldots, n_M \in \mathbb{Z} | \sum_{i=1}^{M} n_i = 1\}} T(n_1, \ldots, n_M) \frac{1}{\prod_{i=1}^{M} p_{ij}^{n_i}} \end{aligned}$$

$$+\ldots$$
$$+\sum_{\{n_1,\ldots,n_M\in\mathbb{Z}|\sum_{i=1}^{M}n_i=\infty\}} T(n_1,\ldots,n_M)\frac{1}{\prod_{i=1}^{M}p_{ij}^{n_i}}) \tag{2.58}$$

where $T(n_1,\ldots,n_M)=\frac{\prod_{i=1}^{M}(m_i)_{n_i}(-m_i\lambda_iK)^{n_i}\frac{1}{n_i!}}{(1+\sum_{i=1}^{M}m_i)_{n_\tau}}$ and $\mathbb{Z}$ is the set of non-negative integers.

Since in the high P_{av} regime, using the approximation $\frac{1}{\prod_{i=1}^{M}p_{ij}^{n_i}}\approx 0$ for $\sum_{i=1}^{M}n_i\geq 1$, we have

$$F'(\mathbf{P}_j)\approx\frac{1}{\Gamma(1+\sum_{i=1}^{M}m_i)}[\prod_{i=1}^{M}(\frac{m_i\lambda_iK}{p_{ij}})^{m_i}] \tag{2.59}$$

From (2.59), we have, for $i=1,\ldots,M$

$$\frac{\partial F'(\mathbf{P}_j)}{\partial p_{ij}}\approx-\frac{m_i}{p_{ij}}\frac{1}{\Gamma(1+\sum_{i=1}^{M}m_i)}\prod_{i=1}^{M}(\frac{m_i\lambda_iK}{p_{ij}})^{m_i} \tag{2.60}$$

Finally, by substituting (2.60) in Theorem 2.1, we have

$$\frac{m_i}{{p_{ij}}^*}\approx\frac{m_l}{{p_{lj}}^*},\quad i,l\in[1,M],i\neq l,j=1,\ldots,L \tag{2.61}$$

which completes the proof of Theorem 2.2.

2.7.4 Proof of Lemma 2.2

In [77], Moschopoulos justified the uniform convergence of the single infinite series in (2.21). With PFPPC, (2.21) can be rewritten as

$$F'(p_j) \;=\; \prod_{i=1}^{M}(\frac{\lambda_i}{\max(\lambda_i)})^{m_i}\sum_{n=0}^{\infty}\frac{\delta_n\gamma(\rho+n,\frac{Km_M\max(\lambda_i)}{p_j})}{\Gamma(\rho+n)} \tag{2.62}$$

where $\rho=\sum_{i=1}^{M}m_i\geq 0.5$ $(M\geq 1,m_i\geq 0.5)$ and the coefficients δ_n are obtained recursively by

$$\delta_{n+1}=\frac{1}{n+1}\sum_{l=1}^{n+1}[\delta_{n+1-l}\sum_{i=1}^{M}m_i(1-\frac{\lambda_i}{\max(\lambda_i)})^l],\ \delta_0=1,\ n=0,1,\ldots \tag{2.63}$$

In high the P_{av} regime ($P_{av} \to \infty$), $r_1 = \frac{K}{p_1} \to 0$, then with PFPPC, the total average power allocated to the outage region $\mathcal{R}_{L,1}$ is

$$\lim_{r_1 \to 0} P_{tot}^{L,1} = \lim_{r_1 \to 0} p_L F'(p_1) \tag{2.64}$$

We have

$$\begin{aligned}
\lim_{r_1 \to 0} p_L F'(p_1) &= \lim_{r_1 \to 0} \frac{p_L}{p_1} p_1 F'(p_1) \\
&= \lim_{r_1 \to 0} \frac{r_1}{r_L} K \frac{\prod_{i=1}^{M} (\frac{\lambda_i}{\max(\lambda_i)})^{m_i} \sum_{n=0}^{\infty} \frac{\delta_n \gamma(\rho+n, r_1 m_M \max(\lambda_i))}{\Gamma(\rho+n)}}{r_1} \\
&= \lim_{r_1 \to 0} \frac{r_1}{r_L} C \sum_{n=0}^{\infty} \frac{\delta_n (r_1 m_M \max(\lambda_i))^{\rho+n-1} e^{-r_1 m_M \max(\lambda_i)}}{\Gamma(\rho+n)} \\
&= \lim_{r_1 \to 0} \frac{r_1^{\rho}}{r_L} C',
\end{aligned} \tag{2.65}$$

where $C = K m_M \max(\lambda_i) \prod_{i=1}^{M} (\frac{\lambda_i}{\max(\lambda_i)})^{m_i}$ and $C' = C \frac{(m_M \max(\lambda_i))^{\rho-1}}{\Gamma(\rho)}$, and the last equality follows from the fact that when $n \geq 1$, the individual terms go to zero for any ρ, as $r_1 \to 0$.

From the proof of Theorem 2.3 (see below), we have

$$p_1 \approx \frac{P_{av}'^{\rho^{L-1}+\ldots+\rho+1}}{L^{\rho^{L-1}+\ldots+\rho+1} c^{\rho^{L-2}+\ldots+\rho+1}} = \frac{P_{av}'^{\sum_{i=0}^{L-1} \rho^i}}{C_1} \tag{2.66}$$

where $C_1 = L^{\rho^{L-1}+\ldots+\rho+1} c^{\rho^{L-2}+\ldots+\rho+1}$. Thus, we have

$$\lim_{r_1 \to 0} \frac{r_1^{\rho}}{r_L} C' = \lim_{P_{av} \to \infty} \frac{p_L}{p_1^{\rho}} C' K^{\rho-1} \approx \lim_{P_{av} \to \infty} p_L \frac{C_1^{\rho} C' K^{\rho-1}}{P_{av}'^{\sum_{i=1}^{L} \rho^i}} \tag{2.67}$$

Since from the proof of Theorem 2.3, we have $p_L \approx \frac{P_{av}'}{L}$,

$$\lim_{r_1 \to 0} \frac{r_1^{\rho}}{r_L} C' \approx \lim_{P_{av} \to \infty} \frac{C_1^{\rho} C' K^{\rho-1}}{L P_{av}'^{(\sum_{i=1}^{L} \rho^i)-1}} \tag{2.68}$$

Thus, if $(\sum_{i=1}^{L} \rho^i) - 1 > 0$, we have

$$\lim_{r_1 \to 0} \frac{r_1^{\rho}}{r_L} C' = 0 \tag{2.69}$$

This completes the proof of Lemma 2.2.

2.7.5 Proof of Theorem 2.3

In the high P_{av} regime, from Theorem 2.2, we have

$$F'(\mathbf{P}_j) \approx \frac{c}{p_j^{\sum_{i=1}^{M} m_i}} = \frac{c}{p_j^{\rho}}, \quad j = 1, \ldots, L \tag{2.70}$$

since $p_{ij} = \frac{m_i}{m_M} p_{Mj} = \frac{m_i}{m_M} p_j$. Here $c = \frac{\prod_{i=1}^{M} (m_M \lambda_i K)^{m_i}}{\Gamma(1+\rho)}$ where $\rho = \sum_{i=1}^{M} m_i$. When $P_{av} \to \infty$, according to [14], all the quantization thresholds approach zero, thus the length between any two quantization thresholds approaches zero as well resulting in the property that the total average power assigned to each quantization region is asymptotically equal. Thus, we have

$$\begin{aligned} p_j(F'(p_{j+1}) - F'(p_j)) &= \frac{P'_{av}}{L}, \quad j = 1, \ldots, L-1 \\ p_L(1 - F'(p_L) + F'(p_1)) &= \frac{P'_{av}}{L} \end{aligned} \tag{2.71}$$

where $P'_{av} = \frac{M m_M}{\rho} P_{av}$. Applying (2.70) to (2.71), we have for $j = 1, \ldots, L-1$,

$$\begin{aligned} p_j\left(\frac{c}{p_{j+1}^{\rho}} - \frac{c}{p_j^{\rho}}\right) &\approx \frac{P'_{av}}{L} \\ \frac{1}{p_{j+1}^{\rho}} &\approx \frac{\left(\frac{P'_{av}}{Lc}\right)}{p_j} + \frac{1}{p_j^{\rho}} \end{aligned} \tag{2.72}$$

It is clear to deduce that in the high P_{av} regime, for $M \geq 2$ and $M = 1,\ m \geq 1$, $\frac{1}{p_j^{\rho}}$ compared to $\frac{\left(\frac{P'_{av}}{Lc}\right)}{p_j}$ is negligible, thus (2.72) can be written as,

$$\begin{aligned} \frac{1}{p_{j+1}^{\rho}} &\approx \frac{\left(\frac{P'_{av}}{Lc}\right)}{p_j} \\ p_j &\approx p_{j+1}^{\rho} \frac{P'_{av}}{Lc} \end{aligned} \tag{2.73}$$

The same approximation can be shown to hold true for $M = 1,\ 0.5 \leq m < 1$ by contradiction, details are omitted due to space restrictions. Thus, we have,

$$p_1 \approx p_2^{\rho}\frac{P'_{av}}{Lc} \approx (p_3^{\rho}\frac{P'_{av}}{Lc})^{\rho}\frac{P'_{av}}{Lc} = p_3^{\rho^2}(\frac{P'_{av}}{Lc})^{\rho+1} \approx \ldots \approx p_L^{\rho^{L-1}}(\frac{P'_{av}}{Lc})^{\rho^{L-2}+\ldots+\rho+1} \quad (2.74)$$

Since $\lim_{P_{av}\to\infty} F'(p_1) = 0$, from (2.71) we have,

$$\begin{aligned} p_L(1 - F'(p_L)) &= \frac{P'_{av}}{L} \\ p_L(1 - \frac{c}{p_L^{\rho}}) &\approx \frac{P'_{av}}{L} \end{aligned} \quad (2.75)$$

Note that $\frac{c}{p_L^{\rho}}$ is negligible ($\to 0$) when P_{av} go to infinity, thus, we have,

$$p_L \approx \frac{P'_{av}}{L} \quad (2.76)$$

Applying (2.76) to (2.74), we have

$$p_1 \approx (\frac{P'_{av}}{L})^{\rho^{L-1}}(\frac{P'_{av}}{Lc})^{\rho^{L-2}+\ldots+\rho+1} = \frac{{P'_{av}}^{\rho^{L-1}+\ldots+\rho+1}}{L^{\rho^{L-1}+\ldots+\rho+1}c^{\rho^{L-2}+\ldots+\rho+1}} \quad (2.77)$$

Since,

$$\begin{aligned} P_{out} &= F'(\mathbf{P}_1) \\ &\approx \frac{c}{p_1^{\rho}} \\ &\approx c(\frac{L^{\rho^{L-1}+\ldots+\rho+1}c^{\rho^{L-2}+\ldots+\rho+1}}{{P'_{av}}^{\rho^{L-1}+\ldots+\rho+1}})^{\rho} \\ &= \frac{L^{\rho^{L}+\ldots+\rho}c^{\rho^{L-1}+\ldots+\rho+1}}{{P'_{av}}^{\rho^{L}+\ldots+\rho}} \\ &= \frac{(\frac{\rho L}{Mm_M})^{\rho^{L}+\ldots+\rho}c^{\rho^{L-1}+\ldots+\rho+1}}{{P_{av}}^{\rho^{L}+\ldots+\rho}} \end{aligned} \quad (2.78)$$

we have,

$$d = -\lim_{P_{av}\to\infty}\frac{\log P_{out}}{\log P_{av}}$$

$$\begin{aligned}
&\approx -\lim_{P_{av}\to\infty}\frac{\log((\frac{\rho L}{Mm_M})^{\rho^L+\ldots+\rho}c^{\rho^{L-1}+\ldots+\rho+1})}{\log P_{av}}+\lim_{P_{av}\to\infty}\frac{\log P_{av}^{\rho^L+\ldots+\rho}}{\log P_{av}}\\
&=0+\rho^L+\ldots+\rho\\
&=\sum_{j=1}^{L}\rho^j. \qquad (2.79)
\end{aligned}$$

This completes the proof of Theorem 2.3.

2.7.6 Proof of Theorem 2.4

Given a random variable $f_i \sim Gamma(m_i, \beta_i)$ (where m_i is the fading parameter satisfying $\frac{1}{2} \le m_i < \infty$) and $E[f_i] = m_i\beta_i = 1$, or $\beta_i = \frac{1}{m_i}$, we have $Var(f_i) = m_i\beta_i^2 = \beta_i$. So $0 < Var(f_i) \le 2 < \infty$.

Let $z_i = log(f_i)$, thus the moment-generating function of random variable z_i is

$$\begin{aligned}
M_{z_i}(t) = E(e^{tz_i}) = E(e^{tlog(f_i)}) &= E((f_i)^t)\\
&= \int_0^\infty f_i^t\,\frac{f_i^{m_i-1}}{\Gamma(m_i)\beta_i^{m_i}}e^{-\frac{f_i}{\beta_i}}df_i\\
&= \frac{\Gamma(m_i+t)\beta_i^{m_i+t}}{\Gamma(m_i)\beta_i^{m_i}}\int_0^\infty\frac{f_i^{t+m_i-1}}{\Gamma(m_i+t)\beta_i^{m_i+t}}e^{-\frac{f_i}{\beta_i}}df_i\\
&= \frac{\Gamma(m_i+t)\beta_i^{m_i+t}}{\Gamma(m_i)\beta_i^{m_i}}\\
&= \frac{\Gamma(m_i+t)\beta_i^{t}}{\Gamma(m_i)} \qquad (2.80)
\end{aligned}$$

Then,

$$\begin{aligned}
E(z_i) &= M_{z_i}^{(1)}(0)\\
&= \frac{d(\frac{\Gamma(m_i+t)\beta_i^t}{\Gamma(m_i)})}{dt}(0)\\
&= (\frac{\Gamma(m_i+t)'\beta_i^t}{\Gamma(m_i)}+\frac{\Gamma(m_i+t)\beta_i^t log(\beta_i)}{\Gamma(m_i)})(0)\\
&= \frac{\Gamma(m_i+t)'(0)}{\Gamma(m_i)}+log(\beta_i)\\
&= \frac{(\psi(m_i+t)\Gamma(m_i+t))(0)}{\Gamma(m_i)}+log(\beta_i)
\end{aligned}$$

$$= \psi(m_i) + log(\beta_i) \tag{2.81}$$

where $\psi(m_i)$ is digamma function [47]. Similarly,

$$\begin{aligned}
E(z_i^2) &= M_{z_i}^{(2)}(0) \\
&= \frac{d^2(\frac{\Gamma(m_i+t)\beta_i^t}{\Gamma(m_i)})}{dt^2}(0) \\
&= (\frac{\Gamma(m_i+t)''\beta_i^t}{\Gamma(m_i)} + 2\frac{\Gamma(m_i+t)'\beta_i^t log(\beta_i)}{\Gamma(m_i)} + \frac{\Gamma(m_i+t)\beta_i^t log^2(\beta_i)}{\Gamma(m_i)})(0) \\
&= \frac{\Gamma(m_i+t)''(0)}{\Gamma(m_i)} + 2\frac{\Gamma(m_i+t)'(0)log(\beta_i)}{\Gamma(m_i)} + log^2(\beta_i) \\
&= \frac{\Gamma(m_i+t)''(0)}{\Gamma(m_i)} + 2\frac{\Gamma(m_i+t)'(0)log(\beta_i)}{\Gamma(m_i)} + log^2(\beta_i) \\
&= \frac{\Gamma(m_i+t)''(0)}{\Gamma(m_i)} + 2\psi(m_i)log(\beta_i) + log^2(\beta_i) \\
&= \frac{(\psi(m_i+t)'\Gamma(m_i+t) + \psi(m_i+t)\Gamma(m_i+t)')(0)}{\Gamma(m_i)} + 2\psi(m_i)log(\beta_i) + log^2(\beta_i) \\
&= \frac{(\psi_1(m_i+t)\Gamma(m_i+t) + \psi(m_i+t)^2\Gamma(m_i+t))(0)}{\Gamma(m_i)} + 2\psi(m_i)log(\beta_i) + log^2(\beta_i) \\
&= \psi_1(m_i) + \psi(m_i)^2 + 2\psi(m_i)log(\beta_i) + log^2(\beta_i) \\
&= \psi_1(m_i) + (\psi(m_i) + log(\beta_i))^2
\end{aligned} \tag{2.82}$$

where $\psi_1(m_i)$ is trigamma function [47].

Let $\sigma_i^2 = Var(z_i)$, then we have

$$\begin{aligned}
\sigma_i^2 &= E(z_i^2) - (E(z_i))^2 \\
&= \psi_1(m_i) + (\psi(m_i) + log(\beta_i))^2 - (\psi(m_i) + log(\beta_i))^2 \\
&= \psi_1(m_i) \\
&= \sum_{n=0}^{\infty} \frac{1}{(m_i+n)^2}
\end{aligned} \tag{2.83}$$

Since $\frac{1}{2} \leq m_i < \infty$, we can obtain,

$$0 < \frac{1}{m_i^2} < \sigma_i^2 = \sum_{n=0}^{\infty} \frac{1}{(m_i+n)^2} \leq \psi_1(\frac{1}{2}) = \frac{\pi^2}{2} < \infty \tag{2.84}$$

Since $m_i < \infty$, there exist a large enough constant $\bar{C}$ so that $m_i \leq \bar{C} < \infty$. From (2.84), we have

$$0 < \frac{1}{\bar{C}^2} < \sigma_i^2 \leq \frac{\pi^2}{2} < \infty \tag{2.85}$$

Let $X_i = z_i - E(z_i)$, $S_n = \sum_{i=1}^{n} X_i$, $\sigma_n^2 = Var(S_n) = \sum_{i=1}^{n} \sigma_i^2$, then from (2.85) we have

$$\sigma_n^2 = \sum_{i=1}^{n} \sigma_i^2 > n\frac{1}{\bar{C}^2} \tag{2.86}$$

Thus, when $n \to \infty$, we have

$$\sigma_n^2 \to \infty \tag{2.87}$$

For every $\epsilon > 0$, using Chebyshev's Inequality, we can obtain,

$$P(|X_i| > \epsilon\sigma_n) \leq \frac{\sigma_i^2}{\epsilon^2\sigma_n^2} \leq \frac{max(\sigma_i^2)}{\epsilon^2\sigma_n^2} = \frac{\frac{\pi^2}{2}}{\epsilon^2\sigma_n^2} \to 0 \quad as \quad n \to \infty \tag{2.88}$$

Thus,

$$\begin{aligned}
\lim_{n\to\infty} \frac{1}{\sigma_n^2} \sum_{i=1}^{n} E(X_i^2 I\{|X_i| > \epsilon\sigma_n\}) &= \lim_{n\to\infty} \frac{1}{\sigma_n^2} \sum_{i=1}^{n} \sigma_i^2 \frac{1}{\sigma_i^2} E(X_i^2 I\{|X_i| > \epsilon\sigma_n\}) \\
&\leq \lim_{n\to\infty} \max(\frac{1}{\sigma_i^2} E(X_i^2 I\{|X_i| > \epsilon\sigma_n\})) \frac{1}{\sigma_n^2} \sum_{i=1}^{n} \sigma_i^2 \\
&= \lim_{n\to\infty} \max(\frac{1}{\sigma_i^2} E(X_i^2 I\{|X_i| > \epsilon\sigma_n\})) \\
&\leq \lim_{n\to\infty} \bar{C}^2 \max(E(X_i^2 I\{|X_i| > \epsilon\sigma_n\}))
\end{aligned} \tag{2.89}$$

where $I(A)$ denotes the indicator function taking the value 1 if the event A is true and taking the value 0 otherwise. Let Y_n denote the random variable $X_i^2 I\{|X_i| > \epsilon\sigma_n\}$, then Y_n is nonzero if and only if $|X_i| > \epsilon\sigma_n$. Since from (2.88), we know that this event has probability approaching zero as $n \to \infty$, we can also conclude that $Y_n \xrightarrow{\mathcal{P}} 0$ where $\xrightarrow{\mathcal{P}}$ denotes convergence in probability. Since $|Y_n| \leq X_i^2$ and $E(X_i^2) = \sigma_i^2 < \infty$, by applying the *Dominated Convergence Theorem*, we can conclude that $E(Y_n) \to 0$, namely,

$$E(X_i^2 I\{|X_i| > \epsilon\sigma_n\}) \to 0 \tag{2.90}$$

Applying the above result into (2.89), we have

$$\lim_{n\to\infty} \frac{1}{\sigma_n^2} \sum_{i=1}^{n} E(X_i^2 I\{|X_i| > \epsilon\sigma_n\}) = 0 \tag{2.91}$$

Thus, the Lindeberg condition holds, and X_i satisfies the Central limit theorem.

Chapter 3

Throughput Maximization in Cognitive Radio with Limited Feedback : Average Interference Constraints

3.1 Introduction

Scarcity of available vacant spectrum is limiting the growth of wireless products and services [59]. Traditional spectrum licensing policies suppress unfavorable interferences at the cost of spectral utilization efficiency. Cognitive radio (CR) technology significantly improves the efficiency of spectral utilization and largely alleviates the spectral scarcity. There are three categories of CR network paradigms: interweave, overlay, and underlay [9]. In the underlay systems, also known as spectrum sharing model, which is the focus of this chapter (also for chapter 4 and 5), the SU can transmit even when the PU is present, but the transmitted power of SU should be controlled properly so as to ensure that the resulting interference does not degrade the received signal quality of PU to an undesirable level [117] by imposing the so called interference temperature [7] constraints at PU (average or peak interference power (AIP/PIP) constraint) and as well as to enhance the performance of the SU-TX to SU-RX links.

It is well known that the knowledge of the channel CSI is crucial in designing the transmit power control of SU. Most of current literatures, such as [7], [45], [66],[117],[28], assume perfect knowledge of full CSI available at SU-TX, which is very difficult to implement in practice, especially the channel information from SU-TX to PU-RX without

PU's cooperation. A few recent papers have emerged that address this concern by investigating performance analysis with various forms of partial CSI at SU-TX, such as noisy CSI and quantized CSI. With assumption of perfect knowledge of the CSI from SU-TX to SU-RX channel, the authors of [67] studied the effect of imperfect channel information for the SU-TX to PU-RX channels under AIP or PIP constraint by considering the channel information from SU-TX to the PU-RX as a noisy estimate of the true CSI, and employing the so-called 'tifr' transmission policy. Another recent work [46] also considers imperfect CSI for the SU-TX to PU-RX channel in the form of noisy channel estimate (a range from near-perfect to seriously flowed estimates) and studied the effect of using midriser uniform quantization CSI, while also assuming SU-TX can access full knowledge of the SU-TX to SU-RX channel. In [84], the authors presented a new coding which can achieve better error performance for cognitive radio when there is only partial CSIT. In [60], the authors has proposed a practical design paradigm for cognitive beamforming based on finite-rate cooperative feedback from the PU-RX to the SU-TX and cooperative feedforward from the SU-TX to the PU-RX. Finally, the authors of [17] studied the issue of channel quantization for resource allocation via the framework of utility maximization in OFDMA based CR networks, but does not investigate the joint channel partitioning and rate/power codebook design problem. Indeed, the lack of a rigorous and systematic design methodology for quantized resource allocation algorithms in the context of cognitive radio networks forms the key motivation for our work.

In this chapter, we consider the uplink of an *infrastructure-based* wideband spectrum sharing system where one SU shares M different frequency bands with M PU's, each PU using a separate band. We address the problem of ergodic capacity maximization of the secondary user subject to an long term average sum (across the bands) transmit power constraint on the secondary user and M individual average interference constraints on each primary user, using quantized channel information about the vector channel space consisting of all SU-TX to SU-Rx (contained in the SU Base station (SU-BS)) channels and all SU-TX to PU-RX (contained in the primary base station (PU-BS)) channels. To this end, we assume the availability of an entity called CR network manager who has access to the full CSI including all secondary-to-secondary and secondary-to-primary

channels via (possibly fibre-optic) links with the primary and secondary base stations, which in turn are assumed to have receiver side full CSI of the secondary to primary and secondary-to-secondary channels, respectively. An optimal power codebook is designed off-line based on the statistical information (channel distributions) of the channels and is known by both the SU-TX the CR network manager, and then in real-time, the CR network manager feeds back the index of the codebook to the secondary transmitter for every channel realization, via a B-bits per band finite-rate feedback link. The secondary transmitter then uses the corresponding power code vector for its transmission.

We make the following key contributions: (1) First and foremost, we present a modified Generalized Lloyd's type algorithm (GLA) for designing the optimal power codebook using quantized channel information. For easier exposition, we focus on the narrowband case first and derive the quantized power allocation algorithm, where we prove that the modified GLA based power codebook design algorithm is globally convergent and empirically consistent. We provide a number of useful and interesting properties of the quantized powers. Then we present a complete description of the optimal power codebook design algorithm for the wideband spectrum sharing case under the average transmit power and average interference power constraints. We believe this chapter is the first to provide a systematic quantized power allocation algorithm with limited feedback for the spectrum sharing scenario in cognitive radio. (2) Although an offline algorithm, GLA based quantizer designs usually require a large number of training samples and can be computationally expensive. We therefore design an approximate quantized power allocation algorithm based on the derived properties of the power codebook, which is computationally significantly faster and is seen to have much better performance compared to other suboptimal algorithms. (3) We then generalize the modified GLA based algorithm for quantized power allocation algorithm to the case where the limited feedback channel is noisy but memoryless. (4) We present a comprehensive set of numerical results which illustrate that (i) the modified GLA-based power codebook can achieve a secondary ergodic capacity with only 3-4 bits of feedback at each band, that is very close to the capacity with full CSI, (ii) the performance of the approximate quantized power allocation algorithm is almost indistinguishable from that of the GLA-based algorithm

with $B \geq 4$ bits per band of feedback and (iii) how the performance of the quantized power allocation degrades when the noisy feedback channel error probability increases.

This chapter is organized as follows. Section 3.2 presents the system model and assumptions about the spectrum sharing problem, and derives the optimal power allocation policy for ergodic capacity of SU maximization problem based on full CSI assumption. In Section 3.3, we provide the modified GLA based quantized power codebook design algorithms along with associated convergence results and some useful properties of the quantized power vectors. The approximate quantized power allocation algorithm (AQPA) and two other suboptimal algorithms are also presented. In Section 3.4, we extend the modified GLA based power codebook design algorithm to a noisy limited feedback channel model. Numerical results are presented in Section 3.5 and finally, concluding remarks and possible extensions are presented in Section 3.6. All proofs are relegated to the appendix section 3.7 in this chapter.

3.2 System Model and Problem Formulation

We consider the uplink of a wideband spectrum sharing scenario in an infrastructure-based cognitive radio network with one SU and Multiple PUs, as shown in Fig. 3.1, where a SU is allowed to use M parallel orthogonal frequency bands ($Band_1$ to $Band_M$) which are individually licensed to $PU_1, \ldots, PU_M$ respectively. Regardless of the ON/OFF status of PU_i, SU uses the i-th channel as long as the impact of the secondary transmission does not substantially degrade the received signal quality PU_i. It is assumed that the channels between the secondary transmitter (SU-TX) and secondary receiver (SU-RX) and those between the secondary transmitter and the each primary receiver are all block fading channels. Let g_0^i and g_1^i denote the real-valued instantaneous channel power gains for the link between the SU-TX and the receiver of PU_i (at the PU-BS) and i-th channel between the SU-TX and SU-RX (at the SU-BS) [1], respectively. These channels are assumed to be stationary ergodic with absolutely continuous probability density functions

[1]Fig. 3.1 also shows that the PU-BS and SU-BS are connected (possibly via fibre-optic links) to a central controller called the CR network manager, the existence of which is crucial in designing the power allocation algorithms in the quantized feedback case (see Section 3.3 for further details).

(pdf) $f_0(g_0^i)$ and $f_1(g_1^i)$. For analytical simplicity, the interference from PU_i-TX to SU-RX is neglected (similarly as in [7, 117]). In the case where the interference caused by the primary transmitter at the secondary receiver is significant, the SU ergodic capacity results derived in this chapter can be taken as upper bounds on the actual capacity under primary-induced interference. This assumption is justified when either the SU is outside the PUs transmission range or the SU receiver is equipped with interference cancellation capability particularly when the PU signal is strong. All g_0^i and g_1^i ($i = 1, \ldots, M$) are statistically mutually independent, and without loss of generality [2] (*w.l.o.g*) are assumed to have unity mean. Similarly, additive noises for each channel are independent Gaussian random variables with zero mean and unit variance *w.l.o.g*. When $M = 1$, this system becomes a typical narrowband spectrum sharing model considered in [7],[123],[117].

Given a channel realization $\mathbf{g}_0 = \{g_0^1, \ldots, g_0^M\}$ and $\mathbf{g}_1 = \{g_1^1, \ldots, g_1^M\}$, we assume that a channel side information (CSI) $\eta(\mathbf{g}_0, \mathbf{g}_1)$ is available at the SU-TX. The power allocated at the SU-TX on the M parallel SU links is represented by the vector $\mathbf{p}(\eta(\mathbf{g}_0, \mathbf{g}_1)) = \{p_1(\eta(\mathbf{g}_0, \mathbf{g}_1)), \ldots, p_M(\eta(\mathbf{g}_0, \mathbf{g}_1))\}$, the ergodic capacity of the SU for this wideband spectrum sharing system can be expressed as

$$C = \frac{1}{M} \sum_{i=1}^{M} E\left[\log\left(1 + g_1^i p_i(\eta(\mathbf{g}_0, \mathbf{g}_1))\right)\right] \tag{3.1}$$

where, for simplicity, we have ignored the factor $\frac{1}{2}$ at the front of the capacity expression and log represents the natural logarithm. Note also that the factor $1/M$ in front of the capacity formula above is not strictly necessary for the problem formulation and since M is fixed for the problem, inclusion or exclusion of it does not change the solution techniques and the results (except for a scaling factor). However, channel capacity is usually expressed in terms of per degree of freedom and in order to have a fair comparison of capacities for various values of M, it is common practice to normalize it by the number of degrees of freedom, in this case, M. A similar formulation can be found in the paper

[2] Note that here the secondary-to-primary and secondary-to-secondary fading channel power gains are modelled as $g_p^i = m_0^i g_0^i$ and $g_s^i = m_1^i g_1^i$, respectively where m_0^i, m_1^i are the corresponding means, and g_0^i, g_1^i have unity mean. It can be easily seen from (3.2) that any non-unity mean m_0^i can be absorbed into the average interference threshold Q_{avg}^i and any non-unity mean m_1^i can be absorbed into $p_i(.)$, the secondary transmission power on the i-th band.

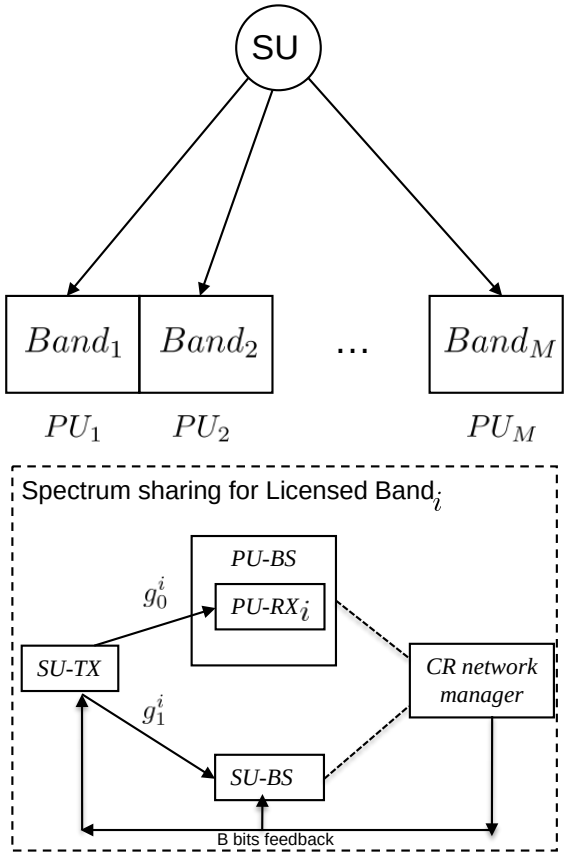

Figure 3.1: System model for wideband spectrum-sharing scenario

[53].

A common way to protect PU's received signal quality is by imposing either an average or a peak interference power (AIP/PIP) constraint at PU-RX [7][123][117], although there are other forms of PU quality of service constraints such as PU's capacity loss and PU's outage probability [91]. It was shown in [123] that an AIP constraint is more favorable than a peak constraint especially in the context of transmission over fading channels, since the AIP constraint is more flexible and can achieve a larger SU capacity with less PU capacity loss than that achieved by PIP.

Motivated by this observation, we consider the following optimal power allocation problem that maximizes the ergodic capacity of SU in a wideband spectrum sharing scenario, under an AIP constraint at each PU_i-RX and an average sum transmit power

constraint (ATP) for the SU, given by,

$$\begin{aligned} \max_{p_i(\eta(\mathbf{g}_0,\mathbf{g}_1))\geq 0,\forall i} \quad & \frac{1}{M}\sum_{i=1}^{M} E\left[\log\left(1+g_1^i p_i(\eta(\mathbf{g}_0,\mathbf{g}_1))\right)\right] \\ s.t. \quad & E\left[g_0^i p_i(\eta(\mathbf{g}_0,\mathbf{g}_1))\right] \leq Q_{avg}^i, \ \ \forall i, \\ & \frac{1}{M}\sum_{i=1}^{M} E\left[p_i(\eta(\mathbf{g}_0,\mathbf{g}_1))\right] \leq P_{avg}. \end{aligned} \tag{3.2}$$

When full channel state information (CSI) is available at the SU-Tx (i.e, $\eta(\mathbf{g}_0,\mathbf{g}_1) = (\mathbf{g}_0,\mathbf{g}_1)$), the optimization problem is convex and the corresponding optimal secondary transmitter power allocation policy is given by the following Theorem (here the term "iff" refers to "if and only if").

Theorem 3.1. *With perfect channel information $\eta(\boldsymbol{g}_0,\boldsymbol{g}_1) = (\boldsymbol{g}_0,\boldsymbol{g}_1)$ at the SU-TX, the optimal power allocation for problem (3.2) is given by*

$$p_i^*(\boldsymbol{g}_0,\boldsymbol{g}_1) = \begin{cases} \left(\frac{1}{\mu_i^f g_0^i} - \frac{1}{g_1^i}\right)^+ & \text{iff } P_{avg} \geq \frac{1}{M}\sum_{i=1}^{M} E\left[\left(\frac{1}{\mu_i^f g_0^i} - \frac{1}{g_1^i}\right)^+\right] \quad (a) \\ \begin{cases} \left(\frac{1}{\lambda^f} - \frac{1}{g_1^i}\right)^+ & \text{iff } E\left[\left(\frac{1}{\lambda^f} - \frac{1}{g_1^i}\right)^+\right] \leq Q_{avg}^i \quad (b) \\ \left(\frac{1}{\lambda^f+\mu_i^f g_0^i} - \frac{1}{g_1^i}\right)^+ & \text{otherwise} \quad (c) \end{cases} & \text{otherwise} \end{cases} \tag{3.3}$$

where $(x)^+ = max(x,0)$ and λ^f, μ_f^i are the nonnegative Lagrange multipliers associated with the ATP constraint and the AIP constraint of PU_i respectively, and condition (a) corresponds to the case $\lambda^f = 0, \mu_f^i > 0, \forall i$ and μ_f^i is determined by solving $E\left[g_0^i\left(\frac{1}{\mu_i^f g_0^i} - \frac{1}{g_1^i}\right)^+\right] = Q_{avg}^i$, condition (b) corresponds to the case $\lambda^f > 0, \mu_f^i = 0$ where λ^f is determined by solving $\frac{1}{M}\sum_{i=1}^{M} E\left[\left(\frac{1}{\lambda^f} - \frac{1}{g_1^i}\right)^+\right] = P_{avg}$, and condition (c) corresponds to the case $\lambda^f > 0, \mu_f^i > 0$ such that λ^f and μ_f^i are determined by solving $\frac{1}{M}\sum_{i=1}^{M} E\left[\left(\frac{1}{\lambda^f+\mu_i^f g_0^i} - \frac{1}{g_1^i}\right)^+\right] = P_{avg}$ and $E\left[g_0^i\left(\frac{1}{\lambda^f+\mu_i^f g_0^i} - \frac{1}{g_1^i}\right)^+\right] = Q_{avg}^i$.

Proof: The proof can be found in the appendix of this chapter.

One can also easily obtain the following *special cases* :

1) When $M = 1$(narrowband spectrum sharing case), from theorem 3.1, the condition

(b)(i.e, $E[(\frac{1}{\lambda^f} - \frac{1}{g_1^1})^+] \leq Q_{avg}$) becomes $P_{avg} \leq Q_{avg}$ (note that we have removed the superscript from Q_{avg} as there is only one primary user), and the optimal power allocation solution specialises to the one presented in [117].

2) When $\mu_i = 0 \ \forall i$, i.e, only ATP is active, for this case, if additionally $\mathbf{g}_1$ are indepedent and identically distributed, we must have $P_{avg} \leq min(Q_{avg}^1, \ldots, Q_{avg}^M)$.

3) If $Q_{avg}^1 = \cdots = Q_{avg}^M = Q_{avg}$ and both $\mathbf{g}_0$ and $\mathbf{g}_1$ are indepedent and identically distributed, the optimal power allocation policy is to assign equal power to each SU link, and the power value is identical to the power allocation policy for the $M = 1$ case.

Appealing to the convexity of Problem (3.2), one can show that in Theorem 3.1, one of the cases must hold, and the corresponding power allocation scheme must be the global optimal solution for the original problem (3.2). An algorithm can be then easily designed to obtain $p_i^*(\mathbf{g}_0, \mathbf{g}_1)$, and the associated non-zero Lagrange multipliers can be obtained by solving the corresponding KKT complementary slackness condition numerically.

3.3 Optimum Quantized Power Control with Finite-Rate Feedback

The assumption of full CSI at the SU-TX (especially that of $\mathbf{g}_0$) is usually unrealistic in practical systems. In this section, we are therefore interested in designing power allocation schemes based on quantized ($\mathbf{g}_0$, $\mathbf{g}_1$) information acquired via a no-delay and error-free feedback link with limited rate. As shown in Fig. 3.1, here we assume that there is a central controller termed as the CR network manager who can obtain perfect information on $\mathbf{g}_1$ from SU-RX at the SU base station and perfect information on $\mathbf{g}_0$ from the PU base station, possibly over fibre-optic links and then forward some appropriately quantized CSI to SU-TX (and SU-RX for decoding purposes) through a finite-rate feedback link. Note that existence of such central controllers is also assumed quite commonly in literature on multi-cell MIMO or macro-diversity based systems with cooperative base stations in a primary network, where several base stations are assumed to be connected to a central controller via a backhaul link so that information about out-of-cell interference

can be obtained resulting in higher capacity [22,88]. If cognitive radio networks are to be successful, it is imperative that the primary users cooperate with the CR service provider at some level. In our model, we assume this cooperation in terms of primary channel information sharing with the CR network manager via the PU-BS. Any cost incurred by the CR service provider as a result of obtaining this information from the PU-BS can be recovered by charging the secondary users a nominal price. This assumption is further (and perhaps more crucially) justified by the fact that having full CSI about the joint channel space $\mathbf{g}_0, \mathbf{g}_1$ allows the CR network manager to design a joint channel quantizer and power codebook that has a far superior performance than quantizing $\mathbf{g}_0$ and $\mathbf{g}_1$ separately in the absence of this central controller, which is clearly suboptimal (see Section 3.5 on *Numerical Results* for further details).

In order to formulate the optimal power allocation with quantized channel feedback, we first make the observation that due to convexity of the original problem (3.2), it can be solved by the Lagrange duality method, namely, by solving the dual problem of (3.2):

$$\min_{\lambda^f \geq 0,\ \mu_i^f \geq 0, \forall i} g(\lambda^f, \{\mu_i^f\}) + \lambda_f P_{avg} + \sum_{i=1}^{M} \mu_i^f Q_{avg}^i, \tag{3.4}$$

where the Lagrange dual function is given by

$$\begin{aligned} g(\lambda^f, \{\mu_i^f\}) = \max_{p_i(\eta(\mathbf{g}_0,\mathbf{g}_1)) \geq 0, \forall i} \quad & \frac{1}{M} \sum_{i=1}^{M} E[\log\left(1 + g_1^i p_i(\eta(\mathbf{g}_0, \mathbf{g}_1))\right) \\ & - \lambda^f p_i(\eta(\mathbf{g}_0, \mathbf{g}_1)) - M\mu_i^f g_0^i p_i(\eta(\mathbf{g}_0, \mathbf{g}_1))]. \end{aligned} \tag{3.5}$$

Here $g(\lambda^f, \{\mu_i^f\})$ can be decomposed into M parallel subproblems, which for band $i, i = 1, \ldots, M$ is given by

$$\max_{p_i(\eta(\mathbf{g}_0,\mathbf{g}_1)) \geq 0, \forall i} E\left[\log\left(1 + g_1^i p_i(\eta(\mathbf{g}_0, \mathbf{g}_1))\right) - \lambda^f p_i(\eta(\mathbf{g}_0, \mathbf{g}_1)) - M\mu_i^f g_0^i p_i(\eta(\mathbf{g}_0, \mathbf{g}_1))\right] \tag{3.6}$$

which implies given λ^f and $\mu_i^f, i = 1, 2, \ldots, M$, we can solve the above problem individually for each band. This observation motivates us to formulate Problem (3.2) with quantization channel feedback individually for each band as described below.

Under the network modelling assumptions described above, given a B-bit per band limited feedback link between the CR network manager and the SU-TX, the power codebook for i-th band ($i = 1, \ldots, M$) given by $\mathcal{P}_i = \{p_{i1}, \ldots, p_{iL}\}$ of cardinality $L = 2^B$, is designed by the CR network manager off-line purely on the basis of the statistics of g_0^i, g_1^i. These codebooks $\mathcal{P}_1, \ldots, \mathcal{P}_M$ are known *a priori* by both SU-TX and CR network manager. For the i-th band, the vector space of (g_0^i, g_1^i) is thus partitioned into L regions $\mathcal{R}_1^i, \ldots, \mathcal{R}_L^i$ using a quantizer $\mathcal{Q}_i$ (such that the codebook element p_{ij} represents the power level used in $\mathcal{R}_j^i$). For the i-th band, the CR network manager maps the current instantaneous (g_0^i, g_1^i) information into one of L integer indices and sends the corresponding index to the SU-TX via the feedback link of rate $B = \log_2 L$ (e.g., if the current (g_0^i, g_1^i) falls in $\mathcal{R}_j^i$, then index j for i-th band will be conveyed back to SU-TX). The SU-TX will use the associated power codebook element p_{ij} as the transmission power to adapt its transmission strategy for the band i.

Remark 3.1. *Note that it is possible to consider different feedback bit rates for different bands and our analysis can be adapted to this scenario, but for simplicity and also due to the fact that all bands are assumed to be statistically* i.i.d.*, we use identical B bits of feedback for each band.*

Let $Pr(\mathcal{R}_j^i)$, $E[\bullet|\mathcal{R}_j^i]$ denote $Pr((g_0^i, g_1^i) \in \mathcal{R}_j^i)$ (the probability that (g_0^i, g_1^i) falls in the region $\mathcal{R}_j^i$) and $E[\bullet|(g_0^i, g_1^i) \in \mathcal{R}_j^i]$, respectively. Then the secondary ergodic capacity maximization problem (3.2) with limited feedback can be formulated as

$$\begin{aligned} \max_{p_{ij} \geq 0, \forall i,j} \frac{1}{M} \sum_{i=1}^{M} \left(\sum_{j=1}^{L} E\left[\log(1 + g_1^i p_{ij}) | \mathcal{R}_j^i\right] Pr(\mathcal{R}_j^i) \right) \\ s.t. \ \sum_{j=1}^{L} E[g_0^i p_{ij} | \mathcal{R}_j^i] Pr(\mathcal{R}_j^i) \leq Q_{avg}^i, \ \forall i, \\ \frac{1}{M} \sum_{i=1}^{M} \left(\sum_{j=1}^{L} E[p_{ij} | \mathcal{R}_j^i] Pr(\mathcal{R}_j^i) \right) \leq P_{avg}. \end{aligned} \tag{3.7}$$

Our objective is thus the joint optimization of the channel partition regions and the power codebooks such that the ergodic capacity of SU is maximized under the above average transmit power and average interference constraints.

3.3.1 Narrowband spectrum-sharing case

For ease of exposition, we first look at the relatively simpler case of $M = 1$ (where SU shares a narrowband spectrum with only one PU). For simplicity (with some abuse of notation), let $p_j, g_1, g_0, Q_{avg}, \mathcal{R}_j$ represent $p_{1j}, g_1^1, g_0^1, Q_{avg}^1, \mathcal{R}_j^1$ respectively. Thus problem (3.7) with $M = 1$ becomes,

$$\begin{aligned} \max_{p_j \geq 0, \forall j} \; & \sum_{j=1}^{L} E\left[\log(1 + g_1 p_j) | \mathcal{R}_j\right] Pr(\mathcal{R}_j) \\ s.t. \; & \sum_{j=1}^{L} E[g_0 p_j | \mathcal{R}_j] Pr(\mathcal{R}_j) \leq Q_{avg}, \\ & \sum_{j=1}^{L} p_j Pr(\mathcal{R}_j) \leq P_{avg} \end{aligned} \tag{3.8}$$

We solve the problem (3.8) based on the Lagrange duality method. First we write the Lagrangian of above problem as $L(P, \lambda, \mu) = \sum_{j=1}^{L} E[\log(1 + g_1 p_j) - \lambda p_j - \mu g_0 p_j | \mathcal{R}_j] Pr(\mathcal{R}_j) + \lambda P_{avg} + \mu Q_{avg}$ where λ and μ are the nonnegative Lagrange multipliers associated with the ATP constraint and AIP constraint respectively. The Lagrange dual function $g(\lambda, \mu)$ is defined as

$$\max_{p_j \geq 0 \; \forall j} \sum_{j=1}^{L} E[\log(1 + g_1 p_j) - \lambda p_j - \mu g_0 p_j | \mathcal{R}_j] Pr(\mathcal{R}_j) \tag{3.9}$$

and the corresponding dual problem is $\min_{\lambda \geq 0, \; \mu \geq 0} g(\lambda, \mu) + \lambda P_{avg} + \mu Q_{avg}$.

We first consider solving the above primal optimization problem with fixed λ and μ. To this end, we employ an algorithm similar to a Generalized Lloyd Algorithm (GLA) [6, 120] to design an optimal power codebook for (3.9), which is based on two optimality conditions : 1) optimum channel partitioning for a given codebook, also called the nearest neighbor condition (NNC) in the context of traditional vector quantization (VQ), and 2) optimum codebook design for a given partition, also known as the centroid condition (CC) (in the context of VQ) [6]. GLA is usually initialized with a random choice of codebook, and then the above two conditions are iterated until some pre-specified convergence criterion is met. The same procedure is used here for designing an optimal quantizer $\mathcal{Q}$, but the design criterion for our case is minimizing the difference between the capacity with perfect CSI and the capacity with quantized power allocation under the given

constraints. This amounts to designing an optimal power codebook $\mathcal{Q}$ that maximizes the Lagrangian function for quantized CSI, $\sum_{j=1}^{L} E[\log(1+g_1p_j) - \lambda p_j - \mu g_0 p_j | \mathcal{R}_j] Pr(\mathcal{R}_j)$. We call the corresponding quantized power allocation algorithm for a given λ, μ as a *modified GLA*.

In practice, this modified GLA is implemented using a sufficiently large number of training samples (channel realizations for g_0, g_1). Beginning with a random initial codebook, one can design the optimal partitions using the fact that the optimal partitions satisfy $\mathcal{R}_j = \{(g_0, g_1) : (\log(1+g_1p_j) - \lambda p_j - \mu g_0 p_j) \geq (\log(1+g_1p_n) - \lambda p_n - \mu g_0 p_n), \forall n \neq j\}$ where $\mathcal{R}_j$ is the corresponding partition region for power level p_j in the codebook, and ties are broken arbitrarily. Once the optimal partitions are designed, the new optimal power codebook is found by solving for $\text{argmax}_{p_j \geq 0} E[\log(1+g_1p_j) - \lambda p_j - \mu g_0 p_j | \mathcal{R}_j] Pr(\mathcal{R}_j)$, $\forall j = 1, 2, \ldots, L$. Given a partition, this optimization problem is convex and by using the KKT conditions, one can obtain the optimal power as $\max(p_j^*, 0)$, where p_j^* is the solution to the equation $E[\frac{g_1}{1+g_1p_j} - (\lambda + \mu g_0) | \mathcal{R}_j] = 0$. These two steps are repeated until the resulting ergodic capacity converges within a pre-specified accuracy. One needs to note that GLA cannot in general guarantee global optimality, since the two optimality conditions (NNC and CC) mentioned above are just necessary conditions [6]. Thus it is very likely that the our resulting quantizer is only locally optimal. While convergence (to a local optimum) of our modified GLA follows immediately by noting that the Lagrangian $\sum_{j=1}^{L} E[\log(1+g_1p_j) - \lambda p_j - \mu g_0 p_j | \mathcal{R}_j] Pr(\mathcal{R}_j)$ is non-decreasing at each iteration and is upper bounded (due to the finite average transmit power and average interference constraints), it is important and instructive to state a more formal result along the lines of [76]. Since GLA is initialized with a random codebook and the optimal partitions and codevectors are found using training samples drawn from empirical distributions, it is crucial that GLA is globally convergent with respect to the choice of initial codebooks and empirically consistent. For more formal definitions of these two properties, see [76]. Under the assumption of absolutely continuous fading distributions for g_0, g_1 and mild regularity assumptions satisfied by these distributions, one can show that the modified GLA satisfies the conditions for global convergence and empirical consistency stated in [76] and thus we have the following result:

Theorem 3.2. *The modified GLA that solves the optimization problem (3.9) satisfies the global convergence and empirical consistency properties of [76].*

Proof: The proof can be found in the appendix of this chapter.

Next, we present some useful properties of the optimal power solutions obtained via the modified GLA. We use the partitions $\mathcal{R}_1, \ldots, \mathcal{R}_L$ and the corresponding power levels $p_1, \ldots, p_L$ to denote the optimal solutions after convergence. First, we state the following Lemma from where we can obtain optimum partition regions structure:

Lemma 3.1. *Given partitions $\mathcal{R}_1, \ldots, \mathcal{R}_L$ and the corresponding power level $p_1, \ldots, p_L$, (where $\mathcal{R}_j$ and $\mathcal{R}_{j+1}, \forall j \in \{1, \ldots, L-1\}$ are adjacent regions and $p_j \neq p_{j+1}$), the boundary between any two adjacent regions $\mathcal{R}_j$ and $\mathcal{R}_{j+1}$ is given by,*

$$g_1 = \frac{e^{(\lambda+\mu g_0)(p_j - p_{j+1})} - 1}{p_j - p_{j+1} e^{(\lambda+\mu g_0)(p_j - p_{j+1})}}. \tag{3.10}$$

When $\mu \neq 0$, g_1 is a monotonically increasing convex function of g_0 and as $g_1 \to \infty$, $g_0 \to \frac{1}{\mu}\left(\frac{\log(\frac{p_j}{p_{j+1}})}{p_j - p_{j+1}} - \lambda\right)$.

Proof: The proof can be found in the appendix of this chapter.

Remark 3.2. *In case $\lambda > 0, \mu = 0$, the AIP constraint is inactive and the ATP constraint is satisfied with equality. In this case, the boundary between any two adjacent regions $\mathcal{R}_j$ and $\mathcal{R}_{j+1}$ becomes $g_1 = \frac{e^{\lambda(p_j - p_{j+1})} - 1}{p_j - p_{j+1} e^{\lambda(p_j - p_{j+1})}}$. Clearly, Problem (3.7) reduces to an ergodic capacity maximization problem with quantized channel information. For the narrowband case, it becomes a scalar quantization problem involving quantizing g_1 only. Note that while for the narrowband case, this no longer pertains to a cognitive radio problem, these properties of the optimal quantized power allocation scheme are still important for the wideband case ($M > 1$). This is due to the fact that in the wideband case, it is possible that for a specific (say the i-th) channel, the AIP constraint is inactive ($\mu_i > 0$) while $\lambda > 0$. See Section 3.3.2 for further details.*

We now give an example to illustrate what the optimum partition regions actually look like. For this example, g_0 and g_1 are both exponentially distributed (Rayleigh fading) with unit mean and $L = 4$ (2 bits of feedback). The optimum partition regions are as

shown in Fig. 3.2 for $\lambda > 0, \mu > 0$, and Fig. 3.3 for $\lambda > 0, \mu = 0$.

We obtain the following properties for the optimal quantized power levels where (as illustrated in Fig. 3.2) the regions $\mathcal{R}_1, \mathcal{R}_2, \ldots$ etc. are sequentially numbered, with $\mathcal{R}_1$ being the region closest to the g_1 axis and $\mathcal{R}_L$ being the region closest to the g_0 axis. Note that these properties apply regardless of whether $\mu > 0$ or $\mu = 0$.

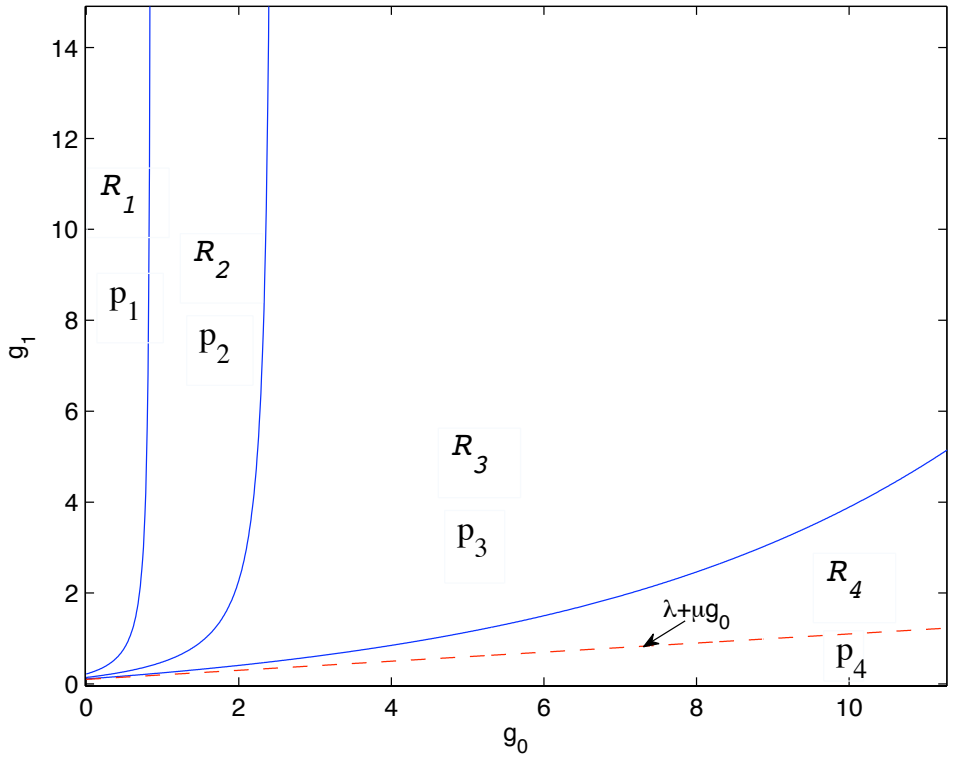

Figure 3.2: The structure of optimum partition regions with $B = 2$ bits of feedback given $\lambda = \mu = 0.1$, $P_{av} = 5.6336$ dB, $Q_{av} = 3.4492$ dB

Theorem 3.3. i). $p_1 > \cdots > p_L$

ii). *All boundaries between any two adjacent partitions satisfy* $g_1 > \lambda + \mu g_0$.

iii). *Given B bits of feedback (or* $L = 2^B$ *regions), for the first L-1 regions, we always have strictly positive power, i.e.* $p_1 > \cdots > p_{L-1} > 0$, *whereas* p_L *is simply nonnegative, i.e.* $p_L \geq 0$.

iv). *When* $\lambda + \mu \geq 1$ *(note that if* $\lambda = 0$, $\mu \geq 1$ *implies* $Q_{avg} < 1$, *and if* $\mu = 0$, $\lambda \geq 1$ *corresponds to* $P_{avg} < 1$*), we always have* $p_L = 0$. *In addition, when L (the number*

of quantized regions) is sufficiently large, no matter what λ, μ are, p_L must be 0. Additionally, as $L \to \infty$ the boundary between $\mathcal{R}_{L-1}$ and $\mathcal{R}_L$ approaches $g_1 = \lambda + \mu g_0$ and $\lim_{L\to\infty} p_{L-1} = 0$.

Proof: The proof can be found in the appendix of this chapter.

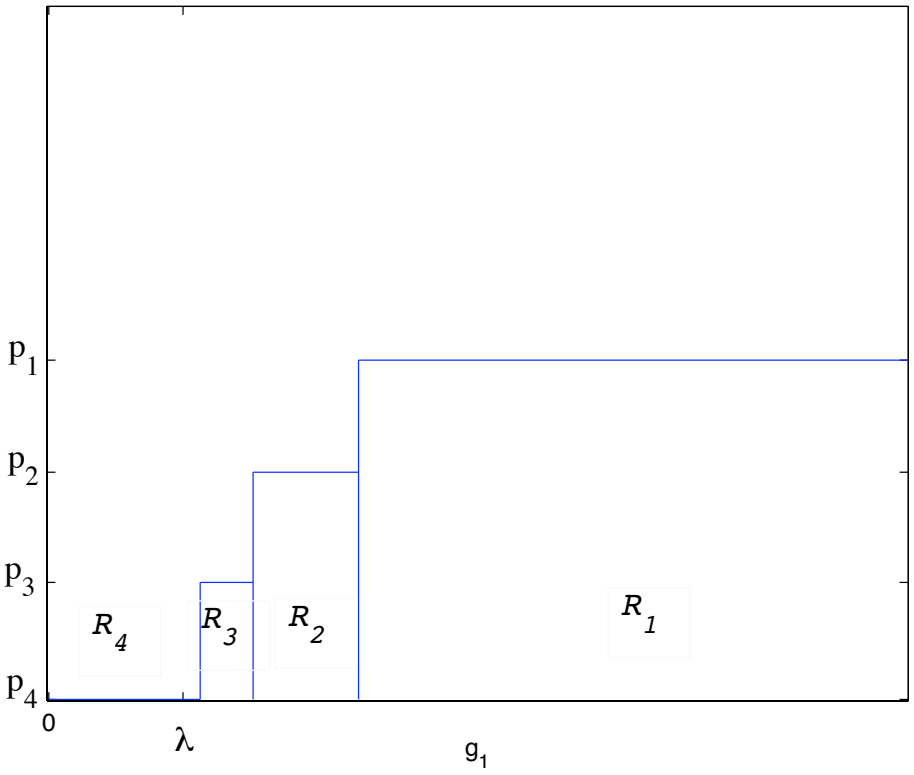

Figure 3.3: The structure of optimum partition regions with $B = 2$ bits of feedback given $\lambda = 1, \mu = 0$, $P_{av} = -8.3298$ dB

Remark 3.3. *The above properties of optimal quantized power values are interesting for two reasons. From property ii), it is clear that $(g_0, g_1) \in \mathcal{R}_j$ for $j = 1, 2, \ldots, L-1$ satisfy the property $g_1 > \lambda + \mu g_0$ whereas for the region $\mathcal{R}_L$, this property may or may not be satisfied. Since the quantized power values in the first $L-1$ regions are strictly positive, it is easy to relate this property to the corresponding property of the full CSI based optimal power value which is strictly positive if and only if when $g_1 > \lambda^f + \mu^f g_0$. Also, as $L \to \infty$, the boundary between $\mathcal{R}_{L-1}$ and $\mathcal{R}_L$ approaches $g_1 = \lambda + \mu g_0$, thus making this relationship between the quantized*

power allocation scheme and the full CSI power allocation scheme stronger. Finally, property iv) allows one to obtain an approximate quantized power allocation scheme (AQPA) for large L by setting $p_L = 0$ *and taking the limit as* $p_{L-1} \to 0$*. This is particularly useful as the modified GLA becomes computationally intensive for large L, whereas AQPA provides a performance that is extremely close to that of the modified GLA, while requiring very little computation time. A detailed description of the AQPA is provided in Section 3.3.3 followed by illustrative numerical simulations in Section 3.5.*

Based on Lemma 3.1 and Theorem 3.3, one also can obtain the optimal quantized power values $p_1, p_2, p_3, \ldots, p_L$ for Problem (3.8) by solving the following set of nonlinear equations:

$$E\left[\frac{g_1}{1+g_1 p_j} - (\lambda + \mu g_0)|\mathcal{R}_j\right] = 0, \quad j = 1, \ldots, L, \; p_L = \max(0, p_L) \tag{3.11}$$

where if $\mu \neq 0$, $E\left[\frac{g_1}{1+g_1 p_j} - (\lambda + \mu g_0)|\mathcal{R}_j\right] = \int_{c_j}^{\infty} \int_{r_{j-1}}^{r_j} (\frac{g_1}{1+g_1 p_j} - (\lambda + \mu g_0)) f(g_0) f(g_1) dg_0 dg_1$, with $c_j = \frac{e^{\lambda(p_j - p_{j+1})} - 1}{p_j - p_{j+1} e^{\lambda(p_j - p_{j+1})}}, j = 1, \ldots, L-1, c_L = 0$ and $r_j = \frac{1}{\mu}\left(\frac{\log \frac{p_j * g_1 + 1}{p_{j+1} * g_1 + 1}}{p_j - p_{j+1}} - \lambda\right), j = 1, \ldots, L-1, r_0 = 0, r_L = \infty$. When $\mu = 0$, $E\left[\frac{g_1}{1+g_1 p_j} - (\lambda + \mu g_0)|\mathcal{R}_j\right] = \int_{c_j}^{c_{j-1}} (\frac{g_1}{1+g_1 p_j} - \lambda) f(g_1) dg_1$, with $c_0 = \infty$. Note that (3.11) can be solved efficiently by a suitable nonlinear equation solver. This particular solution methodology will be very useful in the case of AQPA (see Section 3.3.3 for further details).

We now solve the dual problem for finding the optimal values λ and μ. Since the dual function (3.9) is convex in λ, μ, we can find their optimal values by using an iterative sub-gradient based method [116], where λ and μ are updated until convergence using $\lambda^{l+1} = [\lambda^l - \alpha^l (P_{avg} - \sum_{j=1}^{L} p_j Pr(\mathcal{R}_j))]^+$, $\mu^{l+1} = [\mu^l - \beta^l (Q_{avg} - \sum_{j=1}^{L} E[g_0 p_j | \mathcal{R}_j] Pr(\mathcal{R}_j))]^+$ respectively, where l is the iteration number, α^l, β^l are positive scalar step sizes for the l-th iteration and satisfy $\sum_{l=1}^{\infty} \alpha_l = \infty$, $\sum_{l=1}^{\infty} \beta_l = \infty$, $\sum_{l=1}^{\infty} \alpha_l^2 < \infty$ and $\sum_{l=1}^{\infty} \beta_l^2 < \infty$, and $[x]^+ = \max(x, 0)$. Note that this method is guaranteed to converge to the global optimum of the dual function even though the primal problem is non-convex [116]. One can then repeat the modified GLA based algorithm for finding a locally optimum quantized power values for fixed λ, μ and the sub-gradient based method for updating λ, μ as de-

scribed above until an overall convergence criterion is met. Note that since the primal problem is non-convex, the resultant power allocation and codebook design can only be guaranteed to be locally optimal. An algorithmic format for this procedure is provided for the more general wideband ($M > 1$) case in the next subsection.

Remark 3.4. *Note that the idea of using a Lagrangian based cost function as a modified distortion measure for optimizing via GLA is not new. It has been used for combined adaptive power control and beamforming for MIMO link capacity optimization with limited feedback in [110] and more recently for optimal power and rate allocation and scheduling in TDMA based wireless sensor networks with limited feedback in [118]. However, these papers do not consider average interference constraints and therefore their results cannot be applied to the problem of power allocation in cognitive radio networks with limited feedback. Generic convergence results for the specific GLA used in [110, 118] are also presented in these papers. However, what is unique in this chapter (apart from the novel application to quantized power allocation for secondary throughput maximization in cognitive radio) is that the detailed global convergence and empirical consistency result presented in Theorem 2 and more importantly the properties of the quantized power allocation scheme detailed in Theorem 3, which are specific to the case of the cognitive radio problem. Finally, these properties are used to derive a novel approximate power allocation algorithm (AQPA), which is significantly faster than the GLA based algorithm and as will be seen later, performs very close to it with more than 4 bits of feedback.*

3.3.2 Wideband spectrum-sharing case

The above algorithm for the narrowband case can be easily extended to the wideband case corresponding to the problem (3.7). For this scenario, the Lagrangian function becomes,

$$L(P,\lambda,\mathbf{u}) = \frac{1}{M}\sum_{i=1}^{M}\left(\sum_{j=1}^{L} E\left[\log(1+g_1^i p_{ij})|\mathcal{R}_j^i\right] Pr(\mathcal{R}_j^i)\right) - \lambda\left(\frac{1}{M}\sum_{i=1}^{M}\left(\sum_{j=1}^{L} E[p_{ij}|\mathcal{R}_j^i]Pr(\mathcal{R}_j^i)\right)\right.$$
$$\left. - P_{avg}\right) - \sum_{i=1}^{M}\mu_i\left(\sum_{j=1}^{L} E[g_0^i p_{ij}|\mathcal{R}_j^i]Pr(\mathcal{R}_j^i) - Q_{avg}^i\right) \quad (3.12)$$

where λ and μ_i are the nonnegative Lagrange multipliers associated with the ATP constraint and ith AIP constraint respectively. The Lagrange dual function $g(\lambda, \{\mu_i'\})$ is defined as

$$\max_{p_{ij}\geq 0\ \forall i,j} \quad \frac{1}{M}\sum_{i=1}^{M}\sum_{j=1}^{L} E[\log(1+g_1^i p_{ij}) - \lambda p_{ij} - \mu_i' g_0^i p_{ij}|\mathcal{R}_j^i]Pr(\mathcal{R}_j^i) \tag{3.13}$$

where $\mu_i' = M\mu_i$, and the dual problem is $\min_{\lambda\geq 0,\ \mu_i'\geq 0,\forall i} g(\lambda, \{\mu_i'\}) + \lambda P_{avg} + \sum_{i=1}^{M} \frac{\mu_i'}{M} Q_{avg}^i$.

Similar to the narrowband case, we first consider the problem (3.13) to obtain $g(\lambda, \{\mu_i'\})$ with given λ and $\{\mu_i'\}$. As discussed before, problem (3.13) can be decomposed into M parallel subproblems, where for each band $i, i = 1, \ldots, M$

$$\max_{p_{ij}\geq 0\ \forall j} \sum_{j=1}^{L} E[\log(1+g_1^i p_{ij}) - \lambda p_{ij} - \mu_i' g_0^i p_{ij}|\mathcal{R}_j^i]Pr(\mathcal{R}_j^i) \tag{3.14}$$

is defined as the sub-dual function $g_i(\lambda, \mu_i')$ and $g(\lambda, \{\mu_i'\}) = \frac{1}{M}\sum_{i=1}^{M} g_i(\lambda, \mu_i')$. This kind of duality method is also known as the 'dual decomposition algorithm' [70]. Since each subproblem (3.14) is similar to the problem (3.9) for the narrowband case and can be similarly solved by using a modified GLA. λ and $\{\mu_i'\}$ can be also obtained in a manner similar to the narrowband case. These two steps are then repeated until a satisfactory convergence criterion is met. Due to the increased complexity resulting from the presence of multiple bands, we provide below a description of the overall optimization algorithm (Algorithm 1) for solving (3.7).

Algorithm 1:

1. Let $\lambda = 0$, then all $\mu_i', i = 1, \ldots, M$ must satisfy $\mu_i' > 0$. For each $band_i$, starting with a random initial value for μ_i', obtain the corresponding optimal power codebook $\mathcal{P}_i = \{p_{i1}, \ldots, p_{iL}\}$ using a modified GLA, then update μ_i' by using an iterative subgradient method $\mu_i'(l+1) = [\mu_i'(l) - \beta_i^l(Q_{avg}^i - \sum_{j=1}^{L} E[g_0^i p_{ij}|\mathcal{R}_j^i]Pr(\mathcal{R}_j^i))]^+$, where l denotes the iteration number, $\beta_i^l > 0$ is scalar step size for l-th iteration satisfying $\sum_{l=1}^{\infty}\beta_i^l = \infty$ and $\sum_{l=1}^{\infty}(\beta_i^l)^2 < \infty\ \forall i = 1, 2, \ldots, M$. Repeat these two steps until convergence resulting in M power codebooks $\{\mathcal{P}_1, \ldots, \mathcal{P}_M\}$ (one for each band). With these codebooks, if $\frac{1}{M}\sum_{i=1}^{M}\left(\sum_{j=1}^{L} E[p_{ij}|\mathcal{R}_j^i]Pr(\mathcal{R}_j^i)\right) \leq P_{avg}$, it is

an optimal power codebook and stop; otherwise go to step 2).

2. If 1) is not satisfied, we must have $\lambda > 0$. Starting with a random initial value for λ: for each i, use the modified GLA to find an optimal power codebook first with $\mu_i' = 0$. If $\sum_{j=1}^{L} E[g_0^i p_{ij}|\mathcal{R}_j^i]Pr(\mathcal{R}_j^i) \leq Q_{avg}^i$, then the corresponding optimal codebook $\mathcal{P}_i = \{p_{i1}, \ldots, p_{iL}\}$ is a locally optimal solution for this i-th subproblem, otherwise, we must have $\mu_i' > 0$, the optimal value of which can be found by using an iterative subgradient method as described in step 1). The optimal value of λ can be obtained by a similar iterative subgradient based method given by $\lambda^{l+1} = [\lambda^l - \alpha^l \left(P_{avg} - \frac{1}{M}\sum_{i=1}^{M}\left(\sum_{j=1}^{L} E[p_{ij}|\mathcal{R}_j^i]Pr(\mathcal{R}_j^i)\right)\right)]^+$, where again l is the iteration number, $\alpha^l > 0$ is a scalar step size for the l-th iteration satisfying $\sum_{l=1}^{\infty}\alpha^l = \infty$ and $\sum_{l=1}^{\infty}(\alpha^l)^2 < \infty$. Repeat the modified GLA based step for finding a local optimum for the quantized powers and the subgradient based updates for λ and μ_i', $i = 1, 2, \ldots, M$ until convergence and the final codebook will be a locally optimal codebook for the wideband spectrum sharing Problem (3.7).

Remark 3.5. Convergence of Algorithm 1*: Note that it is straightforward to extend the global convergence and empirical consistency results of Theorem 3.2 to the wideband case for fixed values of λ and μ_i', $i = 1, 2, \ldots, M$. As noted in Section III.A for the narrowband case, the iterative subgradient based methods for updating λ and μ_i' converge to the globally optimal values corresponding to the dual function due to the convexity of the dual function with respect to the Lagrange multipliers [116]. Thus, Algorithm 1 converges to a local optimum (since convergence of the modified GLA can be guaranteed to a local optimum only) of the quantized power values $\{p_{i1}, \ldots, p_{iL}\}$, $i = 1, 2, \ldots, M$.*

Remark 3.6. *Theorem 3.3 also holds for the wideband case in the sense that the properties i)-iv) hold for each $\{p_{i1}, p_{i2}, \ldots p_{iL}\}$, $\forall i = 1, 2, \ldots, M$ with μ replaced by $\mu_i, i = 1, 2, \ldots, M$ and λ representing the Lagrange multiplier associated with the average sum power constraint in (3.12).*

3.3.3 Approximate Quantized Power Allocation Algorithm (AQPA)

Although an offline algorithm, the complexity of modified GLA for determining the optimal quantized power is very high for even a moderately large value of L. This is due to the fact that the optimal channel partitions and the corresponding optimal power codebook are obtained via empirically generating a large number of channel realizations as training samples. As L increases, the number of training samples required will also increase. Thus motivated, we use part iv) of Theorem 3.3 to derive a low-complexity suboptimal scheme for implementing the modified GLA for large L values. Below we describe this scheme for the narrowband case. A similar scheme for the wideband case can be designed accordingly.

Note that part iv) of Theorem 3.3 states that as $L \to \infty$, $p_L = 0$ and $p_{L-1} \to 0$. Applying these approximations to (3.11) allows us to obtain an approximate but computationally efficient algorithm (called approximate quantized power allocation algorithm (AQPA)) for large L. AQPA first solves $E[\frac{g_1}{1+g_1 p_{L-1}} - (\lambda + \mu g_0)|\mathcal{R}_{L-1}] = 0$ for p_{L-2} by substituting $p_L = 0$ and taking the limit $p_{L-1} \to 0$, which, if $\mu > 0$, is equivalent to solving $\int_{\lambda}^{\infty} \int_{\frac{1}{\mu}\left(\frac{\log(1+g_1 p_{L-2})}{p_{L-2}} - \lambda\right)}^{\frac{g_1-\lambda}{\mu}} (g_1 - (\lambda + \mu g_0)) f(g_0) f(g_1) dg_0 dg_1 = 0$ for p_{L-2}. When $\mu = 0$, it is equivalent to solving for p_{L-2} from $\int_{\lambda}^{\frac{e^{\lambda p_{L-2}} - 1}{p_{L-2}}} (g_1 - \lambda) f(g_1) dg_1 = 0$. Note that the above equations (for both $\mu > 0$ and $\mu = 0$) involve only one variable: p_{L-2} and are thus straightforward to solve. One can then recursively compute $p_{L-3}, p_{L-4}, \ldots$, by using the optimality condition (3.11) for the regions $\mathcal{R}_{L-2}, \mathcal{R}_{L-3}, \ldots$, respectively, in the reverse direction. These equations can be solved by appropriate nonlinear equation solvers and do not require the use of large number of training samples. Thus AQPA is significantly faster than GLA and is applicable to the case of large number of feedback bits. Note however, as this is an approximate algorithm only, the performance of this algorithm becomes comparable to modified GLA only for large values of L. Numerical results presented in Section 3.5 illustrate that AQPA performs extremely well for $L \geq 16$. Note also that AQPA will be a suitable algorithm to use if any of the system specifications (such as channel statistics or P_{avg}, Q^i_{avg} etc.) changed and the quantized power values needed to be recalculated.

Other suboptimal algorithms: For comparison purposes, we also propose two other suboptimal methods for finding quantized power allocation in the narrowband case (extension to the wideband case is obvious). (1) In the first method, we quantize g_0 and g_1 separately (i.e. separate scalar quantizations) by minimizing their corresponding distortion $\sum_{n=1}^{L_1} E[(g_0 - g'_{0n})^2|R_n]Pr(R_n)$ and $\sum_{k=1}^{L_2} E[(g_1 - g'_{1k})^2|R'_k]Pr(R'_k)$ respectively, with the Lloyd Algorithm, where g'_{0n}, g'_{1k} are the reconstruction points for g_0 and g_1 respectively, and $L_1 \times L_2 = L$. We then use the resulting (locally) optimal channel quantization regions to solve $E[\frac{g_1}{1+g_1 p_{nk}} - (\lambda + \mu g_0)|R_n, R'_k] = 0$ for finding the optimal power allocation p_{nk} for the region where $g_0 \in R_n, g_1 \in R'_k$. We call this method as "separate channel quantization" (SCQ). (2) In the second method, we jointly quantize g_0 and g_1 by minimizing the distortion $\sum_{m=1}^{L} E[(g_0 - g'_{0m})^2 + (g_1 - g'_{1m})^2|R_m]Pr(R_m)$ with Lloyd Algorithm, and then use the resultant optimal channel quantization regions to solve $E[\frac{g_1}{1+g_1 p_m} - (\lambda + \mu g_0)|R_m] = 0$ for finding the optimal power allocation p_m. We call it "joint channel quantization" (JCQ). Numerical results illustrate that AQPA significantly outperforms these two suboptimal methods.

3.4 Optimum Quantized Power Allocation with Noisy Limited Feedback

In the previous section, we assumed ideal error-free feedback in the limited feedback model. However, feedback channel noise can result in unavoidable erroneous feedback, which can cause the SU-TX to select an incorrect quantized power vector, resulting in an inferior ergodic capacity performance compared to the case of noise-free feedback. In this section, we allow noise in the limited feedback channel model and study the ergodic capacity maximization problem (3.7) with noisy limited feedback. Note that in general modelling of feedback errors in a quantized CSI feedback system is a challenging problem. In the analysis to follow, we make some simplifying assumptions regarding the feedback errors and operating conditions in order to formulate a tractable problem. The noisy feedback link, assumed to be memoryless, is characterized by the index transition probabilities $\rho_{kj}, (k, j = 1, \ldots, L)$, which is defined as the probability of receiving

index k at the SU-TX, given index j was sent from the CR network manager. For each band, given $B = \log_2 L$ bits feedback, denote binary representation of index k and j as $k_1 k_2 \dots k_B$ and $j_1 j_2 \dots j_B$ respectively, where $k_n, j_n \in \{0,1\}$ for $n = 1, \dots B$, and k_1, j_1 represent the most significant bit. For each band with B bits feedback, we model the noisy feedback channel as B independent uses of a binary symmetric channel with crossover probability q_f for every feedback bit. Since bit errors are assumed to be independent, $\rho_{kj} = \prod_{n=1}^{B} \rho_{k_n j_n} = q_f^{d_{k,j}} (1-q_f)^{B-d_{k,j}}$, where $d_{k,j}$ is the Hamming distance between the binary representations of k and j [93].

Thus problem (3.7) with noisy limited feedback can be reformulated as

$$\begin{aligned} \max_{p_{ik} \geq 0, \forall i,k, \mathcal{R}_j^i, \forall i,j} \quad & \frac{1}{M} \sum_{i=1}^{M} \left(\sum_{j=1}^{L} \sum_{k=1}^{L} E[\log(1 + g_1^i p_{ik}) | \mathcal{R}_j^i] \rho_{kj} Pr(\mathcal{R}_j^i) \right) \\ s.t. \quad & \sum_{j=1}^{L} \sum_{k=1}^{L} E[g_0^i p_{ik} | \mathcal{R}_j^i] \rho_{kj} Pr(\mathcal{R}_j^i) \leq Q_{avg}^i, \forall i, \\ & \frac{1}{M} \sum_{i=1}^{M} \left(\sum_{j=1}^{L} \sum_{k=1}^{L} E[p_{ik} | \mathcal{R}_j^i] \rho_{kj} Pr(\mathcal{R}_j^i) \right) \leq P_{avg} \end{aligned} \tag{3.15}$$

Note that for each band the binary codewords representing the feedback indices for a power codebook of size L can be designed in $L!$ different ways. In general, finding the optimal index assignment scheme is computationally prohibitive and sub-optimal or randomized schemes are preferred. However, it was shown in [108] in the context of capacity optimization for MIMO links with noisy limited feedback that when the channel quantizers and the precoder adaptation are jointly optimized for a given index assignment, all index assignment schemes are equally good (see Lemma 2 in [108]). The proof of Lemma 2 in [108] is directly applicable to our scenario due to the specific discrete memoryless nature of the feedback channel and hence all index assignment schemes are equally good for our noisy feedback model as well. Therefore, we simply concentrate on finding the optimum CSI partitions $\mathcal{R}_j^i, \forall j$ and power codebook $\mathcal{P}_i$ for the i-th band, $i = 1, \dots, M$ that jointly optimize the ergodic capacity of SU under the long term average transmit power constraint and average interference constraint given by (3.15), for a fixed index assignment scheme (which can be arbitrarily chosen). Again, to keep things simple, we look at the narrowband spectrum-sharing case (M=1). Using the simplified notations $\mathcal{R}_j, p_j,\ j =$

$1, 2, \ldots, L$, and g_1, g_0, Q_{avg}, we write the Lagrangian for Problem (3.15) with $M = 1$ as $L(P, \lambda, \mu) = \sum_{j=1}^{L} \sum_{k=1}^{L} E[\log(1 + g_1 p_k) - \lambda p_k - \mu g_0 p_k | \mathcal{R}_j] \rho_{kj} Pr(\mathcal{R}_j) + \lambda P_{avg} + \mu Q_{avg}$, where λ and μ are the nonnegative Lagrange multipliers associated with the ATP constraint and AIP constraint respectively. The Lagrange dual function $g(\lambda, \mu)$ is defined as $\max_{p_k \geq 0, \forall k, \mathcal{R}_j, \forall j} \sum_{j=1}^{L} \sum_{k=1}^{L} E[\log(1 + g_1 p_k) - \lambda p_k - \mu g_0 p_k | \mathcal{R}_j] \rho_{kj} Pr(\mathcal{R}_j)$ and the corresponding dual problem is $\min_{\lambda \geq 0, \mu \geq 0} g(\lambda, \mu) + \lambda P_{avg} + \mu Q_{avg}$. It is obvious that this optimization problem with fixed λ and μ can be easily solved using another modified GLA, (termed as modified GLA-2 to distinguish it from the noise free case) resulting in a locally optimum power codebook. For this power codebook, the optimal values λ and μ can then be obtained via subgradient based methods similar to the ones for the noise free case. These two steps are then repeated until a satisfactory convergence criterion is met. It can be easily extented to the wideband case.

3.5 Numerical Results

In this section, we will evaluate the performance of the designed power allocation strategies via numerical simulations. We implement a wideband spectrum sharing system with one SU and M independent frequency bands (each band is originally licensed to a PU), where all the channels involved are assumed to undergo Rayleigh fading, namely all $\mathbf{g}_0$ and $\mathbf{g}_1$ are exponentially distributed with unit mean. For each simulation, 100,000 randomly generated channel realizations for each $\mathbf{g}_0$ or $\mathbf{g}_1$ are used. Any reference to the number of feedback bits should be interpreted in a *per band* sense.

Fig. 3.4 shows, with prefect CSI, the capacity performance of SU-TX, which shares spectrum with four PUs (M=4), with four different AIP constraints thresholds, i.e, (Q_{av1}, Q_{av2}, Q_{av3}, Q_{av4})=(-5 dB, -5 dB, 0 dB, 0 dB), ($Q_{av1}, Q_{av2}, Q_{av3}, Q_{av4}$)=(0 dB, 0 dB, 0 dB, 0 dB), ($Q_{av1}, Q_{av2}, Q_{av3}, Q_{av4}$)=($-5$ dB, 0 dB, 0 dB, 5 dB) and ($Q_{av1}, Q_{av2}, Q_{av3}, Q_{av4}$)=($-5$ dB, 0 dB, 5 dB, 5 dB). An interesting observation from Fig. 3.4 is that when P_{av} is small ($P_{av} \leq -5$ dB), no matter what the value of ($Q_{av1}, Q_{av2}, Q_{av3}, Q_{av4}$) is, the capacity performance of four curves are almost indistinguishable. This is due to the fact that (see Theorem 3.1), when $P_{av} \leq \min(Q_{av1}, Q_{av2}, Q_{av3}, Q_{av4})$ (since $\mathbf{g}_1$ is i.i.d), all AIP con-

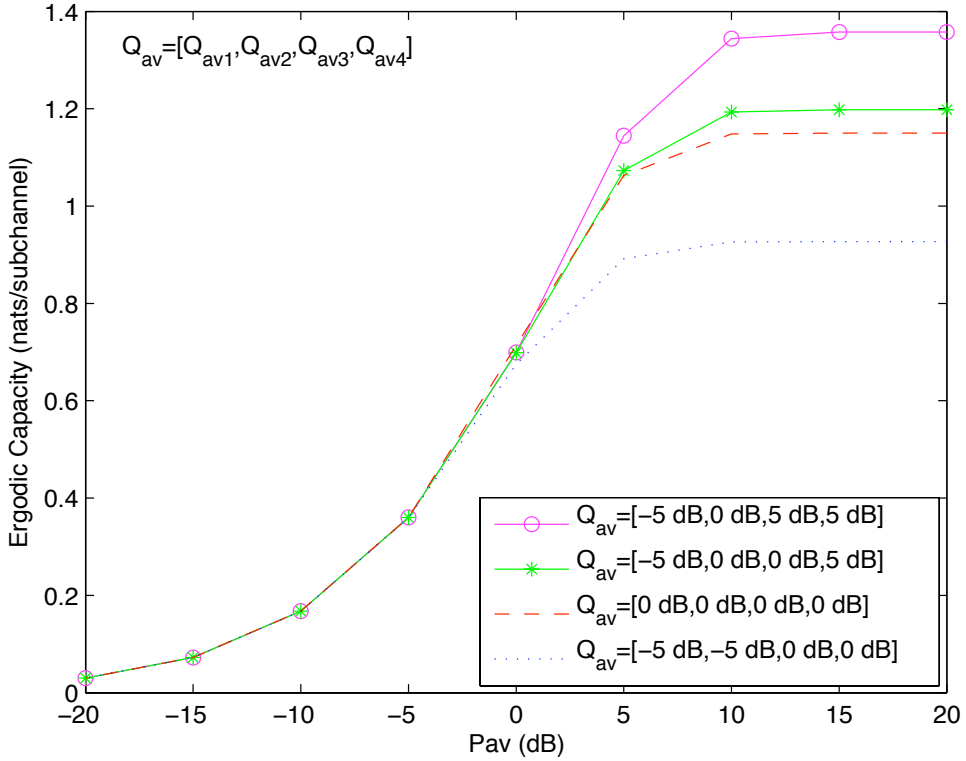

Figure 3.4: Capacity performance for SU-TX in only one PU case with prefect CSI obtained by Algorithm 1.

straints become inactive. As the value of P_{av} increases, the capacity performance with different $(Q_{av1}, Q_{av2}, Q_{av3}, Q_{av4})$ gradually becomes distinguishable, since in this case, the ATP and at least one AIP constraint are effective. However, as P_{av} increases beyond a certain threshold, the capacity curves start to saturate, due to the fact that when $P_{av} \geq \frac{1}{4}\sum_{i=1}^{4} E[(\frac{1}{\mu_i g_0^i} - \frac{1}{g_1^i})^+]$, where μ_i is given by solving $E[g_0^i(\frac{1}{\mu_i g_0^i} - \frac{1}{g_1^i})^+] = Q_{av}^i$, only the AIP constraints are active. Thus no matter how P_{av} changes, if $(Q_{av1}, Q_{av2}, Q_{av3}, Q_{av4})$ are fixed, the capacity will be unchanged. A similar observation for a narrowband spectrum sharing model with full CSI was made in [117]. One should note that theoretically, the ATP corresponding to the optimal power allocation law maximizing the SU ergodic capacity over a Rayleigh fading channel under an AIP constraint with perfect CSI is infinity [67]. Since here we use large numbers of randomly generated channel realizations samples in the simulation studies, the ATP for maximizing SU ergodic capacity under an

AIP constraint is large but not infinite.

Fig. 3.5 shows the capacity performance of SU sharing a narrowband spectrum with

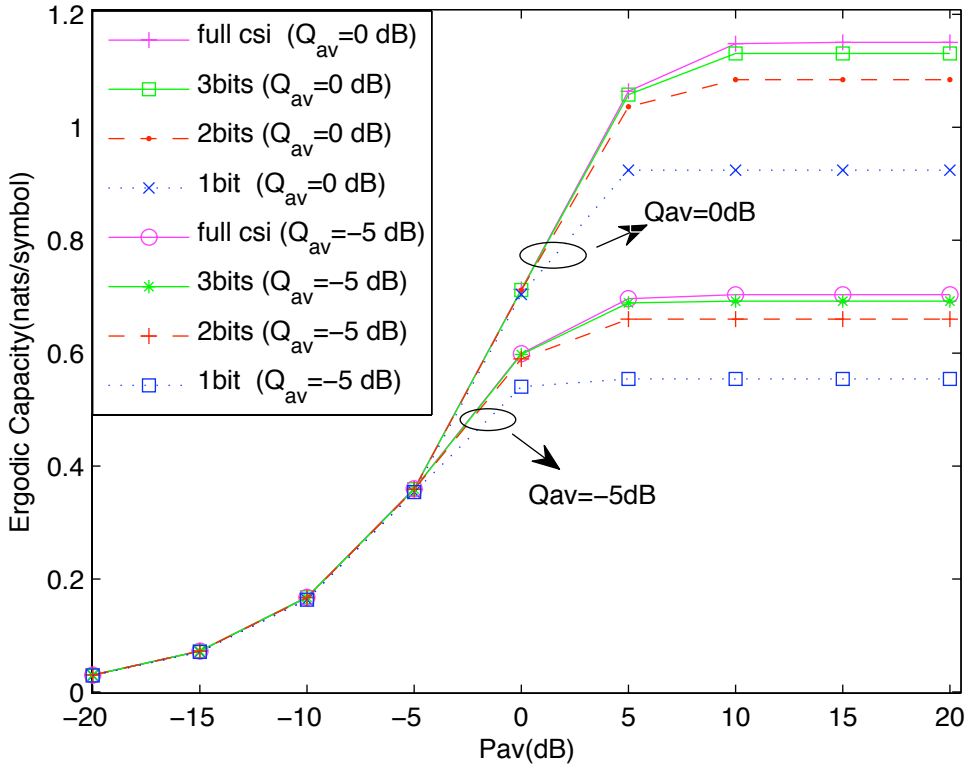

Figure 3.5: SU Ergodic capacity with quantized power allocation (using GLA) with one PU for $Q_{av} = -5$ dB and $Q_{av} = 0$ dB

one PU with limited feedback for $Q_{av} = -5$ dB and $Q_{av} = 0$ dB respectively, and illustrates the effect of increasing the number of feedback bits on the capacity performance. For comparison, we also plot the corresponding capacity performance with full CSI. The striking observation from Fig. 3.5 is that introducing one extra bit of feedback substantially reduces the gap with capacity based on perfect CSI. This property is not very obvious when P_{av} is small, for example when $P_{av} \leq -5$ dB ($P_{av} \leq 0$ dB) for $Q_{av} = -5$ dB ($Q_{av} = 0$ dB). But with increasing P_{av}, it becomes more pronounced. To be specific, for $Q_{av} = -5$ dB case, at $P_{av} = 10$ dB, with 1 bit, 2 bits and 3 bits of feedback, the percentage capacity loss is approximately 21.23%, 6.21% and 1.62% respectively, and for both $Q_{av} = -5$ dB and $Q_{av} = 0$ dB cases, only 3 bits feedback can result in secondary

ergodic capacity very close to that with full CSI. This is very encouraging since only a small number of bits of feedback are required to achieve close performance to the full CSI case. It can be also seen that the capacity performance with a higher AIP threshold

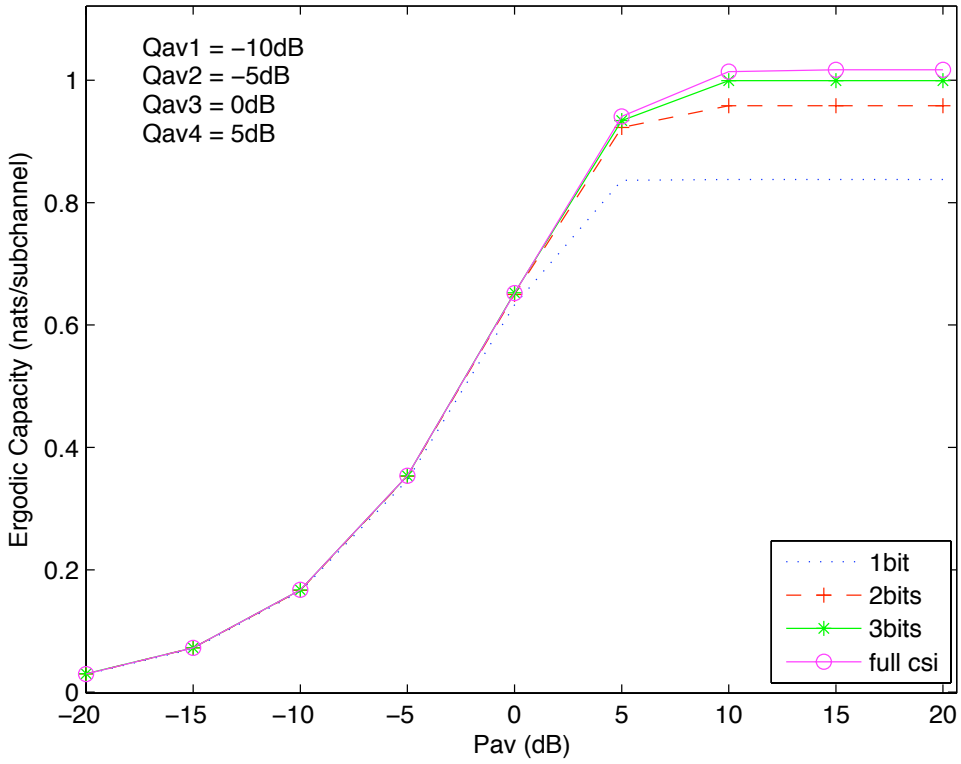

Figure 3.6: SU Ergodic capacity performance with quantized power allocation (GLA) for four PUs ($M = 4$) under various number of feedback bits per band.

($Q_{av} = 0$ dB) outperforms that with a lower AIP threshold ($Q_{av} = -5$ dB), as expected. A similar behaviour can be also observed in Fig. 3.6 for a $M = 4$ wideband spectrum sharing case with $1, 2, 3$ bits of feedback and full CSI performance respectively, where $(Q_{av1}, Q_{av2}, Q_{av3}, Q_{av4}) = (-10$ dB, -5 dB, 0 dB, 5 dB).

In Fig. 3.7 we compare the performance of AQPA with modified GLA, where SU shares the spectrum with four PUs ($M = 4$) and the AIP constraint thresholds (Q_{av1}, Q_{av2}, Q_{av3}, Q_{av4}) = (-10 dB, -5 dB, 0 dB, 5 dB). It is illustrated that with the same number of bits of feedback per band, the gap between AQPA and modified GLA becomes smaller as L increases. For example, when $P_{av} = 15$ dB, the capacity loss by using AQPA

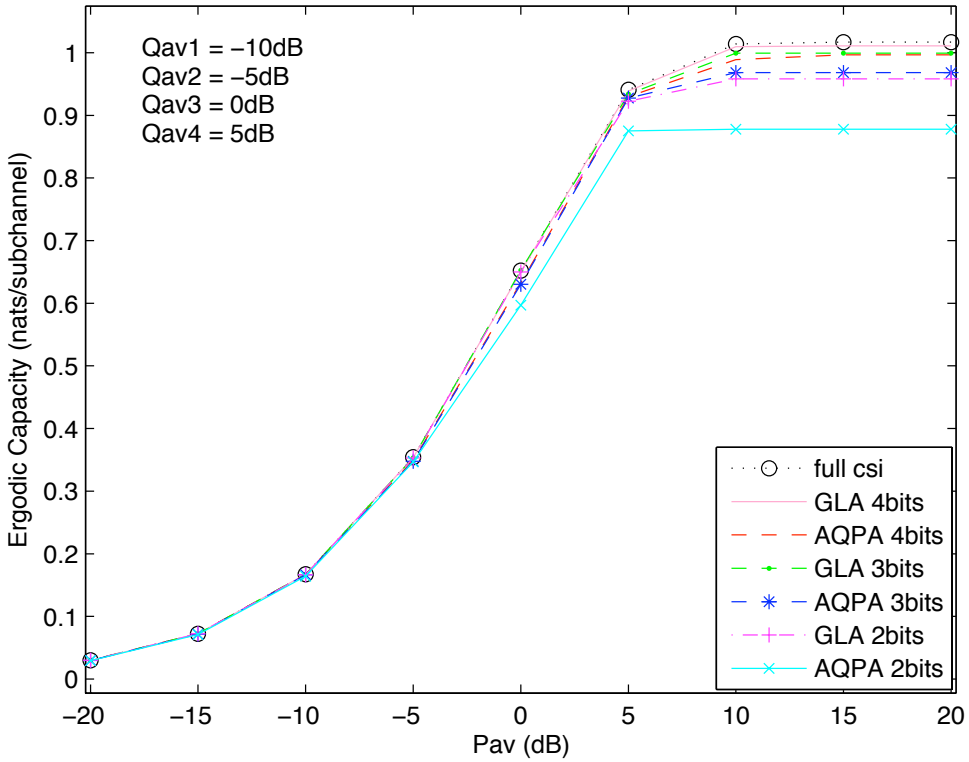

Figure 3.7: Capacity performance of AQPA with four PUs ($M = 4$, feedback bits here refer to bits per band)

instead of GLA is about 8.38%, 3.12% and 1.42% for 2 bits, 3 bits and 4 bits of feedback respectively. It is clearly seen that AQPA with 4 bits of feedback can almost approach the full CSI performance. In order to determine the speedup factor of AQPA compared to GLA for a fixed λ and μ with $M = 4$ and 4 bits of feedback, AQPA and GLA were implemented in MATLAB (version 7.10.0.499 (R2010a)) on an Intel Core 2 Duo processor (CPU T9600 with a clock speed of 2.80 GHz and a memory of 4 GB). It was seen that GLA (with 100,000 training samples) took approximately 7395 seconds or just over 2 hours whereas AQPA took only 5.44 seconds to achieve comparable levels of accuracy. Furthermore, as shown in Fig. 3.8, we also compare capacity performance of AQPA with the two other proposed possible suboptimal methods (SCQ and JCQ) for the narrowband case with $Q_{av} = -5$ dB. For the SCQ case, various combinations of L_1, L_2 such that $L_1 \times L_2 = L$ are investigated and the one with the best performance is reported for every value of P_{av}. We

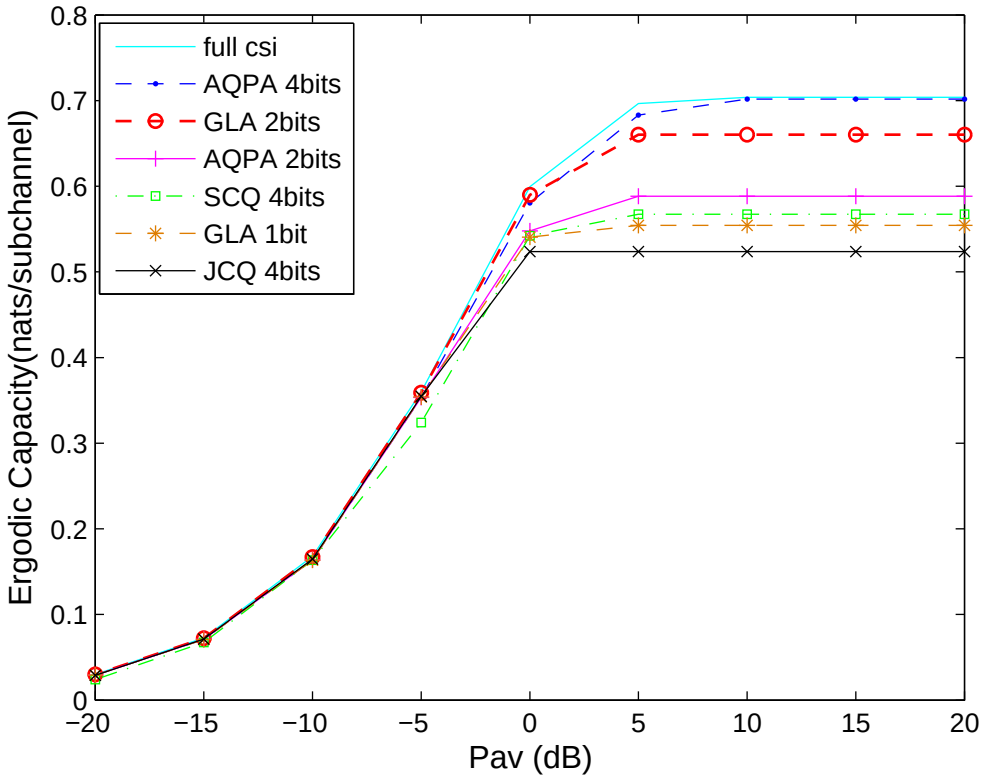

Figure 3.8: Compare capacity performance of AQPA with two other possible suboptimal methods ($M = 1$)

can easily observe that even with 4 bits feedback, the performance of both JCQ and SCQ are worse than AQPA with only 2 bits of feedback, which further confirms the efficiency of AQPA.

Finally, we investigate the SU ergodic capacity performance with noisy limited feedback in Fig. 3.9, with $M = 4$ and $(Q_{av1}, Q_{av2}, Q_{av3}, Q_{av4})$ = (-10 dB, -5 dB, 0 dB, 5 dB). It can be observed that as the feedback becomes less reliable (the crossover probability q_f increases), significant capacity performance degradation occurs, especially in high P_{avg}. For example, when $P_{avg} = 10$ dB, for 3 (2) bits feedback, a noisy feedback channel with $q_f = 0.01$ and $q_f = 0.1$ can result in approximately 3.843% (4.769%) and 17.394% (18.783%) capacity loss respectively, compared to the noise-free case. This clearly illustrates that as the quality of feedback link degrades, the benefit of designing an optimal power codebook diminishes rapidly.

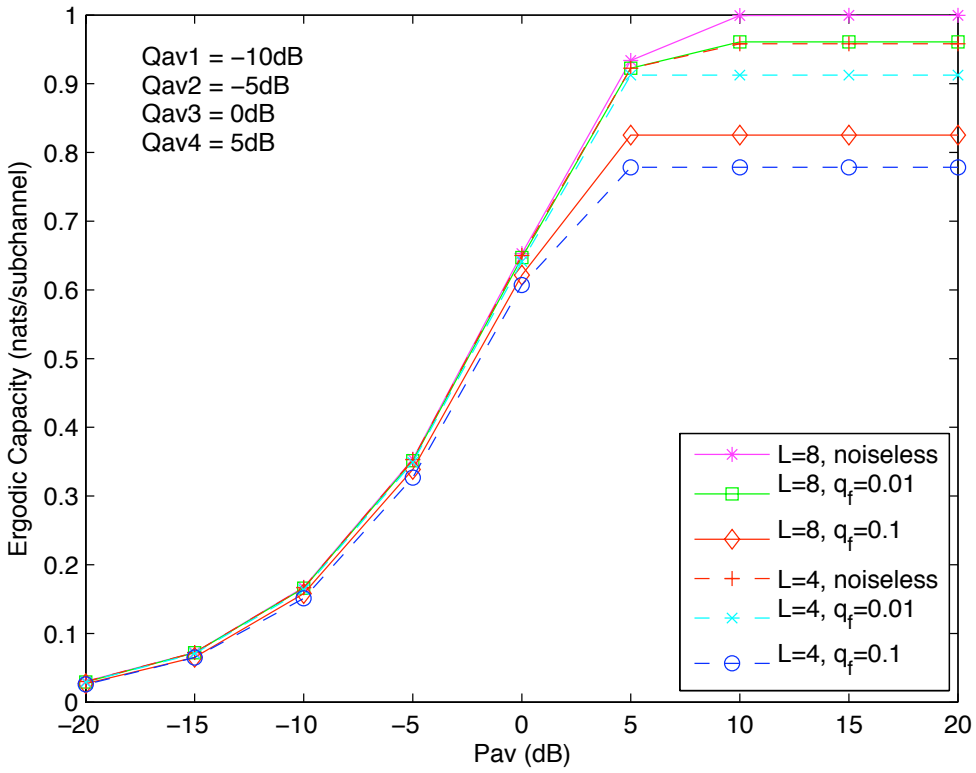

Figure 3.9: Capacity performance of noisy limited feedback with four PUs (M=4) and different BSC crossover probabilities (number of feedback regions L here refer to L per band)

3.6 Conclusions

We have derived quantized power allocation algorithms for a wideband spectrum sharing system with one secondary user and multiple primary users, each licensed to use a separate frequency band, each band modelled as independent block fading channels. The objective has been to maximize the SU ergodic capacity under an average sum transmit power constraint and individual average interference constraints at the PU receivers. Modified Generalized Lloyd-type algorithms (GLA) have been derived and various properties of the quantized power allocation laws have been presented, along with a rigorous convergence and consistency proof of the modified GLA based algorithm. By appropriately exploiting the properties of the quantized power values for large number of bits of feedback, we have also derived approximate quantized power allocation algorithms that

perform very close to the modified GLA based algorithms but are significantly faster. Finally, we have presented an extension of the modified GLA based quantized power allocation algorithm to the case of noisy feedback channels. Future work will include deriving expressions for asymptotic (as the number of feedback bits goes to infinity) capacity loss with quantized power allocation and quantized power allocation with other types of interference constraints at the primary receiver.

3.7 Appendix

3.7.1 Proof of Theorem 3.1

Note that the Karush-Kuhn-Tucker (KKT) conditions are necessary and sufficient for a convex optimization problem. This implies that all the conditions stated in Theorem 3.1 are necessary and sufficient.

1) When $\lambda^f = 0$, from the complementary slackness condition, $\frac{1}{M}\sum_{i=1}^{M} E[p_i(\mathbf{g}_0, \mathbf{g}_1)] \leq P_{avg}$ does not come into play. In this case, the optimization problem (3.2) becomes M completely independent parallel subproblems all having the same structure:

$$\begin{aligned} &\max_{p_i(\mathbf{g}_0,\mathbf{g}_1)\geq 0} \quad E[\log(1+g_1^i p_i(\mathbf{g}_0,\mathbf{g}_1))] \\ &\quad s.t. \quad E[g_0^i p_i(\mathbf{g}_0,\mathbf{g}_1)] \leq Q_{avg}^i, \ \forall i = 1,2,\ldots,M \end{aligned} \tag{3.16}$$

and it is easy to verify that in the above optimization problem, each constraint holds with equality, namely $E[g_0^i p_i(\mathbf{g}_0, \mathbf{g}_1)] = Q_{avg}^i \ \ \forall i$. Thus for each i, from the complementary slackness condition, one can easily show that $\mu_i^f > 0$. Hence, in this case, we have the optimal solution

$$p_i^*(\mathbf{g}_0, \mathbf{g}_1) = (\frac{1}{\mu_i^f g_0^i} - \frac{1}{g_1^i})^+ \qquad \forall i \tag{3.17}$$

where μ_i^f is determined such that $E[g_0^i(\frac{1}{\mu_i^f g_0^i} - \frac{1}{g_1^i})^+] = Q_{avg}^i \ \ \forall i$. From feasibility, we also have $\frac{1}{M}\sum_{i=1}^{M} E[(\frac{1}{\mu_i^f g_0^i} - \frac{1}{g_1^i})^+] \leq P_{avg}$.

2) When $\lambda^f > 0$,we must have $\frac{1}{M}\sum_{i=1}^{M} E[p_i(\mathbf{g}_0, \mathbf{g}_1)] = P_{avg}$.

• If $\mu_i^f > 0$, then corresponding AIP constraint $E[g_0^i p_i(\mathbf{g}_0, \mathbf{g}_1)] = Q_{avg}^i$ and hence the optimal solution for the i-th channel is

$$p_i^*(\mathbf{g}_0, \mathbf{g}_1) = (\frac{1}{\lambda^f + \mu_i^f g_0^i} - \frac{1}{g_1^i})^+ \tag{3.18}$$

where μ_i^f is determined from $E[g_0^i(\frac{1}{\lambda^f + \mu_i^f g_0^i} - \frac{1}{g_1^i})^+] = Q_{avg}^i$ given λ^f.

• If $\mu_i^f = 0$, then the corresponding AIP constraint satisfies $E[g_0^i p_i(\mathbf{g}_0, \mathbf{g}_1)] \leq Q_{avg}^i$, and in this case the optimal solution for the i-th channel is

$$p_i^*(\mathbf{g}_0, \mathbf{g}_1) = (\frac{1}{\lambda^f} - \frac{1}{g_1^i})^+ \tag{3.19}$$

In this scenario we also have $E[g_0^i(\frac{1}{\lambda^f} - \frac{1}{g_1^i})^+] = E[(\frac{1}{\lambda^f} - \frac{1}{g_1^i})^+] \leq Q_{avg}^i$, since $\mathbf{g}_0$ and $\mathbf{g}_1$ are independent, and $E[g_0^i] = 1, \forall i$.

Thus when $\lambda^f > 0$, the optimal solution is given by

$$p_i^*(\mathbf{g}_0, \mathbf{g}_1) = \begin{cases} (\frac{1}{\lambda^f} - \frac{1}{g_1^i})^+ & \text{if } E[(\frac{1}{\lambda^f} - \frac{1}{g_1^i})^+] \leq Q_{avg}^i \\ (\frac{1}{\lambda^f + \mu_i^f g_0^i} - \frac{1}{g_1^i})^+ & otherwise \end{cases} \tag{3.20}$$

where λ^f is determined such that $\frac{1}{M}\sum_{i=1}^M E[p_i] = P_{avg}$.

3.7.2 Proof of Theorem 3.2

For the modified GLA, one can define a distortion measure $d((g_0, g_1), p) = -(\log(1 + g_1 p) - \lambda p - \mu g_0 p)$. For such non-difference distortion measures, following [101], one can ensure nonnegativity of the distortion measure by introducing a modified distortion measure as $\hat{d}((g_0, g_1), p) = d((g_0, g_1), p) - \min_p d((g_0, g_1), p)$. Since $d((g_0, g_1), p)$ is a convex function of p for fixed (g_0, g_1), we get the unique minimum $p^* = (\frac{1}{\lambda + \mu g_0} - \frac{1}{g_1})^+$, thus $\min_p d((g_0, g_1), p) = d((g_0, g_1), p^*)$. Therefore we have $\hat{d}((g_0, g_1), p) \geq 0$. Since $d((g_0, g_1), p^*)$ is constant for a given (g_0, g_1), thus using the distortion measure $\hat{d}((g_0, g_1), p)$ instead of $d((g_0, g_1), p)$ does not affect the results of modified GLA. One can

easily show that $\hat{d}$ satisfies the following properties: (1) $\hat{d}$ is continuous and $\hat{d} \in [0, \infty)$, (2) $\hat{d}((g_0, g_1), p)$ is a convex function of p for each fixed (g_0, g_1), (3) for each (g_0, g_1) and some $\widetilde{(g_0, g_1)}$ not identically equal to (g_0, g_1), $\hat{d}(\widetilde{(g_0, g_1)}, p) \to \infty$, as $\widetilde{(g_0, g_1)} \to (g_0, g_1)$ and $\| p \| \to \infty$, and (4) the partition boundaries in the channel space (g_0, g_1) have zero probability.

Properties 1), 2) and 3) are easy to show and the proofs here are omitted. Property 4) holds due to the assumption of continuous fading channels in this work. Note that this is also a necessary condition for a codebook to be optimal for a given partition [6]. Note also that the popular fading distributions such as Rayleigh, Rician and Nakagami and Log-normal etc. all satisfy the absolutely continuity assumption. It is then easy to show that for these types of fading scenarios, the cumulative distribution function (cdf) of (g_0, g_1), denoted by F, satisfies the following properties [76]: (5) F contains no singular-continuous part and (6) $\int \hat{d}((g_0, g_1), p) dF(g_0, g_1) < \infty$ for each p (implying a finite average distortion). Next, let $\mathbf{g}$ denote (g_0, g_1). Noting that $\{\mathbf{g}(\omega)\}$ is a stationary ergodic sequence with a cdf F, and letting $F_{n,\omega}$ be the empirical distribution function of the first n members of the sequence [76], one can show that for almost every ω, $\{F_{n,\omega}\}$ and F satisfy (see Lemma 4 of [76]) (7) $\{F_n\}$ converges weakly to the F and (8) $\lim_n \int \hat{d}((g_0, g_1), p) dF_n(g_0, g_1) = \int \hat{d}((g_0, g_1), p) dF(g_0, g_1)$, for every p.

Hence, from [76], we can conclude that the modified GLA satisfies properties 1) to 8). Therefore, Lemmas 1-3 of [76] are applicable to the modified GLA designed in this chapter and so the modified GLA satisfies the global convergence and empirical consistency properties as defined in [76].

3.7.3 Proof of Lemma 3.1

From the NNC condition of the modified GLA, the boundary between two adjacent regions $\mathcal{R}_j$ and $\mathcal{R}_{j+1}$ satisfies

$$\log(1 + g_1 p_j) - \lambda p_j - \mu g_0 p_j = \log(1 + g_1 p_{j+1}) - \lambda p_{j+1} - \mu g_0 p_{j+1}. \tag{3.21}$$

Solving the above equation for g_1, the result in the Lemma 3.1 follows. It is straightforward to show that it is an increasing convex function of g_0 by investigating the first and second derivatives.

3.7.4 Proof of Theorem 3.3 i)

We need to prove that for any two adjacent regions $\mathcal{R}_j$ and $\mathcal{R}_{j+1}, j = 1, \ldots, L-1$, $p_j > p_{j+1}$. Given an arbitrary g_0 satisfying $0 \leq g_0 < \frac{1}{\mu}(\frac{\log(\frac{p_j}{p_{j+1}})}{p_j - p_{j+1}} - \lambda)$ (assuming $\mu > 0$), suppose there is a point $(g_0, g_1^a) \in \mathcal{R}_j$ and a point $(g_0, g_1^c) \in \mathcal{R}_{j+1}$ (neither of these two points is on the boundary), and let (g_0, g_1^b) denote the point on the boundary corresponding to the same g_0, which from Lemma 3.1, is given by $g_1^b = \frac{e^{(\lambda+\mu g_0)(p_j - p_{j+1})} - 1}{p_j - p_{j+1}e^{(\lambda+\mu g_0)(p_j - p_{j+1})}}$ Then, we have $g_1^a > g_1^b > g_1^c$. Now suppose $p_j < p_{j+1}$. Since $(g_0, g_1^a) \in \mathcal{R}_j$, we have $\log(1 + g_1^a p_j) - \lambda p_j - \mu g_0 p_j \geq \log(1 + g_1^a p_{j+1}) - \lambda p_{j+1} - \mu g_0 p_{j+1}$ As $p_j < p_{j+1}$, we have $(\lambda + \mu g_0)(p_{j+1} - p_j) \geq \log(\frac{1+g_1^a p_{j+1}}{1+g_1^a p_j})$ which implies $e^{(\lambda+\mu g_0)(p_{j+1}-p_j)} - 1 \geq g_1^a(p_{j+1} - p_j e^{(\lambda+\mu g_0)(p_{j+1}-p_j)})$. We also have $g_1^b = \frac{e^{(\lambda+\mu g_0)(p_j - p_{j+1})} - 1}{p_j - p_{j+1}e^{(\lambda+\mu g_0)(p_j - p_{j+1})}} = \frac{e^{(\lambda+\mu g_0)(p_{j+1}-p_j)} - 1}{p_{j+1} - p_j e^{(\lambda+\mu g_0)(p_{j+1}-p_j)}}$. Note that $p_{j+1} > p_j$ implies $e^{(\lambda+\mu g_0)(p_{j+1}-p_j)} - 1 > 0$. Since $g_1^b > 0$, we have $p_{j+1} - p_j e^{(\lambda+\mu g_0)(p_{j+1}-p_j)} > 0$. Combining the above two results, we obtain $g_1^a \leq \frac{e^{(\lambda+\mu g_0)(p_{j+1}-p_j)} - 1}{p_{j+1} - p_j e^{(\lambda+\mu g_0)(p_{j+1}-p_j)}} = g_1^b$ which is a contradiction to $g_1^a > g_1^b$. Similarly, we can also prove that if $p_j < p_{j+1}$, we have $g_1^c \geq g_1^b$ which is a contradiction to $g_1^c < g_1^b$. Thus we must have $p_j > p_{j+1}$.

3.7.5 Proof of Theorem 3.3 ii)

From Lemma 3.1, the boundary between any two adjacent regions $\mathcal{R}_j$ and $\mathcal{R}_{j+1}$ is given by

$$\begin{aligned} g_1 &= \frac{e^{(\lambda+\mu g_0)(p_j - p_{j+1})} - 1}{p_j - p_{j+1}e^{(\lambda+\mu g_0)(p_j - p_{j+1})}} \\ &= \frac{e^{(\lambda+\mu g_0)p_j} - e^{(\lambda+\mu g_0)p_{j+1}}}{p_j e^{(\lambda+\mu g_0)p_{j+1}} - p_{j+1}e^{(\lambda+\mu g_0)p_j}} \\ &= (\lambda + \mu g_0)\frac{e^{(\lambda+\mu g_0)p_e}(p_j - p_{j+1})}{p_j e^{(\lambda+\mu g_0)p_{j+1}} - p_{j+1}e^{(\lambda+\mu g_0)p_j}} \\ &> \lambda + \mu g_0 \end{aligned} \tag{3.22}$$

where the last equality follows from the mean value theorem for some $p_\epsilon \in (p_{j+1}, p_j)$. The last inequality holds since we have $p_j e^{(\lambda+\mu g_0)p_\epsilon} > p_j e^{(\lambda+\mu g_0)p_{j+1}}$ and $-p_{j+1}e^{(\lambda+\mu g_0)p_\epsilon} > -p_{j+1}e^{(\lambda+\mu g_0)p_j}$. By rearranging, we get $\frac{e^{(\lambda+\mu g_0)p_\epsilon}(p_j-p_{j+1})}{p_j e^{(\lambda+\mu g_0)p_{j+1}}-p_{j+1}e^{(\lambda+\mu g_0)p_j}} > 1$.

3.7.6 Proof of Theorem 3.3 iii)

Given a fixed channel partitioning scheme, the optimal quantized power for $\mathcal{R}_j$ is obtained as $p_j = \max(p_j^*, 0), \forall j$, where p_j^* is determined by solving the equation $E[\frac{g_1}{1+g_1 p_j} - (\lambda + \mu g_0)|\mathcal{R}_j] = 0$. We can see that if $E[g_1|\mathcal{R}_j] \leq E[(\lambda + \mu g_0)|\mathcal{R}_j]$, then to satisfy the equation, $p_j^* < 0$, implying $p_j = \max(p_j^*, 0) = 0$. On the other hand, if $E[g_1|\mathcal{R}_j] > E[(\lambda + \mu g_0)|\mathcal{R}_j]$, p_j^* has to be strictly positive in order to satisfy the optimality equation, implying $\max(p_j^*, 0) = p_j^*$. We know from Theorem 3.3 ii) that all boundaries between any two adjacent regions have a lower bound given by $g_1 > \lambda + \mu g_0$, i.e. for any given (g_0, g_1) belonging to any of the first $L-1$ regions, $g_1 > \lambda + \mu g_0$. Thus for the first $L-1$ regions, $E[g_1|\mathcal{R}_j]Pr\{\mathcal{R}_j\} > E[(\lambda + \mu g_0)|\mathcal{R}_j]Pr\{\mathcal{R}_j\}$. Therefore the optimal quantized power in the first $L-1$ regions is strictly positive. This cannot be said however for p_L as for $\mathcal{R}_L$, we cannot guarantee $g_1 > \lambda + \mu g_0$ for any given (g_0, g_1) pair in that region. It is thus possible to have p_L to be 0. The next result shows under what circumstances one can have p_L to be exactly 0.

3.7.7 Proof of Theorem 3.3 iv)

Step 1: We know from Theorem 3.3 iii) that we always have $E[\frac{g_1}{1+g_1 p_j} - (\lambda + \mu g_0)|\mathcal{R}_j] = 0, j = 1, \ldots, L-1$, and for the region $\mathcal{R}_L$, this equation may not be satisfied when $p_L = 0$. Let us assume that $p_L > 0$. Then we have

$$\sum_{j=1}^{L} E[\lambda + \mu g_0|\mathcal{R}_j]Pr\{\mathcal{R}_j\} = \sum_{j=1}^{L} E[\frac{g_1}{1+g_1 p_j}|\mathcal{R}_j]Pr\{\mathcal{R}_j\}, \tag{3.23}$$

which implies,

$$\lambda + \mu = \sum_{j=1}^{L} E[\frac{g_1}{1+g_1 p_j}|\mathcal{R}_j]Pr\{\mathcal{R}_j\} < \sum_{j=1}^{L} E[g_1|\mathcal{R}_j]Pr\{\mathcal{R}_j\} = 1 \tag{3.24}$$

due to $\sum_{j=1}^{L} E[g_i|\mathcal{R}_j]Pr\{\mathcal{R}_j\} = E[g_i] = 1$, for $i = 0, 1$. Hence if $\lambda + \mu \geq 1$, we must have $p_L = 0$.

From the optimality equation, one can write $p_i = \frac{E[\frac{g_1 p_i}{1+g_1 p_i}|\mathcal{R}_i]}{\lambda+\mu E[g_0|\mathcal{R}_i]}$ when $p_i > 0$, it is obvious that $p_i < \frac{1}{\lambda+\mu E[g_0|\mathcal{R}_i]}$, $i = 1, 2, \ldots, L-1$. Since $p_L \geq 0$, this is also true for region $\mathcal{R}_L$. Therefore when $\mu \neq 0$, $\mu Q_{avg} = \mu \sum_{i=1}^{L} p_i E[g_0|\mathcal{R}_i]Pr(\mathcal{R}_i) < \sum_{i=1}^{L} \frac{\mu E[g_0|\mathcal{R}_i]}{\lambda+\mu E[g_0|\mathcal{R}_i]} Pr(\mathcal{R}_i) < \sum_{i=1}^{L} Pr(\mathcal{R}_i) = 1$. Similarly, if $\lambda \neq 0$, $\lambda P_{avg} < 1$. Thus $\mu > 1$ implies $Q_{av} < 1$ and $\lambda > 1$ implies $P_{av} < 1$.

Step 2: Next, we will show that no matter what λ, μ is, p_L must be zero for a sufficiently large L and $\lim_{L\to\infty} p_{L-1} = 0$. First, we will prove that as $L \to \infty$, the boundary between $\mathcal{R}_{L-1}$ and $\mathcal{R}_L$ approaches its limiting boundary $g_1 = \frac{\lambda+\mu g_0}{1-(\lambda+\mu g_0)\delta^*}$, where $\delta^* = \lim_{L\to\infty} p_L$. Given $p_1 > \cdots > p_L \geq 0$, it is clear that the sequence $\{p_i\}$, $i = 1, 2, \ldots, L$ is a monotonically decreasing sequence bounded below, therefore it must converge to its greatest-lower bound δ^* ($\delta^* = \lim_{L\to\infty} p_L \geq 0$) as $L \to \infty$. Therefore, it can be easily shown that for an arbitrarily small $\epsilon > 0$, we can always find a sufficiently large L such that $p_{L-1} - p_L < \epsilon$. Thus, as $L \to \infty$, $(p_{L-1} - p_L) \to 0$. Using this result, we can show that the boundary between $\mathcal{R}_{L-1}$ and $\mathcal{R}_L$ approaches the limiting boundary $g_1 = \frac{\lambda+\mu g_0}{1-(\lambda+\mu g_0)\delta^*}$ (or $\lambda + \mu g_0 = \frac{g_1}{1+g_1\delta^*}$) as $L \to \infty$, (since this boundary can be written as $\lambda + \mu g_0 = \frac{\log(\frac{1+g_1 p_{L-1}}{1+g_1 p_L})}{p_{L-1}-p_L}$, and $\lim_{L\to\infty}(\lim_{(p_{L-1}-p_L)\to 0} \frac{\log(\frac{1+g_1 p_{L-1}}{1+g_1 p_L})}{p_{L-1}-p_L}) = \lim_{L\to\infty} \frac{g_1}{1+g_1 p_L} = \frac{g_1}{1+g_1\delta^*}$). Now, suppose there exists a pair (λ, μ) such that $p_L > 0$ for any arbitrarily large L (implying $\delta^* > 0$). Thus for any L, p_L satisfies $E[\frac{g_1}{1+g_1 p_L} - (\lambda + \mu g_0)|\mathcal{R}_L] = 0$. From (1), we have as $L \to \infty$, the boundary between $\mathcal{R}_{L-1}$ and $\mathcal{R}_L$ approaches its limit $\lambda + \mu g_0 = \frac{g_1}{1+g_1\delta^*}$. Note that for a finite value of L, the region $\mathcal{R}_L$ can be divided into two parts $\mathcal{R}_{L1}$ and $\mathcal{R}_{L2}$ where $\mathcal{R}_{L1}$ corresponds to $\frac{\log(\frac{1+g_1 p_{L-1}}{1+g_1 p_L})}{p_{L-1}-p_L} \leq \lambda + \mu g_0 < \frac{g_1}{1+g_1\delta^*}$ and $\mathcal{R}_{L2}$ corresponds to $\frac{g_1}{1+g_1\delta^*} \leq \lambda + \mu g_0 < \infty$. As L becomes arbitrarily large, the region $\mathcal{R}_{L1}$ becomes vanishingly small, and one obtains $E(\lambda + \mu g_0|\mathcal{R}_L) > E(\frac{g_1}{1+g_1\delta^*}|\mathcal{R}_L) \geq E(\frac{g_1}{1+g_1 p_L}|\mathcal{R}_L)$ for a sufficiently large L, which is a contradiction to the KKT optimality condition for $p_L > 0$. Hence no matter what λ, μ are, p_L must be zero for a sufficiently large L. And $\delta^* = \lim_{L\to\infty} p_L = 0$. Finally, $\delta^* = 0$ implies the boundary between $\mathcal{R}_{L-1}$ and $\mathcal{R}_L$ approaches $g_1 = \lambda + \mu g_0$ as $L \to \infty$, and since as $L \to \infty$, $(p_{L-1} - p_L) \to 0$ and $p_L = 0$, we have $\lim_{L\to\infty} p_{L-1} = 0$.

Chapter 4

Throughput Maximization in Cognitive Radio with Limited Feedback : Peak Interference Constraints

4.1 Introduction

In chapter 3, we have studied the SU ergodic capacity maximization problem with quantized channel information under an average transmit power (ATP) constraint on the SU-TX and individual average interference power (AIP) constraint on each PU-TX. In this chapter, instead of the AIP constraint, another type of interference constraint at the PU, namely, the peak interference power (PIP) constraint, will be considered. This chapter aims to design optimal power allocation algorithms in a narrowband spectral sharing system where an SU communication link shares the same band with N PUs, that maximizes the SU throughput, while meeting the ATP constraint on SU-TX and the N individual peak interference constraints at each PU receiver (PU-RX), with various forms of imperfect CSI knowledge at the SU-TX. We first look at the throughput maximization problem with full knowledge of the CSI on the SU-TX to SU-RX link, denoted as g_1, and quantized CSI from the SU-TX to each PU-RX links, denoted as $\mathbf{g}_0 = \{g_{01}, \ldots, g_{0N}\}$ being available at the SU-TX. We derive the structure of the optimal quantization regions and the optimal power codebook is then obtained by solving the throughput maximization problem using the Karush-Kuhn Tucker (KKT) necessary conditions. Asymptotic ergodic capacity analysis for a large number of PUs is also provided. For the interference-limited

regime, where only the PIP constraints are active, an alternative algorithm resulting in an optimal quantized transmission rate codebook is also designed. Finally, we investigate the combined effect of imperfect g_1 and imperfect $\mathbf{g}_0$ knowledge at SU-TX in designing the optimal power codebook. With estimated g_1 and quantized $\mathbf{g}_0$ at SU-TX, it is not possible to guarantee that the actual PIP constraints will be satisfied with probability one. Thus a more appropriate approach for this case is to allow the PIP constraints to be violated with a certain small probability (we call it the interference violation probability (IVP)). The relationship between capacity loss due to the effect of estimated g_1 and the IVP is studied. For the case when both quantized g_1 and $\mathbf{g}_0$ available at SU-TX, due to the difficulty and complexity of optimal QPA analysis for this case, we consider a low-complexity suboptimal design of the QPA, in which based on the boundry $v = (\frac{1}{\lambda_l} - \frac{1}{g_1})^+$ (like full CSI case), two different type of power codebooks are derived. Efficiency of the various proposed algorithms is evaluated via numerical simulations.

This chapter is organized as follows. Section 4.2 describes the system model and presents the optimal power allocation scheme for throughput maximization problem with full CSI assumption. In Section 4.3, we design the optimal power codebook for the throughput maximization problem with perfect g_1 information and quantized $\mathbf{g}_0$ knowledge at SU-TX. The asymptotic SU ergodic capacity performance analysis for large number of PUs is also provided. For the interference-limited regime, an alternative algorithm called the quantized rate allocation scheme for solving the throughput maximization problem is studied. In Section 4.4, the throughput maximization problem with both imperfect g_1 and $\mathbf{g}_0$ information at SU-TX is investigated. Some numerical results are presented in Section 4.5 and Section 4.6 contains the conclusions. All proofs are relegated to the appendix section 4.7 in this chapter.

4.2 System Model and Problem Formulation

We consider an infrastructure-based spectrum sharing scenario where a SU communicates to its base station using a narrowband channel shared with multiple PUs for transmission. Regardless of the on/off status of *PUs*, the SU is allowed to use the band

which are licensed to $PU_1, \ldots, PU_N$, as long as the impact of the secondary transmission does not substantially degrade the received signal quality of *PUs*. Let $g_1 = |h_1|^2$ and $g_{0i} = |h_{0i}|^2$ $(i = 1, \ldots, N)$ denote the nonnegative real-valued instantaneous channel power gains for the links from the secondary transmitter (SU-TX) to the secondary receiver (SU-RX) and the SU-TX to the receiver of PU_i $(i = 1, \ldots, N)$ respectively, where h_1 and h_{0i} are corresponding complex channel amplitude gains. These channels are assumed to be Rayleigh block fading channels such that all g_1 and g_{0i} $(i = 1, \ldots, N)$ are statistically mutually independent and, without loss of generality (*w.l.o.g*, similar to the assumption made in Chapter 3), are exponentially distributed with unity mean. Similarly, additive noises for each channel are independent Gaussian random variables with zero mean and unit variance *w.l.o.g*. Note that extensions to other distributions such as Nakagami, Rician etc. can also be handled easily. For analytical simplicity, the interference from the primary transmitter (PU-TX) to SU-RX is neglected following previous work such as [7,117](in the case where the interference caused by the PU-TX at the SU-RX is significant, the SU ergodic capacity results derived in this chapter can be taken as upper bounds on the actual capacity under primary-induced interference). This assumption is justified when either the SU is outside the PU's transmission range or the SU receiver is equipped with interference cancellation capability particularly when the PU signal is strong.

Given a channel realization $\mathbf{g}_0 = \{g_{01}, \ldots, g_{0N}\}$ and g_1, assume that the channel state information (CSI) $(\mathbf{g}_0, g_1)$, is available at the SU-TX, and the power allocated at the SU-TX is represented by $p(\mathbf{g}_0, g_1)$, then the ergodic capacity of the SU for this spectrum sharing system can be expressed as

$$C = E[\log(1 + g_1 p(\mathbf{g}_0, g_1))] \tag{4.1}$$

where log represents the natural logarithm. A common way to protect PU's received signal quality is by imposing either an average or a peak interference power (AIP/PIP) constraint at PU-RX. We studied the optimization problem of maximizing SU capacity under both average transmit power constraint (ATP) at SU and AIP constraints at PUs with quantized CSI in Chapter 3. Although the AIP constraint is more favorable espe-

cially in the context of transmission over fading channels [123], there are other applications where it is desirable to impose a PIP constraint [45]. Thus motivated, we consider the following optimal power allocation problem that maximizes the ergodic capacity of SU in a narrowband spectrum sharing with multiple PUs, under an ATP constraint at SU-TX and a PIP constraint at each PU_i-RX, given by,

$$\begin{aligned} \max_{p(\mathbf{g}_0, g_1)\geq 0} \quad & E[\log(1+g_1 p(\mathbf{g}_0, g_1))] \\ s.t. \quad & E[p(\mathbf{g}_0, g_1)] \leq P_{av}, \\ & g_{0i} p(\mathbf{g}_0, g_1) \leq Q_{pk}, \ \ \forall i \ \ almost\ surely \end{aligned} \tag{4.2}$$

where P_{av} is the average transmit power of SU and the Q_{pk} is the maximum peak interference power tolerated by each PU-RX. It is easy to show that the above PIP constraints can be reformulated as [7][45]

$$p(\mathbf{g}_0, g_1) \leq \frac{Q_{pk}}{\max_i g_{0i}}, \ \ i = 1, \ldots, N \tag{4.3}$$

For the case of $N = 1$, the optimal power allocation for Problem (4.2) with the assumption that full CSI is available at the SU-TX can be found in [117]. A trivial extension of this result for $N > 1$ shows that the optimal solution for Problem (4.2) with full CSI is given by

$$p(\mathbf{g}_0, g_1) = \begin{cases} 0, & g_1 \leq \lambda_f \\ \frac{1}{\lambda_f} - \frac{1}{g_1}, & g_1 > \lambda_f, \ g_m < \frac{Q_{pk}}{\frac{1}{\lambda_f} - \frac{1}{g_1}} \\ \frac{Q_{pk}}{g_m}, & g_1 > \lambda_f, \ g_m \geq \frac{Q_{pk}}{\frac{1}{\lambda_f} - \frac{1}{g_1}} \end{cases} \tag{4.4}$$

where $g_m = \max_i g_{0i}, \ \ i = 1, \ldots, N$, λ_f is the nonnegative Lagrange multiplier associated with the ATP constraint and can be obtained by solving $\lambda_f(E[p(\mathbf{g}_0, g_1)] - P_{av}) = 0$. Actually, (4.4) also can be written as

$$p(\mathbf{g}_0, g_1) = \min([\frac{1}{\lambda_f} - \frac{1}{g_1}]^+, \frac{Q_{pk}}{g_m}) \tag{4.5}$$

Special Case: when P_{av} is sufficiently large [1] to make the ATP constraint inactive and thus only PIP constraints is active, (termed as the 'Interference Limited Regime (ILR)'), Problem (4.2) with full CSI reduces to the problem considered in [7],[45], where the ergodic capacity maximization problem is studied under PIP constraints only and gives the maximum ergodic capacity of SU as

$$C = E[\log(1 + g_1 \frac{Q_{pk}}{g_m})] = E[\log(1 + zQ_{pk})] \tag{4.6}$$

where $Z = \frac{g_1}{g_m}$, and the pdf of Z, is given by [7][45]

$$f(z) = N \sum_{k=0}^{N-1} (-1)^k \binom{N-1}{k} \frac{1}{(1+k+z)^2}. \tag{4.7}$$

However, the assumption of full CSI at the SU-TX (especially that of $\mathbf{g}_0$) is usually unrealistic in practical systems. In the next section, we are therefore interested in designing power allocation schemes of the SU ergodic capacity maximization problem (4.2) based on quantized CSI acquired via a no-delay and error-free feedback link with limited rate, where we assume that SU-TX has perfect knowledge of g_1 but only can access partial knowledge of $\mathbf{g}_0$.

4.3 Optimum Quantized power allocation (QPA) with perfect g_1 and imperfect g_0 at SU-TX

4.3.1 Optimal QPA with limited rate feedback strategy

As shown in Fig.4.1, here we assume that there is a central controller termed as the CR network manager who can obtain perfect information on g_1 from the SU base station and perfect information of $\mathbf{g}_0$ from the PU base station, possibly over fibre-optic links and then forward some appropriately quantized $V = \frac{Q_{pk}}{g_m}$ CSI information to SU-TX through a finite-rate feedback link. Note that the existence of such central controllers is also assumed quite commonly in literature on multi-cell MIMO or macro-diversity based sys-

[1] For $N = 1$ case, this requires $P_{av} \to \infty$, but for $N > 1$, $P_{av} < \infty$ can be sufficiently large

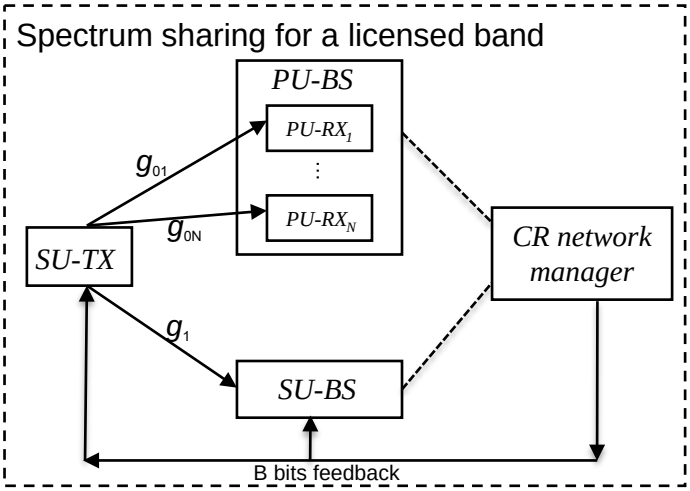

Figure 4.1: System model for QPA strategy

tems with cooperative base stations in a primary network, where several base stations are assumed to be connected to a central controller via a backhaul link so that information about out-of-cell interference can be obtained resulting in higher capacity[88][22]. Under such a network modelling assumption, given B bits of feedback, a power codebook $\mathcal{P}= \{p_1, \ldots, p_L\}$ of cardinality $L = 2^B$, is designed offline based on the statistics of V and g_1. This codebook is made available *a priori* by both SU-TX, SU-RX and CR network manager. Given a channel realization $(\mathbf{g}_0, g_1)$, the CR network manager applies a deterministic mapping $\mathcal{I}(V, g_1)$ from the current instantaneous (V, g_1) information to one of L integer indices, which partitions the vector space of (V, g_1) into L regions $\mathcal{R}_1, \ldots, \mathcal{R}_L$. This mapping is defined as $\mathcal{I}(V, g_1) = j$, if $(V, g_1) \in \mathcal{R}_j$, $j = 1, \ldots, L$), and then sends the corresponding index $j = \mathcal{I}(V, g_1)$ to the SU-TX via the feedback link. The SU-TX then uses the associated power codebook element (e.g., if the feedback signal is j, then p_j will be used as the transmission power) to adapt its transmission strategy.

Let $Pr(\mathcal{R}_j)$, $E[\bullet|\mathcal{R}_j]$ indicate $Pr((V, g_1) \in \mathcal{R}_j)$ (the probability that (V, g_1) falls in the region $\mathcal{R}_j$) and $E[\bullet|(V, g_1) \in \mathcal{R}_j]$, respectively. Then the SU ergodic capacity maximization problem (4.2) with limited feedback can be formulated as

$$\max_{\{p_1, \ldots, p_L\}} C_L(\mathcal{P}) = \sum_{j=1}^{L} E[\log(1 + p_j g_1)|\mathcal{R}_j] Pr(\mathcal{R}_j)$$

$$s.t. \quad \sum_{j=1}^{L} E[p_j|\mathcal{R}_j]Pr(\mathcal{R}_j) \leq P_{av},$$
$$0 \leq p_j \leq \min(v|\mathcal{R}_j), \ \forall j = 1, \ldots, L \tag{4.8}$$

Thus we need to design the joint optimization of the channel partition regions and the power codebook such that the ergodic capacity of SU is maximized under the above constraints.

Lemma 4.1. *Let $\mathcal{P} = \{p_1, \ldots, p_L\}$ and the corresponding channel partitioning $\mathcal{R}_1, \ldots, \mathcal{R}_L$ denote the optimal solution to the optimization problem (4.8). Let $p(V, g_1)$ represent the mapping from instantaneous (V, g_1) to allocated power level, then*

1) When $\lambda > 0$, let $\{v_1, \ldots, v_{L-1}\}$ denote the optimum quantization thresholds on V axis $(0 = v_1 < \cdots < v_{L-1} < \frac{1}{\lambda})$ and let $v_L = \frac{1}{\lambda}$, we have

$$p(V, g_1) = \begin{cases} p_1 = 0, & \text{if } g_1 \leq \lambda \text{ or } V < (\frac{1}{\lambda} - \frac{1}{g_1}),\ v_1 \leq V < v_2 \\ p_j = v_j, & \text{if } V < (\frac{1}{\lambda} - \frac{1}{g_1}),\ v_j \leq V < v_{j+1},\ j = 2, \ldots, L-1 \\ p_L = (\frac{1}{\lambda} - \frac{1}{g_1}), & \text{if } g_1 > \lambda, V \geq (\frac{1}{\lambda} - \frac{1}{g_1}) \end{cases} \tag{4.9}$$

2) When $\lambda = 0$, let $\{v_1, \ldots, v_L\}$ denote the optimum quantization thresholds on V axis $(0 = v_1 < \cdots < v_L < \infty)$ and let $v_{L+1} = \infty$, we have

$$p(V, g_1) = p_j = v_j, \ \text{if } v_j \leq V < v_{j+1},\ j = 1, \ldots, L \tag{4.10}$$

where λ is the nonnegative Lagrange multiplier associated with the ATP constraint of problem (4.8).

Proof: The proof can be found in the appendix of this chapter.

From Lemma 4.1, when $\lambda = 0$, or in other words the ATP constraint is inactive, the quantization structure is pretty straightforward as it only involves quantization of the V axis. Fig.4.2 illustrates the optimum partition regions structure when $\lambda > 0$. Note that here the first region $\mathcal{R}_1$ includes two parts, i.e, $\{g_1 \leq \lambda\}$ and $\{V < (\frac{1}{\lambda} - \frac{1}{g_1}),\ v_1 \leq V < v_2\}$, and $p_1 = 0$ implies that the first region is in outage.

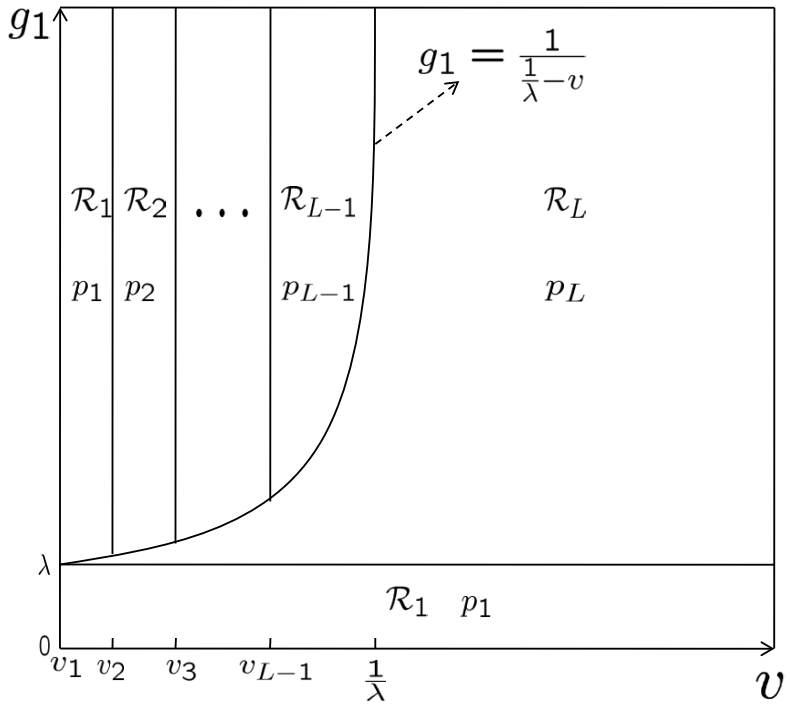

Figure 4.2: The structure of optimum quantization regions when $\lambda > 0$

Below we consider the two cases $\lambda > 0$ and $\lambda = 0$ separately.

1) When $\lambda > 0$ (ATP constraint is active)

Let $F(v), f(v)$ indicate the cdf and pdf of V respectively, from Lemma4.1 the problem (4.8) becomes,

$$\max_{\{v_2,\ldots,v_{L-1}\}} C_L(\mathcal{P}) = \sum_{j=2}^{L-1} E[\log(1+v_j g_1)|\mathcal{R}_j]Pr(\mathcal{R}_j) + E[\log(1+(\frac{1}{\lambda}-\frac{1}{g_1})g_1)|\mathcal{R}_L]Pr(\mathcal{R}_L)$$

$$s.t. \quad \sum_{j=2}^{L-1} E[v_j|\mathcal{R}_j]Pr(\mathcal{R}_j) + E[(\frac{1}{\lambda}-\frac{1}{g_1})|\mathcal{R}_L]Pr(\mathcal{R}_L) \leq P_{av} \tag{4.11}$$

Although the above optimization problem may be verified to be non-convex, we can employ the Karush-Kuhn-Tucker (KKT) necessary conditions to find local maxima for Problem (4.11). Taking the first derivative of the Lagrangian function of problem (4.11)

by using Leibniz integral rule, and setting it to zero, we can obtain

$$\int_{v_j}^{v_{j+1}} \left(\frac{-\exp(\frac{1}{v_j})E_1(\frac{1}{\frac{1}{\lambda}-v}+\frac{1}{v_j})}{v_j^2} + \exp(-\frac{1}{\frac{1}{\lambda}-v})(\frac{1}{v_j}-\lambda)\right) f(v)dv$$
$$= (\hat{f}_j(v_j) - \hat{f}_j(v_{j-1}))f(v_j), \;\; j = 2, \ldots, L-1 \tag{4.12}$$

where $E_1(x)$ is the exponential integral defined as $E_1(x) = \int_x^\infty \frac{\exp(-z)dz}{z}$ and $\hat{f}_2(v_1) = 0$,

$$\hat{f}_j(v) = \exp(\frac{1}{v})E_1(\frac{1}{\frac{1}{\lambda}-v_j}+\frac{1}{v}) + \exp(-\frac{1}{\frac{1}{\lambda}-v_j})\log(1+v\frac{1}{\frac{1}{\lambda}-v_j}) - \lambda v\exp(-\frac{1}{\frac{1}{\lambda}-v_j}), \tag{4.13}$$

and the λ can be obtained by solving

$$\lambda(\sum_{j=2}^{L-1} E[v_j|\mathcal{R}_j]Pr(\mathcal{R}_j) + E[\frac{1}{\lambda} - \frac{1}{g_1}|\mathcal{R}_L]Pr(\mathcal{R}_L) - P_{av}) = 0 \tag{4.14}$$

It is shown in appendix 4.7.2 that

$$F(v) = 1 - (1-\exp(-\frac{Q_{pk}}{v}))^N, \quad f(v) = \frac{NQ_{pk}}{v^2}\exp(-\frac{Q_{pk}}{v})(1-\exp(-\frac{Q_{pk}}{v}))^{N-1}. \tag{4.15}$$

Thus, for fixed λ, given a v_2, from (4.12) we can successively compute $v_3, \ldots, v_{L-1}$ numerically, and then the equation (4.12) with $j = L-1$, which thus has only one unknown variable v_2, can be numerically solved for v_2. Then the optimal value of λ can be obtained by solving (4.14) with a subgradient method, i,e. by updating λ until convergence using

$$\lambda^{l+1} = [\lambda^l - \alpha^l(P_{av} - \sum_{j=2}^{L-1} E[v_j|\mathcal{R}_j]Pr(\mathcal{R}_j) - E[(\frac{1}{\lambda} - \frac{1}{g_1})|\mathcal{R}_L]Pr(\mathcal{R}_L))]^+ \tag{4.16}$$

where l is the iteration number, α^l is positive scalar step size for l-th iteration. One can thus repeat above two steps namely solving (4.12) and (4.16) iteratively until a satisfactory convergence criterion is met.

2) When $\lambda = 0$ (only the PIP constraints are active, namely the ILR case)

In this case, we can see from Lemma 4.1 that none of power levels depends on g_1

information and therefore in this case, SU-TX or CR network manager does not require any knowledge of g_1. And the problem (4.8) becomes,

$$\max_{\{v_2,\ldots,v_L\}} C_L(\mathcal{P}) = \sum_{j=2}^{L} E[\log(1+v_j g_1)](F(v_{j+1}) - F(v_j)) \tag{4.17}$$

By using the KKT necessary conditions we can obtain

$$F(v_{j+1}) = F(v_j) + f(v_j)\frac{\tilde{f}_1(v_j) - \tilde{f}_1(v_{j-1})}{\tilde{f}_2(v_j)}, \quad j = 2,\ldots,L \tag{4.18}$$

where $\tilde{f}_1(v_1) = 0$ and

$$\tilde{f}_1(v) = E[\log(1+vg_1)] = \exp(\frac{1}{v})E_1(\frac{1}{v}), \qquad \tilde{f}_2(v) = \frac{\partial \tilde{f}_1(v)}{\partial v} = \frac{-\exp(\frac{1}{v})E_1(\frac{1}{v})}{v^2} + \frac{1}{v} \tag{4.19}$$

From the expression of $F(v)$ in (4.15), (4.18) can be rewritten as,

$$v_{j+1} = -\frac{Q_{pk}}{\log(1-(1-(F(v_j)+f(v_j)\frac{\tilde{f}_1(v_j)-\tilde{f}_1(v_{j-1})}{\tilde{f}_2(v_j)}))^{\frac{1}{N}})}, \quad j = 2,\ldots,L-1$$

$$F(v_L) + f(v_L)\frac{\tilde{f}_1(v_L) - \tilde{f}_1(v_{L-1})}{\tilde{f}_2(v_L)} = 1. \tag{4.20}$$

Thus, given a specific value of v_2, we can successively compute $v_3,\ldots,v_L$ using (4.20) , and then the last equation in (4.20) , which thus has only one unknown variable v_2, can be numerically solved for v_2.

As the number of feedback bit $B = log_2(L) \to \infty$, the length of quantization interval $[v_j, v_{j+1})$ approaches zero, by using the mean value theorem [13], we can get

$$\frac{\tilde{f}_1(v_j) - \tilde{f}_1(v_{j-1})}{\tilde{f}_2(v_j)} \approx v_j - v_{j-1} \tag{4.21}$$

Substituting (4.21) into (4.18), we have, for $j = 2,\ldots,L$

$$F(v_{j+1}) - F(v_j) \approx f(v_j)(v_j - v_{j-1}) \approx F(v_j) - F(v_{j-1}) \tag{4.22}$$

From (4.22), we have

$$F(v_{L+1}) - F(v_L) \approx \cdots \approx F(v_2) - F(v_1) = \frac{1}{L} \tag{4.23}$$

This implies that one can apply an equal probability per region (EPPR) approximation yielding

$$F(v_j) \approx \frac{j-1}{L}, \quad j = 2, \ldots, L \tag{4.24}$$

Therefore from the expression of $F(v)$, we have,

$$v_j = F^{-1}(v) \approx -\frac{Q_{pk}}{\log(1-(1-\frac{j-1}{L})^{\frac{1}{N}})}, \ j = 2, \ldots, L \tag{4.25}$$

Then we can obtain an approximate expression for the maximum ergodic capacity of SU of problem (4.17) with large L as,

$$C_L \approx \frac{1}{L}\sum_{j=2}^{L} \exp(-\frac{\log(1-(1-\frac{j-1}{L})^{\frac{1}{N}})}{Q_{pk}}) E_1(-\frac{\log(1-(1-\frac{j-1}{L})^{\frac{1}{N}})}{Q_{pk}}) \tag{4.26}$$

Special Case: When in addition, $N \to \infty$ (large number of PUs case), applying the asymptotic cdf of v (see (4.31) below), given by $F(v) \to 1 - e^{-Ne^{-\frac{Q_{pk}}{v}}}$, we have,

$$v_j \approx -\frac{Q_{pk}}{\log(-\frac{\log(1-\frac{j-1}{L})}{N})}, \quad j = 2, \ldots, L \tag{4.27}$$

and

$$C_L \approx \frac{1}{L}\sum_{j=2}^{L} \exp(-\frac{\log(-\frac{\log(1-\frac{j-1}{L})}{N})}{Q_{pk}}) E_1(-\frac{\log(-\frac{\log(1-\frac{j-1}{L})}{N})}{Q_{pk}}) \tag{4.28}$$

So far, we have discussed how to solve the quantization problem (4.8) for the $\lambda > 0$ case and the $\lambda = 0$ case respectively. We can now combine these two procedures to define the following two steps for finding the optimal solution for problem (4.8):

a) First, let $\lambda = 0$, then solving (4.20) gives a power codebook $\{p_1, \ldots, p_L\}$. With this

codebook, if $\sum_{j=1}^{L} E[p_j|\mathcal{R}_j]Pr(\mathcal{R}_j) \leq P_{av}$, then it is an optimal power codebook for problem (4.8) and stop; otherwise go to step b).

b) If a) is not satisfied, we must have $\lambda > 0$. Starting with a random initial value for λ, one can solve (4.12) to obtain the corresponding power codebook $\{p_1, \ldots, p_L\}$, and then update λ by (4.16). Repeat these steps until convergence and the final codebook will be an optimal power codebook for problem (4.8).

4.3.2 Asymptotic Analysis with Large Number of PUs for QPA (ALNPs-QPA)

So far, we have considered one SU and N PUs. As we can see from 4.3.1, the change of N only affects the distribution of V in (4.15). As N increases, the expression of the distribution of V ($F(v)$ and $f(v)$) becomes complex. In this section, we are interested in finding the asymptotic distribution of V as $N \to \infty$, so that we can significantly reduce the computational complexity of solving Problem (4.8) for a large number of PUs.

As we know $V = \frac{Q_{pk}}{g_m}$. Then the cdf of V is given by

$$F(v) = Pr(\frac{Q_{pk}}{g_m} < v) = \int_{\frac{Q_{pk}}{v}}^{\infty} f_{g_m}(g_m) dg_m \tag{4.29}$$

It is shown in appendix 4.7.3 that as $N \to \infty$, the limiting asymptotic pdf of g_m is given by

$$f_{g_m}(g_m) \to N \exp(-g_m) \exp(-Ne^{-g_m}) \tag{4.30}$$

Substituting (4.30) into (4.29), we have

$$F(v) \to 1 - \exp(-Ne^{-\frac{Q_{pk}}{v}}) \tag{4.31}$$

Then after differentiation, the limiting asymptotic pdf of V is given by,

$$f(v) \to \frac{NQ_{pk}}{v^2} \exp(-\frac{Q_{pk}}{v}) \exp(-Ne^{-\frac{Q_{pk}}{v}}). \tag{4.32}$$

This asymptotic distribution can be used as an approximation for $f(v)$ when N becomes large and the same techniques as the previous section can be used to find an optimum QPA.

4.3.3 Quantized rate allocation (QRA) for ILR case

When the ATP constraint is inactive and only PIP constraints are active, we actually can do two alternative quantization methods: 1) QPA strategy (i.e, quantized $V = \frac{Q_{pk}}{g_m}$ information) as shown in 4.3.1 with $\lambda = 0$, or 2) QRA scheme (i.e, quantized ratio $Z = \frac{g_1}{g_m}$ information). It is important to note that unlike QPA with $\lambda = 0$ (here we call it QPA0), the QRA scheme requires the assumption that SU-TX has full knowledge of g_1.

The limited feedback strategy for QRA is similar to QPA case, namely, given B bits of feedback, an operating rate codebook $\mathbf{r}= \{r_1, \ldots, r_L\}$ is designed off line purely on the basis of the statistics of ratio Z information. Again the codebook is known *a priori* by both SU-TX and CR network manager. Given a channel realization ($\mathbf{g}_0$, g_1), the CR network manager applies a deterministic mapping $\mathcal{I}(Z)$ from the current instantaneous ratio Z information to one of L integer indices, which partitions the nonnegative ratio information (scalar space) into L regions $\mathcal{R}_1, \ldots, \mathcal{R}_L$, i.e, $\mathcal{I}(Z) = j$, if $Z \in [z_j, z_{j+1})$, $j = 1, \ldots, L$, where z_j represents the boundary point between $\mathcal{R}_{j-1}$ and $\mathcal{R}_j$, and $z_1 = 0$, $z_{L+1} = \infty$. It then sends the corresponding index $j = \mathcal{I}(Z)$ to the SU-TX via the feedback link. The SU-TX will use the associated rate codebook element to adapt its transmission strategy. We will show later that $r_j = \log(1 + z_j Q_{pk})$, thus with the perfect knowledge of g_1, the actual transmission power at SU is $p_j = \frac{z_j Q_{pk}}{g_1}$, and then the actual received interference power at PU_i is

$$p_j g_{0i} = \frac{z_j Q_{pk}}{\frac{g_1}{g_{0i}}} \leq \frac{z_j Q_{pk}}{\frac{g_1}{\max_i g_{0i}}} \leq Q_{pk} \tag{4.33}$$

since the current ratio CSI $\frac{g_1}{\max_i g_{0i}}$ falls in $\mathcal{R}_j$, $\frac{g_1}{\max_i g_{0i}} \geq z_j$. (4.33) confirms that this limited feedback strategy can guarantee that all PIP constraints are satisfied at the PU receivers.

For any given ratio state information $Z = z$, the corresponding maximum mutual information of SU is given by $\log(1 + zQ_{pk})$, denoted as $R(z)$. Thus, for any $z \in \mathcal{R}_j$, with

the rate level r_j, reliable transmission can be guaranteed only if $R(z) \geq r_j$, which means, when $R(z) < r_j$, an outage will occur. Let $Pr(\mathcal{R}_j)$, $Pr(\bullet|\mathcal{R}_j)$ denote $Pr(Z \in \mathcal{R}_j)$ and $Pr(\bullet|Z \in \mathcal{R}_j)$, respectively. Then the ergodic capacity of SU can be expressed as,

$$C_L(\mathbf{r}) = \sum_{j=1}^{L} r_j Pr(R(z) \geq r_j|\mathcal{R}_j)Pr(\mathcal{R}_j) \tag{4.34}$$

Lemma 4.2. *Let z_j^* be the unique solution for $r_j = \log(1 + z_j^* Q_{pk})$, we have $z_j^* \in [z_j, z_{j+1})$.*

Proof: The proof can be found in the appendix of this chapter.

Let $F(z)$ indicate the cdf of ratio Z, and [45] gives $F(z) = 1 - N\sum_{k=0}^{N-1}(-1)^k\binom{N-1}{k}\frac{1}{1+k+z}$, which actually can be rewritten as

$$F(z) = 1 - NB(N, z+1) \tag{4.35}$$

where $B(a,b)$ is the beta function, defined by $B(a,b) = \frac{\Gamma(a)\Gamma(b)}{\Gamma(a+b)}$. And the pdf $f(z)$ of ratio Z is given in (4.7). Then the secondary ergodic capacity maximization problem (4.6) with QRA can be formulated as

$$\begin{aligned} \max_{\{z_2,\ldots,z_L,z_1^*,\ldots,z_L^*\}} \quad & \sum_{j=1}^{L} log(1 + z_j^* Q_{pk})(F(z_{j+1}) - F(z_j^*)) \\ s.t. \quad & z_j \leq z_j^* \leq z_{j+1} \quad \forall j \end{aligned} \tag{4.36}$$

Lemma 4.3. $z_j = z_j^* \quad j = 2, \ldots, L.$

Proof: The proof can be found in the appendix of this chapter.

Then Problem (4.36) becomes,

$$\max_{z_j^*} \sum_{j=1}^{L} log(1 + z_j^* Q_{pk})(F(z_{j+1}^*) - F(z_j^*)) \tag{4.37}$$

Applying the KKT necessary condition to (4.37), we have

$$\log(\frac{1 + z_{j-1}^* Q_{pk}}{1 + z_j^* Q_{pk}})f(z_j^*) + \frac{Q_{pk}}{1 + z_j^* Q_{pk}}(F(z_{j+1}^*) - F(z_j^*)) = 0 \tag{4.38}$$

where $z_0^* = 0$ and $z_{L+1}^* = \infty$. From (4.38), we have, j=2,...,L

$$z_{j-1}^* = \frac{1}{Q_{pk}}(\exp\{-\frac{Q_{pk}}{1+z_j^* Q_{pk}}\frac{F(z_{j+1}^*)-F(z_j^*)}{f(z_j^*)} + log(1+z_j^* Q_{pk})\} - 1) \tag{4.39}$$

Thus, given a z_L^*, from (4.39) we can successively compute $z_{L-1}^*, \ldots, z_1^*$, and then (4.38) with $j = 1$ becomes an equation with only one unknown variable z_L^*, which can be solved numerically.

QRA has a similar asymptotic behavior in the high resolution quantization as QPA0. From the KKT conditions (4.38), we have that, $j = 1, \ldots, L$

$$\frac{F(z_{j+1}^*)-F(z_j^*)}{f(z_j^*)} = \frac{\log(1+z_j^* Q_{pk}) - \log(1+z_{j-1}^* Q_{pk})}{\frac{Q_{pk}}{1+z_j^* Q_{pk}}} \tag{4.40}$$

Again as the number of feedback bits $B = log_2(L) \to \infty$, by using the mean value theorem, we can get

$$\frac{\log(1+z_j^* Q_{pk}) - \log(1+z_{j-1}^* Q_{pk})}{\frac{Q_{pk}}{1+z_j^* Q_{pk}}} \approx (z_j^* - z_{j-1}^*). \tag{4.41}$$

Substituting (4.41) into (4.40), we have,

$$F(z_{j+1}^*) - F(z_j^*) \approx f(z_j^*)(z_j^* - z_{j-1}^*) \approx F(z_j^*) - F(z_{j-1}^*) \tag{4.42}$$

From (4.42), we have

$$F(z_{L+1}^*) - F(z_L^*) \approx \cdots \approx F(z_1^*) - F(z_0^*) = \frac{1}{L+1} \tag{4.43}$$

Which gives

$$F(z_j^*) \approx \frac{j}{L+1}, \quad j = 1, \ldots, L \tag{4.44}$$

Therefore we have,

$$z_j^* \approx F^{-1}(\frac{j}{L+1}), \quad j = 1, \ldots, L \tag{4.45}$$

From (4.35), we have $F(z) = 1 - NB(N, z+1)$, then $F^{-1}(\frac{j}{L+1})$ is the solution of solving below equation for z.

$$1 - NB(N, z+1) = \frac{j}{L+1} \tag{4.46}$$

Then we can obtain the maximum ergodic capacity of SU as,

$$C_L \approx \frac{1}{L+1} \sum_{j=1}^{L} log(1 + F^{-1}(\frac{j}{L+1}) Q_{pk}) \tag{4.47}$$

Special cases

• $N = 1$ (only one PU case), from (4.46), we can obtain

$$F^{-1}(\frac{j}{L+1}) = \frac{j}{L+1-j} \tag{4.48}$$

Thus (4.47) becomes

$$C_L \approx \frac{1}{L+1} \sum_{j=1}^{L} log(1 + \frac{j}{L+1-j} Q_{pk}) \tag{4.49}$$

• $N \to \infty$ (large number of PU case), applying the asymptotic cdf of z which will be derived below in (4.56), i.e, $F(z) \to 1 - \exp(-N) + N^{-z}(\Gamma(z+1, N) - \Gamma(z+1))$, then $F^{-1}(\frac{j}{L+1})$ can be approximated as the solution of solving below equation for z.

$$1 - e^{-N} + N^{-z}(\Gamma(z+1, N) - \Gamma(z+1)) = \frac{j}{L+1} \tag{4.50}$$

We can further approximate the above equation by applying $\lim_{N\to\infty} \Gamma(z+1, N) = 0$ and $\lim_{N\to\infty} e^{-N} = 0$, therefore equation (4.50) becomes,

$$N^{-z}\Gamma(z+1) \approx c \tag{4.51}$$

where $c = 1 - \frac{j}{L+1}$, and since $j = 1, \ldots, L$, we have $0 < c < 1$.

Lemma 4.4. *For a fixed L, when $N \to \infty$, the solution for equation (4.51) approaches zero, i.e, $z \to 0$.*

Proof: The proof can be found in the appendix of this chapter.

Applying Lemma 4.4, we have as $N \to \infty$, $\Gamma(z+1) \approx 1 - \gamma z$, where $\gamma = 0.57721566...$ is the Euler-Mascheroni constant. Thus (4.51) becomes

$$N^{-z}(1 - \gamma z) \approx c \tag{4.52}$$

which gives the solution $z = \frac{1}{\gamma} - \frac{W(\frac{1}{\gamma} c N^{\frac{1}{\gamma}} \log N)}{\log N}$, where $W(x)$ is Lambert W function which gives the principal solution for w in $x = we^w$. Thus, for a fixed L, as $N \to \infty$, we can obtain

$$F^{-1}(\frac{j}{L+1}) \approx \frac{1}{\gamma} - \frac{W(\frac{1}{\gamma}(1 - \frac{j}{L+1}) N^{\frac{1}{\gamma}} \log N)}{\log N} \tag{4.53}$$

then in this case, (4.47) is given by the following closed form approximation

$$C_L \approx \frac{1}{L+1} \sum_{j=1}^{L} \log(1 + (\frac{1}{\gamma} - \frac{W(\frac{1}{\gamma} \frac{L+1-j}{L+1} N^{\frac{1}{\gamma}} \log N)}{\log N}) Q_{pk}) \tag{4.54}$$

As in the QPA case, we also can find the asymptotic distribution of Z as $N \to \infty$, in order to simplify the solution to Problem (4.37) with large number of PUs, called ALNPs-QRA. As we know $Z = \frac{g_1}{g_m}$. By letting $X = g_m$, the cdf of Z is given by

$$F(z) = \int_0^\infty P(g_1 < xz|x) f_X(x) dx = \int_0^\infty (1 - e^{-xz}) f_X(x) dx \tag{4.55}$$

It is shown in appendix 4.7.3 that as $N \to \infty$, the asymptotic pdf of X is given by $f_X(x) \to Ne^{-x} e^{-Ne^{-x}}$. Substituting it into (4.55), we have

$$F(z) \to 1 - e^{-N} + \int_0^\infty e^{-xz} N e^{-Ne^{-x}} de^{-x} = 1 - e^{-N} + N^{-z}(\Gamma(z+1, N) - \Gamma(z+1)) \tag{4.56}$$

where $\Gamma(a, b)$ is the incomplete gamma function given by $\Gamma(a, b) = \int_b^\infty t^{a-1} e^{-t} dt$ and $\Gamma(a)$ is defined by $\Gamma(a) = \int_0^\infty t^{a-1} e^{-t} dt$. Then the asymptotic pdf of Z is given by ($f(z) =$

$\frac{\partial F(z)}{\partial z}$),

$$f(z) \to \frac{N}{(z+1)^2}\, {}_2F_2(z+1, z+1; z+2, z+2; -N) \tag{4.57}$$

where ${}_2F_2(a_1, a_2; b_1, b_2; x)$ is a generalized hypergeometric function, given by

$${}_2F_2(a_1, a_2; b_1, b_2; x) = \sum_{k=0}^{\infty} \frac{(a_1)_k (a_2)_k x^k}{(b_1)_k (b_2)_k k!} \tag{4.58}$$

in which $(\alpha)_n = \frac{\Gamma(\alpha+n)}{\Gamma(\alpha)}$ is called the Pochhammer symbol.

As we have already shown, these two quantization methods for high P_{av} have some similar nice properties, and both can be very easily extended to other symmetric or asymmetric fading distributions (i.e, the distribution of g_1 and g_{0i} are identical or different). However, there are also a few differences between them:

1. For QPA0, one does not need to know the instantaneous information of g_1 at SU-TX or CR network manager. But for QRA case, both SU-TX and CR network manager are required to have full information of g_1.
2. Compared to QRA, QPA0 requires more complex computations, since it needs to compute expectations with respect to g_1, which may not always have a closed-form solution for arbitrarily general distributions of g_1.
3. When it comes to more general distributions for $\mathbf{g}_0$, e.g. the Rician distribution, for QPA0, we cannot get a nice closed-form expression for the quantization thresholds (like in (4.20) with Rayleigh distribution) and we have to solve (4.18) for the thresholds. But for QRA, no matter what the distribution of g_1 and $\mathbf{g}_0$ is, we always have a closed-form expression for the quantization thresholds (4.39), which can substantially reduce the complexity of solving the optimization problem especially for a large number of feedback bits.

As we will show via simulation studies (Section 4.5), with the same number of feedback bits, QPA0 outperforms QRA, but as the number of feedback bits increases, the capacity gap between them is reduced, which implies that the performances of these two methods are very close for large number of feedback bits. Therefore, when g_1 or $\mathbf{g}_0$ has a complicated distribution, for a large number of feedback bits ($\geq$ 6 bits), we can choose to use

QRA instead of QPA0.

4.4 Optimum QPA with imperfect g_1 and g_0 at SU-TX

In Section 4.3, we have studied optimum QPA scheme with perfect g_1 and quantized $\mathbf{g}_0$ feedback at SU-TX. So it's natural for us to ask, what happens if g_1 information is also imperfect at SU-TX? In this section, we are interested in investigating the effect of imperfect g_1 information at SU-TX in designing the QPA scheme, where two different ways of providing partial g_1 information to SU-TX: estimated g_1 and quantized g_1, will be examined.

4.4.1 Optimum QPA with quantized $\mathbf{g}_0$ and estimated g_1

We exploit the following well estabilised model [62][46] for channel estimate of h_1 at SU-TX, namely $\hat{h}_1$:

$$\hat{h}_1 = \rho_0 h_1 + \sqrt{1-\rho_0^2}\,\eta \tag{4.59}$$

where η is the channel estimation error with standard complex normal distribution (SCND), i.e, $\eta \sim \mathcal{CN}(0,1)$ (which implies that $E[\eta]=0, E[\eta\overline{\eta}]=E[|\eta|^2]=1$) and η is independent of h_1; and $\rho_0 \in [0,1]$ is the correlation coefficient between the true channel coefficient h_1 and its estimate $\hat{h}_1$, given as $\rho_0 = \frac{E[h_1\hat{h}_1]-E[h_1]E[\hat{h}_1]}{\sqrt{Var[h_1]Var[\hat{h}_1]}}$. Thus the estimated g_1, i.e, $\hat{g}_1$, is obtained by $\hat{g}_1 = |\hat{h}_1|^2$. As we mentioned before, $\sqrt{g_1} = |h_1|$ is Rayleigh distributed and $E[|h_1|^2] = E[g_1] = 1$, thus h_1 is also SCND. From (4.59), it's easy to verify that the linear transform $\hat{h}_1$ is distributed also complex-normally, since $E[\hat{h}_1]=0$ and

$$E[\hat{g}_1] = E[|\rho_0 h_1 + \sqrt{1-\rho_0^2}\,\eta|^2] = \rho_0^2 E[g_1] + (1-\rho_0^2)\,E[|\eta|^2] = 1, \tag{4.60}$$

$\hat{h}_1$ is SCND too. Thus the magnitude $|\hat{h}_1|$ of SCND will have the Rayleigh distribution and the squared magnitude $|\hat{h}_1|^2$, namely, $\hat{g}_1$ will have the unit mean exponential distribution.

As stated in section 4.3.1 of optimum QPA with quantized g_0 only, when $\lambda = 0$ (high P_{av} case) implying that only PIP constraints are active, SU-TX is not required to have knowledge of g_1. Thus with partial g_1 information available at SU-TX, the optimum

QPA solution for this case is still the same. But when $\lambda > 0$ (ATP constraints is active), with the estimated g_1 at SU-TX, the transmit power p_L for the last region $\mathcal{R}_L$ becomes $p_L = (\frac{1}{\lambda} - \frac{1}{\hat{g}_1})^+$. The actual PIP becomes $(\frac{1}{\lambda} - \frac{1}{\hat{g}_1})^+ g_m$, which may not necessarily be below Q_{pk}, although one has $(\frac{1}{\lambda} - \frac{1}{g_1})g_m < Q_{pk}$ (region R_L condition) satisfied. Thus with estimated g_1 at SU-TX, it's not possible to guarantee the actual instantaneous PIP remains $\leq Q_{pk}$ with probability 1. It seems that to satisfy the strict PIP constraint, the SU-TX has to transmit at zero power in $\mathcal{R}_L$ [67], which renders the whole $\mathcal{R}_L$ in outage. Actually, a more suitable measure for this case is to allow the actual PIP with estimated g_1 to exceed Q_{pk} with a small certain probability (like 5% or less) [67], which we call as the interference violation probability (IVP), given by

$$\text{IVP} = Pr((\frac{1}{\lambda} - \frac{1}{\hat{g}_1})^+ g_m > Q_{pk} | \mathcal{R}_L) Pr(\mathcal{R}_L) \tag{4.61}$$

In order to achieve a given percentage IVP, we employ a reduced level of Q_{PK} [46], denoted as $\overline{Q}_{PK}$, to design the optimal QPA codebook in section 4.3.1 with $\lambda > 0$, which implies that the maximum IVP of a certain Q_{PK} happens when $\overline{Q}_{PK} = Q_{PK}$. Thus optimum QPA problem (4.11) with estimated g_1 and $\overline{Q}_{PK}$ becomes,

$$\begin{aligned} \max_{\{\overline{v}_2,\ldots,\overline{v}_{L-1}\}} \ & \overline{C}_L = \sum_{j=2}^{L-1} E[\log(1+\overline{v}_j g_1)|\overline{\mathcal{R}}_j] Pr(\overline{\mathcal{R}}_j) + E[\log(1+(\frac{1}{\lambda'} - \frac{1}{\hat{g}_1})^+ g_1)|\overline{\mathcal{R}}_L] Pr(\overline{\mathcal{R}}_L) \\ s.t. \quad & \sum_{j=2}^{L-1} E[\overline{v}_j|\overline{\mathcal{R}}_j] Pr(\overline{\mathcal{R}}_j) + E[(\frac{1}{\lambda'} - \frac{1}{\hat{g}_1})^+ | \overline{\mathcal{R}}_L] Pr(\overline{\mathcal{R}}_L) \leq P_{av} \end{aligned} \tag{4.62}$$

where $\{\overline{v}_2, \ldots, \overline{v}_{L-1}\}$, $\{\overline{\mathcal{R}}_1, \ldots, \overline{\mathcal{R}}_L\}$ denote the new optimum quantization thresholds and regions associated with $\overline{Q}_{PK}$ respectively, and λ' is the nonnegative Lagrange multiplier associated with the ATP constraint of problem (4.62). Problem (4.62) can be solved by using similar methods as us to solve Problem(4.11). Need to note that in Problem (4.62), the capacity of last region is given by

$$\begin{aligned} & E[\log(1+(\frac{1}{\lambda'} - \frac{1}{\hat{g}_1})^+ g_1)|\overline{\mathcal{R}}_L] Pr(\overline{\mathcal{R}}_L) \\ & = \int_{\lambda'}^{\infty} \int_{\lambda'}^{\infty} \log(1+(\frac{1}{\lambda'} - \frac{1}{\hat{g}_1})g_1) f(g_1, \hat{g}_1)(1 - F(\frac{1}{\lambda'} - \frac{1}{g_1})) dg_1 d\hat{g}_1 \end{aligned} \tag{4.63}$$

where $F(x) = 1 - (1 - \exp(-\frac{\overline{Q}_{pk}}{x}))^N$ and $f(g_1, \hat{g}_1)$ is the joint pdf of g_1 and $\hat{g}_1$, which according to the bivariate exponential distributions in Eq.(47.1) of [95], is given as

$$f(g_1, \hat{g}_1) = \frac{1}{1-\rho} I_0(\frac{2\sqrt{\rho g_1 \hat{g}_1}}{1-\rho}) \exp(-\frac{g_1 + \hat{g}_1}{1-\rho}) \tag{4.64}$$

where ρ is the correlation coefficient between g_1 and $\hat{g}_1$, and $I_0(x) = \sum_{k=0}^{\infty} (\frac{x}{2k!})^{2k}$ is the well known modified Bessel function of the first kind with order zero.

With the optimal QPA codebook obtained by $\overline{Q}_{PK}$, the new last region $\overline{\mathcal{R}}_L$ becomes $\{g_1 \geq \lambda', \frac{\overline{Q}_{pk}}{g_m} \geq \frac{1}{\lambda'} - \frac{1}{g_1}\}$ and thus IVP can be expressed as

$$\begin{aligned} \text{IVP} &= Pr((\frac{1}{\lambda'} - \frac{1}{\hat{g}_1})^+ > \frac{Q_{pk}}{g_m} | g_1 \geq \lambda', \frac{\overline{Q}_{pk}}{g_m} \geq \frac{1}{\lambda'} - \frac{1}{g_1}) Pr(\overline{\mathcal{R}}_L) \\ &= Pr(\frac{1}{\lambda'} > \frac{Q_{pk}}{g_m}, \hat{g}_1 > \frac{1}{\frac{1}{\lambda'} - \frac{Q_{pk}}{g_m}} | g_1 \geq \lambda', \frac{\overline{Q}_{pk}}{g_m} \geq \frac{1}{\lambda'} - \frac{1}{g_1}) Pr(\overline{\mathcal{R}}_L) \end{aligned} \tag{4.65}$$

Since $\overline{Q}_{pk} \leq Q_{pk}$, $\frac{1}{\lambda'} > \frac{Q_{pk}}{g_m}$, we have $\frac{1}{\lambda'} > \frac{\overline{Q}_{pk}}{g_m}$. Applying it to (4.65), we have

$$\begin{aligned} \text{IVP} &= Pr(\frac{1}{\lambda'} > \frac{Q_{pk}}{g_m}, \hat{g}_1 > \frac{1}{\frac{1}{\lambda'} - \frac{Q_{pk}}{g_m}} | \lambda' \leq g_1 \leq \frac{1}{\frac{1}{\lambda'} - \frac{\overline{Q}_{pk}}{g_m}}) Pr(\lambda' \leq g_1 \leq \frac{1}{\frac{1}{\lambda'} - \frac{\overline{Q}_{pk}}{g_m}}) \\ &= \int_{\lambda' Q_{pk}}^{\infty} f_{g_m}(g_m) (\int_{\lambda'}^{\overline{c}} \int_{c}^{\infty} f(g_1, \hat{g}_1) d\hat{g}_1 dg_1) dg_m \end{aligned} \tag{4.66}$$

where $\overline{c} = \frac{1}{\frac{1}{\lambda'} - \frac{\overline{Q}_{pk}}{g_m}}$, $c = \frac{1}{\frac{1}{\lambda'} - \frac{Q_{pk}}{g_m}}$, and the pdf of g_m is given by [7], $f_{g_m}(g_m) = N e^{-g_m} (1 - e^{-g_m})^{N-1}$. Let $\triangle = \int_{\lambda'}^{\overline{c}} \int_{c}^{\infty} f(g_1, \hat{g}_1) d\hat{g}_1 dg_1$. Applying (4.64) to $\triangle$, we have,

$$\triangle = \int_{\lambda'}^{\overline{c}} \frac{1}{1-\rho} \exp(-\frac{g_1}{1-\rho}) (\int_{c}^{\infty} I_0(\frac{2\sqrt{\rho g_1 \hat{g}_1}}{1-\rho}) \exp(-\frac{\hat{g}_1}{1-\rho}) d\hat{g}_1) dg_1 \tag{4.67}$$

Change of varible $x = \sqrt{\frac{2\hat{g}_1}{1-\rho}}$, (4.67) becomes

$$\triangle = \int_{\lambda'}^{\overline{c}} e^{-g_1} Q(\sqrt{\frac{2\rho g_1}{1-\rho}}, \sqrt{\frac{2c}{1-\rho}}) \, dg_1 \tag{4.68}$$

where $Q(a,b) = \int_b^\infty xe^{-\frac{x^2+a^2}{2}} I_0(ax)\ dx$ is the first order Marcum Q-function. With a change of variable again, let $y = \sqrt{2g_1}$, (4.68) becomes

$$\triangle = \int_{\sqrt{2\lambda'}}^\infty ye^{-\frac{y^2}{2}} Q(\sqrt{\frac{\rho}{1-\rho}}y, \sqrt{\frac{2c}{1-\rho}})\ dy - \int_{\sqrt{2\bar{c}}}^\infty ye^{-\frac{y^2}{2}} Q(\sqrt{\frac{\rho}{1-\rho}}y, \sqrt{\frac{2c}{1-\rho}})\ dy \quad (4.69)$$

Applying Eq.(14) of [82] to (4.69), we have

$$\begin{aligned}\triangle = {} & e^{-\lambda'} Q(\sqrt{\frac{2\lambda'\rho}{1-\rho}}, \sqrt{\frac{2c}{1-\rho}}) - e^{-c} Q(\sqrt{\frac{2\lambda'}{1-\rho}}, \sqrt{\frac{2c\rho}{1-\rho}}) \\ & - e^{-\bar{c}} Q(\sqrt{\frac{2\bar{c}\rho}{1-\rho}}, \sqrt{\frac{2c}{1-\rho}}) + e^{-c} Q(\sqrt{\frac{2\bar{c}}{1-\rho}}, \sqrt{\frac{2c\rho}{1-\rho}}) \end{aligned} \quad (4.70)$$

Thus, IVP becomes,

$$\begin{aligned}\text{IVP} = \int_{\lambda' Q_{pk}}^\infty f_{g_m}(g_m) \{ & e^{-\lambda'} Q(\sqrt{\frac{2\lambda'\rho}{1-\rho}}, \sqrt{\frac{2c}{1-\rho}}) - e^{-c} Q(\sqrt{\frac{2\lambda'}{1-\rho}}, \sqrt{\frac{2c\rho}{1-\rho}}) \\ & - e^{-\bar{c}} Q(\sqrt{\frac{2\bar{c}\rho}{1-\rho}}, \sqrt{\frac{2c}{1-\rho}}) + e^{-c} Q(\sqrt{\frac{2\bar{c}}{1-\rho}}, \sqrt{\frac{2c\rho}{1-\rho}}) \}\ dg_m \end{aligned} \quad (4.71)$$

which can be calculated numerically.

The capacity loss with estimated g_1 due to using $\overline{Q}_{pk}$ as the PIP to obtain the optimum QPA codebook (so that the IVP can be kept below a desired maximum), is calculated as $C_{loss} = C_L - \overline{C}_L$, where C_L is the maximum SU ergodic capacity obtained from quantization problem (4.11) with PIP Q_{pk} and perfect g_1.

4.4.2 QPA with quantized ($\mathbf{g}_0$, g_1) information

The limited feedback scheme here is similar to QPA in section 4.3.1 except that we quantize both V and g_1, not just V. Let λ_l represent the nonnegative Lagrange multiplier associated with the ATP constraint for this case. Again, when P_{av} is large enough to make the ATP constraint inactive, only PIP constraints are effective ($\lambda_l = 0$) and designing the optimum QPA does not require SU-TX to have knowledge of g_1. Therefore the optimum QPA for this scenario is same as QPA with quantized $\mathbf{g}_0$ only in 4.3.1 with $\lambda = 0$.

When $\lambda_l > 0$, due to the difficulty and complexity of optimal QPA analysis for this case, we consider a low-complexity suboptimal design of the QPA, in which based on the boundry $v = (\frac{1}{\lambda_l} - \frac{1}{g_1})^+$ (like full CSI case), two different type of power codebooks are derived. Let $\mathcal{P} = \{p_1, \ldots, p_{L_1}, p'_1, \ldots, p'_{L_2}\}$ with $L_1 + L_2 = L$ and the corresponding partitioning $\{\mathcal{R}_1, \ldots, \mathcal{R}_{L_1}, \mathcal{R}'_1, \ldots, \mathcal{R}'_{L_2}\}$ denote an optimal solution for current suboptimal setting. Let $\mathcal{V} = \{v_1, \ldots, v_{L_1}\}$, $\mathbf{q} = \{q_1, \ldots, q_{L_2}\}$ denote the quantization thresholds corresponding to this solution on the V axis (where $0 = v_1 < \cdots < v_{L_1} < v_{L_1+1} = \frac{1}{\lambda}$) and the g_1 axis (where $\lambda_l < q_1 < \cdots < q_{L_2} < q_{L_2+1} = \infty$), respectively, and $p(V, g_1)$ represents the mapping from instantaneous (V, g_1) to the allocated power level. Then we have,

$$p(v, g_1) = \begin{cases} p_1 = 0, & \text{if } v \geq (\frac{1}{\lambda_l} - \frac{1}{g_1}), g_1 < q_1 \text{ or } v < (\frac{1}{\lambda_l} - \frac{1}{g_1}),\ v_1 \leq v < v_2 \\ p_j = v_j, & \text{if } v < (\frac{1}{\lambda_l} - \frac{1}{g_1}),\ v_j \leq v < v_{j+1}, \quad j = 2, \ldots, L_1 \\ p'_k = (\frac{1}{\lambda_l} - \frac{1}{q_k}), & \text{if } v \geq (\frac{1}{\lambda_l} - \frac{1}{g_1}), q_k \leq g_1 < q_{k+1},\ k = 1, \ldots, L_2 \end{cases} \tag{4.72}$$

Fig.4.3 illustrates the structure of the partition regions for $\lambda_l > 0$ case.

In this setting, the QPA problem of quantizing both $\mathbf{g}_0$ and g_1 with limited feedback becomes,

$$\begin{aligned} \max_{\{v_1, \ldots, v_{L_1}, q_1, \ldots, q_{L_2}\}} & \sum_{j=1}^{L_1} E[\log(1 + v_j g_1) | \mathcal{R}_j] Pr(\mathcal{R}_j) + \sum_{k=1}^{L_2} E[\log(1 + (\frac{1}{\lambda_l} - \frac{1}{q_k}) g_1) | \mathcal{R}'_k] Pr(\mathcal{R}'_k) \\ s.t. \quad & \sum_{j=1}^{L_1} E[v_j | \mathcal{R}_j] Pr(\mathcal{R}_j) + \sum_{k=1}^{L_2} E[\frac{1}{\lambda_l} - \frac{1}{q_k} | \mathcal{R}'_k] Pr(\mathcal{R}'_k) \leq P_{av} \end{aligned} \tag{4.73}$$

By using the KKT necessary conditions, $v_2, \ldots, v_{L_1}$ can be obtained through solving equations (4.12) with $\lambda = \lambda_l$ and $j = 2, \ldots, L_1$, and $q_1, \ldots, q_{L_2}$ is given by solving following equations:

$$\begin{aligned} & \int_{q_k}^{q_{k+1}} \frac{1}{q_k^2} (\frac{g_1}{1 + (\frac{1}{\lambda_l} - \frac{1}{q_k}) g_1} - \lambda) f_1(g_1) (1 - F(\frac{1}{\lambda_l} - \frac{1}{g_1})) dg_1 \\ & = (\overline{f}_k(q_k) - \overline{f}_k(q_{k-1})) f_1(q_k) (1 - F(\frac{1}{\lambda_l} - \frac{1}{q_k})),\ j = 1, \ldots, L_2, \end{aligned} \tag{4.74}$$

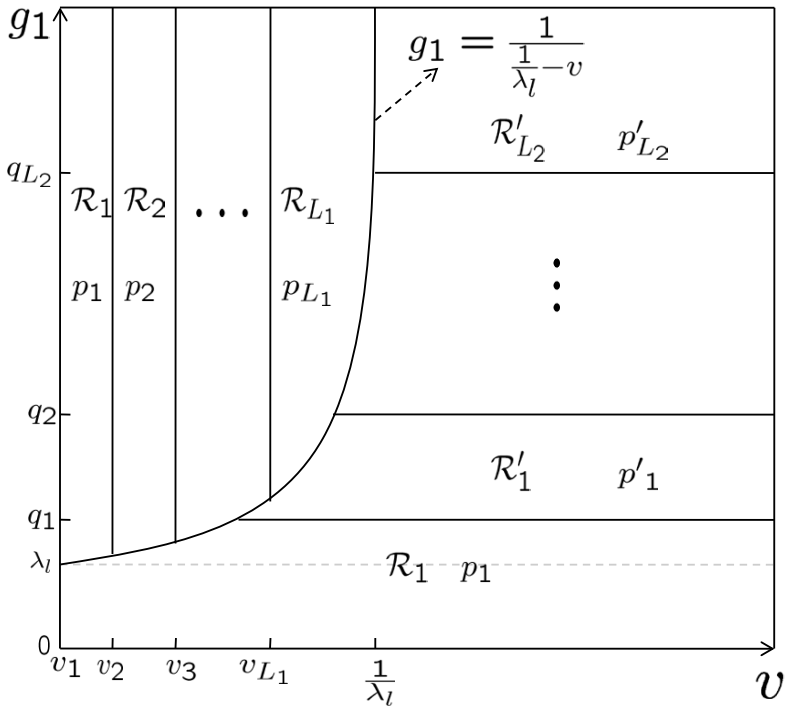

Figure 4.3: A suboptimal quantization regions structure for $\lambda_l > 0$ case

where, $\overline{f}_k(q) = log(1 + (\frac{1}{\lambda_l} - \frac{1}{q})q_k) - 1 + \frac{\lambda_l}{q}$, $f_1(g_1) = e^{-g_1}$, $F(.)$ is given by (4.15) and the λ_l can be obtained by solving

$$\lambda_l(\sum_{j=1}^{L_1} E[v_j|\mathcal{R}_j]Pr(\mathcal{R}_j) + \sum_{k=1}^{L_2} E[\frac{1}{\lambda_l} - \frac{1}{q_k}|\mathcal{R}'_k]Pr(\mathcal{R}'_k) - P_{av}) = 0 \tag{4.75}$$

Thus, for a fixed λ_l, $v_2, \ldots, v_{L_1}$ can be obtained by solving equations (4.12) with $\lambda = \lambda_l$ and $j = 2, \ldots, L_1$, and given a q_1, from (4.74) we can successively compute $q_2, \ldots, q_{L_2}$ numerically. Then the equation (4.74) with $k = L_2$, which has only one unknown variable q_1, can be numerically solved for q_1. Then one can update λ_l until convergence using a subgradient-based method

$$\lambda_l^{n+1} = [\lambda_l^n - \alpha^n(P_{av} - \sum_{j=1}^{L_1} E[v_j|\mathcal{R}_j]Pr(\mathcal{R}_j) - \sum_{k=1}^{L_2} E[\frac{1}{\lambda_l} - \frac{1}{q_k}|\mathcal{R}'_k]Pr(\mathcal{R}'_k))]^+ \tag{4.76}$$

where n is the iteration number and α^n is a positive scalar step size for n-th iteration. One can thus repeat above two steps iteratively until a satisfactory convergence criterion is met.

The above result is based on a given pair of values for L_1 and L_2. To find the optimum L_1 and L_2, we need to exhaustively search all possible combinations of L_1 and L_2 so that $L_1 + L_2 = L$, and pick the one which gives the best SU ergodic capacity.

4.5 Numerical Results

In this section, we examine the analytical results derived in Section 4.3 and 4.4 via numerical simulations. We implement a narrow band spectrum sharing system with one SU and N PUs, where all the channels involved are assumed to undergo identical Rayleigh fading, i.e, all g_{0i} and g_1 are i.i.d and exponentially distributed with unit mean.

Figure 4.4 studies the ergodic capacity performance of SU sharing a narrowband spectrum with various numbers of PUs ($N = 2, 4$ respectively) under both ATP and PIP constraints with QPA strategy (quantizing $\mathbf{g}_0$ only) at $Q_{pk} = 0$ dB, and illustrates the effect of increasing the number of feedback bits on the capacity performance. For comparison, we also plot the corresponding capacity performance with full CSI. First, it can be easily observed that the ergodic capacity increases gradually as P_{av} increases until P_{av} reaches a certain threshold, after which the curves become flat (due to the fact that in high P_{av}, only the PIP constraints are active). The capacity performance also degrades as the number of PUs N gets larger (since the number of PIP constraints increases) as expected. Another striking observation from Figure 4.4 is that for each N, introducing one extra bit of feedback substantially reduces the gap with capacity based on perfect CSI.To be specific, for $N = 4$, at $P_{av} = 10$ dB, with 2 bits, 4 bits and 6 bits of feedback, the percentage capacity gap between them and full CSI case are approximately 25.45%, 6.87% and 1.97% respectively. And for any N, only 6 bits feedback can result in secondary ergodic capacity very close to that with full CSI case. For example, with $P_{pk} = 10$ dB, 6 bits of feedback for $N = 2, 4$ only generate around 2.33% and 1.97% percentage capacity loss respectively compared to their full CSI performance, which is clearly an encouraging result.

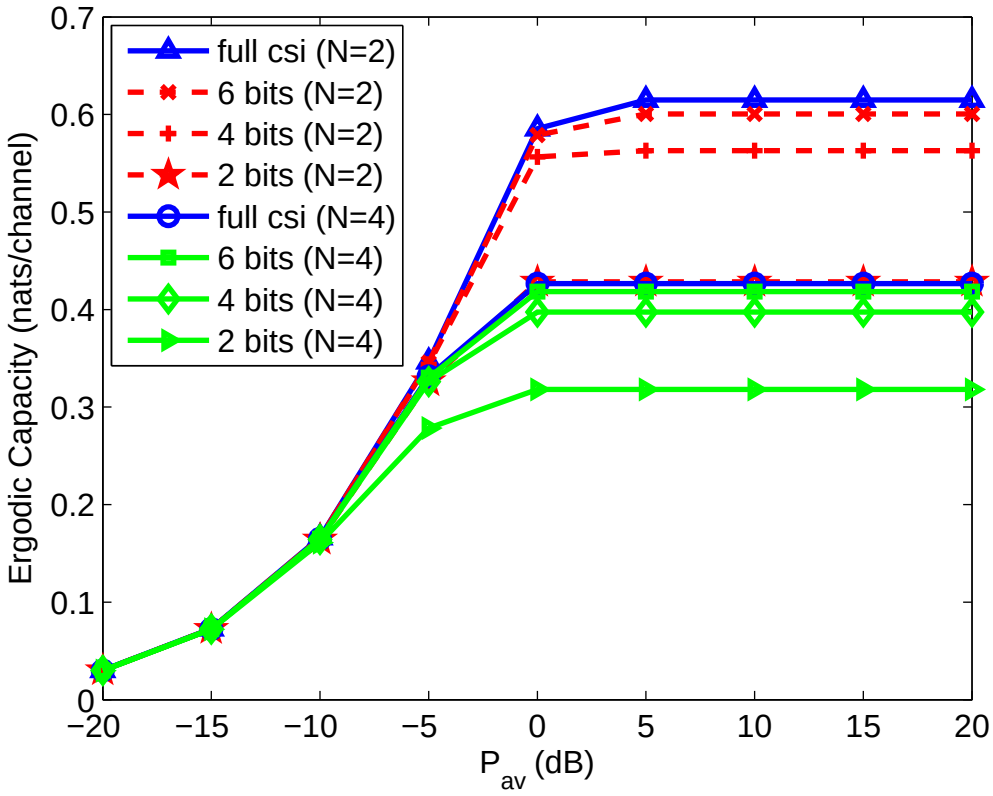

Figure 4.4: Ergodic capacity performance of SU using QPA scheme with perfect g_1 and quantized $\mathbf{g}_0$ for different numbers of PUs ($Q_{pk} = 0$ dB)

Figure 4.5 compares the SU ergodic capacity performance between 6 bits QPA0 with the EPPR approximation and its corresponding optimal 6 bits quantization case for different numbers of PUs ($N = 2, 4, 8$) respectively. An interesting observation from Figure 4.5 is that for any N, the capacity performance of using asymptotic EPPR approximation and optimal scheme (QPA0) are not distinguishable. To be specific, with 6 bits feedback at $Q_{pk} = 10$ dB, for $N = 2, 4, 8$, the percentage capacity loss due to using EPPR approximation instead of using the optimal scheme is only around 0.93%, 0.9% and 0.91% respectively. This implies that the EPPR approximation performs very close to optimum and confirms that EPPR is an very efficient suboptimal scheme of QPA0 for large number of quantization level L. In addition, Figure 4.6 depicts the asymptotic SU capacity behavior of QPA0 obtained from (4.26) versus the number of quantization level L for different numbers of PUs ($N = 1, 2, 4, 8, 16, 32, 64$) with $Q_{pk} = 10$ dB. It can be noted from Figure

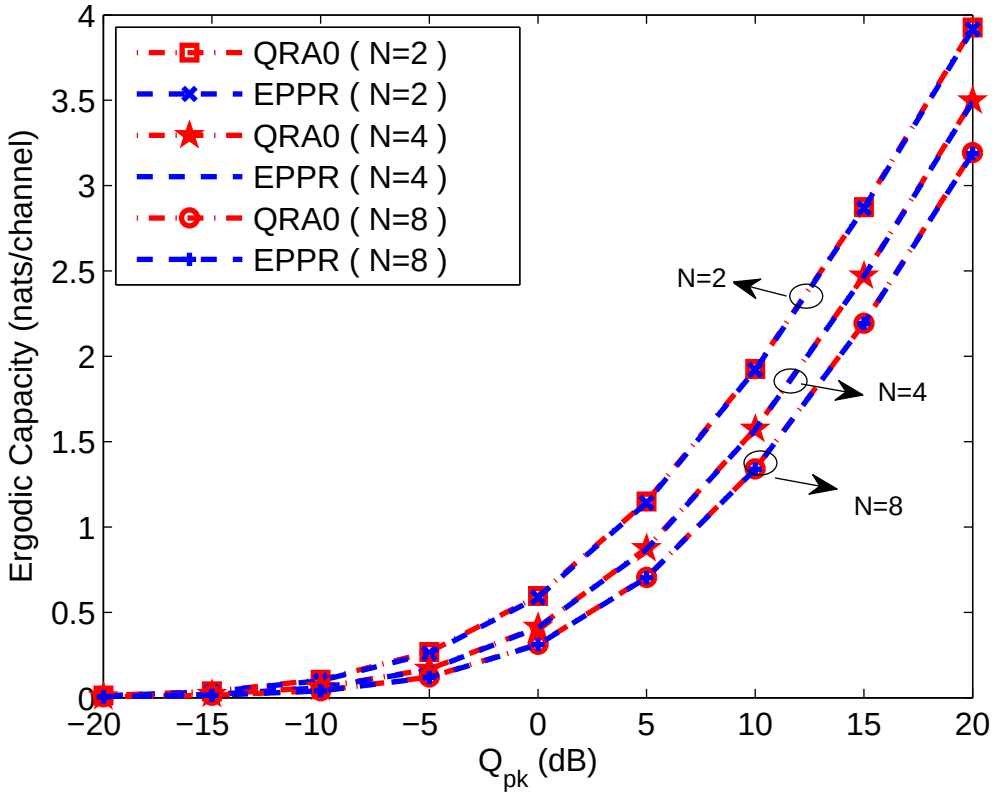

Figure 4.5: Comparison of SU ergodic capacity performance between QPA0 with EPPR approximation and corresponding optimal case for different numbers of PUs under 6 bits of feedback

4.6 that for any N, the capacity increases as the number of quantization level L increases, however, as L increases beyond a certain number ($L \geq 2^6$), the capacity curves start to saturate, which further confirms that only a small number of feedback bits (6 bits) is required to appoach the perfect CSI performance. A similar behavior also can be obtained from QRA scheme case which is ommitted due to avoid repetition.

Next, we test the ALNPs approximation method for QPA and QRA. Here we only plot the results for QRA. A similar observation also can be made for QPA. Figure 4.7 investigates the ergodic capacity performance of SU with quantized feedback (4 bits) using asymptotic analysis method (ALNPs-QRA) for different numbers of PUs ($N = 4, 8, 16$), and compares the results with corresponding optimal QRA (4 bits) case. Interestingly, it can be observed that with same number of feedback bits, increasing the number of PUs

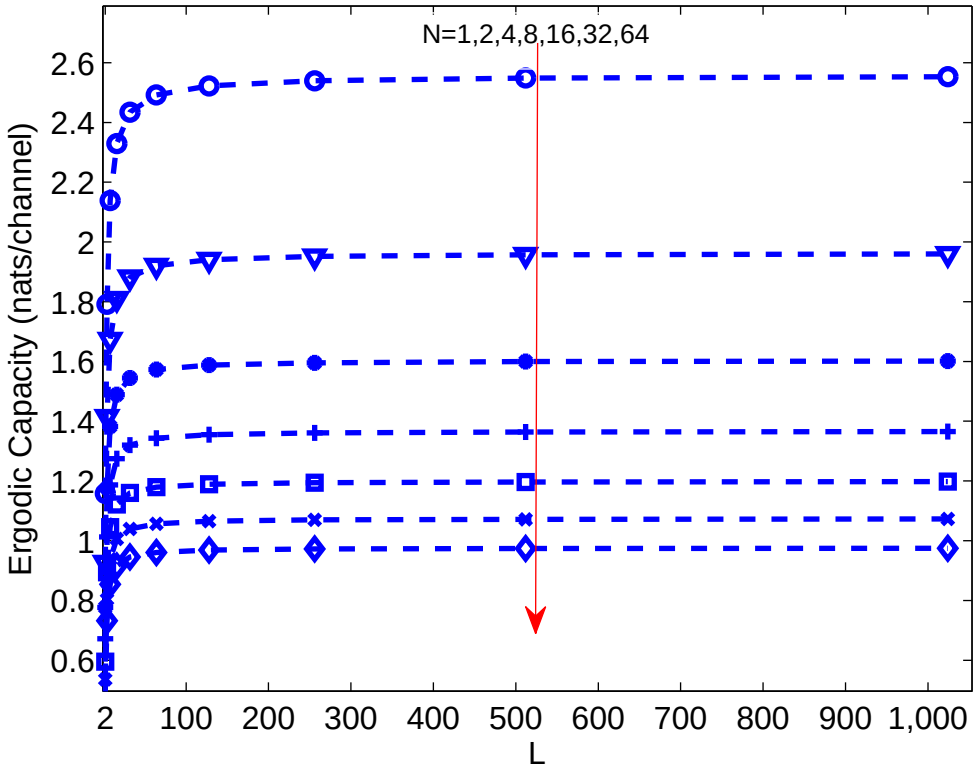

Figure 4.6: Asymptotic capacity behaviour versus the number of quantization level L of QPA0 case

substantially shrinks the capacity performance gap between ALNPs-QRA and the optimal scheme. When $N = 16$, the capacity performance of ALNPs-QRA and the optimal scheme are almost the same. For instance, with 4 bits of feedback at $Q_{pk} = 10$ dB, for $N = 4, 8, 16$, the percentage capacity gap between ALNPs and optimal scheme is around 3.21%, 2.21% and 0.81% respectively. These results confirm that the ALNPs approximation is an efficient alternative, especially for large number of PUs.

Figure 4.8 compares the ergodic capacity performance of two alternative quantization methods (QPA0 and QRA) for high P_{av} case with $N = 4$ for different numbers of bits ($B = 2, 4, 6$ bits). It can be observed from Figure 4.8 that, with same number of feedback bits, QPA outperforms QRA. However, as the number of feedback bits increases, the capacity gap between two methods decreases, and as we can see, with 6 bits feedback, the performance of QRA scheme is very close to QPA case. For example, at $Q_{pk} = 10$ dB,

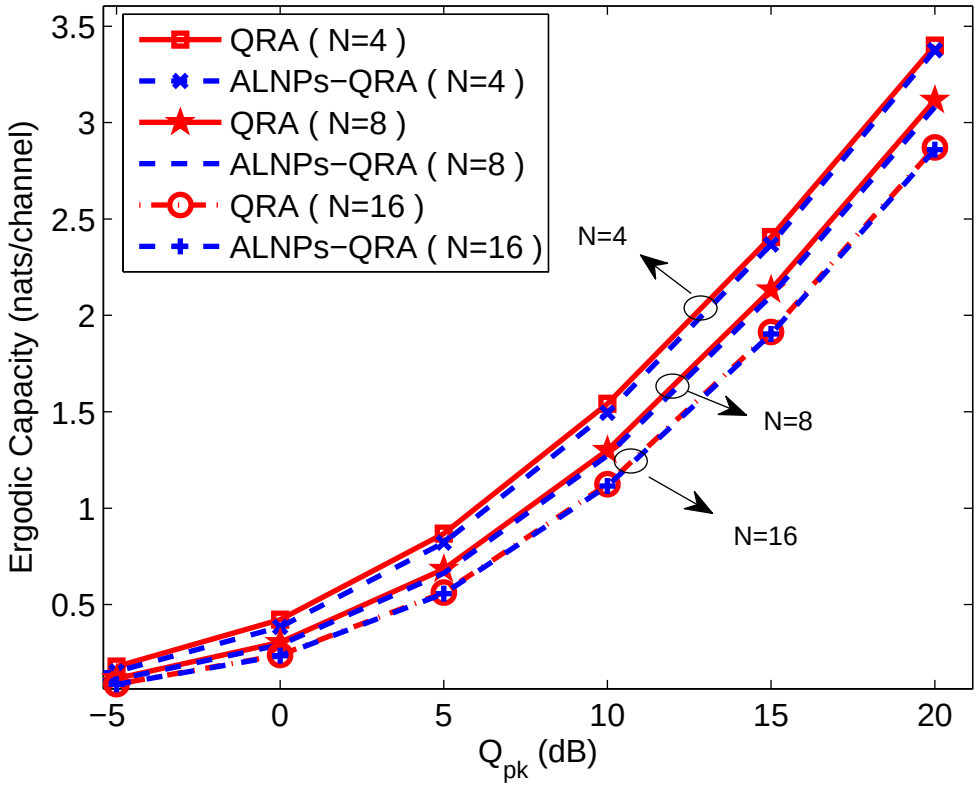

Figure 4.7: Comparison of SU ergodic capacity performance between 4 bits feedback ALNPs-QRA and corresponding optimal 4 bits QRA case for different numbers of PUs

with 2, 4, 6 bits, the percentage capacity gap between two quantization schemes is around 5.56%, 2.86% and 0.84% respectively.

Now we will examine the SU ergodic capacity performance with the additional effect of imperfect g_1 in designing QPA schemes. Figure 4.9 shows (with $Q_{pk} = 0$ dB, $P_{av} = -5$ dB, and $N = 4$), the resulting percentage SU ergodic capacity loss of using QPA schemes with estimated g_1 and $\overline{Q}_{pk}$, against the IVP for different values of the correlation coefficient ρ. Here the range of $\overline{Q}_{pk}$ is from -2.871 dB to 0 dB, corresponding to $IVP = 0$ to the maximum value of IVP. As illustrated in Figure 4.9, for any ρ, capacity loss rises dramatically as IVP decreases, since in order to obtain a lower IVP, we need to further decrease $\overline{Q}_{pk}$, which leads to further capacity loss. Increasing ρ lowers the capacity loss, due to having better estimates of g_1. When $\overline{Q}_{pk} = Q_{pk} = 0$ dB, we obtain the maximum value of IVP which is 0.0450, 0.0365 for $\rho = 0.5$ and $\rho = 0.9$ respectively, and the least value

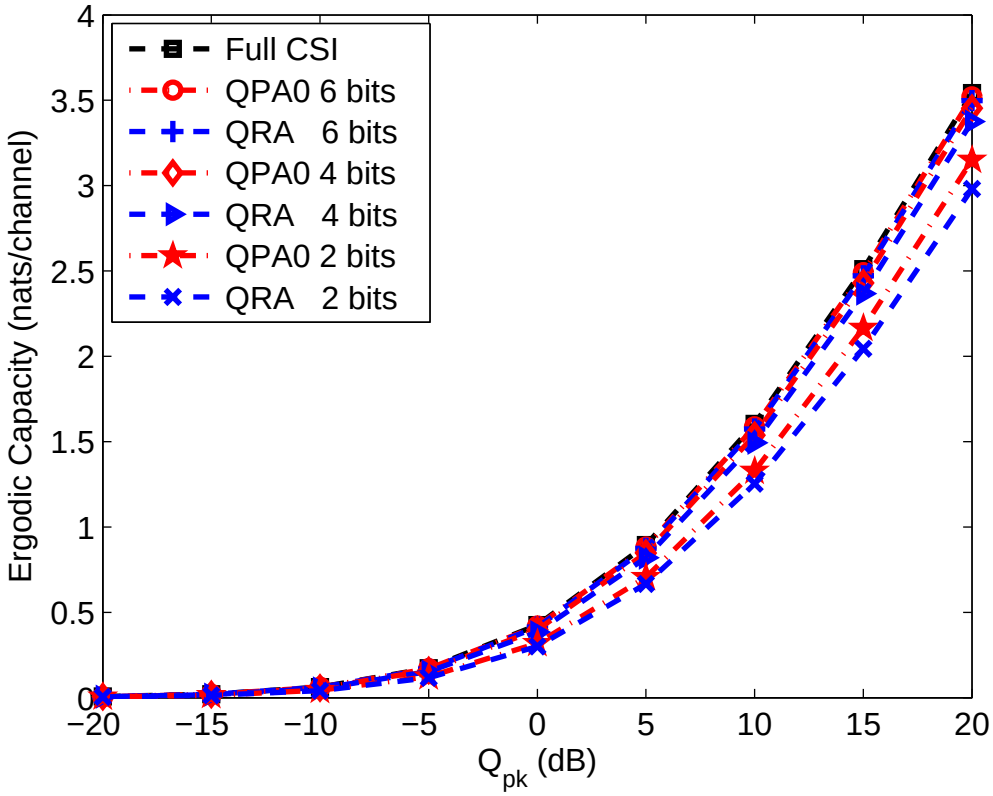

Figure 4.8: Comparison of SU ergodic capacity performance of QPA0 and QRA schemes with $N = 4$

of capacity loss are 2.91% and 1.23% for $\rho = 0.5$ and $\rho = 0.9$, respectively. Interestingly, no matter what ρ is, zero IVP is observed when $\overline{Q}_{pk}$ decreases up to -2.871 dB which achieves the maximum capacity loss, roughly 26.59% for all ρ. This is because when $\overline{Q}_{pk}$ is sufficiently small to make the ATP constraint inactive, and only the PIP constraints active, in this case, the optimum quantized power allocation does not depend on g_1, and hence, even with estimated g_1, IVP=0.

Figure 4.10 depicts the SU ergodic capacity performance of QPA with quantized $\mathbf{g}_0$ and g_1 under $2, 4, 6$ bits of feedback respectively, and compares the results with corresponding performance of QPA with quantized $\mathbf{g}_0$ only (and perfect g_1). From figure 4.10, we can easily observe that with the same number of feedback bits, these two performances almost overlap with each other (recall that when $\lambda_l = 0$, they are identical, and a difference only exists when $\lambda_l > 0$), and with 6 bits of feedback, QPA with quantized $\mathbf{g}_0$

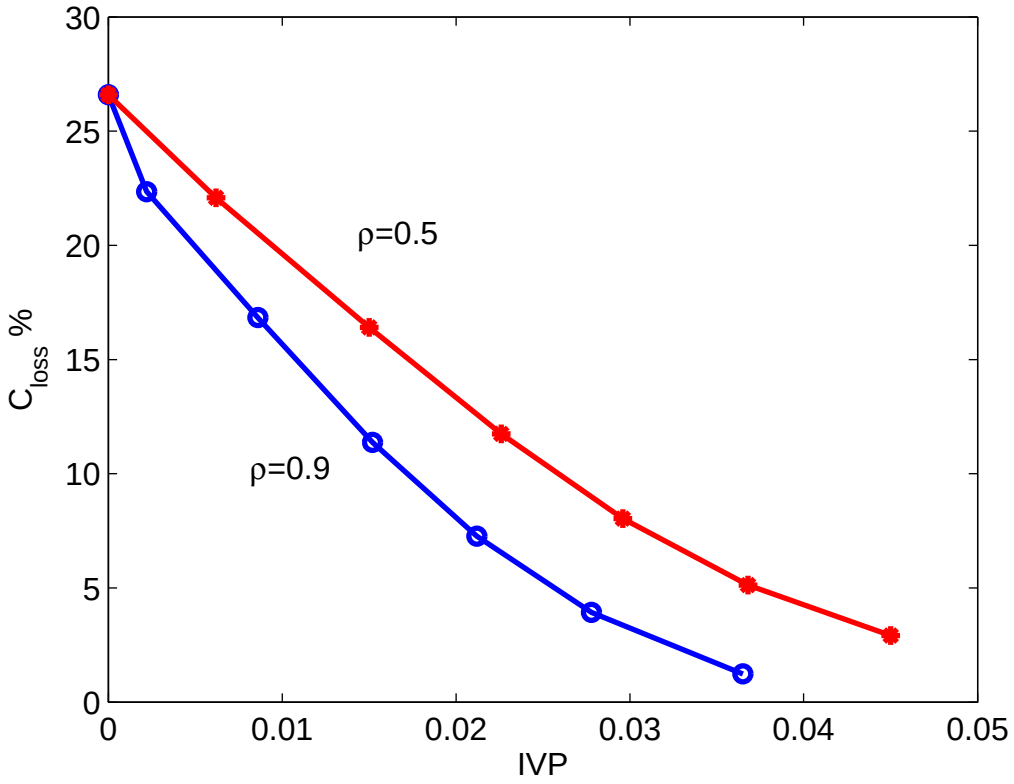

Figure 4.9: The SU ergodic capacity loss of QPA schemes with quantized $\mathbf{g}_0$ and estimated g_1 versus the IVP for difference number of the correlation coefficient ρ ($N = 4, Q_{pk} = 0$ dB, $P_{av} = -5$ dB).

and g_1 are also very close to the full CSI case. For clearer visualization, in figure 4.11 we zoom into the detail of the area of A in the figure 4.10, which shows that with the same number of feedback bits, the performance of QPA with quantized $\mathbf{g}_0$ is only slightly better than QPA with quantized $\mathbf{g}_0$ and g_1, and with increasing number of feedback bits, the capacity loss due to imperfect g_1 information is reduced.

4.6 Conclusions

In this chapter, we have investigated the problem of ergodic capacity maximization of a secondary user sharing the same frequency band with a number of primary users in a narrowband spectrum sharing cognitive radio framework, under an average transmit

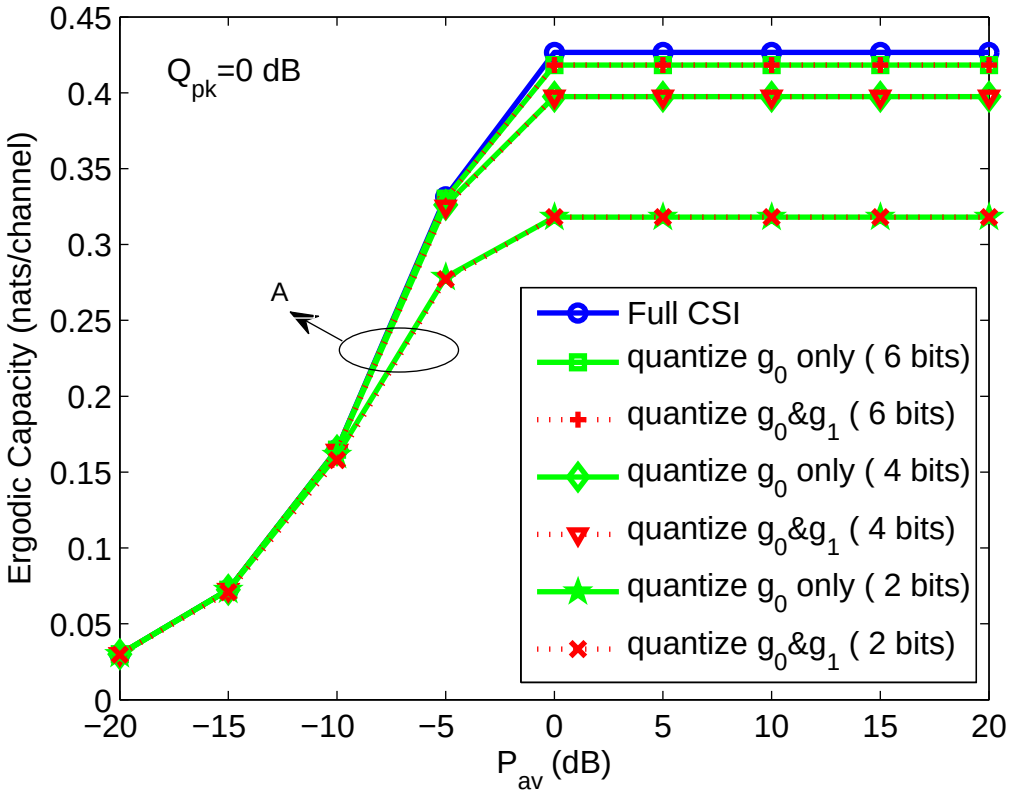

Figure 4.10: The SU ergodic capacity performance of QPA with quantized $(\mathbf{g}_0, g_1)$, and comparing it to the performance of QPA with quantized $\mathbf{g}_0$ only ($N = 4$)

power constraint at SU-TX and individual peak interference constraints at each primary receiver. Three different quantized power codebooks are designed for the throughput maximization problem corresponding to three different forms of channel information of g_1 and g_0 at SU-TX, namely, perfect g_1 and quantized information on g_0, estimated g_1 and quantized g_0, quantized both g_1 and g_0 information. Numerical results present the efficiency of our quantized feedback schemes. A general observation for these schemes is that with only 4-6 bits of feedback, the SU ergodic capacity with quantized channel information closely approximates that with full channel information at the SU transmitter.

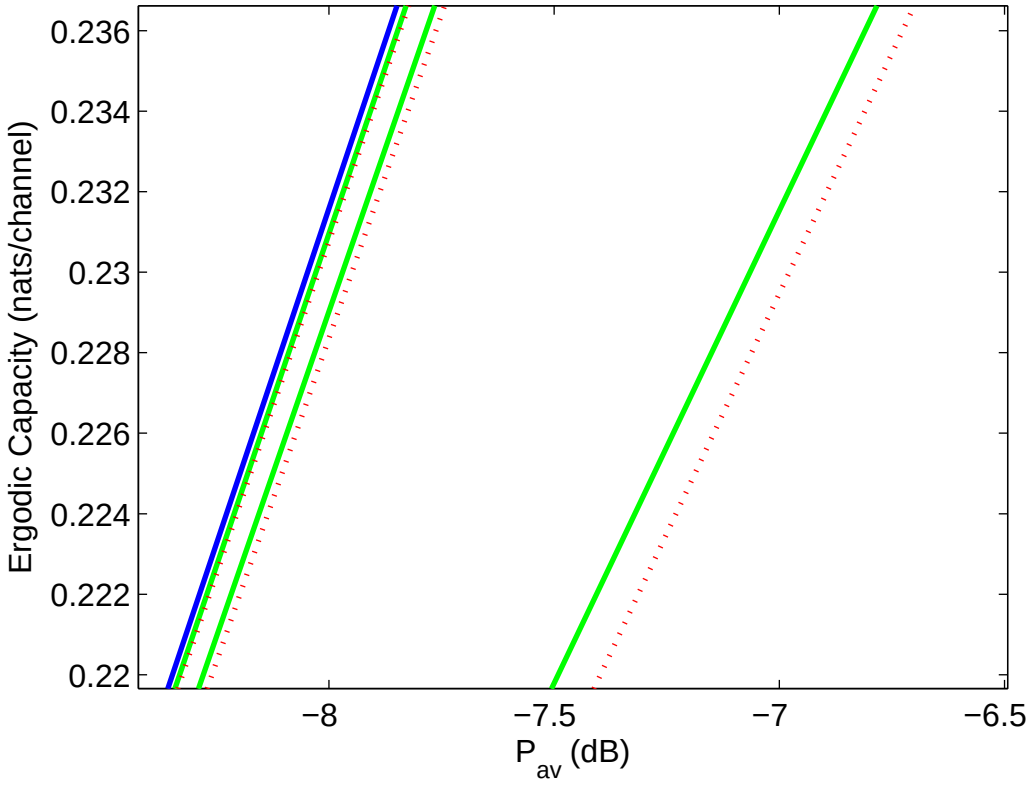

Figure 4.11: Zooming in the area of A in the figure 4.10

4.7 Appendix

4.7.1 Proof of Lemma 4.1

Let λ denotes the nonnegative Lagrange multiplier associated with the ATP constraint of problem (4.8). When $\lambda = 0$ (ATP is inactive), the problem of (4.8) becomes

$$\max_{\{p_1,\ldots,p_L\}} \sum_{j=1}^{L} E[\log(1+p_j g_1)|\mathcal{R}_j] Pr(\mathcal{R}_j)$$
$$s.t. \quad 0 \le p_j \le \min\{v|\mathcal{R}_j\}, \quad j = 1,\ldots,L \tag{4.77}$$

In this case, it's easy to verify that all the constraints in (4.77) is satisfied with equality. Let $\{v_1,\ldots,v_L\}$ denote the optimum quantization thresholds on V axis and $v_{L+1} = \infty$

$(0 = v_1 < \cdots < v_L < \infty)$. We can obtain

$$p(V, g_1) = p_j = v_j, \text{ if } v_j \leq V < v_{j+1},\ j = 1, \ldots, L. \tag{4.78}$$

which is independent of g_1 information

. When $\lambda > 0$, the dual problem of (4.8) is given as

$$\min_{\lambda \geq 0}\ g(\lambda) + \lambda P_{av} \tag{4.79}$$

where the Lagrange dual function $g(\lambda)$ is defined as

$$\begin{aligned} &\max_{\{p_1, \cdots, p_L\}} \sum_{j=1}^{L} E[\log(1 + p_j g_1) - \lambda p_j | \mathcal{R}_j] Pr(\mathcal{R}_j) \\ &s.t. \quad 0 \leq p_j \leq \min\{v | \mathcal{R}_j\},\ \ j = 1, \ldots, L \end{aligned} \tag{4.80}$$

which can be decomposed into L parallel subproblem, i.e, for each region $\mathcal{R}_j, j = 1, \ldots, L$

$$\begin{aligned} &\max_{p_j} \quad E[\log(1 + p_j g_1) - \lambda p_j | \mathcal{R}_j] Pr(\mathcal{R}_j) \\ &s.t. \quad 0 \leq p_j \leq \min\{v | \mathcal{R}_j\} \end{aligned} \tag{4.81}$$

Firstly, from (4.81), we can obtain:

(a) if $\min\{v|\mathcal{R}_j\} < (\frac{1}{\lambda} - \frac{1}{g_1})$, from the power constraint in (4.81) we must have $p_j = \min\{v|\mathcal{R}_j\}$, otherwise we always can increase the p_j up to $\min\{v|\mathcal{R}_j\}$ to achieve better capacity performance of Problem (4.81);

(b) if $\min\{v|\mathcal{R}_j\} \geq (\frac{1}{\lambda} - \frac{1}{g_1})^+$, we must have $p_j = (\frac{1}{\lambda} - \frac{1}{g_1})^+$, due to the capacity of (4.81) in this case is maximum at $p_j = (\frac{1}{\lambda} - \frac{1}{g_1})^+$.

Now, let $\{v_1, \ldots, v_{L-1}\}$ denote the optimum quantization thresholds on V axis, where $0 = v_1 < \cdots < v_{L-1} < \frac{1}{\lambda}$, let $v_L = \frac{1}{\lambda}$, from above (a) and (b), we can easily get:

1) if $\mathcal{R}_1 = \{(v, g_1) | g_1 \leq \lambda\} \bigcup \{(v, g_1) | v < (\frac{1}{\lambda} - \frac{1}{g_1}),\ v_1 \leq v < v_2\}$, then we must have $p_1 = 0$;

2) if $\mathcal{R}_j = \{(v, g_1) | v < (\frac{1}{\lambda} - \frac{1}{g_1}),\ v_j \leq v < v_{j+1}\}$, then we must have $p_j = v_j$, $j = 2, \ldots, L-1$;

3) if $\mathcal{R}_L = \{(v, g_1) | v \geq (\frac{1}{\lambda} - \frac{1}{g_1}) > 0\}$, we must have $p_L = (\frac{1}{\lambda} - \frac{1}{g_1})$.

Secondly, we will show that with the power levels in 1), 2) and 3), the above partition regions are optimal. Let $\mathcal{P} = \{p_1, \ldots, p_L\}$ and the corresponding channel partitioning $\mathcal{R}_1, \ldots, \mathcal{R}_L$ denote the optimal solution to the optimization problem (4.8), such that $p(v, g_1) = p_j$ if $(v, g_1) \in \mathcal{R}_j$.

• Let $\mathcal{R}_1^* = \{(v, g_1) | g_1 \leq \lambda\} \bigcup \{(v, g_1) | v < (\frac{1}{\lambda} - \frac{1}{g_1}),\ v_1 \leq v < v_2\}$ and assume that the set $\mathcal{R}_1^* \setminus \mathcal{R}_1$ is a not-empty set, where $\setminus$ is the set subtraction operation (i.e, if $(v, g_1) \in \mathcal{R}_1^* \setminus \mathcal{R}_1$, then $(v, g_1) \in \mathcal{R}_1^*$ but $(v, g_1) \notin \mathcal{R}_1$). Then we have $\mathcal{R}_1^* \setminus \mathcal{R}_1 \subseteq (\cup_{k=2}^{L} \mathcal{R}_k)$, which gives $\forall\ (v, g_1) \in (\mathcal{R}_1^* \setminus \mathcal{R}_1),\ p(v, g_1) > 0$. However, this violates the power constraint in $\mathcal{R}_1^* \setminus \mathcal{R}_1$, i.e, $0 \leq p(v, g_1) \leq \min\{v | \mathcal{R}_1^* \setminus \mathcal{R}_1\}$ implying $p(v, g_1) = 0$, which is in contradiction with the optimality of the solution $\mathcal{P}, \mathcal{R}_j, \forall j$. Therefore, $\mathcal{R}_1^* \setminus \mathcal{R}_1 = \emptyset$, namely $\mathcal{R}_1^* \subseteq \mathcal{R}_1$.

• $\forall j = 2, \ldots, L-1$, let $\mathcal{R}_j^* = \{(v, g_1) | v < (\frac{1}{\lambda} - \frac{1}{g_1}),\ v_j \leq v < v_{j+1}\}$ and assume that the set $\mathcal{R}_j^* \setminus \mathcal{R}_j$ has nonzero probability. Then, the set $\mathcal{R}_j^* \setminus \mathcal{R}_j$ can be partitioned into two subsets $S_j^- = (\mathcal{R}_j^* \setminus \mathcal{R}_j) \cap (\cup_{k=1}^{j-1} \mathcal{R}_k)$ and $S_j^+ = (\mathcal{R}_j^* \setminus \mathcal{R}_j) \cap (\cup_{k=j+1}^{L} \mathcal{R}_k)$. The set $S_j^- = \emptyset$, otherwise, we can reassign the set S_j^- into region $\mathcal{R}_j$ without violating the power constraints in Problem (4.80), while the total capacity of problem (4.80) is increased, due to the fact that $\forall (v, g_1) \in (\cup_{k=1}^{j-1} \mathcal{R}_k), p(v, g_1) < p_j < (\frac{1}{\lambda} - \frac{1}{g_1})$, and with the reassignment the capacity of set S_j^- achieves better performance, which contradics the optimality of the solution $\mathcal{P}, \mathcal{R}_j, \forall j$. The set $S_j^+ = \emptyset$ too, otherwise the power constraints in S_j^+, i.e, $0 \leq p(v, g_1) \leq v_j$, will be violated, due to $\forall (v, g_1) \in S_j^+, p(v, g_1) > v_j$, which is in contradiction with the optimality. Therefore, we have $\mathcal{R}_j^* \setminus \mathcal{R}_j = \emptyset$, which implies $\mathcal{R}_j^* \subseteq \mathcal{R}_j$.

• Let $\mathcal{R}_L^* = \{(v, g_1) | v \geq (\frac{1}{\lambda} - \frac{1}{g_1}) > 0\}$ and assume that the set $(\mathcal{R}_L^* \setminus \mathcal{R}_L) \neq \emptyset$. Then we have $\mathcal{R}_L^* \setminus \mathcal{R}_L \subseteq (\cup_{k=1}^{L-1} \mathcal{R}_k)$. Again we can repartition the set $\mathcal{R}_L^* \setminus \mathcal{R}_L$ into region $\mathcal{R}_L$ which still satisfies the power constraints in problem (4.80), however, this new partition increases the total capacity of problem (4.80), since $\forall (v, g_1) \in (\cup_{k=1}^{L-1} \mathcal{R}_k), p(v, g_1) < (\frac{1}{\lambda} - \frac{1}{g_1})$, after the repartitioning, the capacity of set $\mathcal{R}_L^* \setminus \mathcal{R}_L$ achieves its maximum value, which contradics the optimality. Therefore, we have $\mathcal{R}_L^* \setminus \mathcal{R}_L = \emptyset$, i.e, $\mathcal{R}_L^* \subseteq \mathcal{R}_L$.

• In summary, we have shown that $\forall j = 1, \ldots, L,\ \mathcal{R}_j^* \subseteq \mathcal{R}_j$. Since $\cup_{j=1}^{L} \mathcal{R}_j^* =$ the whole space of $(v, g_1) = \cup_{j=1}^{L} \mathcal{R}_j$, and $\mathcal{R}_j^* \subseteq \mathcal{R}_j,\ \forall j$, we can obtain that $\mathcal{R}_j^* = \mathcal{R}_j,\ \forall j = 1, \ldots, L$.

4.7.2 Deriving the cdf and the pdf of $V = \frac{Q_{pk}}{\max_i g_{0i}}$

Let $g_0 = \max_i g_{0i}, i = 1, \ldots, N$, then the pdf of g_0 is given by [7],

$$f(g_0) = Ne^{-g_0}(1 - e^{-g_0})^{N-1}. \tag{4.82}$$

The cdf of $V = \frac{Q_{pk}}{\max_i g_{0i}}$ can be obtained as

$$F(v) = Pr(\frac{Q_{pk}}{\max_i g_{0i}} < v) = Pr(g_0 > \frac{Q_{pk}}{v}) = \int_{\frac{Q_{pk}}{v}}^{\infty} f(g_0)dg_0 = 1 - (1 - \exp(-\frac{Q_{pk}}{v}))^N \tag{4.83}$$

After differentiation, the pdf of V is given as

$$f(v) = \frac{NQ_{pk}}{v^2}\exp(-\frac{Q_{pk}}{v})(1 - \exp(-\frac{Q_{pk}}{v}))^{N-1}. \tag{4.84}$$

4.7.3 Deriving the asymptotic pdf of $\max_i g_{0i}, i = 1, \ldots, N$, as $N \to \infty$

Given that $g_{01}, g_{02}, \ldots, g_{0N}$ are i.i.d random variables and exponentially distributed with unit mean, let the cdf $F(x) = Prob(g_{0i} < x) = 1 - e^{-x}$ and pdf $f(x) = e^{-x}$. Let $X = \max(g_{01}, g_{02}, \ldots, g_{0N})$, we want to derive the asymptotic distribution (the pdf) of X as $N \to \infty$. First, it's easy to get that

$$Prob(X < x) = F^N(x) \tag{4.85}$$

Since $f(x) > 0$ and is differentiable for all x in $(x_1, F^{-1}(1))$ for some x_1, and

$$\lim_{x \to F^{-1}(1)} \frac{d}{dx}[\frac{1 - F(x)}{f(x)}] = \lim_{x \to \infty} \frac{d}{dx}[1] = 0, \tag{4.86}$$

according to the Theorem 10.5.2 of [44], we have that there exist constants $a_N > 0$ and b_N, such that

$$F^N(a_N x + b_N) \to e^{-e^{-x}}, \text{as } N \to \infty \tag{4.87}$$

where we can choose,

$$b_N = F^{-1}(1 - \frac{1}{N}) = \log N, \qquad a_N = [Nf(b_N)]^{-1} = 1 \tag{4.88}$$

Therefore,

$$F^N(x + \log N) \to e^{-e^{-x}}, \qquad F^N(x) \to e^{-e^{-(x-\log N)}} \tag{4.89}$$

and,

$$f_X(x) = \frac{\partial F^N(x)}{\partial x} \to Ne^{-x}e^{-Ne^{-x}} \tag{4.90}$$

4.7.4 Proof of Lemma 4.2

Similar to [65], given the optimum quantization thresholds $\mathbf{z}= \{z_2, \ldots, z_L\}$, we assume that the optimum rate codebook $\mathbf{r}= \{r_1, \ldots, r_L\}$ satisfies $z_j^* \notin [z_j, z_{j+1})$ (namely, $z_j^* \geq z_{j+1}$ or $z_j^* < z_j$). We construct a new codebook $\mathbf{r'}= \{r_1, \ldots, r_{j-1}, r'_j, r_{j+1} \ldots, r_L\}$ where $r'_j = R(z_j)$ with corresponding $z_j^{'*} = z_j$. if $z_j^* \geq z_{j+1}$, we have $C_L(\mathbf{r'}) - C_L(\mathbf{r}) = r'_j Pr(\mathcal{R}_j) > 0$, which contradicts with the optimality of rate codebook $\mathbf{r}$. if $z_j^* < z_j$, we have $C_L(\mathbf{r'}) - C_L(\mathbf{r}) = (r'_j - r_j)Pr(\mathcal{R}_j) > 0$, which is also an contradiction with the assumed optimality.

4.7.5 Proof of Lemma 4.3

Given an optimum rate codebook $\mathbf{r}= \{r_1, \ldots, r_L\}$, we assume that the optimum quantization thresholds $\mathbf{z}= \{z_2, \ldots, z_L\}$ satisfies $z_j \neq z_j^*$, thus from Lemma 4.2, we have $z_j < z_j^* < z_{j+1}$. Now, we construct a new quantization thresholds $\mathbf{z'}= \{z_2, \ldots, z_{j-1}, z_j^*, z_{j+1} \ldots, z_L\}$, and we can show that $C_L(\mathbf{z'}) - C_L(\mathbf{z}) = [r_{j-1}(F(z_j^*) - F(z_{j-1}^*)) + r_j(F(z_{j+1}) - F(z_j^*))] - [r_{j-1}(F(z_j) - F(z_{j-1}^*)) + r_j(F(z_{j+1}) - F(z_j^*))] = r_{j-1}(F(z_j^*) - F(z_j)) > 0$, which contradicts with the optimality of optimum quantization thresholds $\mathbf{z}$.

4.7.6 Proof of Lemma 4.4

From (4.51), we have $c = N^{-z}\Gamma(z+1)$, then the derivative of c is,

$$\frac{dc}{dz} = N^{-z}\Gamma(z+1)(\psi^{(0)}(z+1) - logN) = c(\psi^{(0)}(z+1) - logN). \tag{4.91}$$

where $\psi^{(0)}(x)$ is digamma function, defined as $\psi^{(0)}(x) = \frac{\Gamma'(x)}{\Gamma(x)}$, and is monotonically increasing on $x \in [0,\infty)$. Therefore $\psi^{(0)}(z+1) = logN$ only has one solution which is $z = \psi^{-1\ (0)}(logN) - 1$. If $\psi^{(0)}(z+1) < logN$, namely, $0 \leq z < \psi^{-1\ (0)}(logN) - 1$, we have $\frac{dc}{dz} < 0$, which means as c increases, z decreases; on the other hand, if $z \geq \psi^{-1\ (0)}(logN) - 1$,we have $\frac{dc}{dz} \geq 0$, which implies as c increases, z is non-decreasing. As we know, for a fixed L, as $j = 1,\ldots,L$, $c = 1 - \frac{j}{L+1}$ is decreasing, solving (4.51) results in the thresholds $z_1,\ldots,z_L$ respectively, such that $z_1 < \cdots < z_L$. Thus, we must have $0 \leq z < \psi^{-1\ (0)}(logN) - 1$. From $c = N^{-z}\Gamma(z+1)$, we have

$$\log N = \frac{1}{z}\log\frac{\Gamma(z+1)}{c}, \tag{4.92}$$

then

$$\frac{d\log N}{dz} = \frac{1}{z}(\psi^{(0)}(z+1) - \frac{1}{z}\log\frac{\Gamma(z+1)}{c}) = \frac{1}{z}(\psi^{(0)}(z+1) - logN) < 0 \tag{4.93}$$

which indicates that as N increases, z is monotonically decreasing. Since $z \geq 0$, with fixed L, as $N \to \infty$, z must approaches to a non negative constant a (i.e, $\lim_{N\to\infty} z = a$). Now, we assume $a \neq 0$. Then from (4.92), we have

$$\lim_{N\to\infty}\log N = \lim_{N\to\infty}\frac{1}{z}\log\frac{\Gamma(z+1)}{c} = \frac{1}{a}\log\frac{\Gamma(a+1)}{c} < \infty \tag{4.94}$$

which is contradiction with $\lim_{N\to\infty}\log N = \infty$. Therefore, we must have $a = 0$ (i.e, $\lim_{N\to\infty} z = 0$), which gives

$$\frac{1}{a}\log\frac{\Gamma(a+1)}{c} = \frac{1}{a}\log\frac{1}{c} = \infty \tag{4.95}$$

Chapter 5

Outage Minimization in Cognitive Radio with Limited Feedback

5.1 Introduction

In this chapter, we will design optimal quantized power control policy for a different performance measure of SU, i.e, outage probability, with only partial channel information available at SU-TX and subject to both ATP constraint on SU-TX and the individual AIP constraint on each PU-TX (the same constraints as Chapter 3). Similar to Chapter 3, we consider an infrastructure-based narrowband spectrum sharing scenario where a SU communicates to its base station (SU-BS) on a narrowband channel shared with a PU communicating to its receiver PU-RX contained within the primary base station (PU-BS). The key problem of jointly designing the optimal partition regions of the vector channel space consisting of the SU-TX to SU-RX channel (denoted by power gain g_1) and the interfering channel between the SU-TX and PU-RX (denoted by power gain g_0), and computation of an optimal power codebook is solved offline at a central controller called the CR network manager as in Chapter 3, based on the channel statistics. The CR network manager is assumed to be able to obtain the full CSI information of the vector channel space (g_1, g_0) in real-time from the SU-BS and PU-BS, respectively, possibly via wired links (similar to backhaul links in multi-cell MIMO networks connecting multiple base stations). This real-time channel realization is then assigned to the optimal channel partition and the corresponding partition index is sent to the SU-TX (and to the SU-RX for decoding purposes) via a finite-rate feedback link. The SU-TX then uses the power codebook element associated with this index for data transmission. It was shown in Chapter

3 that without the presence of the CR network manager, and thus without the ability to jointly quantize the combined channel space, the SU capacity performance is significantly degraded if one carries out separate quantization of g_1 and g_0. Under these networking assumptions, we prove a 'stepwise' structure of the optimal channel partition regions, which helps us explicitly formulate the outage minimization problem and solve it using the corresponding KKT necessary optimality conditions. As the number of feedback bits go to infinity, we show that the power level for the last region approaches zero, allowing us to derive a useful low-complexity suboptimal quantized power allocation algorithm called 'ZPiORA' for high rate quantization. We also derive some other useful properties related to the channel quantizer structure as the number of feedback bits approaches infinity: (a) under an active AIP constraint, the length of interval between any two adjacent quantization thresholds on the g_0 axis is asymptotically the same, and (b) while when the AIP is inactive, the ratio between any two adjacent quantization thresholds on the g_1 axis asymptotically becomes identical. Finally, with these properties, we derive explicit expressions for asymptotic (as the number of feedback bits increase) behavior of the SU outage probability with quantized power allocation for large resolution quantization. Numerical studies illustrate that with only 6 bits of feedback, the designed optimal algorithms provide secondary outage probability very close to that achieved by full CSI. With 2-4 bits of feedback, ZPiORA provides a comparable performance, thus making it an attractive choice for large number of feedback bits case. Numerical studies also show that ZPiORA performs better than two other suboptimal algorithms constructed using existing approximations in the literature. Finally, it is also shown that the derived asymptotic outage behavior approximates the optimal outage extremely well as the number of feedback bits becomes large.

This chapter is organized as follows. Section 5.2 introduces the system model and the problem formulation based on the full CSI assumption. Section 5.3 presents the joint design of the optimal channel partition regions and an optimal power codebook algorithm. A low-complexity suboptimal quantized power allocation strategy is also derived using novel interesting properties of the quantizer structure and optimal quantized power codebooks. In Section 5.4, the asymptotic behavior of SU outage probability for high res-

olution quantization is investigated. Simulation results are given in Section 5.5, followed by concluding remarks in Section 5.6. All proofs are relegated to the appendix section 5.7 in this chapter.

5.2 System Model and Problem Formulation

We consider an infrastructure-based spectrum sharing network where a SU communication uplink to the SU-BS coexists with a PU link (to the PU-BS) within a narrowband channel. Regardless of the on/off status of PU, the SU is allowed to access the band which is originally allocated to PU, so long as the impact of the transmission of SU does not reduce the received signal quality of PU to an intolerable level. All channels here are assumed to be Rayleigh block fading channels. Let $g_1 = |h_1|^2$ and $g_0 = |h_0|^2$, denote the nonnegative real-valued instantaneous channel power gains for the links from the secondary transmitter (SU-TX) to the secondary receiver (SU-RX) and the SU-TX to the receiver of PU respectively (where h_1 and h_0 are corresponding complex zero-mean circularly symmetric channel amplitude gains). The exponentially distributed channel power gain g_1 and g_0, are statistically mutually independent and, without loss of generality (*w.l.o.g*), are assumed to have unity mean. The additive noises for each channel are independent Gaussian random variables with, *w.l.o.g*, zero mean and unit variance. For analytical simplicity, the interference from the primary transmitter (PU-TX) to SU-RX is neglected following previous work such as [7, 117](in the case where the interference caused by the PU-TX at the SU-RX is significant, the SU outage probability results derived in this chapter can be taken as lower bounds on the actual outage under primary-induced interference). This assumption is justified when either the SU is outside the PU's transmission range or the SU receiver is equipped with interference cancellation capability particularly when the PU signal is strong.

Given a channel realization (g_0, g_1), let the instantaneous transmit power (with full CSI) at the SU-TX represented by $p(g_0, g_1)$, then the maximum mutual information of the

SU for this narrowband spectrum sharing system can be expressed as

$$R(g_1, p(g_0, g_1)) = \frac{1}{2}\log(1 + g_1 p(g_0, g_1)) \tag{5.1}$$

where log represents the natural logarithm. The outage probability of SU-TX with a pre-specified transmission rate r_0, is given as,

$$P_{out} = Pr\{R(g_1, p(g_0, g_1)) < r_0\} \tag{5.2}$$

where $Pr\{A\}$ indicates the probability of event A occurring. Using the interference temperature concept in [7], a common way to protect PU's received signal quality is by imposing either an average or a peak interference power (AIP/PIP) constraint at the PU-RX. In [123], it was demonstrated that the AIP constraint is more flexible and favorable than the PIP constraint in the context of transmission over fading channels, for both the SU and the PU. Let Q_{av} denote the average interference power limit tolerated by PU-RX, then the AIP constraint can be written as,

$$E[g_0 p(g_0, g_1)] \leq Q_{av} \tag{5.3}$$

The following optimal power allocation problem that minimizes the outage probability of SU in a narrowband spectrum sharing with one PU, under both a long term average transmit power (ATP) constraint at SU-TX and an AIP constraint at the PU-RX, was considered in [117]

$$\begin{aligned} \min_{p(g_0,g_1)\geq 0} \quad & Pr\{\frac{1}{2}\log(1 + g_1 p(g_0, g_1)) < r_0\} \\ s.t. \quad & E[p(g_0, g_1)] \leq P_{av}, \\ & E[g_0 p(g_0, g_1)] \leq Q_{av} \end{aligned} \tag{5.4}$$

where P_{av} is the maximum average transmit power at SU-TX.

With the assumption that perfect CSI on g_0 and g_1 is available at the SU-TX, the opti-

mal power allocation scheme for Problem (3.2) is given by [117]

$$p(g_0, g_1) = \begin{cases} \frac{c}{g_1}, & \lambda_f + \mu_f g_0 < \frac{g_1}{c}, \\ 0, & \text{otherwise} \end{cases} \tag{5.5}$$

where $c = e^{2r_0} - 1$, and λ_f, μ_f are the nonnegative Lagrange multipliers associated with the ATP constraint and the AIP constraint, respectively, and the optimal values of which can be obtained by solving $\lambda_f(E[p(g_0, g_1)] - P_{av}) = 0$ and $\mu_f(E[g_0 p(g_0, g_1)] - Q_{av}) = 0$.

However, the assumption of full CSI at the SU-TX (especially that of g_0) is usually unrealistic and difficult to implement in practical systems, especially when this channel is not time-division duplex (TDD). In the next section, we are therefore interested in designing a power allocation strategy of the outage probability minimization Problem (5.4) based on quantized CSI at the SU-TX acquired via a no-delay and error-free feedback link with limited rate.

5.3 Optimum Quantized power allocation (QPA) with imperfect g_1 and g_0 at SU-TX

5.3.1 Optimal QPA with limited rate feedback strategy

As shown in Fig.5.1, following our earlier work in Chapter 3, we assume that there is a central controller termed as the CR network manager who can obtain perfect information on g_0 and g_1, from PU-RX at the PU base station and SU-RX at the SU base station respectively, possibly over fibre-optic links, and then forward some appropriately quantized (g_0, g_1) information to SU-TX through a finite-rate feedback link. For further details on the justification of and resulting benefits due this assumption, see Chapter 3. Under such a network modelling assumption, given B bits of feedback, a power codebook $\mathcal{P} = \{p_1, \ldots, p_L\}$ of cardinality $L = 2^B$, is designed offline purely on the basis of the statistics of g_0 and g_1 information at the CR network manager. This codebook is known *a priori* by both SU-TX and the SU-RX for decoding purposes. Given a channel realization (g_0, g_1), the CR network manager employs a deterministic mapping from the current

instantaneous (g_0, g_1) information to one of L integer indices (let $\mathcal{I}(g_0, g_1)$ denote the mapping, which partitions the vector space of (g_0, g_1) into L regions $\mathcal{R}_1, \ldots, \mathcal{R}_L$, defined as

$$\mathcal{I}(g_0, g_1) = j, \text{ if } (g_0, g_1) \in \mathcal{R}_j, \ j = 1, \ldots, L \tag{5.6}$$

) and then sends the corresponding index $j = \mathcal{I}(g_0, g_1)$ to the SU-TX (and the SU-RX) via the feedback link. The SU-TX then uses the associated power codebook element (e.g., if the feedback signal is j, then p_j will be used as the transmission power) to adapt its transmission strategy.

Remark 5.1. *Note that the CR network manager could be assumed to be located at the SU-BS for the current setup and in this case, the PU-BS simply has to cooperate with the SU-BS by sending the real-time full CSI information of g_0. However, for future generalization of our work to a multi-cell cognitive network scenario, we assume that the CR network manager is a separate entity, which can obtain information from multiple PU-BS and SU-BS if necessary.*

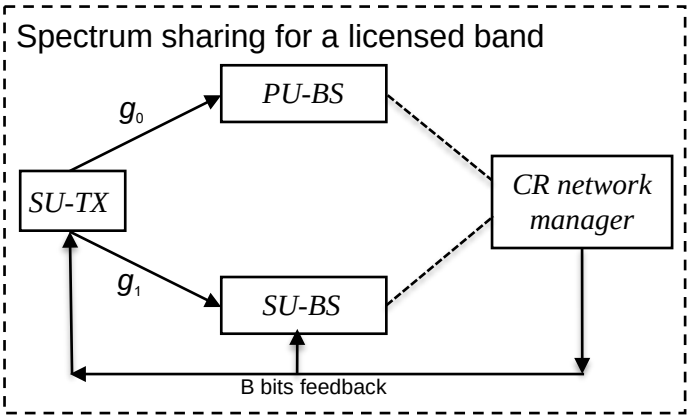

Figure 5.1: System model for narrowband spectrum sharing scenario with limited rate feedback

Define an indicator function $x_j, \ j = 1, \ldots, L$, as

$$X_j = \begin{cases} 1, & \frac{1}{2}\log(1 + g_1 p_j) < r_0, \\ 0, & \text{otherwise} \end{cases} . \tag{5.7}$$

Let $Pr(\mathcal{R}_j)$, $E[\bullet|\mathcal{R}_j]$ represent $Pr((g_0, g_1) \in \mathcal{R}_j)$ and $E[\bullet|(g_0, g_1) \in \mathcal{R}_j]$, respectively. Then the SU outage probability minimization Problem (5.4) with limited feedback can be formulated as

$$\begin{aligned} \min_{p_j \geq 0,\ \mathcal{R}_j\ \forall j} \quad & \sum_{j=1}^{L} E[X_j|\mathcal{R}_j] Pr(\mathcal{R}_j) \\ s.t. \quad & \sum_{j=1}^{L} E[p_j|\mathcal{R}_j] Pr(\mathcal{R}_j) \leq P_{av} \\ & \sum_{j=1}^{L} E[g_0 p_j|\mathcal{R}_j] Pr(\mathcal{R}_j) \leq Q_{av} \end{aligned} \tag{5.8}$$

Thus the key problem to solve here is the joint optimization of the channel partition regions and the power codebook such that the outage probability of SU is minimized under the above constraints.

The dual problem of (5.8) is expressed as

$$\max_{\lambda \geq 0,\ \mu \geq 0} \ g(\lambda, \mu) - \lambda P_{av} - \mu Q_{av}, \tag{5.9}$$

where λ, μ are the nonnegative Lagrange multipliers associated with the ATP and AIP constraints in Problem (5.8), and the Lagrange dual function $g(\lambda, \mu)$ is defined as

$$g(\lambda, \mu) = \min_{p_j \geq 0,\ \mathcal{R}_j,\ \forall j} \ \sum_{j=1}^{L} E[X_j + (\lambda + \mu g_0) p_j|\mathcal{R}_j] Pr(\mathcal{R}_j) \tag{5.10}$$

The procedure to solve the above dual problem is:

Step 1: With fixed values of λ and μ, find the optimal solution (power codebook and quantization regions) for the Lagrange dual function (5.10).

Step 2: Find the optimal λ and μ by solving the dual problem using subgradient search method, i.e, updating $\lambda,\ \mu$ until convergence using

$$\lambda^{l+1} = [\lambda^l - \alpha^l (P_{av} - \sum_{j=1}^{L} E[p_j|\mathcal{R}_j] Pr(\mathcal{R}_j))]^+,$$

$$\mu^{l+1} = [\mu^l - \beta^l (Q_{av} - \sum_{j=1}^{L} E[g_0 p_j | \mathcal{R}_j] Pr(\mathcal{R}_j))]^+, \tag{5.11}$$

where l is the iteration number, α^l, β^l are positive scalar step sizes for the l-th iteration satisfying $\sum_{l=1}^{\infty} \alpha_l = \infty$, $\sum_{l=1}^{\infty} (\alpha_l)^2 < \infty$ and similarly for β_l.

Remark 5.2. *A general method to solve Step 1 is to employ a simulation-based optimization algorithm called the Simultaneous Perturbation Stochastic Approximation algorithm (SPSA) (for a step-by-step guide to implementation of SPSA, see [100]), where one can use the objective function of Problem (5.10) as the loss function, and the optimal power codebook elements for each channel partition are obtained via a randomized stochastic gradient search technique. Note that due to the presence of the indicator function and no explicit expression being available for the outage probability with quantized power allocation, we can't directly exploit the Generalized Lloyd Algorithm (GLA) with a Lagrangian distortion, as we used in Chapter 3, to solve Problem (5.10). SPSA uses a simulation-based method to compute the loss function and then estimates the gradient from a number of loss function values computed by randomly perturbing the power codebook. Note that SPSA results in a local minima (similar to GLA), but is computationally highly complex and the convergence time is also quite long.*

Due to the high computational complexity of SPSA and its long convergence time, to solve Problem (5.10), we will next derive a low-complexity approach for solving Problem (5.10). However, due to the original problem (5.8) not being convex with respect to the power codebook elements, the optimal solution we can obtain is also locally optimal.

Let $\mathcal{P} = \{p_1, \ldots, p_L\}$, where $p_1 > \cdots > p_L \geq 0$, and the corresponding channel partitioning $\mathcal{R}_1, \ldots, \mathcal{R}_L$ denote the optimal solution to Problem (5.10). And let $p(g_0, g_1)$ represents the mapping from instantaneous (g_0, g_1) to the allocated power level. We can obtain,

Lemma 5.1. *Let $\{v_1, \ldots, v_L\}$ denotes the optimum quantization thresholds on the g_1 axis ($0 < v_1 < \cdots < v_L$) and $\{s_1, \ldots, s_{L-1}\}$ indicates the optimum quantization thresholds on the g_0 axis*

($0 < s_1 < \cdots < s_{L-1}$). Then we have $\forall j, j = 1, \ldots, L-1$:

$$p(g_0, g_1) = \begin{cases} p_j, & v_j \leq g_1 < v_{j+1}, 0 \leq g_0 < s_j; \\ p_L, & \text{otherwise.} \end{cases} \tag{5.12}$$

where $v_j = \frac{c}{p_j}$, and when $\mu > 0$, $s_j = \frac{1}{\mu(p_j - p_L)} - \frac{\lambda}{\mu}$; when $\mu = 0$, $s_j = \infty$, condition $0 \leq g_0 < s_j$ becomes $\lambda < \frac{1}{p_j - p_L}$. The region $\mathcal{R}_L$ includes two parts : the set $\mathcal{R}_{L1} = \{(g_0, g_1) : v_j \leq g_1 < v_{j+1}, g_0 \geq s_j, \forall j = 0, \ldots, L-1\}$ with $s_0 = 0, v_0 = 0$ and the set $\mathcal{R}_{L2} = \{(g_0, g_1) : g_1 \geq v_L, g_0 \geq 0\}$. The entire set $\mathcal{R}_{L1}$ is in outage.

Proof: The proof can be found in the appendix of this chapter.

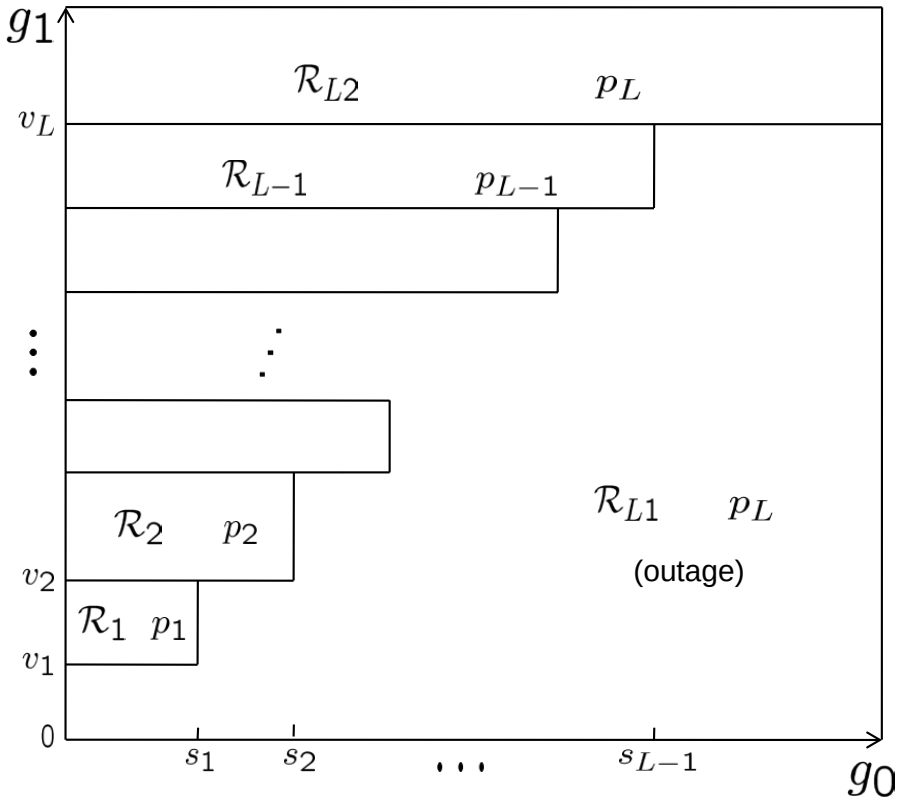

Figure 5.2: The 'stepwise structure' of optimum quantization regions for $\mu > 0$ case

Remark 5.3. *When $\mu > 0$, which implies that the AIP constraint is active, from Lemma 5.1, the*

optimum partition regions possess a stepwise structure, as shown in Fig.5.2; When $\mu = 0$, i.e, the AIP constraint is inactive and only ATP constraint is active (we must have $\lambda > 0$), Problem (5.8) becomes a scalar quantization problem involving quantizing g_1 only, and Lemma 5.1 reduces to $\forall j, j = 1, \ldots, L-1$:

$$p(g_1) = \begin{cases} p_j, & v_j \leq g_1 < v_{j+1}; \\ p_L, & otherwise. \end{cases} \tag{5.13}$$

where $\lambda < \frac{1}{p_j - p_L}$ and the two parts of $\mathcal{R}_L$ becomes $\mathcal{R}_{L1} = \{g_1 : 0 \leq g_1 < v_1\}$ and $\mathcal{R}_{L2} = \{g_1 : g_1 \geq v_L\}$, and $\mathcal{R}_{L1}$ is in outage. Note that in this case we must have $Q_{av} \geq P_{av}$, due to $Q_{av} \geq \sum_{j=1}^{L} E[g_0 p_j | \mathcal{R}_j] Pr(\mathcal{R}_j) = \sum_{j=1}^{L} E[p_j | \mathcal{R}_j] Pr(\mathcal{R}_j) = P_{av}$.

From Lemma5.1, (due to the fading channels being independently exponentially distributed with unity mean) Problem (5.8) becomes,

$$\begin{aligned} \min_{p_j \geq 0,\ \forall j} \ & P_{out}^L = 1 - e^{-v_1} + \sum_{j=1}^{L-1} (e^{-v_j} - e^{-v_{j+1}}) e^{-s_j} \\ s.t. \ & p_L + \sum_{j=1}^{L-1} (p_j - p_L)(e^{-v_j} - e^{-v_{j+1}})(1 - e^{-s_j}) \leq P_{av} \\ & p_L + \sum_{j=1}^{L-1} (p_j - p_L)(e^{-v_j} - e^{-v_{j+1}})(1 - e^{-s_j}(1 + s_j)) \leq Q_{av} \end{aligned} \tag{5.14}$$

where P_{out}^L denotes the outage probability with $B = \log_2 L$ bits feedback QPA, $v_j = \frac{c}{p_j}$ and when $\mu > 0$, $s_j = \frac{1}{\mu(p_j - p_L)} - \frac{\lambda}{\mu}$, whereas when $\mu = 0$, $s_j = \infty$. Although the above optimization problem may be verified to be non-convex, we can employ the Karush-Kuhn-Tucker (KKT) necessary conditions to find local minima for Problem (5.14). Taking the partial derivative of first order of the Lagrangian of Problem (5.14) over $p_j, j = 1, \ldots, L-1$, and setting it to zero, we can obtain

$$\begin{aligned} & (e^{-v_j} - e^{-v_{j+1}})[\lambda(1 - e^{-s_j}) + \mu(1 - e^{-s_j}(1 + s_j))] \\ & = e^{-v_j} \frac{c}{p_j^2} [\hat{f}(p_{j-1}) - \hat{f}(p_j)], \ \ j = 1, \ldots, L-1; \end{aligned} \tag{5.15}$$

where $\hat{f}(p_0) = 1$ and

$$\hat{f}(p_j) = (p_j - p_L)(\lambda + \mu(1 - e^{-s_j})),\ 1 \leq j \leq L-1. \tag{5.16}$$

(5.15) also can be rewritten as $j = 1, \ldots, L-1$,

$$p_{j+1} = \frac{c}{v_j - \ln(1 - \frac{\frac{c}{p_j^2}[\hat{f}(p_{j-1}) - \hat{f}(p_j)]}{\lambda(1-e^{-s_j}) + \mu(1-e^{-s_j}(1+s_j))})}, \tag{5.17}$$

Equating the partial derivative of the Lagrangian function of Problem (5.14) over p_L to zero gives,

$$\begin{aligned} &\sum_{j=1}^{L-1}(e^{-v_j} - e^{-v_{j+1}})[\lambda(1 - e^{-s_j}) + \mu(1 - e^{-s_j}(1+s_j))] \\ &+ e^{-v_L}\frac{c}{p_L^2}\hat{f}(p_{L-1}) = \lambda + \mu, \end{aligned} \tag{5.18}$$

Optimal values of λ and μ can be determined by solving

$$\begin{aligned} \lambda[p_L + \sum_{j=1}^{L-1}(p_j - p_L)(e^{-v_j} - e^{-v_{j+1}})(1 - e^{-s_j}) - P_{av}] = 0 \\ \mu[p_L + \sum_{j=1}^{L-1}(p_j - p_L)(e^{-v_j} - e^{-v_{j+1}})(1 - e^{-s_j}(1+s_j)) - Q_{av}] = 0 \end{aligned} \tag{5.19}$$

Thus, for fixed λ and μ, we need solve L equations of (5.17)(5.18) for the power codebook. Given p_1 and p_L, from (5.17) we can successively compute $p_2, \ldots, p_{L-1}$, and then we can jointly solve the equation (5.17) with $j = L-1$ and equation (5.18) numerically for p_1 and p_L. The optimal value of λ and μ can be obtained by solving (5.19) with a subgradient method, i,e. by updating λ and μ until convergence using (5.11). One can thus repeat the above two steps (i.e, given λ and μ find the optimal power levels, and then using the resulting optimal power levels update λ and μ) iteratively until a satisfactory convergence criterion is met. This procedure can be formally summarized as:

a) First, if $P_{av} \leq Q_{av}$, we must have $\mu = 0,\ \lambda > 0$. Starting with an arbitrary positive initial value for λ, solve (5.15), (5.18) to obtain a power codebook $\{p_1, \ldots, p_L\}$, and

then use this codebook to update λ by (5.11). Repeat these steps until convergence and the final codebook will be an optimal power codebook for Problem (5.14).

b) If $P_{av} > Q_{av}$, we must have $\mu > 0$. Let $\lambda = 0$, then solving KKT conditions gives an optimal value of μ and corresponding power codebook $\{p_1, \ldots, p_L\}$. With this codebook, if $\sum_{j=1}^{L} E[p_j|\mathcal{R}_j]Pr(\mathcal{R}_j) \leq P_{av}$, then it is an optimal power codebook for Problem (5.14). Otherwise we must have $\lambda > 0$ too, in which case, starting with arbitrary positive initial values for λ and μ, obtain the corresponding power codebook $\{p_1, \ldots, p_L\}$, and then update λ and μ by (5.11). Repeat these steps until convergence and the final codebook will be an optimal power codebook for Problem (5.14).

5.3.2 Suboptimal QPA Algorithm

When the number of feedback bit B is large, the following Lemma allows us to obtain a suboptimal but computationally efficient algorithm for large L.

Lemma 5.2. $\lim_{L\to\infty} p_L = 0$

Proof: The proof can be found in the appendix of this chapter.

Remark 5.4. *Lemma 5.2 shows that regardless of whether $\mu > 0$ or $\mu = 0$, with high rate quantization, the power level for the last region $\mathcal{R}_{\mathcal{L}}$ approaches zero, which implies that as $L \to \infty$,*
1) The non-outage part of $\mathcal{R}_{\mathcal{L}}$, given by $\mathcal{R}_{\mathcal{L}2}$, disappears gradually. In other words, $\mathcal{R}_{\mathcal{L}} \to \mathcal{R}_{\mathcal{L}1}$. Thus, when $L \to \infty$, $\mathcal{R}_{\mathcal{L}}$ becomes the outage region with zero power.
2) When $\mu > 0$, the quantization thresholds on g_0 axis $s_j \to s'_j$ ($s'_j = \frac{1}{\mu p_j} - \frac{\lambda}{\mu}$), which gives $v_j = c\lambda + c\mu s'_j$, and it means all the points given by coordinates (s'_j, v_j) lie on the line of $g_1 = c\lambda + c\mu g_0$. Therefore, as $L \to \infty$, the stepwise shape of the structure in $\mu > 0$ case (i.e, the boundary between non-outage and outage regions) approaches the straight line $g_1 = c\lambda + c\mu g_0$, which is consistent with the full CSI-based power allocation result in (5.5).

Thus, when L is large, applying Lemma 5.2 (i.e, $p_L \to 0$) to Problem (5.14), the above L

KKT conditions (5.15) and (5.18) can be simplified into $L-1$ equations: $\forall j, j = 1, \ldots, L-1$

$$\begin{aligned}&(e^{-v_j} - e^{-v_{j+1}})[\lambda(1-e^{-s'_j}) + \mu(1-e^{-s'_j}(1+s'_j))] \\ &= e^{-v_j}\frac{c}{p_j^2}[p_{j-1}(\lambda+\mu(1-e^{-s'_{j-1}})) - p_j(\lambda+\mu(1-e^{-s'_j}))]\end{aligned} \tag{5.20}$$

where when $\mu > 0$, the quantization thresholds on g_0 axis $s'_j = \frac{1}{\mu p_j} - \frac{\lambda}{\mu}$, $s'_0 = 0$, and $p_0 = \frac{1}{\lambda+\mu s'_0}$; when $\mu = 0$, $s'_j = \infty, s'_0 = 0$, and $p_0 = \frac{1}{\lambda}$. (5.20) also can be written as

$$\begin{aligned}p_{j+1} &= \frac{c}{v_j - \ln(1 - \frac{\frac{c}{p_j^2}[p_{j-1}(\lambda+\mu(1-e^{-s'_{j-1}})) - p_j(\lambda+\mu(1-e^{-s'_j}))]}{\lambda(1-e^{-s'_j})+\mu(1-e^{-s'_j}(1+s'_j))})}, \quad j = 1, \ldots, L-2; \\ &\frac{\lambda(1-e^{-s'_{L-1}}) + \mu(1-e^{-s'_{L-1}}(1+s'_{L-1}))}{\frac{c}{p_{L-1}^2}[p_{L-2}(\lambda+\mu(1-e^{-s'_{L-2}})) - p_{L-1}(\lambda+\mu(1-e^{-s'_{L-1}}))]} = 1.\end{aligned} \tag{5.21}$$

Thus, with fixed values of λ and μ, starting with a specific value of p_1, we can successively compute $p_2, \ldots, p_{L-1}$ using (5.21). Then the second equation in (5.21) becomes an equation in only p_1, which can be easily numerically solved. We call this suboptimal QPA algorithm as 'Zero Power in Outage Region Approximation'(ZPiORA), which is applicable to the case of large number of feedback bits. Through simulation studies, we will illustrate that ZPiORA performs well even for 4 bits of feedback.

Alternative suboptimal algorithms: For comparison purposes, we also propose two alternative suboptimal algorithms described below:

(1) The first suboptimal algorithm is based on the Equal average power per region approximation (EAPPR) algorithm, originally proposed in [13] in a non-cognitive or typical primary network setting for an outage minimization problem with only an ATP constraint. Alternatively, a related Equal Probability Per Region (excluding the outage region) approximation (EPrPR) algorithm may be also used. These two methods (both have $p_L \neq 0$) can be applied to our cognitive radio outage minimization problem. However, ZPiORA is computationally simpler than these two methods, especially when $\mu > 0$. In addition, when P_{av} or Q_{av} is small, ZPiORA always outperforms EPrPR and EAPPR. It is seen however that when both

P_{av} and Q_{av} are large, for a small number of feedback bits, EPrPR and EAPPR may outperform ZPiORA, whereas with a sufficiently large number of feedback bits, ZPiORA is a more accurate approximation due to Lemma 5.2.

(2) The second algorithm is based on GLA with a sigmoid function approximation (GLASFA) method proposed by [18], where the sigmoid function is used to approximate the indicator function in the Lagrange dual function (5.10). More specifically, given a random initial power codebook, we use the nearest neighbor condition of Lloyd's algorithm with a Lagrangian distortion $d((g_0, g_1), j) = X_j + (\lambda + \mu g_0)p_j$ to generate the optimal partition regions [83] given by, $\mathcal{R}_j = \{(g_0, g_1) : X_j + (\lambda + \mu g_0)p_j \leq X_i + (\lambda + \mu g_0)p_i, \forall i \neq j\}$, $i, j = 1, \ldots, L$,. We then use the resulting optimal partition regions to update the power codebook by $p_j \approx \text{argmin}_{p_j \geq 0} E[\sigma(k(\frac{1}{2}\log(1 + g_1 p_j) - r_0)) + (\lambda + \mu g_0)p_j | R_j] Pr(R_j)$ for $j = 1, \ldots, L$, where we use the approximation $X_j \approx \sigma(k(\frac{1}{2}\log(1 + g_1 p_j) - r_0))$, $\sigma(x) = \frac{1}{1+e^x}$ being the sigmoid function where the coefficient k controls the sharpness of the approximation (for detailed guidelines on choosing k see [18]). The above two steps of GLA are repeated until convergence. Numerical results illustrate that ZPiORA significantly outperforms this suboptimal method. See Section 5.5 for more details.

5.4 Asymptotic outage behaviour of QPA under high resolution quantization

In this section, we derive a number of asymptotic expressions for the SU outage probability when the number of feedback bits becomes very large. To this end, we will first derive some useful properties regarding the quantizer structure at high rate quantization:

Lemma 5.3. *As the number of quantization regions $L \to \infty$, we can obtain the following results: 1) when $\mu > 0$, the optimum quantization thresholds on the g_0 axis satisfy*

$$s'_1 - s'_0 \approx s'_2 - s'_1 \approx \cdots \approx s'_{L-1} - s'_{L-2} \tag{5.22}$$

where $s'_j = \frac{1}{\mu p_j} - \frac{\lambda}{\mu}, j = 1, \ldots, L-1$ and $s'_0 = 0$.

2) when $\mu = 0$, the optimum quantization thresholds on the g_1 axis satisfy

$$\frac{v_1}{v_0} \approx \frac{v_2}{v_1} \cdots \approx \frac{v_{L-1}}{v_{L-2}} \tag{5.23}$$

where $v_j = \frac{c}{p_j}, j = 1, \ldots, L-1$ and $v_0 = c\lambda$.

Proof: The proof can be found in the appendix of this chapter.

Lemma 5.4. *In the high rate quantization regime, as $L \to \infty$, we have*

$$\sum_{j=1}^{L-1} (e^{-v_j} - e^{-v_{j+1}})[\lambda(1 - e^{-s'_j}) + \mu(1 - e^{-s'_j}(1 + s'_j))] \approx \frac{\lambda P_{av} + \mu Q_{av}}{L-1} \sum_{j=1}^{L-1} \frac{1}{p_j}. \tag{5.24}$$

where for $\mu > 0$, $s'_j = \frac{1}{\mu p_j} - \frac{\lambda}{\mu}$. When $\mu = 0$, $s'_j = \infty$, and (5.24) simplifies to

$$ce^{-v_1} \approx \frac{P_{av}}{L-1} \sum_{j=1}^{L-1} v_j, \tag{5.25}$$

where $v_j = \frac{c}{p_j}$.

Proof: The proof can be found in the appendix of this chapter.

With Lemma 5.3 and Lemma 5.4, the main result of this section can be obtained in the below Theorem.

Theorem 5.1. *The asymptotic outage probability of SU for a large number of feedback bits is given as,*
1) when $\mu > 0$,

$$P_{out}^L \approx 1 - e^{-c\lambda_f}[1 - (1 - e^{-\frac{a}{L}}) \frac{1 - e^{-a(1+\frac{1}{c\mu_f})}}{1 - e^{-\frac{a(1+\frac{1}{c\mu_f})}{L}}}] \tag{5.26}$$

where a is a constant satisfying: $(\lambda_f P_{av} + \mu_f Q_{av})(\lambda_f + \frac{a}{2c})e^{c\lambda_f} \approx [(\lambda_f + \mu_f)(1 - \frac{c\mu_f}{1+c\mu_f}(1 - e^{-a(1+\frac{1}{c\mu_f})})) - \frac{c\mu_f^2}{(1+c\mu_f)^2}(1 - e^{-a(1+\frac{1}{c\mu_f})}(1 + a(1 + \frac{1}{c\mu_f})))]$. And We also have $\lim_{L\to\infty} P_{out}^L = 1 - e^{-c\lambda_f}[1 - \frac{1-e^{-a(1+\frac{1}{c\mu_f})}}{1+\frac{1}{c\mu_f}}]$.

2) when $\mu = 0$,

$$P_{out}^{L} \approx 1 - e^{-c\lambda_f(1+\frac{\beta}{L})} \tag{5.27}$$

where β *is a constant, given by* $e^{-c\lambda_f} \approx \lambda_f P_{av} \frac{e^{\beta}-1}{\beta}$. *In this case we also have* $\lim_{L\to\infty} P_{out}^{L} = 1 - e^{-c\lambda_f}$.

Proof: The proof can be found in the appendix of this chapter.

5.5 Numerical Results

In this section, we will examine the outage probability performance of the SU in the narrow band spectrum sharing system with the proposed power allocation strategies via numerical simulations. All the channels involved are assumed to undergo identical Rayleigh fading, i.e, channel power gain g_0 and g_1 are i.i.d and exponentially distributed with unit mean. And the required transmission rate is taken to be $r_0 = 0.25$ nats per channel use.

Fig. 5.3 displays the SU outage probability performance of the suboptimal algorithm ZPiORA versus P_{av} with feedback bits $B = \{1, 2\}$, under $Q_{av} = -5$ dB and $Q_{av} = 0$ dB respectively, and compares these results with the corresponding outage probability performance using optimal QPA. As observed from Fig. 5.3, when $Q_{av} = -5$ dB, with B fixed, the outage performance of ZPiORA and corresponding optimal QPA case almost overlaps each other. When $Q_{av} = 0$ dB, with $P_{av} \leq -5$ dB, with same number of feedback bits, the outage performances of these two methods are still indistinguishable; and with $P_{av} > -5$ dB, the outage performance gap between ZPiORA and corresponding optimal QPA is decreasing with increasing B. For example, with 1 bit feedback, at $P_{av} = 10$ dB, the outage gap between ZPiORA and optimal QPA is 0.0347, but with 2 bits of feedback, the outage performance of these two methods are very close to each other, which agrees with Lemma 5.2 that ZPiORA is a near-optimal algorithm for large number of feedback bits. Furthermore, Fig. 5.4 compares the outage performance of ZPiORA with another suboptimal method (GLASFA) with $Q_{av} = -5$ dB. We can easily observe that with a

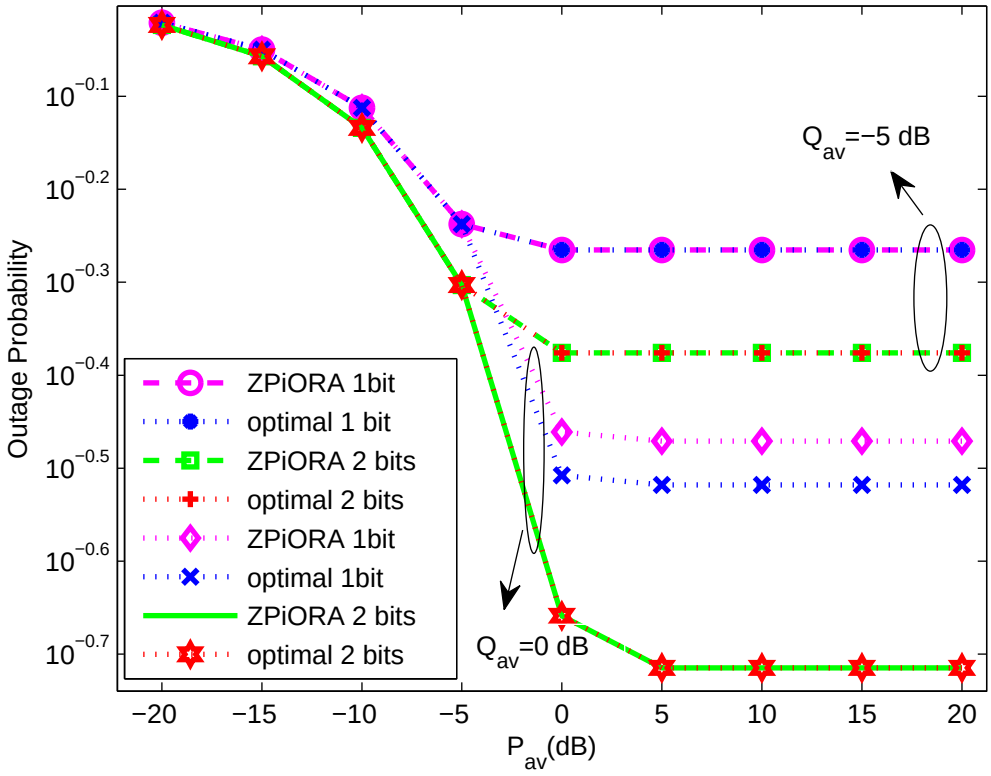

Figure 5.3: Outage probability performance comparison between ZPiORA and optimal QPA

fixed number of feedback bits (2 bits or 4 bits), ZPiORA always outperforms GLASFA. And ZPiORA is also substantially faster than GLASFA. For example, with fixed λ and μ and 4 bits of feedback ($Q_{av} = -5$dB, $P_{av} = 10$ dB), when implemented in MATLAB (version 7.11.0.584 (R2010b)) on a AMD Quad-Core processor (CPU P940 with a clock speed of 1.70 GHz and a memory of 4 GB), it was seen that GLASFA (with 100,000 training samples, starting $k = 20$ and increasing it by a factor of 1.5 at each step which finally converged at about $k = 768.8672$) took approximately 299.442522 seconds (different initial guesses of the power codebook may result in different convergence time). In comparison, ZPiORA took only 0.006237 seconds to achieve comparable levels of accuracy. These results further confirm the efficiency of ZPiORA.

Fig. 5.5 illustrates the outage performance of SU with optimal QPA strategy versus P_{av} with feedback bits $B = \{2, 4, 6\}$, under $Q_{av} = -5$ dB and $Q_{av} = 0$ dB respectively, and

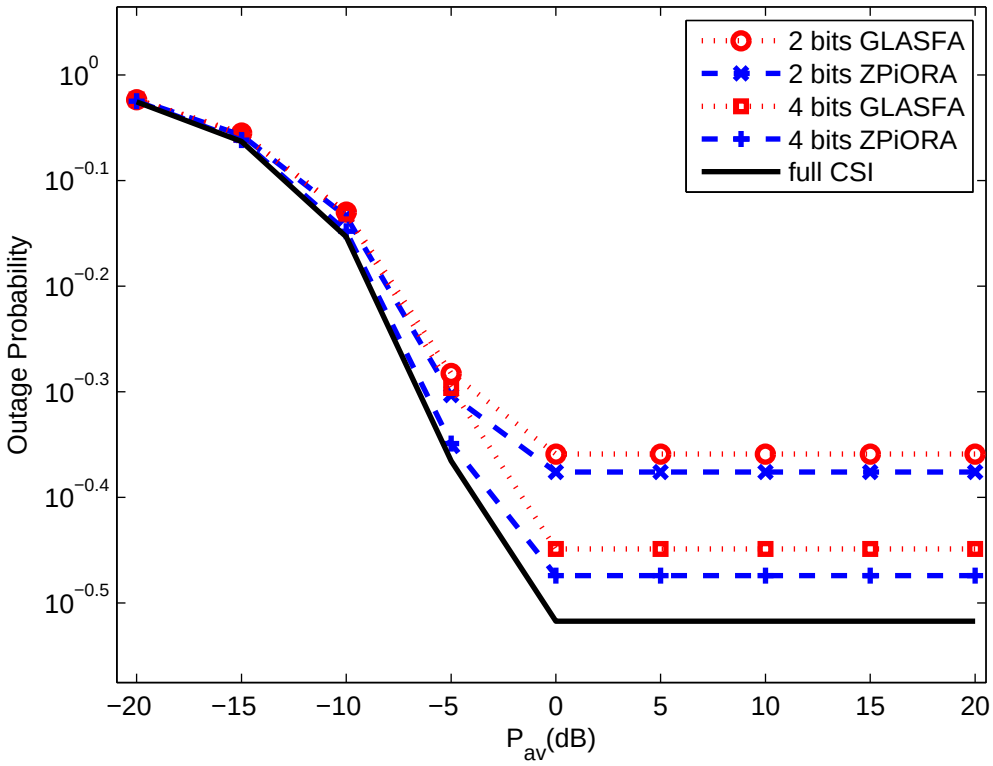

Figure 5.4: Outage probability performance comparison between ZPiORA and other possible suboptimal algorithm : GLASFA

studies the effect of increasing the number of feedback bits on the outage performance. For comparison, we also plot the corresponding SU outage performance with full CSI case. Since ZPiORA is an efficient suboptimal method for large number of feedback bits, we employ ZPiORA to obtain the outage performance instead of using optimal QPA for $B = 6$ bits. First, it can be easily observed that all the outage curves decreases gradually as P_{av} increases until P_{av} reaches a certain threshold, when the outage probability attains a floor. This is due to the fact that in the high P_{av} regime, the AIP constraint dominates. For a fixed number of feedback bits, the higher Q_{av} is, the smaller the resultant outage probability is, since higher Q_{av} means PU can tolerate more interference. Fig. 5.5 also illustrates that for fixed Q_{av}, introducing one extra bit of feedback substantially reduces the outage gap between QPA and the perfect CSI case. To be specific, for $Q_{av} = 0$ dB and $P_{av} = 10$ dB, with 2 bits, 4 bits and 6 bits of feedback, the outage gaps with the full CSI

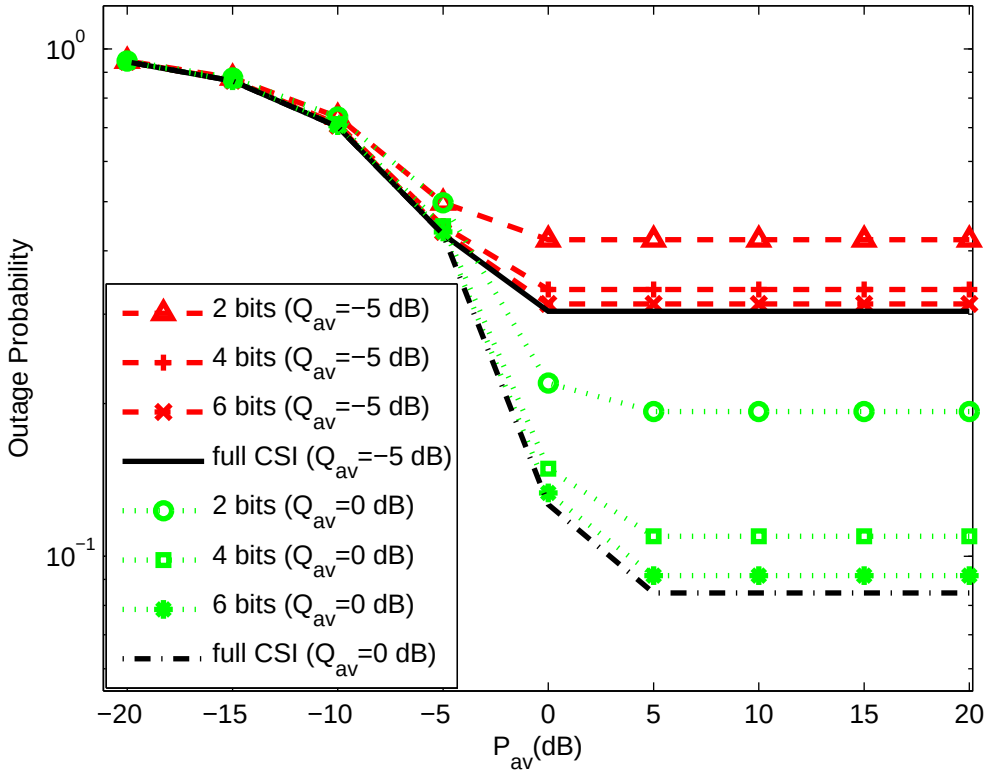

Figure 5.5: Effect of increasing feedback bits on outage performance of SU

case are approximately 0.1083, 0.0249 and 0.006979 respectively. And for any Q_{av}, only 6 bits of feedback seem to result in an SU outage performance very close to that with full CSI case.

Figure 5.6 compares the asymptotic outage performance derived in Theorem 5.1 and the optimal QPA performance $B = \{4, 6, 8\}$ under $Q_{av} = 0$ dB. It is clearly observed that increasing number of feedback bits substantially shrinks the outage performance gap between the asymptotic outage approximation and the corresponding optimal QPA performance. For instance, with 4, 6, 8 bits of feedback at $P_{av} = 10$ dB, the outage gap between the asymptotic outage approximation and the corresponding optimal QPA are around 0.0325, 0.00618, 0.000168 respectively. These results confirm that the derived asymptotic outage expressions in Theorem 5.1 are highly accurate for $B \geq 8$ bits of feedback. In addition, Figure 5.7 depicts the asymptotic outage probability behavior of SU versus the

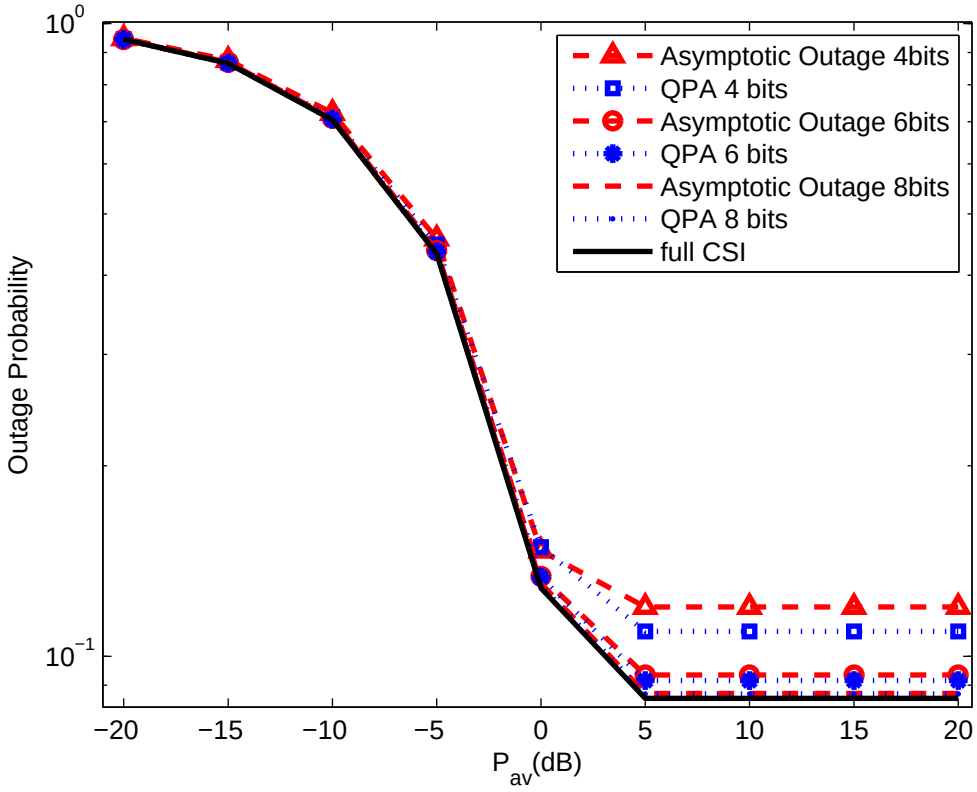

Figure 5.6: Comparison between asymptotic outage performance and QPA performance with $Q_{av} = 0dB$

number of quantization level L at $Q_{av} = 0$ dB, $P_{av} = 10$ dB, and compares the result with corresponding full CSI performance. It can be seen from Figure 5.7 that the outage decreases as the number of quantization level L increases, however, as L increases beyond a certain number ($L \geq 2^8$, i.e, $B \geq 8$ bits), the capacity curve starts to saturate and approaches the full CSI performance. This further confirms that only a small number of feedback bits is enough to obtain an outage performance close to the perfect CSI-based performance.

5.6 Conclusions

In this chapter, we designed optimal power allocation algorithms for secondary outage probability minimization with quantized CSI information for a narrowband spectrum

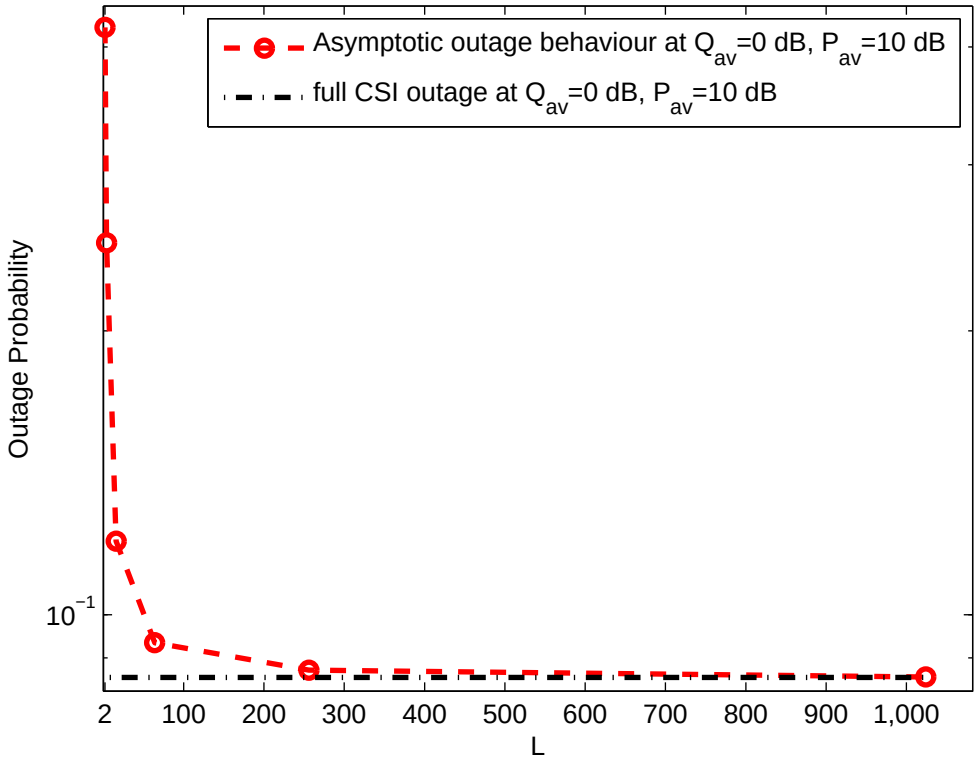

Figure 5.7: Asymptotic outage behavior versus the number of quantization level L

sharing cognitive radio framework under an ATP constraint at SU-TX and an AIP constraint at PU-RX. We prove that the optimal channel partition structure has a "stepwise" pattern based on which an efficient optimal power codebook design algorithm is provided. In the case of a large number of feedback bits, we derive a novel low-complexity suboptimal algorithm ZPiORA which is seen to outperform alternative suboptimal algorithms based on approximations used in the existing literature. We also derive explicit expressions for asymptotic behavior of the SU outage probability for a large number of feedback bits. Although the presented optimal power codebook design methods result in locally optimal solutions (due to the non-convexity of the quantized power allocation problem), numerical results illustrate that only 6 bits of feedback result in SU outage performance very close to that obtained with full CSI at the SU transmitter. Future work will involve extending the results to more complex wideband spectrum sharing scenario

along with consideration of other types of interference constraints at the PU receiver.

5.7 Appendix

5.7.1 Proof of Lemma 5.1

We use an analysis method similar to [71] to prove our problem's optimal quantizer structure. Let $\mathcal{P} = \{p_1, \ldots, p_L\}$, where $p_1 > \cdots > p_L \geq 0$, and the corresponding channel partitioning $\mathcal{R} = \{\mathcal{R}_1, \ldots, \mathcal{R}_L\}$ denote the optimal solution to the optimization problem (5.8), and $p(g_0, g_1) = p_j$, if $(g_0, g_1) \in \mathcal{R}_j$.

Let $\mathcal{R}_j^* = \{(g_0, g_1) : v_j \leq g_1 < v_{j+1}, 0 \leq g_0 < s_j\}$, $j = 1, \ldots, L-1$ and $\mathcal{R}_L^* = \mathcal{R}_{L1}^* \cup \mathcal{R}_{L2}^* = \{(g_0, g_1) : v_j \leq g_1 < v_{j+1},\ g_0 \geq s_j, \forall j = 0, 1, \ldots, L-1\} \cup \{(g_0, g_1) : g_1 \geq v_L, g_0 \geq 0\}$, where $s_0 = 0$ and $v_0 = 0$. We assume that the set $\mathcal{R}_j^* \setminus \mathcal{R}_j$ is a non-empty set, where $\setminus$ is the set subtraction operation (i.e, if $(g_0, g_1) \in \mathcal{R}_j^* \setminus \mathcal{R}_j$, then $(g_0, g_1) \in \mathcal{R}_j^*$ but $(g_0, g_1) \notin \mathcal{R}_j$). Then, the set $\mathcal{R}_j^* \setminus \mathcal{R}_j$ can be partitioned into two subsets $S_j^- = (\mathcal{R}_j^* \setminus \mathcal{R}_j) \cap (\cup_{k=1}^{j-1} \mathcal{R}_k)$ and $S_j^+ = (\mathcal{R}_j^* \setminus \mathcal{R}_j) \cap (\cup_{k=j+1}^{L} \mathcal{R}_k)$. In what follows, we denote the empty set by $\emptyset$.

(1): We will show that $S_j^- = \emptyset$, $\forall j = 1, \ldots, L$.

(a): When $j = 1$, it is obvious that $S_1^- = \emptyset$. When $1 < j < L$, if $S_j^- \neq \emptyset$, then we can always reassign the set S_j^- into region $\mathcal{R}_j$ without changing the overall outage probability. This is due to the fact that within the set $S_j^- \in \mathcal{R}_j^*$, we have $v_j \leq g_1 < v_{j+1}$ resulting in $\frac{1}{2}\log(1 + g_1 p_j) \geq r_0$, and the power level in $(\cup_{k=1}^{j-1} \mathcal{R}_k)$ satisfies $p_k > p_j$. Thus S_j^- is never in outage. However, the new assignment can achieve a lower Lagrange dual function (LDF) in (5.10), due to $g'(\lambda, \mu) - g(\lambda, \mu) = E[(\lambda + \mu g_0)(p_j - p_k)|S_j^-]Pr(S_j^-) < 0$, where $g'(\lambda, \mu)$ denotes the LDF with the new assignment, which contradicts the optimality of the solution $\mathcal{P}, \mathcal{R}$.

(b) When $j = L$, if $S_L^- \neq \emptyset$, we can again reassign the set S_L^- into region $\mathcal{R}_L$. 1) If some part of S_L^- is in the set $\{(g_0, g_1) : 0 \leq g_1 < v_1,\ g_0 \geq 0\}$ of $\mathcal{R}_{L1}^*$, we have $\frac{1}{2}\log(1 + g_1 p_1) < r_0$, which implies that this part of S_L^- is always in outage. Therefore, this reassignment for this part of S_L^- will not change the outage probability but will decrease the LDF due to the power level p_L in $\mathcal{R}_L$ is the lowest. 2) For any j ($j = 1, \ldots, L-1$), if some part

of S_L^- (called it 'S_{Lp}^-') exists in the set $\{(g_0, g_1) : v_j \leq g_1 < v_{j+1},\ g_0 \geq s_j\}$ of $\mathcal{R}_{L1}^*$, we have $\frac{1}{2}\log(1+g_1 p_j) \geq r_0$, $\frac{1}{2}\log(1+g_1 p_{j+1}) < r_0$ and $(\lambda+\mu g_0)(p_j - p_L) \geq 1$. And given $S_{Lp}^- \subset (\cup_{k=1}^{L-1}\mathcal{R}_k)$, let the power level for S_{Lp}^- be p_k (where k could be any value from $\{1,\ldots,L-1\}$). Reassigning this part of set S_L^- into region $\mathcal{R}_L$ will deminish the value of the LDF, since if $k \leq j$ (implying $p_k \geq p_j$), $g'(\lambda,\mu) - g(\lambda,\mu) = E[1 + p_L(\lambda+\mu g_0) - p_k(\lambda+\mu g_0)|S_{Lp}^-]Pr(S_{Lp}^-) < 0$ and if $k > j$ (implying $p_k < p_j$), $g'(\lambda,\mu) - g(\lambda,\mu) = E[1 + p_L(\lambda+\mu g_0) - 1 - p_k(\lambda+\mu g_0)|S_{Lp}^-]Pr(S_{Lp}^-) < 0$. 3) If some part of S_L^- belongs to the set $\mathcal{R}_{L2}^*$, similar to (a), we can show that the new partition for this part of S_L^- does not change the overall outage probability and meanwhile reduces the value of the LDF. These all contradict the optimality.

(2): We will now show that the set $S_j^+ = \emptyset$, $j = 1,\ldots,L$. When $j = L$, it's straightforward that $S_L^+ = \emptyset$. When $j < L$, we assume that $S_j^+ \neq \emptyset$. Within the set $S_j^+ \in \mathcal{R}_j^*$, we have $v_j \leq g_1 < v_{j+1}$, implying $\frac{1}{2}\log(1+g_1 p_{j+1}) < r_0$, or in other words, $S_j^+ \in (\cup_{k=j+1}^{L}\mathcal{R}_k)$ is in outage. We can reallocate the set S_j^+ into region $\mathcal{R}_j$. This reassignment not only lowers the outage probability (S_j^+ with p_j will not be in outage) but also lowers the value of the LDF, given by $g'(\lambda,\mu) - g(\lambda,\mu) = E[(\lambda+\mu g_0)(p_j - p_k) - 1|S_j^+]Pr(S_j^+) \leq E[(\lambda+\mu g_0)(p_j - p_L) - 1|S_j^+]Pr(S_j^+) < 0$, due to $g_0 < s_j = \frac{1}{\mu(p_j - p_L)} - \frac{\lambda}{\mu}$. This also contradicts optimality.

Therefore, we have $\mathcal{R}_j^* \setminus \mathcal{R}_j = \emptyset$, $\forall j = 1,\ldots,L$, i.e, $\mathcal{R}_j^* \subseteq \mathcal{R}_j$, $\forall j = 1,\ldots,L$. Since $\cup_{j=1}^{L}\mathcal{R}_j^* =$ the whole space of $(g_0, g_1) = \cup_{j=1}^{L}\mathcal{R}_j$, and $\mathcal{R}_j^* \subseteq \mathcal{R}_j$, $\forall j$, we can obtain that $\mathcal{R}_j^* = \mathcal{R}_j$, $\forall j = 1,\ldots,L$.

5.7.2 Proof of Lemma 5.2

We assume that $\lim_{L\to\infty} p_L \neq 0$. Let $\delta = \lim_{L\to\infty} p_L > 0$. From the KKT condition (5.18), we have

$$\begin{aligned}
&e^{-v_L}\frac{c}{p_L^2}(p_{L-1} - p_L)(\lambda + \mu(1 - e^{-s_{L-1}})) \\
&= (\lambda+\mu)(P_{out}^L + e^{-v_L}) + \mu\sum_{j=1}^{L-1}(e^{-v_j} - e^{-v_{j+1}})e^{-s_j}s_j \\
&\geq (\lambda+\mu)(P_{out}^L + e^{-v_L}) \qquad (5.28)
\end{aligned}$$

Let P_{out}^{f} denotes the outage probability with full CSI at SU-TX, then we have $P_{out}^{L} \geq P_{out}^{f}$ and $\lim_{L\to\infty} P_{out}^{L} = P_{out}^{f}$. Taking the limit $L \to \infty$ at both side of (5.28), gives,

$$\begin{aligned}&\lim_{L\to\infty} e^{-v_L}\frac{c}{p_L^2}(p_{L-1}-p_L)(\lambda+\mu(1-e^{-s_{L-1}}))\\&\geq(\lambda+\mu)(P_{out}^{f}+e^{-\frac{c}{\delta}})\neq 0\end{aligned} \tag{5.29}$$

Given $p_1 > \cdots > p_L > 0$, it is clear that the sequence $\{p_j\},\ j = 1, 2, \ldots, L$ is a monotonically decreasing sequence bounded below, therefore it must converge to its greatest-lower bound δ, as $L \to \infty$. Therefore, it can be easily shown that for an arbitrarily small $\epsilon > 0$, we can always find a sufficiently large L such that $p_{L-1} - p_L < \epsilon$. Thus, as $L \to \infty$, $(p_{L-1} - p_L) \to 0$, which implies when $\mu > 0$, $s_{L-1} = \frac{1}{\mu(p_{L-1}-p_L)} - \frac{\lambda}{\mu} \to \infty$). This implies that,

$$\begin{aligned}&\lim_{L\to\infty} e^{-v_L}\frac{c}{p_L^2}(p_{L-1}-p_L)(\lambda+\mu(1-e^{-s_{L-1}}))\\&=e^{-\frac{c}{\delta}}\frac{c}{\delta^2}(\lambda+\mu)\lim_{L\to\infty}(p_{L-1}-p_L)\\&=0.\end{aligned} \tag{5.30}$$

Which is in contradiction with (5.29). Thus, we must have

$$\lim_{L\to\infty} p_L = 0. \tag{5.31}$$

5.7.3 Proof of Lemma 5.3

As $L \to \infty$, from Lemma 5.2, we have $p_L \to 0$. Applying it to Problem (5.14), we have KKT conditions become (5.20).

1) $\mu > 0$:

From $s_j' = \frac{1}{\mu p_j} - \frac{\lambda}{\mu}$, we have $p_j = \frac{1}{\lambda+\mu s_j'}$, and we also have $p_0 = \frac{1}{\lambda+\mu s_0'}$. Applying it to (5.20), the right hand side (RHS) of equation (5.20) becomes,

$$RHS = e^{-v_j}\frac{c}{p_j^2}[\frac{\lambda+\mu(1-e^{-s_{j-1}'})}{\lambda+\mu s_{j-1}'} - \frac{\lambda+\mu(1-e^{-s_j'})}{\lambda+\mu s_j'}]$$

$$= e^{-v_j} \frac{c(s'_{j-1} - s'_j)}{p_j^2} \frac{\frac{\lambda+\mu(1-e^{-s'_{j-1}})}{\lambda+\mu s'_{j-1}} - \frac{\lambda+\mu(1-e^{-s'_j})}{\lambda+\mu s'_j}}{s'_{j-1} - s'_j} \tag{5.32}$$

From the mean value theorem (MVT), we have

$$\frac{\frac{\lambda+\mu(1-e^{-s'_{j-1}})}{\lambda+\mu s'_{j-1}} - \frac{\lambda+\mu(1-e^{-s'_j})}{\lambda+\mu s'_j}}{s'_{j-1} - s'_j} = \frac{-\mu}{(\lambda+\mu s')^2}[\lambda(1-e^{-s'}) + \mu(1-e^{-s'}(1+s'))] \tag{5.33}$$

where $s' \in [s'_{j-1}, s'_j)$. As the number of feedback bits $B = \log_2 L \to \infty$, the length of quantization interval on g_0 axis $[s'_{j-1}, s'_j), j = 1, \ldots, L-1$ approaches zero [13]. Hence (5.33) becomes,

$$\frac{\frac{\lambda+\mu(1-e^{-s'_{j-1}})}{\lambda+\mu s'_{j-1}} - \frac{\lambda+\mu(1-e^{-s'_j})}{\lambda+\mu s'_j}}{s'_{j-1} - s'_j} \approx \frac{-\mu}{(\lambda+\mu s'_j)^2}[\lambda(1-e^{-s'_j}) + \mu(1-e^{-s'_j}(1+s'_j))] \tag{5.34}$$

Applying (5.34) to (5.32), we have

$$RHS \approx e^{-v_j} c\mu(s'_j - s'_{j-1})[\lambda(1-e^{-s'_j}) + \mu(1-e^{-s'_j}(1+s'_j))] \tag{5.35}$$

Similarly, as $L \to \infty$, we also have the length of quantization interval on g_1 axis $[v_j, v_{j+1}), j = 1, \ldots, L-2$ approaches zero, thus from MVT,

$$e^{-v_j} - e^{-v_{j+1}} \approx e^{-v_j}(v_{j+1} - v_j) \tag{5.36}$$

Thus the left hand side (LHS) of equation (5.20) can be approximated as,

$$LHS \approx e^{-v_j}(v_{j+1} - v_j)[\lambda(1-e^{-s'_j}) + \mu(1-e^{-s'_j}(1+s'_j))] \tag{5.37}$$

From (5.35) and (5.37), we have $j = 1, \ldots, L-2$,

$$v_{j+1} - v_j \approx c\mu(s'_j - s'_{j-1}) \tag{5.38}$$

since $v_j = c\lambda + c\mu s'_j$, (5.38) becomes, $j = 1, \ldots, L-2$,

$$s'_{j+1} - s'_j \approx s'_j - s'_{j-1} \tag{5.39}$$

namely,

$$s'_{L-1} - s'_{L-2} \approx \cdots \approx s'_1 - s'_0 \tag{5.40}$$

2) $\mu = 0$:

In this case, we have $s'_j = \infty$, $j = 1, \ldots, L-1$, (5.20) becomes,

$$e^{-v_j} - e^{-v_{j+1}} = e^{-v_j} \frac{c}{p_j^2}(p_{j-1} - p_j) \tag{5.41}$$

where $j = 1, \ldots, L-1$ and $p_0 = \frac{1}{\lambda}$. (5.41) can be rewritten as

$$\frac{1}{v_j}(e^{-v_j} - e^{-v_{j+1}}) = \frac{1}{v_{j-1}} e^{-v_j}(v_j - v_{j-1}) \tag{5.42}$$

where $v_0 = \frac{c}{p_0} = c\lambda$. Applying (5.36) into (5.42), we have $j = 1, \ldots, L-2$,

$$\frac{1}{v_j} e^{-v_j}(v_{j+1} - v_j) \approx \frac{1}{v_{j-1}} e^{-v_j}(v_j - v_{j-1}) \tag{5.43}$$

which gives, $j = 1, \ldots, L-2$

$$\frac{v_{j+1}}{v_j} \approx \frac{v_j}{v_{j-1}} \tag{5.44}$$

namely,

$$\frac{v_{L-1}}{v_{L-2}} \approx \cdots \approx \frac{v_1}{v_0} \tag{5.45}$$

Here completes the proof for Lemma 5.3.

5.7.4 Proof of Lemma 5.4

As $L \to \infty$, from Lemma 5.2, we have $p_L \to 0$. Adding the two equations of (5.19) together and applying $p_L \to 0$, we have

$$\sum_{j=1}^{L-1} p_j(e^{-v_j} - e^{-v_{j+1}})[\lambda(1 - e^{-s'_j}) + \mu(1 - e^{-s'_j}(1 + s'_j))] = \lambda P_{av} + \mu Q_{av} \tag{5.46}$$

The KKT conditions (5.20), also can be rewritten as,

$$\begin{aligned} &p_j(e^{-v_j} - e^{-v_{j+1}})[\lambda(1 - e^{-s'_j}) + \mu(1 - e^{-s'_j}(1 + s'_j))] \\ &= p_{j-1}e^{-v_j}(v_j - v_{j-1})\frac{[\hat{f}'(p_{j-1}) - \hat{f}'(p_j)]}{p_{j-1} - p_j} \end{aligned} \tag{5.47}$$

where $\hat{f}'(p_j) = p_j(\lambda + \mu(1 - e^{-s'_j}))$. As mentioned before, as $L \to \infty$, we have the length of quantization interval on g_1 axis $[v_{j-1}, v_j), j = 2, \ldots, L-1$ approaches zero, then we also have $[p_{j-1}, p_j), j = 2, \ldots, L-1$ approaches zero, due to $v_j = \frac{c}{p_j}$. Thus from MVT, we have

$$\begin{aligned} e^{-v_{j-1}} - e^{-v_j} &\approx e^{-v_j}(v_j - v_{j-1}) \\ \frac{\hat{f}'(p_{j-1}) - \hat{f}'(p_j)}{p_{j-1} - p_j} &\approx \lambda(1 - e^{-s'_{j-1}}) + \mu(1 - e^{-s'_{j-1}}(1 + s'_{j-1})) \end{aligned} \tag{5.48}$$

Applying (5.48) into (5.47), we can obtain, $j = 2, \ldots, L-1$

$$\begin{aligned} &p_j(e^{-v_j} - e^{-v_{j+1}})[\lambda(1 - e^{-s'_j}) + \mu(1 - e^{-s'_j}(1 + s'_j))] \approx \\ &p_{j-1}(e^{-v_{j-1}} - e^{-v_j})[\lambda(1 - e^{-s'_{j-1}}) + \mu(1 - e^{-s'_{j-1}}(1 + s'_{j-1}))] \end{aligned} \tag{5.49}$$

Then applying the result of (5.49) into (5.46), we can have $j = 1, \ldots, L-1$

$$p_j(e^{-v_j} - e^{-v_{j+1}})[\lambda(1 - e^{-s'_j}) + \mu(1 - e^{-s'_j}(1 + s'_j))] \approx \frac{\lambda P_{av} + \mu Q_{av}}{L-1} \tag{5.50}$$

which gives,

$$\sum_{j=1}^{L-1}(e^{-v_j}-e^{-v_{j+1}})[\lambda(1-e^{-s'_j})+\mu(1-e^{-s'_j}(1+s'_j))] \approx \frac{\lambda P_{av}+\mu Q_{av}}{L-1}\sum_{j=1}^{L-1}\frac{1}{p_j}. \tag{5.51}$$

Here completes the proof for Lemma 5.4.

5.7.5 Proof of Theorem 5.1

1) when $\mu > 0$

From the (5.22) of Lemma 5.3, we can easily obtain, $j = 1, \ldots, L-1$,

$$\begin{aligned} s'_j &\approx j s'_1 \\ \frac{1}{p_j} &= \lambda + \mu s'_j \approx \lambda + j\mu s'_1 \\ v_j &= \frac{c}{p_j} \approx c\lambda + jc\mu s'_1 \end{aligned} \tag{5.52}$$

Let

$$z = \sum_{j=1}^{L-1}(e^{-v_j}-e^{-v_{j+1}})[\lambda(1-e^{-s'_j})+\mu(1-e^{-s'_j}(1+s'_j))] \tag{5.53}$$

where implies that $0 < z < \lambda + \mu$. Then from Lemma 5.4, we have

$$\frac{1}{L-1}\sum_{j=1}^{L-1}\frac{1}{p_j} \approx z' \tag{5.54}$$

where $z' = \frac{z}{\lambda P_{av}+\mu Q_{av}}$ and $0 < z' < \frac{\lambda+\mu}{\lambda P_{av}+\mu Q_{av}}$. Applying (5.52) into (5.54) gives,

$$s'_1 \approx \frac{2(z'-\lambda)}{\mu L} = \frac{d}{L} \tag{5.55}$$

where $d = \frac{2(z'-\lambda)}{\mu}$. Let $a = c\mu d = 2(z'-\lambda)c$, then $s_1' \approx \frac{a}{c\mu L}$. Due to $0 < z' < \frac{\lambda+\mu}{\lambda P_{av}+\mu Q_{av}}$, we have

$$\lim_{L\to\infty} \frac{a}{L} = 0. \tag{5.56}$$

From (5.53), we have

$$\begin{aligned} z &= (\lambda+\mu)e^{-v_1} - \sum_{j=1}^{L-1}(e^{-v_j} - e^{-v_{j+1}})[(\lambda+\mu)e^{-s_j'} + \mu e^{-s_j'}s_j'] \\ &\approx e^{-c\lambda}[(\lambda+\mu)e^{-\frac{a}{L}} - (1-e^{-\frac{a}{L}})(\lambda+\mu)\sum_{j=1}^{L-1} e^{-j(\frac{a}{L}+s_1')} - (1-e^{-\frac{a}{L}})\mu s_1' \sum_{j=1}^{L-1} je^{-j(\frac{a}{L}+s_1')}] \\ &\approx e^{-c\lambda}[(\lambda+\mu)e^{-\frac{a}{L}} - (1-e^{-\frac{a}{L}})(\lambda+\mu)\sum_{j=1}^{L-1} e^{-j\frac{b}{L}} - (1-e^{-\frac{a}{L}})\frac{a}{cL}\sum_{j=1}^{L-1} je^{-j\frac{b}{L}}] \end{aligned} \tag{5.57}$$

where $b = a + Ls_1' = a(1+\frac{1}{c\mu})$ and we also have $\lim_{L\to\infty}\frac{b}{L} = 0$. Since,

$$\begin{aligned} \sum_{j=1}^{L-1} e^{-j\frac{b}{L}} &= \frac{1-e^{-b}}{1-e^{-\frac{b}{L}}} - 1, \\ \sum_{j=1}^{L-1} je^{-j\frac{b}{L}} &= -\frac{e^{(-\frac{b}{L}-b)}(Le^{\frac{b}{L}} - e^b - L + 1)}{(1-e^{-\frac{b}{L}})^2}, \end{aligned} \tag{5.58}$$

(5.57) becomes

$$z \approx e^{-c\lambda}[(\lambda+\mu)(1-(1-e^{-\frac{a}{L}})\frac{1-e^{-b}}{1-e^{-\frac{b}{L}}}) - (1-e^{-\frac{a}{L}})\frac{a}{cL}\frac{e^{-\frac{b}{L}}(1-e^{-b}) - Le^{-b}(1-e^{-\frac{b}{L}})}{(1-e^{-\frac{b}{L}})^2}] \tag{5.59}$$

Since $\lim_{L\to\infty}\frac{a}{L} = 0$ and $\lim_{L\to\infty}\frac{b}{L} = 0$, we have

$$\begin{aligned} 1-e^{-\frac{a}{L}} &\approx \frac{a}{L} \\ 1-e^{-\frac{b}{L}} &\approx \frac{b}{L} \end{aligned} \tag{5.60}$$

And when $L \to \infty$, we have

$$\begin{aligned} \lambda &\approx \lambda^f \\ \mu &\approx \mu^f \end{aligned} \tag{5.61}$$

Applying (5.60), (5.61) into (5.59) gives

$$\begin{aligned} z &\approx e^{-c\lambda_f}[(\lambda_f+\mu_f)(1-\frac{a}{b}(1-e^{-b}))-\frac{a^2}{cb^2}((1-\frac{b}{L})(1-e^{-b})-be^{-b})] \\ &\approx e^{-c\lambda_f}[(\lambda_f+\mu_f)(1-\frac{a}{b}(1-e^{-b}))-\frac{a^2}{cb^2}(1-e^{-b}(1+b))] \end{aligned} \tag{5.62}$$

Since

$$\begin{aligned} z &= (\lambda P_{av}+\mu Q_{av})z' \\ &= (\lambda P_{av}+\mu Q_{av})(\lambda+\frac{a}{2c}) \\ &\approx (\lambda_f P_{av}+\mu_f Q_{av})(\lambda_f+\frac{a}{2c}) \end{aligned} \tag{5.63}$$

we can obtain a by solving following equation,

$$\begin{aligned} &(\lambda_f P_{av}+\mu_f Q_{av})(\lambda_f+\frac{a}{2c})e^{c\lambda_f} \\ &\approx [(\lambda_f+\mu_f)(1-\frac{c\mu_f}{1+c\mu_f}(1-e^{-a(1+\frac{1}{c\mu_f})}))-\frac{c\mu_f^2}{(1+c\mu_f)^2}(1-e^{-a(1+\frac{1}{c\mu_f})}(1+a(1+\frac{1}{c\mu_f})))] \end{aligned} \tag{5.64}$$

From (5.64), with given P_{av} and Q_{av}, a is a constant. Then when L is large,

$$\begin{aligned} P_{out}^L &\approx 1-e^{-v_1}+\sum_{j=1}^{L-1}(e^{-v_j}-e^{-v_{j+1}})e^{-s_j'} \\ &\approx 1-e^{-c\lambda}[e^{-\frac{a}{L}}-(1-e^{-\frac{a}{L}})\sum_{j=1}^{L-1}e^{-j\frac{b}{L}}] \\ &= 1-e^{-c\lambda}[1-(1-e^{-\frac{a}{L}})\frac{1-e^{-b}}{1-e^{-\frac{b}{L}}}] \end{aligned}$$

$$\approx 1 - e^{-c\lambda_f}[1 - (1 - e^{-\frac{a}{L}})\frac{1 - e^{-a(1+\frac{1}{c\mu_f})}}{1 - e^{-\frac{a(1+\frac{1}{c\mu_f})}{L}}}] \tag{5.65}$$

and

$$\lim_{L\to\infty} P_{out}^{L} = 1 - e^{-c\lambda_f}[1 - \frac{1 - e^{-a(1+\frac{1}{c\mu_f})}}{1 + \frac{1}{c\mu_f}}] \tag{5.66}$$

2) when $\mu = 0$

Let $y = \frac{v_1}{v_0} = \frac{v_1}{c\lambda} > 1$, then from the (5.23) of Lemma 5.3, we can get, $j = 1, \ldots, L-1$,

$$v_j \approx c\lambda y^j \tag{5.67}$$

Applying (5.67) into the (5.25) of Lemma 5.4, we have,

$$e^{-c\lambda y} \approx \frac{\lambda P_{av}}{L-1} \sum_{j=1}^{L-1} y^j = \frac{\lambda P_{av}}{L-1} \frac{y^L - y}{y-1} \tag{5.68}$$

Let $x = y - 1$. (5.68) becomes,

$$e^{-c\lambda(1+x)} \approx \lambda P_{av}(1+x)\frac{(1+x)^{L-1} - 1}{x(L-1)} \tag{5.69}$$

Now, suppose $\lim_{L\to\infty} xL = \infty$. Since

$$(1+x)^{L-1} > 1 + (L-1)x + \frac{1}{2}(L-2)(L-1)x^2, \tag{5.70}$$

we have

$$\lim_{L\to\infty} \frac{(1+x)^{L-1} - 1}{(L-1)x} > \lim_{L\to\infty} 1 + \frac{1}{2}(L-2)x = \infty. \tag{5.71}$$

Then taking the limit as $L \to \infty$ on the both sides of the equation (5.69), gives

$$\lim_{L\to\infty} e^{-c\lambda(1+x)} = \infty \tag{5.72}$$

which contradicts with $\lim_{L\to\infty} e^{-c\lambda(1+x)} < 1$, thus we must have $\lim_{L\to\infty} xL = \beta < \infty$ (where constant $\beta \geq 0$), implying

$$\text{as} \quad L \to \infty, \qquad x \to \frac{\beta}{L}. \tag{5.73}$$

Applying (5.73), (5.69) becomes,

$$e^{-c\lambda(1+\frac{\beta}{L})} \approx \lambda P_{av}(1+\frac{\beta}{L})\frac{(1+\frac{\beta}{L})^{L-1}-1}{\frac{\beta}{L}(L-1)} \tag{5.74}$$

and then taking the limit as $L \to \infty$ on the both sides of above equation, we have

$$e^{-c\lambda_f} \approx \lambda_f P_{av}\frac{e^{\beta}-1}{\beta} \tag{5.75}$$

Note that $\lim_{L\to\infty}(1+\frac{\beta}{L})^{L-1} = e^{\beta}$ and when L is large, $\lambda \approx \lambda_f$. Thus, we can obtain constant β through solving (5.75). Therefore, when L is large,

$$\begin{aligned} P_{out}^{L} &= 1 - e^{-v_1} \\ &= 1 - e^{-c\lambda(1+x)} \\ &\approx 1 - e^{-c\lambda_f(1+\frac{\beta}{L})} \end{aligned} \tag{5.76}$$

and

$$\lim_{L\to\infty} P_{out}^{L} = 1 - e^{-c\lambda_f} \tag{5.77}$$

Here completes the proof for Theorem 5.1.

Chapter 6
Conclusion

The thesis has designed various optimal resource allocation algorithms and provided corresponding analytial justifications for wireless communication networks with limited feedback to largely improve their system performance, as opposed to the prevalent assumption of full CSI in most existing work. Below we will summarise our work, and present some possible ideas for the future research related to the topics in this thesis.

6.1 Summary of Contributions

In chapter 2, we have studied the outage probability minimization problem with quantized CSI for an M-parallel Nakagami block-fading channels under a long term average power constraint. We formulated the outage problem with limited feedback and provide a numerical iterative algorithm to find the optimal power codebook, followed by the modified explicitly problem formulation using the power ordering and linearized approximation. Two low-complexity suboptimal algorithms were also presented for high average power regime. The diversity order for the outage probability was derived for the Nakagami fading case using our power allocation algorithm based on the power ordering and linearized approximation. For large number of parallel channels system, a valid Gaussian approximation based sub-optimal algorithm was also provided.

In chapter 3, quantized power allocation algorithms for a wideband spectrum sharing system were investigated. To maximize the SU ergodic capacity under an average sum transmit power constraint and individual average interference constraints at the PU

receivers, a Modified Generalized Lloyd-type algorithms (GLA) have been derived and various properties of the quantized power allocation laws have been presented, along with a rigorous convergence and consistency proof of the modified GLA based algorithm. For large number bits of feedback, we have also derived an approximate quantized power allocation algorithms that perform very close to the modified GLA based algorithms but with much lower complexity and significantly faster. Finally, we have extended the modified GLA based quantized power allocation algorithm to the case of noisy limited feedback.

Chapter 4 considered the problem of throughput maximization for a narrowband spectrum sharing cognitive radio network where a secondary user sharing the same frequency band with a number of primary users, subject to a long term ATP constaint at SU-TX and individual PIP constaints at each primary receiver. Three dissimilar quantized power codebooks were derived along with their associated theoretical properties for the throughput maximization problem associated with three different forms of obtaining the partial channel informantion of g_1 and g_0 at SU-TX, i.e, perfect g_1 and quantized g_0, estimated g_1 and quantized g_0, quantized g_1 and quantized g_0.

In Chapter 5, we considered the optimal transmit power control design with quantized CSI information for a narrowband spectrum sharing cognitive radio framework to minimize the outage probability performance and meet the ATP constraint at SU-TX and the AIP constraint at PU-RX. A complex general numerical algorithm for finding the optimal power codebook with SPSA and another more efficient low-complexity power codebook design approach were provided. With various useful properties, we developed a suitable explicit expression for asymptotic behavior of the SU outage probability as number of feedback bits increases.

6.2 Future Research

For the quantized power allocation problem for parallel channels studied in Chapter 2, possible future work will include extension of these results to correlated fading channels, different fading environment such as rician fading, consideration of noisy or erroneous

feedback as investigated in [92][20] and quantized CSIT based power allocation to more general optimization problems such as the service-outage based power and rate allocation in [53].

For the work of quantized power control in cognitive radio networks, deriving expressions for asymptotic (as the number of feedback bits goes to infinity) capacity loss with quantized power allocation in Chapter 3, extending the results of Chapter 4 and Chapter 5 to more complex wideband spectrum sharing scenario can be done. Possible future work also include consideration of primary interference at the secondary receiver and quantized power allocation with other types of interference constraints at the primary receiver, such as PU's capacity loss and PU's outage probability [91]. It also can be done the extension of these results to other fading environment such as Nakagami fading. And It would be interesting to consider the asymmetric fading channels scenario. Consideration of multiple secondery users and multiple primary users in quantized power allocation design can also be investigated.

Random vector quantization (RVQ) is a simple approach to a beamforming codebook design for multiple-antenna systems that generates the beamforming vectors independently from a uniform distribution on the complex unit sphere. It is possible to employ RVQ to design the power codebooks in this thesis. However, RVQ is generally suboptimal (compared to the generalized Lloyd algorithm developed in this thesis) for a finite-size codebook and asymptotically optimal when the codebook size goes to infinity. Hence it is more suitable for an asymptotic performance analysis. On the other hand, the distribution of the optimal transmission power allocation policies as a function of full channel information, as derived in the thesis are complex and do not have closed-form expressions. Therefore the process of generating a codebook using RVQ from this distribution is difficult and is possible only via numerical simulation. This defeats the purpose of using RVQ, which is generally used to obtain an asymptotic analytical performance of resource allocation based on quantized systems. However, we agree that as asymptotic analysis of our quantized power allocation scheme for spectrum sharing cognitive radio networks is necessary and although beyond the scope of the current thesis, will be investigated in future work.

Bibliography

[1] M. Peacock, I. B. Collings and M. L. Honig, "Analysis of multiuser peer-to-peer mc-cdma with limited feedback," in *Proc. IEEE ICC '04*, vol. 2, Paris, France, Jun. 2004, pp. 968–972.

[2] A. D. Dabbagh and D. J. Love, "Feedback rate-capacity loss tradeoff for limited feedback MIMO systems," *IEEE Trans. Inform. Theory*, vol. 52, no. 5, pp. 2190–2202, May 2006.

[3] A. E. Ekpenyong and Y. Huang, "Feedback-detection strategies for adaptive modulation systems," *IEEE Trans. Commun.*, vol. 54, no. 10, pp. 1735–1740, Oct. 2006.

[4] A. G. Marques, G. B. Giannakis, F. F. Digham and F. J. Ramos, "Power-efficient wireless OFDMA using limited-rate feedback," *IEEE Trans. Wireless Commun.*, vol. 7, no. 2, pp. 685–696, Feb. 2008.

[5] A. G. Marques, X. Wang and G. B. Giannakis, "Optimizing energy efficiency of tdma with finite rate feedback," in *Proc. IEEE ICASSP 2007*, vol. 3, Honolulu, Hawai'i, USA, April 2007, pp. III–117 – III–120.

[6] A. Gersho and R. Gray, *Vector quantization and signal compression*. Kluwer Academic Publishers, 1992.

[7] A. Ghasemi and E. S. Sousa, "Fundamental limits of spectrum-sharing in fading environments," *IEEE Trans. Wireless Commun.*, vol. 6, no. 2, pp. 649–658, Feb. 2007.

[8] ——, "Fundamental limits of spectrum-sharing in fading environments," *IEEE Trans. Wireless Commun.*, vol. 6, no. 2, pp. 649–658, Feb. 2007.

[9] A. Goldsmith, S.A. Jafar, I. Maric and S. Srinivasa, "Breaking spectrum gridlock with cognitive radios: an information theoretic perspective," *Proceedings of the IEEE*, vol. 97, no. 5, pp. 894–914, May 2009.

[10] A. J. Goldsmith and P. Varaiya, "Capacity of fading channels with channel side information," *IEEE Trans. Information Theory*, vol. 43, no. 6, pp. 1986–1992, Nov. 1997.

[11] A. K. Karmokar and V. K. Bhargava, "Coding rate adaptation for hybrid arq systems over time varying fading channels with partially observable state," in *Proc. IEEE ICC '05*, vol. 4, Seoul, Korea, May 2005, pp. 2797–2801.

[12] A. Khoshnevis and A. Sabharwal, "Performance of quantized power control in multiple antenna systems," in *Proc. IEEE ICC'04*, Paris, France, Jun. 2004, pp. 803–807.

[13] ——, "Performance of quantized power control in multiple antenna systems," in *Proc. IEEE International Conference on Commun. (ICC' 04)*, Paris, France, Jun. 2004, pp. 803–807.

[14] ——, "On the asymptotic performance of multiple antenna channels with quantized feedback," *IEEE Trans. Wireless Commun.*, vol. 7, no. 10, pp. 3869–3877, Oct. 2008.

[15] A. Narula, M. J. Lopez, M. D. Trott and G. W. Wornell, "Efficient use of side information in mulitiple-antenna data transmission over fading channels," *IEEE J. Select. Areas Commun.*, vol. 16, no. 8, pp. 1423–1436, Oct. 1998.

[16] A. Omar and A. R. Ali, "Adaptive channel characterization for wireless communication," in *Proc. IEEE Radio and Wireless Symposium*, Orlando, FL , USA, Jan. 2008, pp. 543–546.

[17] A.G. Marques, X. Wang and G.B. Giannakis, "Dynamic resource management for cognitive radios using limited-rate feedback," *IEEE Trans. on Signal Processing*, vol. 57, no. 9, pp. 3651–3666, Sept. 2009.

[18] B. Khoshnevis and W. Yu, "Joint power control and beamforming codebook design for miso channels with limited feedback," in *Proc. IEEE Global Telecommunications Conference (GLOBECOM 2009)*, Honolulu, HI, USA, Dec. 2009, pp. 1–6.

[19] B. Kim and S. Oh , "Optimal rate and power allocation in uplink packet cdma transmission," in *Proc. IEEE WCNC'09*, Budapest, Hungary, Apr. 2009, pp. 1–5.

[20] B. Makki and T. Eriksson, "Data transmission in the presence of noisy channel state feedback and outage probability constraint," in *Proc. IEEE ISITA 2010*, Taichung, Taiwan, Oct. 2010, pp. 458 – 463.

[21] D. P. Bertsekas, *Nonlinear Programming*. Belmont, Massachusetts: Athena Scientific, 1999.

[22] B.L. Ng, J.S. Evans, S. Hanly and D. Aktas, "Distributed downlink beamforming with cooperative base stations," *IEEE Trans. on Information Theory*, vol. 54, no. 12, pp. 5491–5499, Dec. 2008.

[23] R. S. Blum, "MIMO with limited feedback of channel state information," in *Proc. IEEE Int. Conf. Acoust., Speech and Sig. Proc.*, vol. 4, Bethlehem, PA, USA, April 2003, pp. 89–92.

[24] ——, "MIMO with limited feedback of channel state information," in *Proc. IEEE ICASSP'03*, vol. 4, Hong Kong, China, Apr. 2003, pp. IV 89–92.

[25] B.M. Hochwald, T.L. Marzetta and V. Tarokh, "Multiple-antenna channel hardening and its implications for rate feedback and scheduling," *IEEE Trans. Information Theory*, vol. 50, no. 9, pp. 1893–1909, Sep. 2004.

[26] C. A. Jotten, P. W. Baier, M. Meurer, T. Weber and M. Haardt, "Efficient representation and feedback signaling of channel state information in frequency division duplexing MIMO systems," in *Proc. IEEE WPMC '02*, vol. 2, Honolulu, Hawaii, USA, Oct. 2002, pp. 444–448.

[27] C. B. Chae, D. Mazzarese, N. Jindal and R. W. Heath, Jr., "Coordinated beamforming with limited feedback in the MIMO broadcast channel," *IEEE J. Select. Areas Commun.*, vol. 26, no. 8, pp. 4712–4724, Oct. 2008.

[28] C. H. Chen and C. L. Wang, "Joint subcarrier and power allocation in multiuser OFDM-based cognitive radio systems," in *Proc. IEEE ICC 2010*, Cape Town, South Africa, May 2010, pp. 1–5.

[29] C. K. Au-Yeung and D. J. Love , "On the performance of random vector quantization limited feedback beamforming in a miso system," *IEEE Trans. Wireless Commun.*, vol. 6, no. 2, pp. 458 – 462, Feb. 2007.

[30] F. C. Commission, "Spectrum policy task force report, (et docket no. 02-135)," *[Online]. Available: http://transition.fcc.gov/sptf/files/E&UWGFinalReport.pdf*, Nov. 2002.

[31] D. J. Love and R. W. Heath, "Grassmanian beamforming for multiple-input multiple-output wireless systems," *IEEE Trans. Information Theory*, vol. 49, no. 10, pp. 2735–2747, Oct. 2003.

[32] D. J. Love and R. W. Heath, Jr., "OFDM power loading using limited feedback," *IEEE Trans. on Veh. Technol.*, vol. 54, no. 5, pp. 1773–1780, Sept. 2005.

[33] D. J. Love, R. W. Heath Jr. and T. Strohmer, "Grassmannian beamforming for multiple-input multiple-output wireless systems," *IEEE Trans. Inform. Theory*, vol. 49, no. 10, pp. 2735–2747, Oct. 2003.

[34] D. J. Love, R. W. Heath, V. K. N. Lau, D. Gesbert, B. D. Rao and M. Andrews, "An overview of limited feedback in wireless communication systems," *IEEE Journal on Selected Areas in Communications*, vol. 26, no. 8, pp. 1341–1365, Oct. 2008.

[35] D. Tse and P. Viswanath, *Fundamentals of Wireless Communication*. Cambridge, UK ; New York : Cambridge University Press, 2005.

[36] E. Biglieri, J. Proakis and S. Shamai, "Fading channels: Information-theoretic and communications aspects," *IEEE Trans. Information Theory*, vol. 44, no. 6, p. 2619C2692, Oct. 1998.

[37] E. Cianca, A. D. Luise, M. Ruggieri, and R. Prasad, "Channel-adaptive techniques in wireless communications: an overview," *Wireless Communications and Mobile Computing*, vol. 2, no. 8, pp. 799–813, Dec. 2002.

[38] H. Exton, *Multiple Hypergeometric Functions and Applications*. New York: Wiley, 1976.

[39] W. Feller, *An Introduction to Probability Theory and Its Applications*, 3rd ed. New York: Wiley, 1971, vol. 2.

[40] G. Caire, G. Taricco and E. Biglieri, "Optimum power control over fading channels," *IEEE Trans. Information Theory*, vol. 45, no. 5, pp. 1468–1489, Jul. 1999.

[41] G. Dietl and G. Bauch, "Linear precoding in the downlink of limited feedback multiuser MIMO systems," in *Proc. IEEE GLOBECOM '07*, Washington, DC, USA, Nov. 2007, pp. 4359–4364.

[42] G. Wunder and T. Michel, "Optimal resource allocation for parallel gaussian broadcast channels: Minimum rate constraints and sum power minimization," *IEEE Trans. Information Theory*, vol. 53, no. 12, pp. 4817 – 4822, Dec. 2007.

[43] M. Gastpar, "On capacity under received-signal constraints," in *Proc. 42nd Annual Allerton Conf. on Commun., Control and Comp.*, Monticello, IL, USA, Sept. 2004.

[44] H. A. David and H. N. Nagaraja, *Order statistics (third edition)*. Wiley Interscience, 2003.

[45] H. A. Suraweera, J. Gao, P. J. Smith, M. Shafi and M. Faulker, "Channel capacity limits of cognitive radio in asymmetric fading environments," in *Proc. IEEE International Conference on Commun. (ICC 2008)*, Beijing, China, May 2008, pp. 4048–4053.

[46] H. A. Suraweera, P. J. Smith and M. Shafi, "Capacity limits and performance analysis of cognitive radio with imperfect channel knowledge," *IEEE Trans. on Vehicular Technology*, vol. 59, no. 4, pp. 1811–1822, May 2010.

[47] H. Jeffreys and B. S. Jeffreys, *The Digamma $\mathcal{F}$ and Trigamma $\mathcal{F}'$ Functions*, 3rd ed. Cambridge, England: Methods of Mathematical Physics, Cambridge University Press, 1988.

[48] I. H. Kim and D. J. Love, "On the capacity and design of limited feedback multiuser MIMO uplinks," *IEEE Trans. Information Theory*, vol. 54, no. 10, pp. 4712–4724, Oct. 2008.

[49] J. M. III, "Cognitive radio for flexible mobile multimedia communications," in *IEEE Int. Workshop on Mobile Multimedia Commun. (MoMuC)*, San Diego, CA, USA, Nov. 1999, pp. 3–10.

[50] J. C. Roh and B. D. Rao, "Transmit beamforming in multiple-antenna systems with finite rate feedback: A vq-based approach," *IEEE Trans.Inform. Theory*, vol. 52, no. 3, pp. 1101–1112, Mar. 2006.

[51] J. Chen, R. A. Berry and M. L. Honig, "Large system performance of downlink OFDMA with limited feedback," in *Proc. IEEE ISIT 2006*, Seattle, Washington, USA, Jul. 2006, pp. 1399–1403.

[52] J. Choi and R. W. Heath, Jr., "Interpolation based transmit beamforming for MIMO-OFDM with limited feedback," *IEEE Trans. Signal Processing*, vol. 53, no. 11, pp. 4125–4135, Nov. 2005.

[53] J. H. Luo, R. Yates and P. Spasojević, "Service outage based power and rate allocation for parallel fading channels," *IEEE Trans. Information Theory*, vol. 51, no. 7, pp. 2594–2611, Jul. 2005.

[54] J. Leinonen, J. Hamalainen and M. Juntti, "Performance analysis of downlink OFDMA frequency scheduling with limited feedback," in *Proc. IEEE ICC '08*, Beijing, China, May 2008, pp. 3318–3322.

[55] ——, "Performance analysis of downlink OFDMA resource allocation with limited feedback," *IEEE Trans. on Wireless Commun.*, vol. 8, no. 6, pp. 2927–2937, Jun. 2009.

[56] J. Lopez Vicario, R. Bosisio, U. Spagnolini and C. Anton-Haro, "A throughput analysis for opportunistic beamforming with quantized feedback," in *Proc. IEEE PIMRC '06*, Helsinki, Finland, Sept. 2006, pp. 1–5.

[57] J. Zhang, Z. Fang and B. Bensaou, "Adaptive power control for single channel ad hoc networks," in *Proc. IEEE ICC '05*, vol. 5, Seoul, Korea, May 2005, pp. 3156–3160.

[58] N. Jindal, "MIMO broadcast channels with finite-rate feedback," *IEEE Trans. Inform. Theory*, vol. 52, no. 11, pp. 5045–5060, Nov. 2006.

[59] J.M. Peha, "Sharing spectrum through spectrum policy reform and cognitive radio," *Proc. of the IEEE*, vol. 97, no. 4, pp. 708–719, Apr. 2009.

[60] K. Huang and R. Zhang, "Cooperative feedback in multi-antenna cognitive radio networks," in *Proc. VTC'2010-Spring*, Taipei, Taiwan, May 2010, pp. 1–5.

[61] K. K. Mukkavilli, A. Sabharwal, E. Erkip and B. Aazhang, "On beamforming with finite rate feedback in multiple-antenna systems," *IEEE Trans. Information Theory*, vol. 49, no. 10, pp. 2563–2579, Oct. 2003.

[62] K. S. Ahn and R. W. Heath Jr., "Performance analysis of maximum ratio combining with imperfect channel estimation in the presence of cochannel interferences," *IEEE Trans. Wireless Commun.*, vol. 8, no. 3, pp. 1080–1085, Mar. 2009.

[63] K. S. Lee, B.-H. Ryu, and C.-H. Lee, "Power efficient frequency domain packet scheduling for OFDMA systems," in *Proc. ICCIT 2007*, Gyeongju, Korea, Nov. 2007, pp. 1906–1911.

[64] L. A. Imhof and R. Mathar, "Capacity regions and optimal power allocation for cdma cellular radio," *IEEE Trans. Information Theory*, vol. 51, no. 6, pp. 2011 – 2019, Jun. 2005.

[65] L. Lin, R. D. Yates and P. Spasojevic, "Adaptive transmission with discrete code rates and power levels," *IEEE Trans. Commun.*, vol. 51, no. 12, pp. 2115–2125, Dec. 2003.

[66] L. Musavian and S. Aissa, "Capacity and power allocation for spectrum-sharing communications in fading channels," *IEEE Trans. Wireless Commun.*, vol. 8, no. 1, pp. 148–156, Jan. 2009.

[67] ——, "Fundamental capacity limits of cognitive radio in fading environments with imperfect channel information," *IEEE Trans. Commun.*, vol. 57, no. 11, pp. 3472–3480, Nov. 2009.

[68] L. Ozarow, S. Shamai and A. D. Wyner, "Information theoretic considerations for cellular mobile radio," *IEEE Trans. Veh. Technol.*, vol. 43, pp. 359–378, May 1994.

[69] L. Ruan and V. K.N. Lau , "Power control and performance analysis of cognitive radio systems under dynamic spectrum activity and imperfect knowledge of system state," *IEEE Trans. on Wireless Commun.*, vol. 8, no. 9, pp. 4616 – 4623, Sep. 2009.

[70] L. Zhang, Y. Xin and Y. Liang, "Optimal power allocation for multiple access channels in cognitive radio networks," in *Proc. VTC'2008-Spring*, Singapore, May 2008, pp. 1550–2252.

[71] M. A. Khojastepour, G. Yue, X. Wang and M. Madihian, "Optimal power control in MIMO systems with quantized feedback," *Trans. Wireless Commun.*, vol. 7, no. 12, pp. 4859–4866, Dec. 2008.

[72] M. A. Khojastepour, X. Wang and M. Madihian, "MIMO throughput optimisation via quantised rate control," *IET Communications*, vol. 1, no. 3, pp. 333–340, Jun. 2007.

[73] M. A. Sadrabadi, M. A. Maddah-Ali and A. K. Khandani, "On the capacity of time-varying channels with periodic feedback," *IEEE Trans.Inform. Theory*, vol. 53, no. 8, pp. 2910–2915, Aug. 2007.

[74] M. Agarwal, D. Guo and M.L. Honig, "Multi-carrier transmission with limited feedback: power loading over sub-channel groups," in *Proc. IEEE ICC '08*, Beijing, China, May 2008, pp. 981 – 985.

[75] M. Pausini and G. J. M. Janssen, "Performance analysis of uwb autocorrelation receivers over nakagami-fading channels," *IEEE Journal of Selected Topics in Signal Processing*, vol. 1, no. 3, pp. 443–455, Oct. 2007.

[76] M. Sabin and R. Gray, "Global convergence and empirical consistency of the generalized lloyd algorithm," *IEEE Trans. Information Theory*, vol. 32, no. 2, pp. 148–155, Mar. 1986.

[77] P. G. Moschopoulos, "The distribution of the sum of independent gamma random variables," *Annals of the Institute of Statistical Mathematics*, vol. 37, no. 1, pp. 541–544, Dec. 1985.

[78] N. Ahmed, M. A. Khojastepour, A. Sabharwal and B. Aazhang, "Outage minimization with limited feedback for the fading relay channel," *IEEE Trans. Commun.*, vol. 54, no. 4, pp. 659–669, Apri. 2006.

[79] N. Jindal and A. Goldsmith, "Capacity and optimal power allocation for fading broadcast channels with minimum rates," *IEEE Trans. Information Theory*, vol. 49, no. 11, pp. 2895 – 2909, Nov. 2003.

[80] N. Ravindran and N. Jindal, "Limited feedback-based block diagonalization for the MIMO broadcast channel," *IEEE J. Select. Areas Commun.*, vol. 26, no. 8, pp. 1423–1436, Oct. 2008.

[81] S. Nadarajah, "Simplified expressions for the outage and error rate performance of ds-cdma with mrc in nakagami-m fading," *International Journal of Electronics*, vol. 96, no. 4, pp. 365–369, Apri. 2009.

[82] A. H. Nuttall, "Some integrals involving the q_m function (corresp.)," *IEEE Trans. Information Theory*, vol. 21, no. 1, pp. 95–96, Apri. 1975.

[83] P. A. Chou, T. Lookabaugh and R. M. Gray, "Entropy-constrained vector quantization," *IEEE Trans. Acoustics, Speech and Signal Processing*, vol. 31, no. 1, pp. 31–42, Jan. 1989.

[84] P. H. Lin, S. C. Lin, C. P. Lee and H. J. Su, "Cognitive radio with partial channel state information at the transmitter," *IEEE Trans. Wireless Commun.*, vol. 9, no. 11, pp. 3402–3413, Nov. 2010.

[85] R. Agarwal and J. Cioffi, "Capacity of fading broadcast channels with limited rate feedback," in *Proc. of Forty-Fourth Annual Allerton Conf. on Comm. Cont. and Comp.*, UIUC, Illinois, USA, Sept.-Oct. 2006, pp. 336–343.

[86] R. Agarwal, R. Vannithamby and J. Cioffi, "Optimal allocation of feedback bits for downlink OFDMA systems," in *Proc. IEEE ISIT 2008*, Toronto, ON, Canada, Jul. 2008, pp. 1686–1690.

[87] R. Agarwal, V. Abhishek, R. Vannithamby and J. Cioffi, "Opportunistic feedback protocol for minimizing power in uplink with heterogeneous traffic," in *Proc. IEEE VTC-2007 Fall*, Baltimore, MD, USA, Sept.-Oct. 2007, pp. 1882–1886.

[88] R. Chen, J.G. Andrews, R.W. Heath and A. Ghosh, "Uplink power control in multi-cell spatial multiplexing wireless systems," *IEEE Trans. on Wireless Commun.*, vol. 6, no. 7, pp. 2700–2711, Jul. 2007.

[89] R. McEliece and W. Stark, "Channels with block interference," *IEEE Trans. Information Theory*, vol. IT-30, pp. 44–53, Jan. 1984.

[90] R. Zhang, S. Cui and Y. Liang, "On ergodic sum capacity of fading cognitive multiple-access and broadcast channels," *IEEE Trans. Information Theory*, vol. 55, no. 11, pp. 5161 – 5178, Nov. 2009.

[91] R. Zhang, Y-C. Liang and S. Cui, "Dynamic resource allocation in cognitive radio networks," *IEEE Signal Processing Magazine*, vol. 27, no. 3, pp. 102–114, Mar. 2010.

[92] S. Ekbatani, F. Etemadi and H. Jafarkhani, "Outage behaviour of quasi-static fading channels with partial power control and noisy feedback," in *Proc. IEEE GLOBECOM'07*, Washington DC, USA, Nov. 2007, pp. 1556–1560.

[93] ——, "Throughput maximization over slowly fading channels using quantized and erroneous feedback," *IEEE Trans. Commun.*, vol. 57, no. 9, pp. 2528–2533, Sep. 2009.

[94] S. Hwang, B. H. Kim and Y. Kim, "A hybrid arq scheme with power ramping," in *Proc. IEEE VTC-2001 Fall*, vol. 3, San Francisco, CA, USA, Oct. 2001, pp. 1579–1538.

[95] S. Kotz, N. Balakrishnan and N. L. Johnson, *Continuous multivariate distributions, volume 1: models and applications (second edition)*. New York : Wiley, 2000.

[96] S. Ren, K.B. Letaief and J.R.B. de Marca, "Outage reduction in cooperative networks with limited feedback," *IEEE Trans. on Commun.*, vol. 58, no. 3, pp. 748 – 752, Mar. 2010.

[97] S. Sanayei and A. Nosratinia, "Opportunistic beamforming with limited feedback," *IEEE Trans. Wireless Commun.*, vol. 6, no. 8, pp. 2765–2771, Aug. 2007.

[98] ——, "Opportunistic downlink transmission with limited feedback," *IEEE Trans. Inform. Theory*, vol. 53, no. 11, pp. 4363–4372, Nov. 2007.

[99] S. V. Hanly and D. N. C. Tse, "Multi-access fading channels - part II: Delay-limited capacities," *IEEE Trans. Information Theory*, vol. 44, no. 7, pp. 2816–2831, Nov. 1998.

[100] J. C. Spall, "Implementation of the simultaneous perturbation algorithm for stochastic optimization," *IEEE Trans. on Aerospace and Electronic Systems*, vol. 34, no. 3, pp. 817–823, Jul. 1998.

[101] T. Linder and R. Zamir, "High-resolution source coding for non-difference distortion measures: the rate-distortion function," *IEEE Trans. Information Theory*, vol. 45, no. 2, pp. 533–547, Mar. 1999.

[102] T. linder, G. Lugosi and K. Zeger, "Empirical quantizer design in the presence of source noise or channel noise," *IEEE Trans. Information Theory*, vol. 43, no. 2, pp. 612–623, Mar. 1997.

[103] T. Pande, D. J. Love and J. V. Krogmeier, "Reduced feedback MIMO-OFDM precoding and antenna selection," *IEEE Trans. Signal Processing*, vol. 55, no. 5, pp. 2284–2293, May 2007.

[104] T. Renk, H. Jaekel and F. K. Jondral , "Outage regions and optimal power allocation for wireless relay networks," in *Proc. Information Theory Workshop (ITW'09)*, Taormina, Oct. 2009, pp. 168 – 172.

[105] T. T. Kim and M. Skoglund, "Partial power control for slowly fading MIMO channels," in *Proc. IEEE ICC'06*, Istanbul, Turkey, Jun. 2006, pp. 1362–1367.

[106] ——, "Diversity-multiplexing tradeoff in MIMO channels with partial csit," *IEEE Trans. Information Theory*, vol. 53, no. 8, pp. 2743–2759, Aug. 2007.

[107] ——, "On the expected rate of slowly fading channels with quantized side information," *IEEE Trans. Commun.*, vol. 55, no. 4, pp. 820–829, Apri. 2007.

[108] T. Wu and V. K. N. Lau, "Robust precoder adaptation for MIMO links with noisy limited feedback," *IEEE Trans. Information Theory*, vol. 55, no. 4, pp. 1640–1649, Apri. 2009.

[109] V. A. Aalo, T. Piboongungon and G. P. Efthymoglou, "Another look at the performance of mrc schemes in nakagami-m fading channels with arbitrary parameters," *IEEE Trans. Commun.*, vol. 53, no. 12, pp. 2002–2005, Dec. 2005.

[110] V. Lau, Y. Liu and T-A. Chen, "On the design of MIMO block-fading channels with feedback-link capacity constraint," *IEEE Trans. Commun.*, vol. 52, no. 1, pp. 62–70, Jan. 2004.

[111] V. Nagarajan, Y. Liu and J. Hou, "The effect of channel side information at transmitter on coding complexity," in *Proc. IEEE ISIT 2004*, Chicago, Illinois, USA, Jun. 2004, p. 148.

[112] V.K.N. Lau and T. Wu, "Optimal transmission and limited feedback design for OFDM/MIMO systems in frequency selective block fading channels," *IEEE Trans. Wireless Commun.*, vol. 6, no. 5, pp. 1569 – 1573, May 2007.

[113] W. Dai, Y. Liu and B. Rider, "Quantization bounds on grassmann manifolds and applications to MIMO communications," *IEEE Trans. Inform. Theory*, vol. 54, no. 3, pp. 1108–1123, Mar. 2008.

[114] W. Santipach and M. L. Honig, "Asymptotic performance of MIMO wireless channels with limited feedback," in *Proc. IEEE Mil. Comm. Conf.*, vol. 1, Honolulu, Hawaii, USA, Oct. 2003, pp. 141–146.

[115] ——, "Signature optimization for cdma with limited feedback," *IEEE Trans. Inform. Theory*, vol. 51, no. 10, pp. 3475–3492, Oct. 2005.

[116] W. Yu and R. Lui, "Dual methods for nonconvex spectrum optimization of multicarrier systems," *IEEE Trans. Commun.*, vol. 54, no. 7, pp. 1310–1322, Jul. 2006.

[117] X. Kang, Y. Liang, A. Nallanathan, H. K. Garg and R. Zhang, "Optimal power allocation for fading channels in cognitive radio networks: Ergodic capacity and outage capacity," *Trans. Wireless Commun.*, vol. 8, no. 2, pp. 940–950, Feb. 2009.

[118] X. Wang, A.G. Marques and G.B. Giannakis, "Power-efficient resource allocation and quantization for tdma using adaptive transmission and limited-rate feedback," *IEEE Trans. on Signal Processing*, vol. 56, no. 9, pp. 4470–4485, Sept. 2008.

[119] X. Zheng, Y. Xie, J. Li and P. Stoica, "MIMO transmit beamforming under uniform elemental power constraint," *IEEE Trans. Signal Processing*, vol. 55, no. 11, pp. 5395–5406, Nov. 2007.

[120] Y. Linde, A. Buzo and R. Gray, "An algorithm for vector quantizer design," *IEEE Trans. Commun.*, vol. 28, no. 1, pp. 84–95, Jan. 1980.

[121] Y. Sun and M. L. Honig, "Asymptotic capacity of multicarrier transmission over a fading channel with feedback," in *Proc. IEEE ISIT 2003*, Pacifico Yokohama, Yokohama, Japan, Jun.-Jul. 2003, p. 40.

[122] Y. Y. He and S. Dey, "Power allocation in spectrum sharing cognitive radio networks with quantized channel information," *IEEE Trans. Commun.*, vol. 59, no. 6, pp. 1644–1656, Jun. 2011.

[123] R. Zhang, "On peak versus average interference power constraints for protecting primary users in cognitive radio networks," *IEEE Trans. Wireless Commun.*, vol. 8, no. 4, pp. 2112–2120, Apri. 2009.